

CONFERENCE GUIDE NORTH AMERICAN PARTICLE ACCELERATOR CONFERENCE 2016



October 9 – 14, 2016
Chicago, IL USA

SPONSORED BY:



Image credit (front cover): <http://lpmfc375762dcvmc48alm81c.wpengine.netdna-cdn.com/wp-content/uploads/2014/11/chicago8.jpg>



North American Particle Accelerator Conference 2016

Chicago, Illinois USA
October 9-14, 2016

Sponsored by

American Physical Society

and

Institute of Electrical and Electronics Engineers (IEEE)

Hosted by

Argonne National Laboratory

and

Fermi National Accelerator Laboratory





North American Particle Accelerator Conference 2016

October 9-14, 2016

napac2016.aps.anl.gov ♦ e-mail: NAPAC16@aps.anl.gov

WELCOME

Dear Attendee,

The 2016 North American Particle Accelerator Conference (NAPAC16) will be held in the heart of downtown Chicago at the Sheraton Grand Chicago. The conference covers the entire spectrum of accelerator science and technology topics and will bring together hundreds of experts in all fields of accelerator science and technology. Our industrial partners, without whom today's modern accelerator facilities could not have been built, will present their latest offerings and capabilities. We are sincerely grateful for their support of our field and of this conference. Many students from all over the world will be in attendance. Students are the experts of tomorrow, and we know there will be many opportunities over this week for the students, exhibitors, accelerator scientists, engineers, and technicians to interact and develop networks and new ideas that will eventually become the basis for accelerators of the future.

This conference is sponsored by IEEE and the American Physical Society.

We hope you enjoy the excellent program of talks and posters and also take the opportunity to enjoy our beautiful city on the shores of Lake Michigan.

Sincerely,

Marion White, Conference Chair

Vladimir Shiltsev, Program Chair

Maria Power, Scientific Secretariat/Proceedings Editor

Argonne National Laboratory, Building 401/Room B4191
9700 S. Cass Ave., Lemont, IL 60439 U.S.A.
Phone: +1 630 252-6158 ♦ Fax: +1 630 252-7187



ORGANIZING COMMITTEE

Marion White, Argonne (Conference Chair)
Vladimir Shiltsev, FNAL (SPC Chair)
Armando Antillón Díaz, UNAM
Bill Barletta, MIT
Ed Bonnema, Meyer Tool & Mfg. Inc.
John Cary, CIPS
John Erickson, LANL
Steve Gourlay, LBNL
Don Hartill, Cornell U.
Ed Hartouni, LLNL
Mark Hogan, SLAC
Andrew Hutton, JLab
Kevin Jones, ORNL
Shane Koscielniak, TRIUMF
Liu Lin, LNLS
Stephen Milton, Colorado State U.
Brian Richter, GMW Assoc.
Thomas Roser, BNL
Stan Schriber, APS/IEEE
Linda Spentzouris, IIT
Bruce Strauss, DOE
Dave Sutter, U. Maryland
Alan Todd, AMMTodd Consulting
Yoshishige Yamazaki, Michigan State U.

LOCAL ORGANIZING COMMITTEE

Marion White, Argonne (Conference Chair)
Vladimir Shiltsev, FNAL (SPC Chair)
Maria Power, Argonne (Scientific Secretariat/
Proceedings Editor)
Patty Cameli, Argonne
Bruce Carlsten, LANL
Kelly Cunningham, Argonne
Linda DeVito, Argonne
Auralee Edelen, Colorado State U.
Richard Fenner, Argonne
Katherine Harkay, Argonne
Stuart Henderson, Argonne
Kelly Jaje, Argonne
Jacque LeBreck, Argonne
Christine McGhee, Argonne
Joy Pomillo, FNAL
Melody Saperston, FNAL
Nihan Sipahi, Colorado State U.
Linda Spentzouris, IIT
Suzanne Weber, FNAL

SCIENTIFIC PROGRAM COMMITTEE

Vladimir Shiltsev, FNAL (SPC Chair)	Rolland Johnson, Muons Inc	Claudio Rivetta, SLAC
Alexander Aleksandrov, ORNL	Chad Joshi, UCLA	Alexandr Romanenko, FNAL
Yuri Alexahin, FNAL	Osamu Kamigaito, Riken	James Rosenzweig, UCLA
Giorgio Apollinari, FNAL	Robert Kephart, FNAL	Lucio Rossi, CERN
Mei Bai, COSY	Tim Koeth, UMD	GianLuca Sabbi, LBNL
Michael Benedikt, CERN	Bob Laxdal, TRIUMF	Vadim Sajaev, Argonne
Maria Biagini, INFN	Valeri Lebedev, FNAL	Carl Schroeder, LBNL
Sandra Biedron, Colorado State	Evgeny Levichev, BINP	Andrei Seryi, JAI
Michael Blaskiewicz, BNL	Vladimir Litvinenko, BNL	Pitamber Singh, BARC
Michael Borland, Argonne	John Lewellen, LANL	Nikolay Solyak, FNAL
Salime Boucher, Radiabeam	David McGinnis, ESS	Panagiotis Spentzouris, FNAL
John Byrd, LBNL	Peter McIntyre, Texas A&M	Markus Steck, FAIR/GSI
Mark Champion, ORNL	Francois Meot, BNL	Christoph Steier, LBNL
Swapan Chattopadhyay, NIU/FNAL	Michiko Minty, BNL	Gennady Stupakov, SLAC
Yu-Jiuan Chen, LLNL	Nikolai Mokhov, FNAL	Michael Syphers, MSU
Eric Colby, SLAC/DOE	Marie-Hélène Moscatello Di Giacomo, GANIL	Takashi Tanaka, SPring8
Sarah Cousineau, ORNL	Patric Muggli, MPIAlex Murokh, Radiabeam	Jingyu Tang, IHEP
Glenn Decker, Argonne	Sergei Nagaitsev, FNAL	Pedro Tavares, MAX IV Lab - Lund Univ
Jean Delayen, ODU	Olivier Napoly, CEA	Alan Todd, AMMTodd Consulting
Vladimir Derenchuk, ProNova Solutions	Patrick Naulleau, LBNL	Aaron Tremaine, SLAC
Paul Derwent, FNAL	Kazuhito Ohmi, KEK	Grigoriy Trubnikov, JINR
Lyn Evans, CERN	Yukiyoshi Ohnishi, KEK	Alex Valishev, FNAL
Wolfram Fischer, BNL	Peter Ostroumov, Argonne	Jean-Luc Vay, LBNL
John Fox, SLAC	Hasan Padamsee, FNAL	Nikolay Vinokurov, BINP
John Galambos, ORNL	Mark Palmer, FNAL	Nicholas Walker, DESY
Camille Ginsburg, FNAL	Fulvia Pilat, JLab	Dong Wang, SSRF
Terry Grimm, Niowave, Inc	Philippe Piot, NIU	Jie Wei, MSU/FRIB
Kazuo Hasegawa, JPARC	John Power, Argonne	Marion White, Argonne
Erik Hemsing, SLAC	Qing Qin, IHEP BEIJING	Ferdinand Willeke, BNL
Stuart Henderson, Argonne	Pantaleo Raimondi, ESRF	Johnathan Wurtele, UC Berkeley
Robert Hettel, SLAC	Alex Ratti, LBNL	Zhentang Zhao, SINAP
Georg Hoffstaetter, Cornell U.	Sven Reiche, PSI	Alexander Zholents, Argonne
Mark Hogan, SLAC		Mikhail Zobov, INFN
Patrick Hurh, FNAL		Robert Zwaska, FNAL

TABLE OF CONTENTS

General Information	vii
Conference Venue	vii
Registration/Information Desk	vii
Welcome Reception - Sunday, October 9	vii
Breaks and Lunches	vii
Mobile Application	vii
Internet & Wireless Service.....	viii
Information for Speakers and Presenters	viii
NAPAC 2016 Louis Costrell Honorary Awards Session	ix
List of Participants	x
Security	x
Vendor Exhibits.....	x
Tipping	x
No-Smoking Policy	x
About Chicago.....	x
About The American Physical Society (APS)	xi
About The Institute of Electrical and Electronics Engineers (IEEE)	xi
Transportation.....	xi
Tours of Argonne And Fermilab – Saturday, October 15	xi
Sheraton Floor Plans.....	xii
Exhibitors	xiv
Programme and Abstracts	1
Author Index	105
List of Participants	129
Program.....	135

GENERAL INFORMATION

CONFERENCE VENUE

Sheraton Grand Chicago
301 East North Water Street
Chicago, IL 60611 USA
Telephone: 1-312-464-1000
Fax: 1-312-464-9140
E-mail: info@sheratonchicago.com
www: www.sheratonchicago.com

REGISTRATION/INFORMATION DESK

Registration materials (i.e., conference badge, banquet tickets) will be available at the registration desk located outside Chicago VI & VII.

Sunday, October 9	12:00 – 20:00
Monday, October 10	08:00 – 18:00
Tuesday, October 11	08:00 – 18:00
Wednesday, October 12	08:00 – 18:00
Thursday, October 13	08:00 – 12:00
Friday, October 14	Closed

WELCOME RECEPTION - SUNDAY, OCTOBER 9

You are invited to join us at a Welcome Reception on Sunday from 18:00-21:00 in the Sheraton Grand Chicago (Riverwalk A & B).

BREAKS AND LUNCHESES

Refreshment breaks will be served at 10:30 and 15:30 in Riverwalk A & B, where our exhibitors will be located. Lunch breaks are from 12:30–14:00. There are many great restaurants within walking distance of the Sheraton Grand Chicago. Please feel free to ask the concierge for additional recommendations.

MOBILE APPLICATION

The NAPAC2016 mobile application is available for both iPhone via the AppStore and Android devices via the Google Play Store. It allows you to view the schedule, posters, presentations, exhibitors, and speaker details from the conference. Users can take notes on presentations and posters inside the app. Note-taking is also available in the exhibitor module.

Additionally, users can share information with attendees and colleagues within app messaging, tweeting, and emailing.

When creating your account for the app, use the event code: NAPAC2016.

INTERNET & WIRELESS SERVICE

Complimentary WiFi, computer workstation, and online printing are available at the internet cafe called “The Link” located one level below the Lobby.

INFORMATION FOR SPEAKERS AND PRESENTERS

The deadline for the submission of contributions to the Proceedings is October 5, 2016, at 11:59 PM in Chicago (GMT-6). All papers should be submitted through SPMS. A monitor will be available near the registration area to view the editing status of your paper, and a link to the status page is available from the Mobile App.

Invited Talks

Invited talks will take place in Chicago Ballrooms VI & VII starting at 08:30 each morning. Speakers should upload a PDF of their slides through SPMS the day before the talk at the very latest.

Poster Sessions

Poster Sessions are Monday afternoon (October 10) through Thursday morning (October 13), and will take place in the Riverwalk Hall A & B. The morning session runs from 08:30 until 12:30. Morning posters should be staffed from 11:00 until 12:30. The afternoon session runs from 14:00 until 17:30. Afternoon posters should be staffed from 16:00 until 17:30.

The student poster session will be held on Sunday, October 9, in Riverwalk A & B. Posters should be set up from 13:30-14:00 on Sunday, October 9, and students should attend their posters for interactions with judges and arriving conference delegates from 14:00 to 18:00.

Poster Display and Removal

For the morning poster session, you may put your poster up any time after 08:00 on the day of your poster session. For the afternoon poster session, you may put your poster up any time after 13:00 on the day of your poster session. Please set up your poster before the session begins. Each poster will be presented on half a single display board. The area available for your poster has width 4 feet (122 cm) and height 4 feet (122 cm). **All posters must be attended during the poster session, and removed promptly when the poster session is over.**

Proceedings

All work properly submitted and presented for NAPAC16 will be included in the conference proceedings, which will be published at the JACoW website shortly after the conference. All contributions must be uploaded via SPMS according to the electronic submission guidelines.

Questions concerning the proceedings may be addressed to the Scientific Secretariat/ Proceedings Editor, Maria Power (mpower@anl.gov). The Proceedings Office will be located in Columbus A/B on the Lobby Level of the Sheraton.

NAPAC2016 LOUIS COSTRELL HONORARY AWARDS SESSION

The awards session will take place on Thursday, October 13, from 16:00-17:30, and will include the following:

What Life is Like as a Scientist in Congress, presented by Rep. Bill Foster

2016 IEEE Fellow, presented by Ilan Ben-Zvi

B. Carlsten, Los Alamos National Laboratory

"For contributions to high-brightness electron beams and vacuum electron devices."

IEEE NPSS Awards, presented by Ilan Ben-Zvi

S. Posen, Fermilab National Accelerator Laboratory

"For contributions to the development of Nb₃Sn SRF cavities."

W. Leemans, Lawrence Berkeley National Laboratory

"For pioneering development of laser-plasma accelerators."

A. Grassellino, Fermi National Accelerator Laboratory

"For pioneering nitrogen-doping of superconducting RF cavities."

2016 APS DPB Fellows (5), presented by Tor Raubenheimer

NAPAC16 Student Poster Awards and APS DPB Outstanding Doctoral Thesis Award winners, presented by Vladimir Shiltsev

APS DPB Outstanding Doctoral Thesis award winner talk

Panagiotis Baxevanis, SLAC National Accelerator Laboratory

"In recognition of outstanding contributions to the theory of three dimensional effects in free electron lasers."

2016 APS Wilson Prize (V. Parkhomchuk), presented by Maury Tigner

2016 APS Wilson Prize winner talk

Vasily Parkhomchuk, Budker Institute of Nuclear Physics

“For crucial contributions in the proof of principle of electron cooling, for leading contribution to the experimental and theoretical development of electron cooling, and for achievement of the planned parameters of coolers for facilities in laboratories around the world.”

LIST OF PARTICIPANTS

A list of NAPAC2016 attendees at the time of printing is included in this book. Complete information will also be posted on the NAPAC2016 website following the conference.

SECURITY

Participants are asked not to leave their baggage or conference bags unattended and to wear conference badges at all times. The conference organizers cannot accept liability for personal injuries sustained, or for loss of, or damage to, property belonging to conference participants (or accompanying persons), either during or as a result of the conference.

VENDOR EXHIBITS

Vendor Exhibits are located in Riverwalk A & B.

TIPPING

Tipping in the United States is generally 15-20% for restaurant service; more for exceptional service. Tips are typically 10-15% for taxis and \$1.00 per bag for luggage.

NO-SMOKING POLICY

Illinois has a no-smoking policy that restricts smoking in all public and work places; smoking is only permitted outside (15 feet beyond building entrances).

ABOUT CHICAGO

Chicago is the third largest city in the United States, with a population of nearly three million people. Its scenic lakeside location, world-class cultural offerings and unique architecture are just some of the reasons why Chicago is a great place to live and visit. You can explore the city by bus, boat, or on foot. There are many attractions such as the Hancock and Willis Towers, Millennium Park, Navy Pier, The Art Institute of Chicago, Museum of Science & Industry, Field Museum, Adler Planetarium & Lincoln Park Zoo. Please visit the conference website at <https://napac2016.aps.anl.gov/General-Info/About-Chicago> for more information.

ABOUT THE AMERICAN PHYSICAL SOCIETY (APS)

The American Physical Society (APS) is a non-profit membership organization working to advance and diffuse the knowledge of physics through its outstanding research journals, scientific meetings, and education, outreach, advocacy, and international activities. APS represents over 51,000 members, including physicists in academia, national laboratories, and industry in the United States and throughout the world. Society offices are located in College Park, MD (Headquarters), Ridge, NY, and Washington, D.C. See www.aps.org for information about APS.

ABOUT THE INSTITUTE OF ELECTRICAL AND ELECTRONICS ENGINEERS (IEEE)

IEEE is the world's largest technical professional organization dedicated to advancing technology for the benefit of humanity. IEEE and its members inspire a global community to innovate for a better tomorrow through its highly cited publications, conferences, technology standards, and professional and educational activities. IEEE is the trusted “voice” for engineering, computing, and technology information around the globe. See www.ieee.org for information about IEEE.

TRANSPORTATION

Within Chicago, transportation is usually by taxi cab or through the Chicago Transit Authority (CTA) bus and rail systems. Transit Cards can be purchased and value can be added to Transit Cards at Ventra vending machines located at all CTA rail stations. Vending machines accept \$1, \$5, \$10, and \$20 USD bills, and all coins except pennies and half dollars. Credit/debit cards are also accepted at Ventra vending machines. Taxicabs are available outside the main hotel entrance. The Chicago Transit Authority (CTA) provides bus and ‘L’ (subway) service. See www.transitchicago.com for more information.

Uber and Lyft serve the Chicago area. Apps for these transportation services can be downloaded at <http://get.uber.com> and www.lyft.com/app.

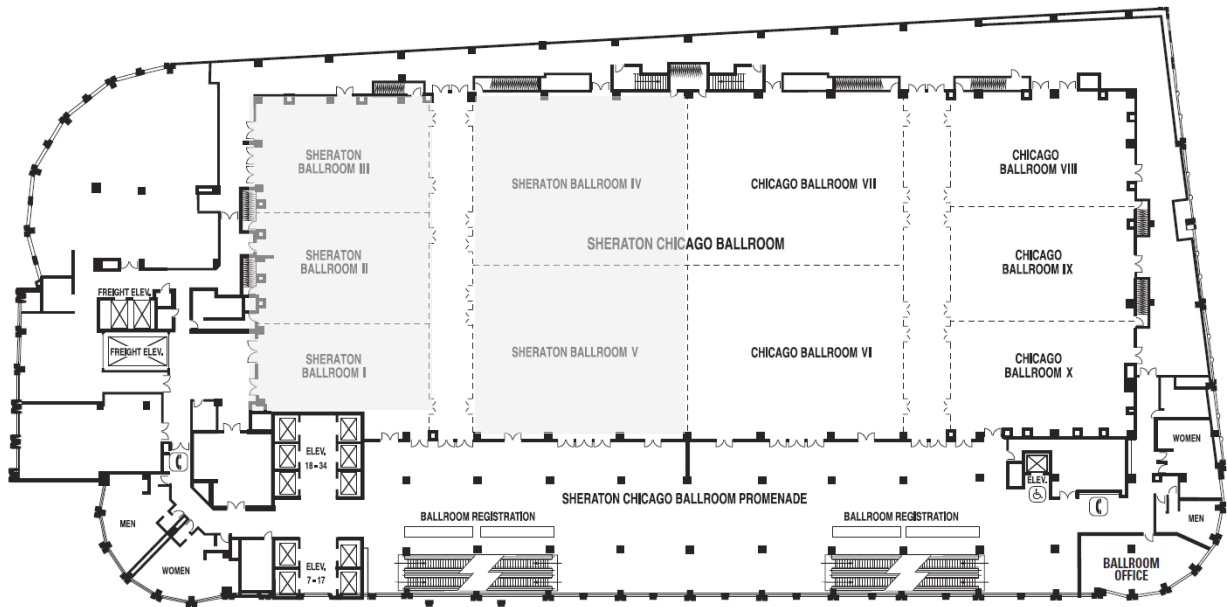
Airport and additional travel information can be found on the conference web page: <https://napac2016.aps.anl.gov/General-Info/Getting-to-Chicago>.

TOURS OF ARGONNE AND FERMILAB – SATURDAY, OCTOBER 15

Tours of Argonne National Laboratory and Fermi National Accelerator Laboratory have been organized. The bus will leave Saturday, October 15, at 08:00 a.m. from the Lobby Level Convention Entrance of the hotel. The tour will last approximately eight hours. As part of your registration fee, assorted boxed lunches will be provided.

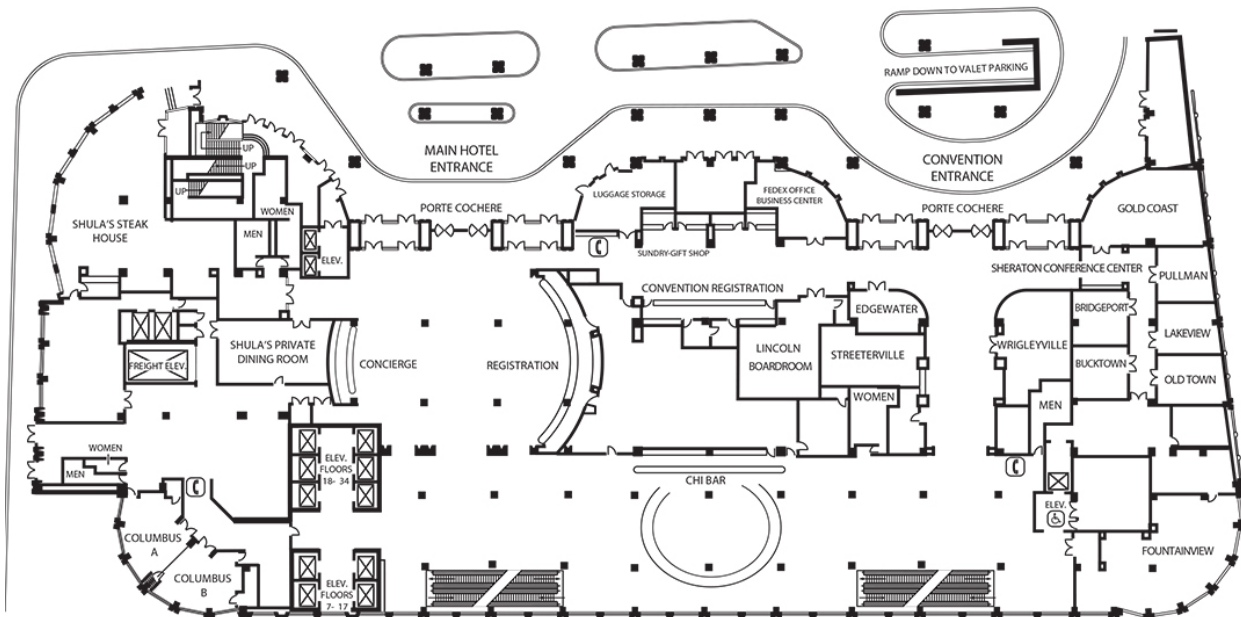
In order to attend the tour at Argonne National Laboratory, you **MUST** be pre-registered. All visitors (except children under the age of 17) are required to present photo identification, such as a driver's license or passport, to receive a gate pass.

SHERATON FLOOR PLANS



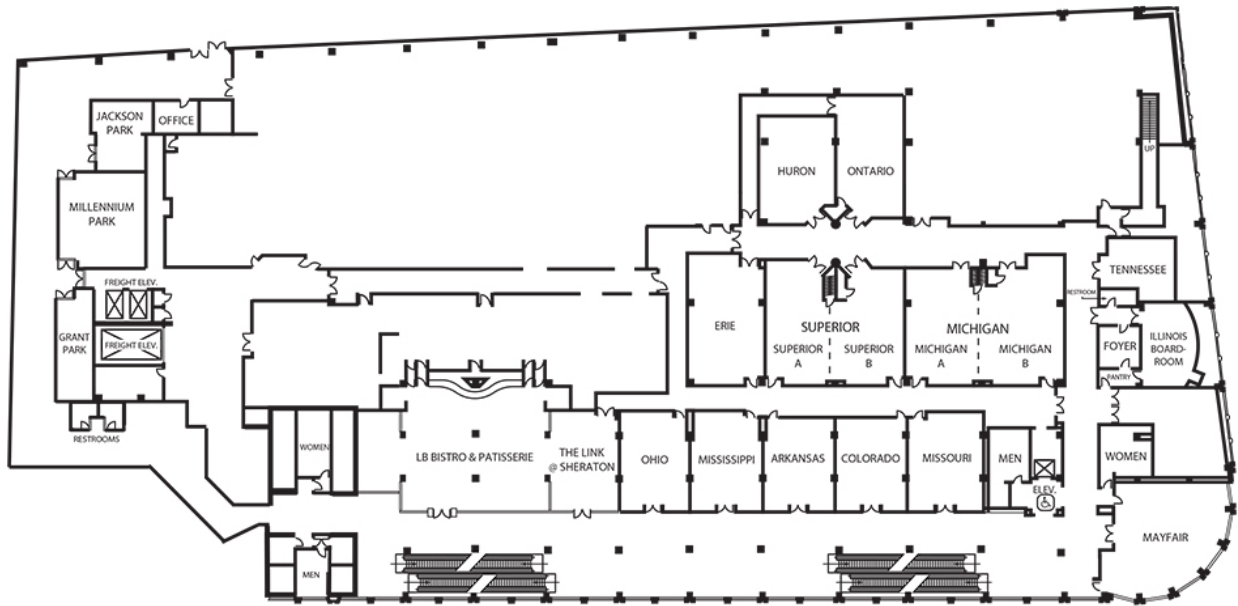
Ballroom – Level 4

General Sessions – Chicago Ballrooms VI & VII

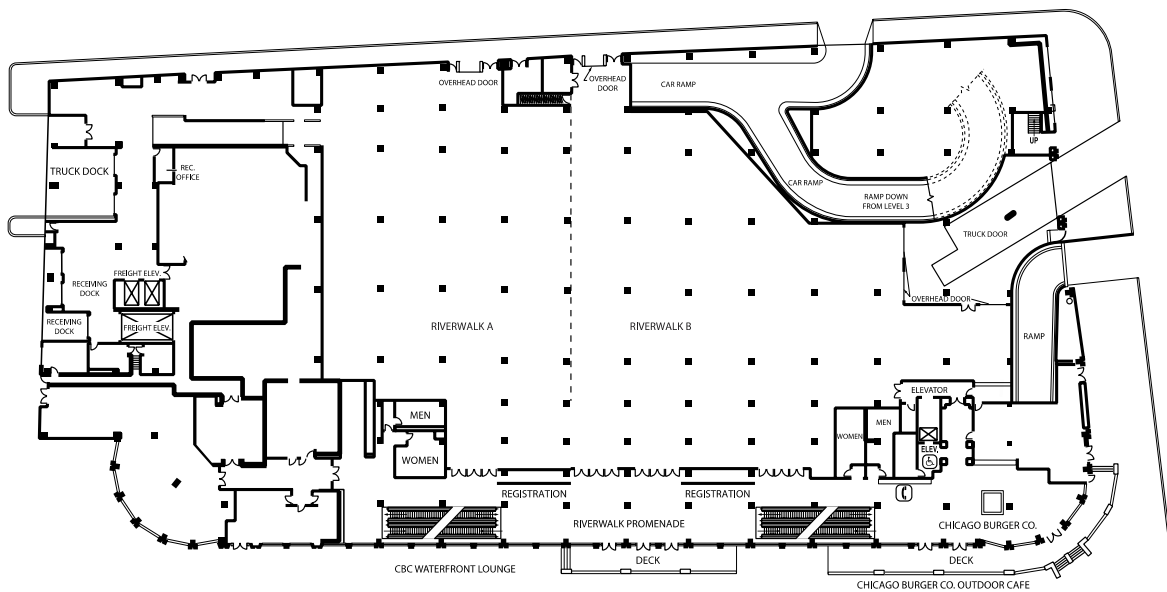


Lobby Level – Level 3

Proceedings Office – Columbus A/B



Meeting Rooms– Level 2
Internet Access – The Link @ Sheraton Café



Riverwalk– Level 1
Poster Sessions / Exhibitors – Riverwalk A & B

EXHIBITORS

Advanced Energy Industries, Inc.

1625 Sharp Point Drive
Fort Collins, Colorado 80525
(970) 407-5296
www.advanced-energy.com

COSMOTEC, Inc.

229 Polaris Ave
Mountain View, California 94043
(408) 428-9741
www.cosmotec.us

Argonne National Laboratory

9700 S. Cass Avenue
Lemont, Illinois 60439
(630) 252-2000
www.anl.gov

CST of America

492 Old Connecticut Path
Suite 500
Framingham, Massachusetts 01701
(508) 665-4400
www.cst.com

Buckley Systems Ltd.

19 Turcotte Memorial Drive
Rowley, Massachusetts 01969
(978) 948-3403
Buckleysystems.com

Danfysik A/S

Gregersensvej 8
Taastrup, 3600
Denmark
+4572202400
www.danfysik.com

C.F. Roark Welding & Engineering Co. Inc.

136 North Green Street
Brownsburg, Indiana 46112
(317) 852-3163
www.roarkfab.com

Dean Technology, Inc.

4117 Billy Mitchell Drive
Addison, Texas 75001
(972) 248-7691
www.deantechnology.com

Communication Power Corporation

80 Davids Drive, Suite 3
Hauppauge, New York 11788
(631) 805-0474
www.cpcamps.com

Eagle Harbor Technologies, Inc.

169 Western Ave W., Suite 263
Seattle, Washington 98119-4211
(206) 402-5241
www.eagleharbortech.com/

Elytt Energy

Calle de Orense 11, 2b
Madrid, Madrid 28020
Spain
+34914110963
www.elytt.com

Euclid Techlabs, LLC

5900 Harper Rd # 102
Solon, Ohio 44139
(440) 519-0410
www.euclidtechlabs.com

GMW Associates

955 Industrial Road
San Carlos, California 94070
(650) 802-8292
www.gmw.com

Hamamatsu Corporation

360 Foothill Road
Bridgewater, New Jersey 08807
(908) 231-0960
www.hamamatsu.cm

Hi-Tech Manufacturing, LLC

9815 W. Leland
Schiller Park, Illinois 60176
(847) 678-1616
www.hi-tech-mfg.com

Instrumentation Technologies d.d.

Velika pot 22, Solkan, Nova Gorica 5250
Slovenia
+38653352600
www.i-tech.si/

Lake Shore Cryotronics

575 McCorkle Boulevard
Westerville, Ohio 43082
(614) 891-2243
www.lakeshore.com

Mega Industries, LLC

28 Sanford Drive
Gorham, Maine 04038
(207) 854-1700
www.megaind.com

Muons, Inc.

552 N. Batavia Ave.
Batavia, Illinois 60510
(757) 870-6943
www.muonsinc.com

RadiaBeam Technologies

1717 Stewart Street
Santa Monica, California 90404
(310) 822-5845
www.radiabeam.com

SAES Group

1122 E Cheyenne Mnt Blvd
Colorado Springs, Colorado 80906
(719) 576-3200
www.saesgetters.com

ScandiNova Systems

Ultunaallén 2A
75651 Uppsala
Sweden
+460184805900
www.scandinovasystems.com

Scanditronix Magnet AB

Olvägen 28
Vislanda, Kronobergs Lan 34250
Sweden
+4647248680
www.scanditronix-magnet.se

SIGMAPHI

Rue des frères Montgolfier
Vannes, 56000
France
+33297010880
www.sigmaphi.fr

SmarAct Inc.

2140 Shattuck Ave, STE 1103
Berkeley, California 94131
(415) 766-9006
www.smaract.com/

Solid Sealing Technology

44 Daliba Ave
Watervliet, New York 12189
(518) 874-3600
www.solidsealing.com

TDK-Lambda Americas High Power Division

405 Essex Rd.
Neptune, New Jersey 07753
(732) 922-9300
www.us.tdk-lambda.com/hp

Time Co. Ltd.

73-48 Obara, Nutanishi chou
Mihara city, Hiroshima 729-0473
Japan
(0848) 85-066
www.time-merit.co.jp

Tomco Technologies

38 Payneham Road
Stepney
South Australia 5069
(202) 657-6844
www.tomcorf.com

Programme and Abstracts

SUPO — Student Poster Session	5
MOPL — Conference Opening	13
MOPLI001 Welcome	13
MOPLI002 High Energy Physics as a Global Enterprise: Report from ICHEP XXVIII (Chicago, Aug. 2016)	13
MOPLI003 A Billion Times Brighter: An Overview of the Scientific Impact and Future Opportunities of X-Ray Free Electron Lasers	13
MOPLI004 Nuclear Physics at the Electron Ion Collider Plenary	13
MOA2 — Oral Presentations (MC6)	14
MOA2I001 Towards Attosecond Synchronization in Ultrafast Light Sources	14
MOA2I002 The BNL/LBNL BPM Electronics, High Performance for Next Generation Storage Rings	14
MOA2C003 Measurement of Tune Shift with Amplitude from BPM Data with a Single Kicker Pulse	14
MOA2C004 MICE Operation and Demonstration of Muon Ionization Cooling	14
MOB2 — Oral Presentations (MC1)	15
MOB2I001 Beam Dynamics Issues in Very High Energy Circular p-p Colliders	15
MOB2I002 Overview of Jefferson Lab EIC Design and R&D	15
MOB2C003 Collider in the Sea: A New Vision for a 700 TeV World Laboratory	15
MOB2C004 Multiphysics Analysis of Crab Cavities for High Luminosity LHC Upgrade	15
MOA3 — Oral Presentations (MC6)	16
MOA3I001 High Energy Coulomb Scattered Electrons Detected in Air Used as the Main Beam Overlap Diagnostics for Tuning the RHIC Electron Lenses	16
MOA3I002 Precision Vector Control of a Superconducting RF Cavity Driven by an Injection Locked Magnetron	16
MOA3C003 The Bunch Shape Monitor Measurements At The LANSCE Linac	16
MOA3C004 Operational Experience with Fast Fiber-Optic Beam Loss Monitors for the Advanced Photon Source Storage Ring Superconducting Undulators	16
MOB3 — Oral Presentations (MC1)	17
MOB3I001 Commissioning of the Phase-I SuperKEKB B-Factory and Update on the Overall Status	17
MOB3I002 LHC Operation at 6.5 TeV : Status and Beam Physics Issues	17
MOB3C003 RHIC Au-Au Operation at 100 GeV in Run16	17
MOB3C004 High Luminosity 100 TeV Proton-Antiproton Collider	17
MOA4 — Oral Presentations (MC4)	18
MOA4I001 Performance of the Low Charge State Laser Ion Source in BNL	18
MOA4I002 Recent Progress in High Intensity Operation of the Fermilab Accelerator Complex	18
MOA4C003 Complete Beam Dynamics of the JLEIC Ion Collider Ring Including Imperfections, Corrections, and Detector Solenoid Effects	18
MOA4C004 Compact Carbon Ion Linac	18
MOB4 — Oral Presentations (MC1)	19
MOB4I001 Specifics of Electron Dynamics in High Energy Circular e^+e^- Colliders	19
MOB4I002 Linac-ring and Ring-ring designs for the eRHIC Electron-Ion Collider	19
MOB4C003 Design of Muon Collider Lattices	19
MOB4C004 Design of the Room-Temperature Front-End for a Multi-Ion Linac Injector	19
MOPOB — Poster Session (MC7)	20
TUA1 — Oral Presentations (MC4)	31
TUA1I001 Status of FRIB	31
TUA1I002 Status Report on the SPIRAL2 Facility at GANIL	31
TUA1I003 Technological Challenges in the Path to 3.0 MW at the SNS Accelerator	31
TUA1C004 Simulation of Beam Dynamics in a Strong-Focusing Cyclotron	31
TUA1C005 Design of a Compact Ring for Pulse Structure Manipulation of Heavy Ion Beams at the NSCL	31
TUB1 — Tutorial (MC9) / Oral Presentation (MC2)	32
TUB1TU01 A Discussion on Phase Space and Beam Emittance	32
TUB1C002 Operating Synchrotron Light Sources with a High Gain Free Electron Laser	32
TUB1C003 ALS-U: A Soft X-Ray Diffraction Limited Light Source	32
TUA2 — Oral Presentations (MC3)	33
TUA2I001 AWAKE - a Proton Driven Plasma Wakefield Acceleration Experiment at CERN	33
TUA2I002 Staging Results at the Argonne DLA facility	33
TUA2C003 A Novel Technique of Power Control in Magnetrons	33

TUA2C004 Vacuum Breakdown Research at 110 GHz	33
TUB2 — Oral Presentations (MC2)	34
TUB2I001 Accelerator Physics Challenges in the Design of Multi Bend Achromat Based Storage Rings	34
TUB2I002 Advanced Concepts for Seeded FELs	34
TUB2C003 Fokker-Planck Analysis of Transverse Collective Instabilities in Electron Storage Rings	34
TUB2C004 Corrugated Structure Insert to Extend SASE Bandwidth Up to 3% at the European XFEL	34
TUPOA — Poster Session (MC6 & MC8)	35
TUA3 — Oral Presentations (MC3)	45
TUA3I001 Possible Road Maps for High-Energy Collider Based on Advanced Acceleration Techniques	45
TUA3I002 FACET Results and FACET II Perspective	45
TUA3C003 Compact Ring-Based X-Ray Source With on-Orbit and on-Energy Laser-Plasma Injection	45
TUA3C004 Kinetic Limits to Average Power in Plasma Wakefield Accelerators	45
TUB3 — Oral Presentations (MC2)	46
TUB3I001 Commissioning of Max-IV, the First Light Source Using a Multi Bend Achromat	46
TUB3I002 Overview of Electron Source Development for High Repetition Rate FEL Facilities	46
TUB3C003 Demonstration of fresh slice self seeding in a hard X-ray free electron laser	46
TUB3C004 A New Thermionic RF Electron Gun for Synchrotron Light Sources	46
TUA4 — Oral Presentations (MC3)	47
TUA4I001 Staging Results at BELLA and Plans for BELLA	47
TUA4I002 Eupraxia: A Compact European Plasma Accelerator With Superior Beam Quality	47
TUA4C003 Loading of Wakefields in a Plasma Accelerator Section Driven by a Self-Modulated Proton Beam	47
TUA4C004 High-Power Tunable THz Generation in Corrugated Plasma Waveguides	47
TUB4 — Oral Presentations (MC2)	48
TUB4I001 Status of the MaRIEProject	48
TUB4I002 Accelerator Technical Progress and First Commissioning Results from the European XFEL	48
TUB4C003 Optimization of Compton source Performance through Electron Beam Shaping	48
TUB4C004 Progress on the Magnetic Performance of Planar Superconducting Undulators	48
TUPOB — Poster Session (MC1 & MC5)	49
WEA1 — Oral Presentations (MC5)	57
WEA1I001 Demonstration of Energy-Chirp Control in Relativistic Electron Bunches at LCLS Using a Corrugated Structure	57
WEA1I002 Computation of Electromagnetic Fields Generated by Relativistic Beams in Complicated Structures	57
WEA1C003 Simulations of Booster Injection Efficiency for the APS-Upgrade	57
WEA1C004 Hollow Electron Beam Collimation for HL-LHC - Effect on the Beam Core	57
WEA1C005 Microwave Instability Studies in NSLS-II	57
WEA1C006 Analytical theory for McMillan map	57
WEB1 — Tutorial & Oral Presentation (MC7)	58
WEB1TU01 Superconducting Accelerators Magnets	58
WEB1C002 Investigation of Structure and Composition Development in the Two-Step Diffusion Coating of Nb ₃ Sn on Niobium	58
WEB1C003 Surface Impurity Content Optimization to Maximize Q-factors of Superconducting Resonators	58
WEA2 — Oral Presentations (MC5)	59
WEA2I001 Calculating Spin Lifetime	59
WEA2I002 Proposed Experimental Validation of Hamiltonian Perturbation Theory in IOTA	59
WEA2C003 Incoherent Vertical Emittance Growth from Electron Cloud at CsrTA	59
WEA2C004 Vlasov Analysis of Microbunching Gain for Magnetized Beams	59
WEB2 — Oral Presentations (MC7)	60
WEB2I001 Development of Higher Harmonic Superconducting Cavity for Light Sources	60
WEB2I002 Compact Crabbing Cavity Systems for Particle Colliders	60
WEB2C003 High Power Production Target for FRIB	60
WEB2C004 Nb ₃ Sn SRF Coatings at Fermilab	60
WEPOA — Poster Session (MC3 & MC4)	61
WEA3 — Oral Presentations (MC5)	70
WEA3I001 Emittance Growth from Modulated Focusing in Bunched Beam Cooling	70
WEA3I002 Start-to-End Beam Dynamics Optimization of X-Ray FEL Light Source Accelerators	70
WEA3C003 Efficiency of Feedbacks for Suppression of Transverse Instabilities of Bunched Beams	70
WEA3C004 Impedance Characterization and Collective Effects in the MAX IV 3 GeV Ring	70
WEB3 — Oral Presentations (MC7)	71
WEB3I001 Superconducting Cryomodule Development and Production for the FRIB Linac	71
WEB3I002 First Test Results of the 150 mm Aperture IR Quadrupole Models for the High Luminosity LHC	71
WEB3C003 650 MHz Elliptical Superconducting RF Cavities for PIP-II Project	71
WEB3C004 Preliminary Tests of Plasma Cleaning as an in-Situ Superconducting RF Cavity Cleaning Technique	71

WEA4 — Oral Presentations (MC5)	72
WEA4I001 Dynamics of Beams With Canonical Angular Momentum in Non-Axisymmetric Optical Elements	72
WEA4C002 Impact of Space Charge on Beam Dynamics and Integrability in the IOTA Ring	72
WEA4C003 Intrinsic Landau Damping of Bunched Beams at Transverse Coupling Resonance	72
WEA4C004 Suppression of Half-Integer Resonance in FNAL Booster and Space Charge Losses at Injection	72
WEA4C005 Accelerator Physics Design and Challenges of RF Based Electron Cooler LEReC	72
WEB4 — Oral Presentations (MC7)	73
WEB4I001 Advanced High Gradient, High Efficiency RF Technology	73
WEB4I002 CLIQ: a New Quench Protection Technology for Superconducting Accelerator Magnets	73
WEB4C003 Phase Shift Calibration of CEBAF Linac Cavities	73
WEB4C004 100 kW Very Compact Pulsed Solid-State RF Amplifier. Development and Tests	73
WEPOB — Poster Session (MC2)	74
THA1 — Oral Presentations (MC7)	83
THA1I001 Progress in High Q SRF cavities development: from Single Cell to Cryomodule	83
THA1I002 Results of the 2015 Helium Processing of CEBAF Cryomodules	83
THA1C003 MAX IV and Solaris 1.5 GeV Storage Rings Magnet Block Production Series Measurement Results	83
THA1C004 Persistent Current Effect in 15-16 T Nb3Sn Accelerator Dipoles and its Correction	83
THA1C005 Thermal Modeling and Cryogenic Design of a Helical Superconducting Undulator Cryostat	83
THA1C006 Status of Development of Superconducting Undulators for Storage Rings and Free Electron Lasers at the Advanced Photon Source*	83
THB1 — Tutorial (MC6) / Invited Oral (MC8)	84
THB1TU01 Risk Management of Complex Systems	84
THB1I002 Lightweight Superconducting Magnet Technology for Medical Applications	84
THA2 — Oral Presentations (MC7)	85
THA2I001 High Field SC Magnet Program in the US and Worldwide: Goals, Challenges, Plans	85
THA2I002 High Gradient Permanent Magnet Technology for Ultra-High Brightness Rings	85
THA2C003 S-Band 1.4 Cell Photoinjector Design for High Brightness Beam Generation	85
THA2C004 Bench Measurement of a Multifrequency Cavity of the Ultra-fast RF Kicker for ERL Circular Cooler Ring of JLEIC	85
THB2 — Oral Presentations (MC8)	86
THB2I001 Applications of High-Power Accelerators to Cargo Inspection	86
THB2I002 Production of Medical Isotopes With Electron Linacs	86
THB2I003 Fulfilling the Mission of Brookhaven ATF as a DOE's Flagship User Facility in Accelerator Stewardship	86
THPOA — Poster Session (MC2 & MC5)	87
THA3 — Oral Presentations (MC4)	96
THA3I001 FNAL Accelerator Complex Upgrade Possibilities	96
THA3I002 The ESS Accelerator	96
THA3C003 Beam Commissioning Activities and Issues at Demo Facility of C-ADS Injector II	96
THA3C004 Space Charge Compensation Using Electron Columns and Electron Lenses at IOTA	96
THB3 — Oral Presentations (MC8)	97
THB3I001 Development of a High Brightness Source for Fast Neutron Imaging*	97
THB3I002 Review of Potential Accelerator Systems for Energy and Environmental Applications	97
THB3C003 Thermoacoustic Range Verification for Ion Therapy	97
THB3C004 The Design and Monte Carlo Simulation of the Energy Loss Used in Proton Radiography	97
THPL — Louis Costrell Honorary Awards Session	98
THPLI001 What Life Is Like as a Scientist in Congress	98
FRA1 — Oral Presentations (MC6)	99
FRA1I001 Single Particle Detection With a Schottky Resonator	99
FRA1I002 State of the Art X-Ray Photon BPMs for Next Generation Storage Ring Light Sources	99
FRA1C003 An Ultra-High Resolution Pulsed-Wire Magnet Measurement System	99
FRA1C004 6D Phase Space Measurement of Low Energy, High Intensity Hadron Beam	99
FRA1C005 Progress of Gas-Filled Multi-RF-Cavity Beam Profile Monitor for Intense Neutrino Beam	99
FRA1C006 Measurement of Coherent Transition Radiation Using Interferometer and Photoconductive Antenna	99
FRB1 — Tutorial (MC7) / Oral Presentation (MC8)	100
FRB1TU01 RF Superconductivity	100
FRB1I002 ADAM: LIGHT a Linear Accelerator for Proton Therapy	100
FRA2 — Oral Presentations (MC6)	101
FRA2I001 Development and Application of on-Line Accelerator Optimization Algorithms	101
FRA2I002 High Precision RF Control for the LCLS-II	101
FRA2C003 Study of the Electrical Center of a Resonant Cavity Beam Position Monitor (RF-BPM) and Its Integration With the a Main Beam Quadrupole for Alignment Purposes	101
FRA2C004 Status of the SRF Cavities Resonance Control F&D Work at FNAL	101

FRB2 — Oral Presentations (MC8)	102
FRB2I001 Application of Superconducting Technology for Proton Therapy	102
FRB2I002 4 K Superconducting Linacs for Commercial Applications	102
FRB2I003 GEM*STAR Accelerator-Driven Subcritical System for Improved Safety, Waste Management, and Pluto- nium Disposition	102
FRPL — Closing Session	103
FRPLI001 The Need for Compact Coherent Light Sources - an Example - X-Ray Phase Contrast Tomography Reveals the Secrets of Herculaneum Papyri	103
Author List	105

SUPO — Student Poster Session

Chair: K.C. Harkay (ANL)

- SUP001 An Accurate and Efficient Numerical Integrator for Pair-Wise Interaction**
A.A. Al Marzouk, B. Erdelyi (Northern Illinois University) **B. Erdelyi** (ANL)
 We are developing a new numerical integrator based on Picard iteration method for Coulomb collisions. The aim is to achieve a given prescribed accuracy most efficiently. The integrator is designed to have adaptive time stepping, variable order, and dense output. It also has an automatic selection of the order and the time step. We show that with a good estimation of the radius of convergence of the expansion, we can obtain the optimal time step size. We also show how the optimal order of the integration is chosen to maintain the required accuracy. For efficiency, particles are distributed over time bins, and propagated accordingly with the use of parallelization.
- SUP002 Preliminary Tests of Plasma Cleaning as an in-Situ Superconducting RF Cavity Cleaning Technique**
B.R. Barber (University of Chicago)
 Oxygen plasmas have shown promise for removing surface hydrocarbons from niobium in superconducting RF cavities. These techniques are candidates for in-situ cleaning techniques for installed accelerating cavities. The goal is to improve the performance of cavities that have degraded over time, without removing them from their cryomodule. By varying the governing parameters of the plasma, the primary cleaning method can be varied between a primarily physical process (sputtering) and a primarily chemical process. We extend this work from organic contaminants to more general contaminants, including metallic species. These preliminary tests are primarily concerned with characterizing the cleaning power of various plasma compositions. A variety of gas species are used to create different plasma compositions, including Ar, Ne, O₂, N₂, H₂, and He. Cleaning power is determined by performing surface characterization analysis on room-temperature niobium samples before and after plasma treatment. Samples are maintained in a clean environment between characterization and treatment, to prevent surface recontamination. Measurements of surface contamination and surface character are presented.
- SUP003 Minimization of Emittance at the Cornell Electron Storage Ring With Sloppy Models**
W.F. Bergan, A.C. Bartnik, I.V. Bazarov, H. He, D. L. Rubin (Cornell University (CLASSE), Cornell Laboratory for Accelerator-Based Sciences and Education) **J.P. Sethna** (Cornell University)
 Our current method to minimize the vertical emittance of the beam at the Cornell Electron Storage Ring (CESR) involves measurement and correction of the dispersion, coupling, and orbit of the beam and lets us reach emittances of 10 pm, but is limited by finite dispersion measurement resolution.* For further improvement in the vertical emittance, we propose using a method based on the theory of sloppy models.** The storage ring lattice permits us to identify the dependence of the dispersion and emittance on our corrector magnets, and taking the singular value decomposition of the Jacobian of the dispersion/corrector matrix gives us the combinations of these magnets which will be effective knobs for emittance tuning, ordered by singular value. These knobs will permit us to empirically tune the emittance based on direct measurements of the vertical beam size. Simulations show that when starting from a lattice with realistic alignment errors which has been corrected by our existing method to have an emittance of a few pm, this new method will enable us to reduce the emittance to nearly the quantum limit, assuming that vertical dispersion is the primary source of our residual emittance.
- SUP004 Measurement of Internal Quality Factor in Cryogenic Copper Accelerators at High Power**
A.D. Cahill, J.B. Rosenzweig (UCLA) **V.A. Dolgashev, S.G. Tantawi** (SLAC)
 Recent SLAC experiments with cryogenically cooled X-band standing wave copper accelerating cavities have shown that these structures can operate with accelerating gradients of ~250 MV/m and low breakdown rates. To better understand what is happening in the copper structure we would like to measure the internal Q factor during a pulse of 1-10 MW of power in an X-Band accelerating structure. This work is to verify previous work measuring Q at low power, and to discover if rf pulse heating will have effects on the internal Q during a single pulse, if there is any time-dependence to the internal Q. These measurements are part of studies with the goal of reaching very high operating accelerating gradients in normal conducting rf structures*.
- SUP005 Magnetic Cloaking of Charged Particle Beams**
K.G. Capobianco-Hogan (SBU)
 In order to measure the momentum of particles produced by asymmetric collisions in the proposed Electron Ion Collider, a magnetic field must be introduced perpendicular to the path of the beam without bending or depolarizing it. A magnetic cloak consisting of a superconducting magnetic shield surrounded by a ferromagnetic layer is capable of shielding the interior from a magnetic field – thereby protecting the beam – without distorting the field outside of the cloak – permitting detector coverage at high pseudorapidity.
- SUP006 Electron Cloud Trapping in Recycler Combined Function Dipole Magnets**
S. A. Antipov (University of Chicago) **S. Nagaitsev** (Fermilab)
 Electron cloud can lead to a fast instability in intense proton and positron beams in circular accelerators. In the Fermilab Recycler the electron cloud is confined within its combined function magnets. We show that combined function magnets trap the electron cloud with their magnetic field, present the results of analytical estimates of trapping, and compare them to numerical simulations of electron cloud formation. The electron cloud in a combined function magnet is located at the beam center and up to 1% of the particles can be trapped by its magnetic field. Since the process of electron cloud build-up is exponential, once trapped this amount of electrons significantly increases the density of the cloud on the next revolution. In a Recycler combined function dipole this multi-turn accumulations allows the electron cloud reaching final intensities orders of magnitude greater than in a pure dipole. The multi-turn build-up can be stopped by injection of a single clearing bunch of 1×10^{10} p at any position in the ring.
- SUP007 6D Phase Space Measurement of Low Energy, High Intensity Hadron Beam**
B.L. Cathey (ORNL RAD)
 The goal of this project is to demonstrate a method for measuring the full 6D phase space of an low energy, high intensity hadron beam. This is done by combining 4D emittance measurement techniques along with dispersion measurement and a beam shape monitor to provide the energy and phase space components. The measurement will be performed on new Beam Testing Facility (BTF) at the Spallation Neutron Source (SNS), a 2.5 MeV functional duplicate of the SNS accelerator front end.

- SUP008 Accelerating Field Enhancement in Superconducting Resonators**
M. Checchin, A. Grassellino, M. Martinello, S. Posen, A. Romanenko (Fermilab) M. Martinello (Illinois Institute of Technology) J. Zasadzinski (IIT)
 Superconducting radio-frequency resonators are limited in terms of accelerating gradient by their superconducting nature. Above the field of first penetration the magnetic field is free to penetrate the superconductor increasing abruptly the dissipation and quenching the superconducting state. Ideally, the field of first penetration corresponds to the superheating field, but experimental evidences suggest that only the so-called 120 C baked cavities can reach fields above the lower critical field. Differently from others treatments, the 120 C bake generates a dirty layer at the surface with thickness comparable to the magnetic field penetration depth. Starting from the Ginzburg-Landau equations, I calculated numerically the energy barrier to the flux penetration in presence of a dirty layer at the surface. Such calculation suggests the energy barrier enhancement due to the dirty layer, explaining why 120 C baked cavities can reach higher fields. By N-doping the superficial layer high quality factor at high accelerating gradients should then be possible.
- SUP009 High Reliability LLRF System for High Beam Current Proton Accelerator**
Q. Chen (IMP/CAS) J.M. Byrd, L.R. Doolittle, G. Huang (LBNL)
 High beam current proton accelerator need a high stability, flexibility, reliability low level radio frequency (LLRF) control system for future manufacture produce. Separated the RF front-ended, AD/DA converter, FPGA digital control board for LLRF control system into three modules. Each module can upgrade independently. With the industry standard connectors, they can design individually. Considering high reliability, imported hardware and software interlock protection, monitoring, protection and redundancy circuits are also designed for cavity and equipment protection. For high accuracy measurements and data acquisition, analog differential signals also be chosen for common noise rejection.
- SUP010 Machine Learning and Artificial Intelligence Based Controls for Particle Accelerators**
A.L. Edelen, S. Biedron, S.V. Milton (CSU) D.L. Bowring, B.E. Chase, J.P. Edelen, J. Steimel (Fermilab)
 Particle accelerators have nonlinear and complex physical phenomena. They involve a multitude of interacting systems, are subject to tight performance demands, and should be able to run for extended periods of time with minimal interruptions. Machine learning and artificial intelligence constitutes a versatile set of techniques that are particularly well-suited to modeling, control, and diagnostic analysis of complex, nonlinear, and time-varying systems, as well as systems with large parameter spaces. Consequently, the use of adaptive, machine learning and artificial intelligence-based modeling and control techniques could be of significant benefit to particle accelerators and the scientific endeavors that they support. Recently, we have developed and tested a set of neural network-based control systems at Fermilab for the PXIE RFQ. The control systems - based on model predictive control and reinforcement learning - regulate the resonant frequency of the RFQ by adjusting the temperature of the water in the wall and vane cooling circuits. Results of our tests and description of the systems are presented herein, along with the results of test cases conducted on various machines.
- SUP011 Demonstration of fresh slice self seeding in a hard X-ray free electron laser**
C. Emma, C. Pellegrini (UCLA) M.W. Guetg, A.A. Lutman, A. Marinelli, T.J. Maxwell, C. Pellegrini, J. Wu (SLAC)
 We discuss the first demonstration of fresh slice self seeding (FSSS) in a hard X-ray Free Electron Laser (XFEL). The FSSS method utilizes a single electron beam to generate a strong seed pulse and amplify it with a small energy spread electron slice. This extends the capability of self seeded XFELs by producing short pulses, not limited by the duration set by the self-seeding monochromator system, with high peak intensity. The scheme relies on using a parallel plate dechirper to impart a spatial chirp on the beam, and appropriate orbit control to lase with different electron beam slices before and after the self-seeding monochromator. The performance of the FSSS method is analyzed with start-to-end simulations for the Linac Coherent Light Source (LCLS). The simulations include the effect of the parallel plate dechirper and propagation of the radiation field through the monochromator. We also present results of the first successful demonstration of FSSS at LCLS. The radiation properties of FSSS X-ray pulses are compared with the Self-Amplified Spontaneous Emission (SASE) mode of FEL operation for the same electron beam parameters.
- SUP012 Dynamics of Intense Beam in Quadrupole-Duodecapole Lattice Near Sixth Order Resonance**
Y.K. Batygin, T.T. Fronk (LANL)
 The presence of duodecapole components in quadrupole focusing field results in excitation of sixth-order single-particle resonance if the phase advance of the particles transverse oscillation is close to 60 deg. This phenomenon results in intensification of beam losses. We present analytical and numerical treatment of particle dynamics in the vicinity of sixth-order resonance. The topology of resonance in phase space is analyzed. Beam emittance growth due to crossing of resonance islands is determined. Halo formation of intense beams in presence of resonance conditions is examined.
- SUP013 Implementing the Fast Multipole Boundary Element Method With High-Order Elements**
A.J. Gee, B. Erdelyi (Northern Illinois University) B. Erdelyi (ANL)
 The next generation of beam applications will require high-intensity beams with unprecedented control. For the new system designs, simulations that model collective effects must achieve greater accuracies and scales than conventional methods allow. The fast multipole method is a strong candidate for modeling collective effects due to its linear scaling. It is well known the boundary effects become important for such intense beams. We implemented a constant element fast boundary element method (FMBEM) * as our first step in studying the boundary effects. To reduce the number of elements and discretization error, our next step is to allow for high-order elements using differential algebraic methods. In this paper we will present the theory and status of the implementation using high-order boundary elements.
- SUP014 Performance of a Combined System Using an X-Ray FEL Oscillator and a High-Gain FEL Amplifier**
L. Gupta (University of Chicago) K.-J. Kim, R.R. Lindberg (ANL)
 The LCLS-II at SLAC will feature a 4 GeV CW superconducting (SC) RF linac [1] that can potentially drive a 5th harmonic X-Ray FEL Oscillator to produce fully coherent, 1 MW photon pulses with a 5 meV bandwidth at 14.4 keV [2]. The XFEL output can serve as the input seed signal for a high-gain FEL amplifier employing fs electron beams from the normal conducting SLAC linac, thereby generating coherent, fs x-ray pulses with ~TW peak powers using a tapered undulator after saturation [3]. Coherent, intense output at several tens of keV will also be feasible if one considers a harmonic generation scheme. Thus, one can potentially reach the 42 keV photon energy required for the MaRIE project [4] by beginning with an XFEL operating at the 5th harmonic to produce 8.4 keV photons using a 3.1 GeV SCRF linac, and then subsequently using the high-gain harmonic generation scheme to generate and amplify the 5th harmonic at 42 keV [5]. We report extensive GINGER simulations that determine an optimized parameter set for the combined system. [1] "Linac Coherent Light Source-II Conceptual Design Report," SLAC-R-978 (2011)

- SUP015 Simple Method for Measuring the Electron-Beam Magnetization**
A. Halavanau, P. Piot (Northern Illinois University) P. Piot (Fermilab)
 There are a number of projects that require magnetized beams for applications, such as electron cooling or aiding in flat beam transforms. Here we explore a simple technique to characterize the magnetization, observed through angular momentum, of magnetized beams. These beams are produced through photoemission, the generating drive laser first passed through a microlens arrays (fly-eye light condensers) to form a transversely modulated pulse incident on the photocathode surface. The resulting charge distribution accelerated from the photocathode, we explore the evolution of the pattern with the relative shearing of the beamlets providing information on the angular momentum. This method is illustrated through numerical simulation and preliminary measurements carried out at the Fermilab Accelerator Science & Technology (FAST) facility are presented.
- SUP016 Search for X-Ray Channeling Radiation at FAST**
P. Hall (Fermilab)
 Channeling Radiation (CR) is generated by charged beams (typically electrons or positrons) passing through a crystal parallel with a crystallographic plane*. Electrons may oscillate perpendicular to the plane and generate CR which propagates in the same direction as the incident beam**. Electron beams with moderate energy ranging from 4 to 50 MeV can be used to produce x-rays through Channeling Radiation. The x-ray spectrum from electron beams extends up to 140 keV, and this range covers the demand for most practical applications***. The beam experiment at the Fermilab Accelerator Science and Technology (FAST) facility will have a beam energy of 50 MeV, and offers the possibility of a precise, tunable X-ray source. This poster will give a brief overview of FAST's channeling radiation experiment, and the progress made in achieving x-ray channeling radiation.
- SUP017 Bench Measurement of a Multifrequency Cavity of the Ultra-fast RF Kicker for ERL Circular Cooler Ring of JLEIC**
Y.L. Huang (IMP/CAS) R.A. Rimmer, H. Wang, S. Wang (JLab)
 An ultra-fast kicker system is being developed for the ERL based electron Circular Cooler Ring (CCR) in the proposed Jefferson Lab Electron Ion Collider (JLEIC, previously named MEIC). In the CCR, the injected electron bunches can be recirculating and performing cooling for 10^{-30} turns before the extraction, thus reducing the ERL beam current to 1/10 - 1/30 (150mA - 50mA) of the cooling beam current (up to 1.5A). Assuming a bunch repetition rate of 476.3MHz and a recirculating factor of 10 in the CCR, the kicker is required to operate at a pulse repetition rate of 47.63MHz with pulse width of around 2ns, so that only every 10th bunch in the CCR will experience the transverse kick while the rest of the bunches won't be disturbed. Such a kicker pulse can be synthesized by 10 harmonic modes of the 47.63MHz kicker pulse repetition frequency, using four quarter wavelength resonator based deflecting cavities. A prototype cavity which could excite 5 odd modes simultaneously was fabricated with copper, and a 3-D bead pull system was built. Bench measurement for the kick scheme, electric center, stub tuner and multipole field was done on the prototype cavity.
- SUP018 Characterization of Laser-Compton X-Rays at LLNL**
Y. Huang, T. Tajima (UCI) G.G. Anderson, C.P.J. Bart, D.J. Gibson, R.A. Marsh (LLNL)
 Laser-Compton X-rays have been produced at LLNL using the unique compact X-band accelerator at LLNL operated in a novel multibunch mode, and results agree very well with modeling predictions. Flux, source size and bandwidth of the 30 keV X-ray beam were measured using an X-ray CCD camera and image plates. K-edge absorption images using thin foils confirm the narrow bandwidth of the source and offer electron beam diagnostics through matched imaging simulation. Future plans for medically relevant imaging will be discussed with facility upgrades to enable 100 keV x-ray production.
- SUP019 Update of the SEY Measurement at Fermilab Main Injector**
Y. Ji (IIT)
 The studies of in-situ Secondary electron yield (SEY) measurement at Main Injector started at 2013. These studies aimed at understand how the conditioning of different materials evolve at Main Injector. The engineering run was finished at 2014. From 2014 to 2016 the Fermilab accelerator intensity has increased from $24 \cdot 10^{12}$ Protons to $42 \cdot 10^{12}$ Protons. The conditioning effect of SS116L and TiN coated SS116L have been observed during such period. A on going process of improving the data acquisition procedure and hardware has been performed. A deconditioning process was observed during the accelerator annual shut down at 2016.
- SUP020 Transverse and Longitudinal Beam Dynamics Studies for an Energy-Recovery Experiment at CEBAF**
P. Korysko, F. Méot, G. Robert-Demolaize (BNL)
 A proposal for a multiple-pass, high energy, energy-recovery experiment using CEBAF is under preparation within a JLab-BNL collaboration. In order to prepare for beam dynamics studies and in addition to the existing Elegant model, a version of the CEBAF lattice is developed for MAD-X. In the following, results from numerical simulations are presented, with the focus being transverse and longitudinal beam dynamics, in particular issues related to the longitudinal matching over the course of multiple-pass tracking.
- SUP021 FEL Wiggler Bussbar Field Compensation**
B. Li, H. Hao, Y.K. Wu (FEL/Duke University) J.Y. Li (USTC/NSRL)
 Abstract The Duke storage ring is a dedicated driver for the storage ring based free-electron laser (FEL) and the High Intensity Gamma-ray Source (HIGS). The high intensity gamma-ray beam is produced using Compton scattering between the electron and FEL photon beams. The beam displacement and angle at the collision point need to be maintained constant in the gamma-ray beam production. The magnetic field of the copper bussbars carrying the current to the FEL wigglers can impact the beam orbit. The compensation scheme ingeneral is complicated. In this work, we report preliminary results of a bussbar compensation scheme for one of the wiggler and power supply configurations. Significant reductions of the orbit distortions have been realized using this compensation.
- SUP022 LCLS Injector Laser Profile Shaping Using Digital Micromirror Device**
S. Li (Stanford University) S.C. Alverson, D.K. Bohler, A.R. Fry, S. Gilevich, Z. Huang, A. Miahnahri, D.F. Ratner, J. Robinson, F. Zhou (SLAC)
 In the Linear Coherent Light Source (LCLS) at SLAC, the injector laser plays an important role as the source of the electron beam for the Free Electron Laser (FEL). The emittance of the beam is highly related to the transverse shape of the injector laser. Currently the LCLS injector laser has hot spots that degrade the FEL performance. The goal of this project is to use adaptive optics to modulate the transverse shape of the injector laser, in order to produce a desired shape of electron beam. With a more controllable electron transverse profile, we can achieve lower emittance for the FEL, improve the FEL performance, and operation reliability. We use a digital micromirror device (DMD) to achieve the laser's transverse profile shaping. In this paper, we demonstrate the experiment set up to shape and transport the beam in the LCLS injector laser lab. We present testing results of the device damage threshold, pulse front tilt correction, and demonstration of beam shaping.

SUP023 Diffusion Measurement From Transverse Echoes**Y.S. Li** (*Carleton College*) **T. Sen** (*Fermilab*)

Beam diffusion is an important measure of stability in high intensity beams. Traditional methods of diffusion characterization (e.g. beam scraping) can be very time-consuming. In this study, we investigated transverse beam echoes as a novel technique for measuring beam diffusion. With aid of both analytical and numerical solutions, we analyzed variations in maximum echo amplitude with and without diffusion. We performed a self-consistent measurement of linear diffusion coefficient via a parameter scan over delay time τ . We also demonstrated the effectiveness of pulsed quadrupoles as a means to boost echo amplitude. Results from this study will support the planned echo experiments in the IOTA proton ring under construction at Fermilab.

SUP024 Future Prospects of RF Hadron Beam Profile Monitors for Intense Neutrino Beam**Q. Liu** (*Case Western Reserve University*) **M. Backfish**, **A. Moretti**, **V. Papadimitriou**, **A.V. Tollestrup**, **K. Yonehara**, **R.M. Zwaska** (*Fermilab*) **M.A.C. Cummings**, **R.P. Johnson**, **G.M. Kazakevich** (*Muons, Inc*) **B.T. Freemire**, **Y. Torun** (*IIT*)

A novel beam monitor based on a gas-filled RF resonator is proposed to measure the precise profile of secondary particles downstream of a target in the LBNF beam line at high intensity. The RF monitor is so simple that it promises to be radiation robust in extremely high-radiation environment. When a charged beam passes through a gas-filled microwave RF cavity, it produces electron-ion pairs in the RF cavity. The induced plasma changes the gas permittivity in proportion to the beam intensity. The permittivity shift can be measured by the modulated RF frequency and quality factor. The beam profile can thus be reconstructed from the signals from individual RF cavity pixels built into the beam profile monitor. A demonstration test is underway, and the current results has shown technical feasibility. The next phase consists of two stages, (1) to build and test a new multi-cell 2.45 GHz RF cavity that can be used for the NuMI beamline, and (2) to build and test a new multi-cell 9.3 GHz RF cavity that can be put in service in a future beamline at the LBNF for spatial resolution. These two resonant frequencies are chosen since they are the standard frequencies for magnetron RF source.

SUP025 Novel Metallic Structures for Wakefield Acceleration**X.Y. Lu**, **M.A. Shapiro**, **R.J. Temkin** (*MIT/PSFC*)

Three novel ideas for wakefield acceleration (WFA) of electrons with metallic periodic subwavelength structures will be presented. The first idea is a deep corrugation structure for collinear WFA. A design for the Argonne Wakefield Accelerator is shown. An analytical model is developed and it agrees with the CST wakefield solver. A scaling study has been performed, and ways to increase the gradient will be discussed. The deep corrugation structure can generate a higher gradient than a dielectric tube with the same beam aperture when excited by the same bunch. The second idea is an elliptical structure for two-beam acceleration (TBA). The unit cell is an elliptical cavity, and the drive beam hole and the witness beam hole are located around the two focal points. The TBA process has been calculated and will be presented. The third idea is a metamaterial ‘wagon wheel’ structure for a power extractor design. The fundamental mode is a TM mode with a negative group velocity. A power extractor at 11.7 GHz based on the structure can reach a GW power level when a train of 40 nC bunches with 1.3 GHz rep rate are sent in.

SUP026 Modulator Simulations for Coherent Electron Cooling**J. Ma** (*SBU*) **V. Litvinenko**, **V. Samulyak**, **G. Wang** (*BNL*) **V. Litvinenko** (*Stony Brook University*) **V. Samulyak** (*SUNY SB*)

Cooling high-energy hadron beams is one of major challenges in modern accelerator physics. Coherent electron cooling (CEC) is a novel technique for rapidly cooling high-energy, high-intensity hadron beams. CEC consists of three sections: a modulator, where the ion imprints a density wake on the electron distribution, an amplifier, where the density wake is amplified, and a kicker, where the amplified wake interacts with the ion, resulting in dynamical friction for the ion. In this work, we perform highly resolved numerical simulations based on modulator, the first section of CEC. SPACE, a 3D electromagnetic particle-in-cell code is used. The beam parameters for simulations are relevant to the Relativistic Heavy Ion Collider (RHIC) at Brookhaven National Laboratory. Kappa-2 velocity distribution is used to model the electron temperature. We calculate the number density modulation and energy modulation of a longitudinal slice of electrons, induced by a single ion. Various moving velocities for ion are studied and compared with theoretical results. Our simulations are consistent with theoretical values in number density modulation and energy modulation.

SUP027 Real-Time Magnetic Electron Energy Spectrometer for Use With Medical Linear Accelerators**P.E. Maggi**, **H.R. Hogstrom**, **K.L. Matthews II** (*LSU*) **R.L. Carver** (*Mary Bird Perkins Cancer Center, Our Lady of the Lake*)

Accelerator characterization and quality assurance is an integral part of electron linear accelerator (linac) use in a medical setting. The current clinical method for radiation metrology of electron beams (dose deposition versus depth in water) only provides a surrogate for the underlying performance of the accelerator, and does not provide direct information about the electron energy spectrum. We have developed an easy to use real-time magnetic electron energy spectrometer for characterizing the electron beams of medical linacs. Our spectrometer uses a 0.54 T permanent magnet block as the dispersive element, and scintillating fibers coupled to a CCD camera as the position sensitive detector. The goal is to have a device capable of 0.3 MeV energy resolution (which corresponds to a range shift of approximately 1 mm), with a minimum readout rate of 1 Hz, over an energy range of 3 to 25 MeV. This work describes the real-time spectrometer system, the detector response model, and the spectrum unfolding method. Measured energy spectra from multiple electron beams are presented.

SUP028 Surface Impurity Content Optimization to Maximize Q-factors of Superconducting Resonators**M. Martinello** (*Fermilab*)

The superconducting properties of niobium RF cavities are enhanced when nitrogen impurities are dissolved as interstitial in the material. In this paper we study how the surface resistance is affected by this impurities introduction, in comparison with standard surface treatment for niobium resonators. A variety of 1.3 GHz cavities with different surface treatments are studied in order to cover a large range of interstitial impurities content: from few to thousand of nanometers of mean free path. Different contributions of the surface resistance are studied in this paper, focusing on the BCS and the trapped flux surface resistance. We found that interstitial impurities help to lower the BCS resistance contribution, allowing to obtain mean free path close to the predicted minimum of BCS resistance as a function of mean free path. Also we found that the trapped flux surface resistance follow a bell-shaped trend as a function of the mean free path. Adding these results together we show that optimal Nitrogen doping (N-doping) treatment allows to maximize Q-factor at 2 K and 16 MV/m as long as the magnetic field fully trapped during the cavity cooldown stays below 10 mG.

SUP029 Emittance Measurements in 112 MHz Superconducting SRF Electron Gun with CsK2Sb Photo-Cathode**K. Mihara** (*Stony Brook University*) **V. Litvinenko**, **I. Pinayev** (*BNL*)

The proof principle experiment to test a coherent electron cooling (CeC) is currently ongoing the commissioning phase. A 112 MHz superconducting radio frequency gun with CsK2Sb photocathode is generating CW electron beam with kinetic energy of 1.2 MeV and charges per bunch from 100 pC to 3 nC. In this paper we present experimental result of beam emittance measurement from our gun at various charges per bunch. We compare these measurements with simulations.

- SUP030 Simulated Measurements of Beam Cooling in Muon Ionization Cooling Experiment**
T.A. Mohayai (IIT) *D.V. Neuffer, D.V. Neuffer, P. Snopok (Fermilab) C.T. Rogers (STFC/RAL/ASTeC) P. Snopok (Illinois Institute of Technology)*
 Cooled muon beams are essential to enable future Neutrino Factory and Muon Collider facilities. The international Muon Ionization Cooling Experiment (MICE) aims to demonstrate muon beam cooling through ionization energy loss in material. A figure of merit for muon beam cooling in MICE is the transverse root-mean-square (RMS) emittance reduction and to measure this, the individual muon positions and momenta are reconstructed using two scintillating-fiber tracking detectors housed in spectrometer solenoid modules. The reconstructed positions and momenta before and after a low-Z absorbing material are then used for constructing the covariance matrix and measuring normalized transverse RMS emittance of MICE muon beam. However, RMS emittance is sensitive to nonlinear effects in beam optics. In this study, the direct measurement of phase-space density as an alternative approach to measuring the muon beam cooling using the novel Kernel Density Estimation (KDE) method, is described.
- SUP031 Benchmark of RF Photoinjector and Beamline in OPAL-T and GPT**
N.R. Neveu (IIT) *G. Ha (POSTECH) G. Ha, J.G. Power (ANL)*
 Accurate simulations of RF photoinjector beamlines is critical to many modern accelerator applications, including SASE FEL light sources and advanced accelerator concepts such as two beam acceleration. These beamlines typically start with an RF photocathode gun and are followed by accelerating structures, bunch compressors, and a variety of magnets. Accurate beam dynamics simulations must include single particle effects (e.g. time step) as well as collective effects such as space charge, wakefields, and coherent synchrotron radiation (CSR). Using portions of the Argonne Wakefield Accelerator as the benchmark model, we simulated beam dynamics using OPAL-T, and GPT for several charge values between 0.1nC and 100nC. In this paper, we present the results, and discuss the similarities or differences between the codes in each case.
- SUP032 Multipacting Behaviour Study for the 112 MHz Superconducting Photo-Electron Gun**
I. Petrushina (SUNY SB)
 Superconducting 112 MHz quarter-wave resonator (QWR) photo-electron gun is used as a source of electron beam for the Coherent electron Cooling experiment (CeC PoP) at BNL. During the CeC commissioning, numerous multipacting zones were encountered in the cavity. It was also observed that introduction of CsK2Sb photocathode creates additional multipacting zone. This paper presents experimental study of the multipactor discharge in the QWR along with possible ways of crossing the multipacting levels. The results of numerical simulations of multipactor discharge are discussed and compared with the experimental data.
- SUP033 S-Band 1.4 Cell Photoinjector Design for High Brightness Beam Generation**
E. Pirez, P. Musumeci (UCLA) *D. Alesini (INFN/LNF) J.M. Maxson (Cornell University)*
 In this paper, we study in detail the design of a novel S-band radiofrequency photogun structure to maximize the accelerating field at the time of injection. This is a critical quantity for electron sources as it directly sets a limit of the maximum brightness achievable. The proposed design is based on a modification of the latest generation of S-band RF photoinjectors including novel fabrication approaches. The gun is designed to operate at a 120MV/m gradient and at an optimal injection phase of 70 degrees providing the beam quality required to enable novel electron beam applications such as single shot time-resolved transmission electron microscopy and ultrafast electron nanodiffraction.
- SUP034 Investigation of Structure and Composition Development in the Two-Step Diffusion Coating of Nb3Sn on Niobium**
U. Pudasaini, M.J. Kelley (The College of William and Mary) *G.V. Eremeev, M.J. Kelley, C.E. Reece (JLab) M.J. Kelley, J. Tuggle (Virginia Polytechnic Institute and State University)*
 The potential for higher operating temperatures and increased accelerating gradient has attracted SRF researchers to Nb3Sn coatings on niobium or other substrates for nearly 50 years. Its seeming simplicity has made the two-step tin vapor diffusion process the leading candidate, despite the almost universal finding of quality factor of coated cavities falling with increasing gradient. We have undertaken a fundamental materials study of the nucleation and deposition steps. Nucleation was accomplished within the usual parameter range: 400oC-500oC, 1-5 hours duration, 5 mg to 1 g SnCl2 and 1-3 g Sn. The resulting deposit consists of a low (< 10%) coverage of micron-sized tin particles by SEM/EDS and a high (> 50%) coverage of few nm thick tin film by XPS and Scanning Auger Microscopy. The crystallography by EBSD and the topography of the substrate by AFM and SEM had no evident effect on the nucleation or the final film.
- SUP035 Thermal Analysis for the Higher Order Mode Waveguide and Fundamental Power Coupler for the 647 MHz Accelerating Cavity for the Electron Ion Collider**
D. Ravikumar, R. Than, C. Xu (BNL)
 The work focuses on the thermal analysis for the cryogenically cooled waveguide for the Higher Order Mode RF energy dampers and Fundamental mode Power Coupler [FPC] for the 647 MHz 5-cell accelerating cavities being proposed for the Electron Ion Collider's Linear Accelerator. We develop a model to execute thermal analysis for the aforementioned waveguide/power coupler using SLAC's multiphysics program ACE3p running on NERSC computing facility or using the ANSYS multiphysics program running on a workstation. The goal would be to complete a thermal design optimized for either a 2 or 3 thermal intercept configuration.
- SUP036 Early Results and Experimental Plans for Single-Channel Strong Octupole Fields at the University of Maryland Electron Ring**
K.J. Ruisard, B. Beaudoin, I. Haber, T.W. Koeth (UMD)
 Nonlinear quasi-integrable optics is a promising development on the horizon of high-intensity ring design. Large amplitude-dependent tune spreads, driven by strong nonlinear magnet inserts, lead to decoupling from incoherent tune resonances. This reduces intensity-driven beam loss while quasi-integrability ensures a well-contained beam. In this paper we discuss on-going work to install and interrogate a long-octupole channel at the University of Maryland Electron Ring (UMER). This is a discrete insert that occupies 20 degrees of the ring, consisting of independently powered printed circuit octupole magnets. Transverse confinement is obtained with quadrupoles external to this insert. Operating UMER as a non-FODO lattice, in order to meet the beam-envelope requirements of the quasi-integrable lattice, is a challenge. We discuss efforts to match the beam and optimize steering solutions. We also discuss our experiences operating a distributed strong octupole lattice.

SUP037 Development of a Fiber Laser for Improving the Pulse Radiolysis System**Y. Saito** (*Waseda University*)

When material is irradiated by the ionizing radiation, short-lived and highly reactive substance intermediate active species are made and then react with substances. The chemical reaction is determined by intermediate active species in early process. Proving the behavior of intermediate active species is important for understanding and controlling radiation chemical reaction. In Waseda university we been developing a Pulse Radiolysis System, a method to measure the behavior of intermediate species, for radiation chemical analysis with RF electron gun. Currently we are developing a Supercontinuum ray(SC ray) as a probe ray to improve Pulse Radiolysis System. We have introduced a SC ray using Yb fiber laser and PCF(Photonic Crystal Fiber). But this type of probe light isn't stable enough in the visible light region. Therefore we started to study Er fiber laser oscillator as new probe ray source. We have succeeded to oscillate a Er fs laser pulse, second harmonic generation and measurement of hydrated electron in ns time resolution. In this presentation we will report current research about generation of SC ray, Er fiber laser system and dose rate effect against the hydrated electron.

SUP038 Impedance Measurement of the Vacuum Chamber Components for the Advance Photon Source (APS) Upgrade**M.P. Sangroula, C.U. Segre** (IIT) **R.R. Lindberg** (ANL)

The Advanced Photon Source (APS) at Argonne National Lab has proposed an upgrade to a multi-bend achromat (MBA) that would improve the x-ray brightness by two to three orders of magnitude. One of the main design challenges of the upgrade is to minimize rf heating and collective instabilities associated with the impedance of the small-aperture vacuum components. As part of this effort, my research focuses on impedance measurement and simulation of various MBA vacuum components. Here, we present our planned measurement technique with some preliminary simulation and measurement results.

SUP039 Application of Accelerators in the Measurement of Reaction Cross-Section Data**M.K. Sharma** (*Aligarh Muslim University, Accelerator Laboratory*)

In recent years there is an interest for development of high-energy and high-current accelerators due to the potential of accelerator-driven sub-critical reactor systems (ADS). The experimental cross-section data is required in the basic research for nuclear reaction mechanism as well as in the applied research for designing the energy generation devices such as the ADS reactors. In ADS systems, a high energy proton beam (GeV) is used to produce spallation neutrons from some heavy target. In such systems, light heavy charged particles such as like ^8Be , ^{12}C , ^{14}N , ^{16}O , ^{19}F etc., are also produced as a result of spallation. As such, information regarding the cross-section for reactions initiated by these particles produced in such devices is required for modeling of the system. In view of the above cross-section data for a large number of reactions produced in $^{12}\text{C}+^{128}\text{Te}$, $^{13}\text{C}+^{159}\text{Tb}$, $^{16}\text{O}+^{159}\text{Tb}$, $^{16}\text{O}+^{169}\text{Tm}$ and $^{16}\text{O}+^{181}\text{Ta}$ systems have been measured. The analysis of data within the framework of statistical model indicates reaction mechanisms such as complete fusion, incomplete fusion, direct reaction and pre-equilibrium emission involved in these systems.

SUP040 Simulation of Beam-Beam Noise Effect in Linac-Ring Scheme eRHIC**K. Shih, Y. Hao** (BNL)

The linac-ring scheme eRHIC promises higher luminosity and versatile upgradability than its ring-ring counterpart. However the fresh electron beam may heat up the ion beam in the ring through beam-beam interaction. The noise effect of the electron beam had been studied theoretically, while detailed simulation is needed to explore the effect beyond linear theories. In this paper, we will present the simulation results of the electron beam noise effect to the ion beam considering the nonlinearity of the beam-beam force and effect of the finite bunch length.

SUP041 Nonlinear Behavior of Multipactor: 3D Simulations**M. Siddiqi, R.A. Kishek** (UMD)

Multipactor is a discharge induced by the impact of electrons on a surface due to radio-frequency (RF) electromagnetic fields and secondary electron emission (SEE). Depending on the impact energy and RF phase of the incident electron, a growth in the electron density is possible. Multipactor can lead to device breakdown in many applications, such as particle accelerator structures and rf systems, satellite communication equipment, and microwave components. Multipactor can also be a precursor for electron cloud effects. Due to the critical need to mitigate multipactor, a more comprehensive theory has been introduced that views multipactor as a global effect that can be analyzed through the concepts of iterative maps and nonlinear dynamics *. In order to test this novel approach, multipactor is simulated in a parallel-plate waveguide using the WARP particle-in-cell code. Different parameters are varied in the simulation to determine the conditions that add to multipactor growth, such as geometry dimensions, electron seeding scenarios, and an applied DC electric field. These computational results and their implications on the further development of this theory will be presented.

SUP042 Design of a High Average Beam-Power SRF Electron Source**N. Sipahi, S. Biedron, S.V. Milton** (CSU) **S. Biedron** (*University of Ljubljana, Faculty of Electrical Engineering*)

There is a significant interest in achieving high-average power electron sources particularly in the area of electron sources integrated with Superconducting Radio Frequency (SRF) systems. For these systems, the electron gun and cathode parts are critical components for stable intensity and high-average powers. In this initial design study, we will present the design of 9-cell accelerator cavity having 1.3-GHz frequency and field optimization studies by comparing simulation results.

SUP043 Wakefield Excitation in Power Extraction Cavity (PEC) of Co-Linear X-Band Energy Booster (CXEB) in Time Domain (T3P) with ACE3P**T. Sipahi, S. Biedron, S.V. Milton** (CSU)

We provide the general concept and the design details of our proposed Co-linear X-band Energy Booster (CXEB) in our previous papers. In addition to that we present more advanced 3D simulations of our system with frequency domain modules Omega3P and S3P of ACE3P code suite in another paper at this conference. In here, using the time domain module T3P of ACE3P we provide the single bunch and multiple bunch wakefield excitations with a symmetric Gaussian bunch distribution and related power extraction mechanism in our traveling wave (TW) X-band power extraction cavity (PEC) are discussed further.

SUP044 Preparation of LCLS-II 1.3 GHz Prototype Cryomodule Testing at Fermilab**K. Sirovattanakul** (*Lehigh University*) **E.R. Harms** (*Fermilab*)

Linac Coherent Light Source II (LCLS-II) is a next generation x-ray free electron laser to be constructed in SLAC National Accelerator Laboratory's existing tunnel. The first prototype 1.3 GHz cryomodule was delivered to Fermilab's Cryomodule Testing Facility (CMTF) from Fermilab's Technical division on July 20, 2016 for testing. In preparation for the testing, we analyze the performance of testing facility's RF system, as well as develop necessary graphical interfaces to monitor the test. Results from test runs using test

loads reveal that complete calibrations for power measurements are still needed for multiple cavities. In the meantime, the direct output from the amplifiers are stable with RMS less than 2 percent. It should be possible to make gradient calculations to within 5-10 percent.

SUP045 **High Efficiency Energy Extraction Results from the Nocibur Experiment**

N.S. Sudar, J.P. Duris, P. Musumeci (UCLA)

We present results from the Nocibur experiment recently performed at Brookhaven National Laboratory's Accelerator Test Facility. Using a 54 cm long strongly tapered undulator to couple a 65 MeV beam to a 200 GW CO₂ laser seed we are able to decelerate 45% of the electrons to a final energy of 35 MeV, extraction 30% of the electron beams initial energy. These results demonstrate a great improvement in electro-optical conversion efficiencies for an electron beam-undulator interaction, serving as an important step in the further development of high peak and average power coherent radiation sources.

SUP046 **Analysis of Microbunching Structures in Transverse and Longitudinal Phase Spaces**

C.-Y. Tsai (Virginia Polytechnic Institute and State University) R. Li (JLab)

Microbunching instability (MBI) has been a challenging issue in high-brightness electron beam transport for modern accelerators. The existing Vlasov analysis of MBI is based on single-pass configuration*. For multi-pass recirculation or a long beamline, the intuitive argument of quantifying MBI, by successive multiplication of MBI gains, was found to underestimate the effect**. More thorough analyses based on concatenation of gain matrices aimed to combine both density and energy modulations for a general beamline**. Yet, quantification still focuses on characterizing longitudinal phase space; microbunching residing in (x,z) or (x',z) was observed in particle tracking simulation. Inclusion of such cross-plane microbunching structures in Vlasov analysis shall be a crucial step to systematically characterize MBI for a beamline complex in terms of concatenating individual beamline segments. We derived a semi-analytical formulation to include the microbunching structures in longitudinal and transverse phase spaces. Having numerically implemented the generalized formulae, an example lattice*** is studied and reasonable agreement achieved when compared with particle tracking simulation.

SUP047 **Proton Beam Defocusing as a Result of Self-Modulation in Plasma**

M. Turner, E. Gschwendtner, A.V. Petrenko (CERN) K.V. Lotov, A. Sosedkin (Budker INP & NSU)

The AWAKE experiment, currently under construction at CERN, will use a 400 GeV/c proton beam with a longitudinal bunch length of $\sigma_z = 12$ cm to create and sustain GV/m plasma wakefields over meters. A 12 cm long bunch can only drive strong wakefields in a plasma with $n_p = 7 \cdot 10^{14}$ atoms/cm³ after the self-modulation instability (SMI) developed, and microbunches -spaced at the plasma wavelength- formed. The fields present during SMI focus and defocus the protons in the transverse plane. By inserting two imaging screens downstream the plasma, we can measure the angle of the defocused protons. Measuring maximum defocusing angles around 1 mrad indirectly proves that SMI developed successfully and that GV/m plasma wakefields were created. In this paper we present numerical studies on how and when the wakefields defocus protons in plasma, the expected measurement results of the two screen diagnostics and the physics we can deduce from it.

SUP048 **Bend Magnet Head Loads and Out of Orbit Scenarios**

T.T. Valicenti, J.A. Carter, K.J. Suthar (ANL)

This paper presents an analytical calculation of the spatial power spectrum emitted from relativistic electrons passing through a series of bend magnets. Using lattice files from the software Elegant, both the ideal and missteered trajectories taken by the beam are considered in determination of the power profile. Calculations were performed for the Advanced Photon Source Upgrade multi-bend-achromat storage-ring. Results were validated with Synrad, a monte-carlo based program designed at CERN. The power distribution and integrated total power values are in agreement with Synrad's results within one percent error. The analytic solution used in this software gives a both quick and accurate tool for calculating the heat load on a photon absorber. The location and orientation can be optimized in order to reduce the peak intensity and thus the maximum thermal stress. This can be used with any optimization or FEA software and gives rise to a versatile set of uses for the developed program.

SUP049 **Planned High Density Material Imaging Experiments Using Relativistic Electron Beam at the Argonne Wakefield Accelerator**

Y.R. Wang (AAI/ANL) M.E. Conde, D.S. Doran, W. Gai, W. Liu, J.G. Power, J.Q. Qiu, C. Whiteford, E.E. Wisniewski (ANL) Z.M. Zhang (IMP/CAS)

A test facility, AWA, has been commissioned and in operation since last year. It can provide beam of several bunches in a train of nano-seconds and 10s of nC with energy up to 70 MeV. In addition, the AWA can accommodate various beamlines for experiments. One of the proposed experiments is to use the AWA beam as a diagnostics for time resolved high density material, typically a target with high Z and time dependent, imaging experiments. When electron beam scatters after passing through the target, and the angular and energy distribution of beam will depend on the density and thickness of the target. A small aperture is used to collimate the scattered electron beam for off axis particles, and the target image will be detected by imaging plate. By measuring the scattered angle and energy at the imaging plate would yield information of the target. In this paper, we will report on the planned experiments setup, which consist of a target, imaging optics and 4 meters of beam transport. The imaging beamline is currently under installation and experiment will be performed soon. This work will have implication on the high energy density physics and even future nuclear fusion studies.

SUP050 **Dynamics of Beams With Canonical Angular Momentum in Non-Axisymmetric Optical Elements**

C.Y. Wong (NSCL) S.M. Lund (FRIB)

Magnetized beams emerging from electron cyclotron resonance (ECR) ion sources have large statistical canonical angular momentum that substantially alters the beam dynamics. This paper examines the single-particle dynamics of such beams in non-axisymmetric lattice elements. The work supports commissioning activities at the FRIB Front End by illustrating how xy projections of the components of a multi-species beam become tilted due to dipoles and quadrupoles, which can complicate charge state selection with slits. The results help guide simulations performed using the PIC code WARP to achieve better optimization of the collimation in the charge selection system (CSS). Beam statistical angular momentum also evolves in the CSS which in turn changes the x- and y-plane emittances. Possible implications of this effect on the final thermalized beam emittances delivered by the Front End are discussed.

SUP051 **Dark Current Simulation of a Standing Wave Disk-Loaded Waveguide Structure at 17 GHz**

H. Xu, B.J. Munroe, M.A. Shapiro, R.J. Temkin (MIT/PSFC)

We present calculations of the dark current in a high gradient accelerator with the intent of understanding its role in breakdown.

The initial source of the dark current is the field emission of electrons from the surfaces where the electric field is maximum. For a 17 GHz single-cell standing wave disk-loaded waveguide structure, the 3-d particle-in-cell simulation shows that only a small portion of the charge emitted is reaching the current monitors at the ends of the structure, while most of the current collides on the structure inner surfaces, causing secondary electron emission. In the simulation, a two-point multipactor process is observed on the side wall of cell due to the low electric field on the surface. The multipactor reaches a steady state within nanoseconds when the electric field is suppressed by the electron cloud formed so that the average secondary electron yield equals to unity. In the steady state when operating at 80 MV/m, the multipactor current on the side wall goes up to 100'1000 A with an average electron energy of around 30 eV. This multipactor current can cause the ionization of the metal material and surface outgassing, leading to breakdown.

SUP052 **FPGA Control in Laser Pulse Stacking**

Y.L. Xu, J.M. Byrd, L.R. Doolittle, Q. Du, G. Huang, R.B. Wilcox, Y. Yang (LBNL)

Laser pulse stacking (LPS) is a new time-domain coherent addition technique that stacking several optical pulses into a single output pulse, enabling high average power and kHz repetition rate. Due to advantages of precise timing and fast processing, FPGA processes digital signals and does feedback control so as to realize the stacking-cavity stabilization. We develop a hardware and firmware design platform to support the laser pulse stacking application. Bias control module for the modulator is implemented to stabilize the bias operating point at the minimum of its transfer function. Cavity control module ensures that each optical cavity is kept at a certain individually-prescribed and stable round-trip phase in this pulse stacking system.

SUP053 **Second Harmonic Generation in Nonlinear Crystal Using Extracted FEL Beam on the Duke Storage Ring**

J. Yan, H. Hao, T. He, S.F. Mikhailov, V. Popov, Y.K. Wu (FEL/Duke University)

A new pulsed FEL operational mode using an rf frequency switching technique is developed for the Duke storage ring FEL system. With this operational mode, the peak FEL power is enhanced by two to three orders of magnitude. Taking advantage of this substantial enhancement of peak FEL power, we have experimentally achieved the second harmonic generation (SHG) in a BBO crystal with an extracted FEL beam around 530 nm. The nonlinear optical effect of the FEL beam in the crystal is investigated in terms of its wavelength tunability and the SHG conversion efficiency. The wavelength dependency of the crystal phase-matching angle is also examined.

SUP054 **Study of the Electrical Center of a Resonant Cavity Beam Position Monitor (RF-BPM) and Its Integration With the a Main Beam Quadrupole for Alignment Purposes**

S. Zorzetti, M. Wendt (CERN) L. Fanucci (Università di Pisa)

To achieve the luminosity goals in a next generation linear collider, acceleration and preservation of ultra-low emittance particle beams is mission critical and requires a precise alignment between the main accelerator components. PACMAN is an innovative doctoral training program, hosted by CERN, with the goal of developing high accuracy metrology and alignment methods and tools to integrate those components in a standalone, automatic test bench. The method will be validated on CLIC components, a proposed Compact Linear Collider currently studied at CERN. The alignment between the electrical center of the Beam Position Monitor (BPM) and the magnetic center of the associated Main Beam Quadrupole (MBQ) is of particular importance to minimize the emittance blow-up, and therefore in the focus of the PACMAN project. The two components have been independently characterized on separated test benches by stretched and vibrating wire techniques. Preliminary conclusions are presented in this paper, with emphasis on the characterization of the electrical center of the BPM.

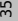
SUP055 **Quantification of Octupole Magnets for the University of Maryland Electron Ring**

H. Baumgartner, B. Beaudoin, I. Haber, T.W. Koeth, D.B. Matthew, K.J. Ruisard, M.R. Teperman (UMD)

The intensity frontier is limited by the ability to propagate substantial amounts of beam current without resulting in particle scrapping and/or losses from resonant growth and halo formation. Modern accelerators are based on the theories developed in the 1950's that assume particle motion is bounded and subject to linear forces. Recent theoretical developments have demonstrated that a strongly nonlinear lattice can be used to stably transport an intense beam has resulted in a fundamental rethinking of the conventional wisdom. A lattice composed of strong nonlinear magnets is predicted by theory to damp resonances while maintaining dynamic aperture. Results of rotating coil measurements, magnetic field scans and simulations will be presented, quantifying the multi-pole moments and fringe fields in the 1st generation Printed Circuit Board (PCB) octupoles for UMER's nonlinear lattice experiments.

MOPL — Conference Opening**Chair:** V.D. Shiltsev (Fermilab)**MOPLI001 Welcome**08:30  **M. White** (ANL)

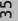
Welcome by Argonne National Laboratory Director, Peter Littlewood

MOPLI002 High Energy Physics as a Global Enterprise: Report from ICHEP XXVIII (Chicago, Aug. 2016)08:45  **Y.K. Kim** (University of Chicago)

Worldwide High Energy Physics goes through revolutionary transformations following the Higgs and neutrino discoveries. This presentation will give an overview of international trends in the HEP, recent results, expectations from the LHC and other facilities and brief report on the ICHEP XXVIII conference (Chicago, Aug. 2016)

MOPLI003 A Billion Times Brighter: An Overview of the Scientific Impact and Future Opportunities of X-Ray Free Electron Lasers09:20  **A.M. Dunne** (SLAC)

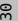
FEL Accelerators : Backbone of Modern Science (status and perspectives)- an overview talk on what FELs do and will do for science, review of facilities, BESAC recommendations, users perspective on them, etc.

MOPLI004 Nuclear Physics at the Electron Ion Collider Plenary09:55  **R. Ent** (JLab) *A. Deshpande (Stony Brook University) R. Milner (MIT)*

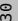
NSAC has recently recommended the EIC as the next large project for the field of nuclear physics. Talk presents a review of relevant nuclear physics to be explored in such a machine.

MOA2 — Oral Presentations (MC6)


Chair: J.M. Byrd (LBNL)

MOA2I001 Towards Attosecond Synchronization in Ultrafast Light Sources11:00  **R.B. Wilcox** (LBNL) *N.J. Evans* (ORNL RAD)

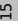
This presentation will report on the latest results of the SNS fast feedback system commissioning and Beam Transfer Function experimental study

MOA2I002 The BNL/LBNL BPM Electronics, High Performance for Next Generation Storage Rings11:30  **K. Vetter** (ORNL) *W.X. Cheng, K. Ha, J. Mead, B. Podobodov* (BNL) *G.J. Portmann* (LBNL)

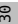
A custom state-of-the-art RF BPM has been developed and commissioned at the Brookhaven National Laboratory (BNL) NSLS-II. A collaboration between Lawrence Berkeley National Laboratory (LBNL) and BNL has been a key driver in the success of the NSLS-II RF BPM which has resulted in a derivative RF BPM recently deployed at the LBNL Advanced Light Source (ALS). High stability coherent signal processing has allowed for demonstrated 200nm RMS spatial resolution and true turn-by-turn position measurement capability. Sub-micron stability has been achieved at BNL by 0.1C thermal regulation of the electronics rack, and by use of a pilot-tone at LBNL. The intentional partitioning of the RF and digital processing into separate boards has resulted in derivative instrumentation platforms including the Cell Controller for the NSLS-II Fast Orbit Feedback computation, an X-ray BPM at NSLS-II, and a CVD diamond beamline BPM incorporating local feedback for photon beam stability control. The systematic design of the NSLS-II RF BPM electronics, measured operational performance at NSLS-II, and derivative Instrumentation will be presented in this paper.

MOA2C003 Measurement of Tune Shift with Amplitude from BPM Data with a Single Kicker Pulse12:00  **Y. Hidaka**, *B. Podobodov* (BNL)

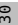
Measurements of amplitude-dependent tune shift are critical to understanding of nonlinear single particle dynamics in storage rings. The standard method involves scanning of the kicker amplitude while having a short bunch train at the flattop area of the kicker pulse. In this paper we present a novel, alternative technique which uses a long bunch train, or a sequence of bunch trains, that are spread along the kicker pulse (including the rising and/or falling edges), such that different bunches experience significantly different kick amplitudes. BPM ADC signals are subsequently processed to separate the bunches with different kick amplitudes, so the entire curve for the tune-shift vs. amplitude is obtained from the data taken on a single kicker pulse. This technique is immune to the pulse-to-pulse kicker jitter and other undesirable effects from machine drifts. This paper describes our measurements with this technique at NSLS-II ring, as well as their comparison to those done using the standard approach.

MOA2C004 MICE Operation and Demonstration of Muon Ionization Cooling12:15  **A. Liu** (Fermilab)


Muon beams of low emittance provide the basis for the intense, well characterised neutrino beams necessary to elucidate the physics of flavour at the Neutrino Factory and to provide lepton-antilepton collisions up to several TeV at the Muon Collider. The international Muon Ionization Cooling Experiment (MICE) will demonstrate muon ionization cooling, the technique proposed to reduce the phase-space volume occupied by the muon beam at such facilities. In an ionization cooling channel, the muon beam traverses a material (the absorber) losing energy, which is replaced using RF cavities. The combined effect is to reduce the transverse emittance of the beam (transverse cooling). The configuration of MICE required to deliver the demonstration of ionization cooling is being prepared in parallel to the execution of a programme of measurement designed to characterise the cooling properties of liquid hydrogen and lithium hydride. The design of the cooling demonstration experiment will be presented together with a summary of the performance of each of its components and the cooling performance of the experiment. The status of the construction project will be summarized.

MOB2 — Oral Presentations (MC1)**Chair:** T.O. Raubenheimer (SLAC)**MOB2I001 Beam Dynamics Issues in Very High Energy Circular p-p Colliders**11:00 **M.J. Syphers** (*Northern Illinois University*) **M.J. Syphers** (*Fermilab*)


Design and beam dynamics issues facing very high energy circular hadron colliders will be explored. Results from past studies and projects within the U.S. will be reviewed as well as recent developments in hadron collider studies being pursued throughout the world, particularly in Europe and Asia.

MOB2I002 Overview of Jefferson Lab EIC Design and R&D11:30 **V.S. Morozov** (*JLab*)

An Electron Ion Collider (EIC) has been identified in the Nuclear Physics Long Range Plan as the priority facility for new construction. This talk presents the overview and status of the Jefferson Lab design of an EIC (JLEIC). It features frequent collisions of small electron and ion bunches providing a luminosity of 10^{33} - 10^{34} cm⁻²s⁻¹ in a broad range of the center-of-mass energy. The small size of ion bunches is maintained against intra-beam scattering by a novel high-energy bunched beam electron cooling system. The figure-8 shape of the electron and all ion rings allows for preservation and ease of manipulation of the electron polarization and the spin of any ion species. The interaction region is designed to accommodate a full-acceptance detector with complete coverage and geometry tagging in the forward and ultra-forward directions. The talk highlights recent progress in the JLEIC accelerator design and various aspects of R&D including the electron and ion complexes, integrated interaction region design, optimization of non-linear dynamics, electron and light ion polarization schemes, RF systems, crab crossing scheme, high-energy electron cooling, and magnet design.

MOB2C003 Collider in the Sea: A New Vision for a 700 TeV World Laboratory12:00 **P.M. McIntyre, J. Breitschopf, J. Gerity, J.N. Kellams, A. Sattarov** (*Texas A&M University*) **S. Assadi** (*HiTek ESE LLC*) **D. Chavez** (*DCI-UG*) **N. Pogue** (*LLNL*)

A design is presented for a hadron collider in which the magnetic storage ring is configured as a circular pipeline, supported in neutral buoyancy in the sea at a depth of ~100 m. Each collider detector is housed in a bathysphere the size of the CMS hall at LHC, also neutral-buoyant. Each half-cell of the collider lattice is ~300 m long, housed in a single pipe that contains one dipole, one quadrupole, a correction package, and all umbilical connections. A choice of ~4 T dipole field, 2000 km circumference provides a collision energy of 700 TeV. Beam dynamics is dominated by synchrotron radiation damping, which sustains luminosity for >10 hours. Issues of radiation shielding and abort can be accommodated inexpensively. There are at least ten sites world-wide where the collider could be located, all near major urban centers. The paper summarizes several key issues; how to connect and disconnect half-cell segments of the pipeline at-depth using remote submersibles; how to maintain the lattice in the required alignment; provisions for the injector sequence.

MOB2C004 Multiphysics Analysis of Crab Cavities for High Luminosity LHC Upgrade12:15 **O. Kononenko, Z. Li** (*SLAC*) **R. Calaga, C. Zaroni** (*CERN*)

Development of superconducting RF crab cavities is one of the major activities under the high luminosity LHC upgrade project that aims to increase the machine discovery potential. The crab cavities will be used for maximizing and leveling the LHC luminosity hence having tight tolerances for the operating voltage and phase. RF field stability in its turn is sensitive to Lorentz force and external loads, so an accurate modeling of these effects is very important. Using the massively parallel ACE3P simulation suite developed at SLAC, we perform a corresponding multiphysics analysis of the electro-mechanical interactions for the baseline cavity designs in order to ensure the operational reliability of the LHC crabbing system.

MOA3 — Oral Presentations (MC6)**Chair:** P.N. Ostroumov (ANL)**MOA3I001 High Energy Coulomb Scattered Electrons Detected in Air Used as the Main Beam Overlap Diagnostics for Tuning the RHIC Electron Lenses**14:00 **P. Thieberger**, Z. Altinbas, C. Carlson, C. Chasman, M.R. Costanzo, C. Degen, K.A. Drees, W. Fischer, D.M. Gassner, X. Gu, K. Hamdi, J. Hock, Y. Luo, A. Marusic, T.A. Miller, M.G. Minty, A.I. Pikin (BNL) S.M. White (ESRF)

A new type of electron-ion beam overlap monitor has been developed for the RHIC electron lenses. Low energy electrons acquire high energies in small impact parameter Coulomb scattering collisions with relativistic ions. Such electrons can traverse thin vacuum windows and be conveniently detected in air. Counting rates are maximized to optimize beam overlap. Operational experience with the electron backscattering detectors during the 2015 p-p RHIC run will be presented. Other possible real-time non-invasive beam-diagnostic applications of high energy Coulomb-scattered electrons will be briefly discussed.

MOA3I002 Precision Vector Control of a Superconducting RF Cavity Driven by an Injection Locked Magnetron14:30 **B.E. Chase** (Fermilab)


The technique presented in this paper enables the regulation of both radio frequency amplitude and phase in narrow band devices such as a Superconducting RF (SRF) cavity driven by constant power output devices i.e. magnetrons. The ability to use low cost high efficiency magnetrons for accelerator RF power systems, with tight vector regulation, presents a substantial cost savings in both construction and operating costs compared to current RF power system technology. An operating CW system at 2.45 GHz has been experimentally developed. Vector control of an injection locked magnetron has been extensively tested and characterized with a SRF cavity as the load. Amplitude dynamic range of 30 dB, amplitude stability of 0.3% r.m.s, and phase stability of 0.26 degrees r.m.s. has been demonstrated.

MOA3C003 The Bunch Shape Monitor Measurements At The LANSCE Linac15:00 **I.N.D. Draganic**, D. Baros, C.M. Fortgang, R.W. Garnett, R.C. McCrady, J.F. O'Hara, L. Rybarczyk (LANL) A. Feschenko, V. Gaidash, Yu. V. Kiselev (RAS/INR)

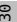
Two Bunch Shape Monitors (BSM) [1] have been developed, fabricated and assembled for the first direct longitudinal beam measurements at the Los Alamos Neutron Science Center (LANSCE) linear accelerator (linac). The BSM detectors use different radio frequencies for the deflecting field: first harmonic (201.25 MHz) and second harmonic (402.5 MHz) of fundamental accelerator radio frequency. The first BSM is designed to record the proton beam longitudinal phase distribution after the new RFQ accelerator at a beam energy of 750 keV with phase resolution of 1.0 degree and covering phase range of 180 degree at 201.25 MHz. The second BSM is installed between DTL tanks 3 and 4 of the LANSCE linac in order to scan both H^+ and H^- beams at a beam energy of 73 MeV with a phase resolution up to 0.5 degree in the phase range of 90 degree at 201.25 MHz. Preliminary results of bunch shape measurements for both beams under different beam gates (pulse length of 150 us, 1 Hz repetition rate, etc.) will be presented and compared high performance simulation results (HPSIM) [2].

MOA3C004 Operational Experience with Fast Fiber-Optic Beam Loss Monitors for the Advanced Photon Source Storage Ring Superconducting Undulators15:15 **J.C. Dooling**, K.C. Harkay, V. Sajaev, H. Shang (ANL)

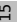
Fast fiber-optic (FFO) beam loss monitors (BLMs) installed with the first two superconducting undulators (SCUs) in the Advanced Photon Source storage ring have proven to be a useful diagnostic for measuring deposited charge (energy) during rapid beam loss events. The first set of FFOBLMs were installed outside the cryostat of the short SCU, a 0.33-m long device, above and below the beam centerline. The second set are mounted with the first 1.1-m-long SCU within the cryostat, on the outboard and inboard sides of the vacuum chamber. The next 1.1-m-long SCU is scheduled to replace the short SCU later in 2016 and will be fitted with FFOBLMs in a manner similar to original 1.1-m device. The FFOBLMs were employed to set timing and voltage for the abort kicker (AK) system. The AK helps to prevent quenching of the SCUs during beam dumps* by directing the beam away from the SC magnet windings. The AK is triggered by the Machine Protection System (MPS). In cases when the AK fails to prevent quenching, the FFOBLMs show that losses often begin before detection by the MPS. We describe the different loss distributions generated by beam dumps as well as injection and fast instabilities.

MOB3 — Oral Presentations (MC1)**Chair:** R. Wichmann (DESY)**MOB3I001 Commissioning of the Phase-I SuperKEKB B-Factory and Update on the Overall Status**14:00  **Y. Ohnishi, Y. Funakoshi (KEK)**


The SuperKEKB B-Factory at KEK (Japan), after few years of shutdown for the construction and renovation, has finally come to the Phase⁻¹ stage with the commissioning of the LER and HER rings, without the Final Focus and Belle detector. In this phase beam scrubbing for vacuum cleaning and optics and backgrounds measurements will be performed. Low emittance tuning techniques will also be applied in order to set up the rings for the Phase-2 with colliding beams next year. An update of the Final Focus doublet system construction, as well as the status of the injection system with the new positron damping ring and high current/low emittance electron gun is also presented.

MOB3I002 LHC Operation at 6.5 TeV : Status and Beam Physics Issues14:30  **G. Papotti, M. Albert, R. Alemany-Fernandez, E. Bravin, G.E. Crookford, K. Fuchsberger, R. Giachino, M. Giovannozzi, G.H. Hemelsoet, W. Höfle, D. Jacquet, M. Lamont, D. Nisbet, L. Normann, M. Pojer, L. Ponce, S. Redaelli, B. Salvachua, M. Solfaroli Camillocci, R. Suykerbuyk, J. Wenninger (CERN)**

Operation of the LHC at record high energy 6.5 TeV and at the design luminosity is a great success and remarkable achievement of the CERN team. This presentation will give a comprehensive overview of the machine status, challenges and plans with particular focus on the beam physics issues.

MOB3C003 RHIC Au-Au Operation at 100 GeV in Run1615:00  **X. Gu, J.G. Alessi, E.N. Beebe, M. Blaskiewicz, J.M. Brennan, K.A. Brown, D. Bruno, J.J. Butler, R. Connolly, T. D'Ottavio, K.A. Drees, W. Fischer, C.J. Gardner, D.M. Gassner, Y. Hao, M. Harvey, T. Hayes, H. Huang, R.L. Hulsart, P.F. Ingrassia, J.P. Jamilkowski, J.S. Laster, V. Litvinenko, C. Liu, Y. Luo, M. Mapes, G.J. Marr, A. Marusic, G.T. McIntyre, K. Mernick, R.J. Michnoff, M.G. Minty, C. Montag, J. Morris, C. Naylor, S. Nemesure, I. Pinayev, V.H. Ranjbar, D. Raparia, G. Robert-Demolaize, T. Roser, P. Sampson, J. Sandberg, V. Schoefer, F. Severino, T.C. Shrey, K.S. Smith, S. Tepikian, R. Than, P. Thieberger, J.E. Tuozzolo, G. Wang, Q. Wu, A. Zaltsman, K. Zeno, S.Y. Zhang, W. Zhang (BNL)**

In order to achieve higher instantaneous and integrated luminosities, the average Au bunch intensity in RHIC has been increased by 30% compared to the preceding Au run. This increase was accomplished by merging bunches in the RHIC injector AGS. Luminosity leveling for one of the two interaction points (IP) with collisions was realized by continuous control of the vertical beam separation. Parallel to RHIC physics operation, the electron beam commissioning of a novel cooling technique with potential application in eRHIC, Coherent electron Cooling as a proof of principle (CeCPoP), was carried out. In addition, a 56 MHz superconducting RF cavity was commissioned and made operational. In this paper we will focus on the RHIC performance during the 2016 Au-Au run.

MOB3C004 High Luminosity 100 TeV Proton-Antiproton Collider15:15  **S.J. Oliveros, J.G. Acosta, L.M. Cremaldi, T.L. Hart, D.J. Summers (UMiss)**

The energy scale for new physics is known to be in the multi-TeV range, signaling the possible need for a collider beyond the LHC energy scale. A $10^{34} \text{ cm}^{-2} \text{ s}^{-1}$ luminosity 100 TeV proton-antiproton collider is explored. Engineering studies for 233 and 270 km circumference tunnels have been done for Illinois dolomite and Texas chalk, respectively. The cross section for many high mass states is 10x higher with antiproton collisions. Antiquarks can come directly from an antiproton rather than gluon splitting. The higher cross sections reduce the synchrotron radiation in superconducting magnets, because lower beam currents can produce the same rare event rates. Increased momentum acceptance ($11 \pm 2.7 \text{ GeV}/c$) in a Fermilab-like antiproton source is used with septa to collect 12x more antiprotons in 12 channels. Because stochastic cooling scales as the number of particles, 12 cooling systems would be used, each with one debuncher/momentum equalizer ring and two accumulator rings. One electron cooling ring would follow. Finally antiprotons would be recycled during runs without leaving the collider ring, by joining them to new bunches with synchrotron damping.

MOA4 — Oral Presentations (MC4)

Chair: Y. Ohnishi (KEK)

MOA4I001 Performance of the Low Charge State Laser Ion Source in BNL16:00 **M. Okamura, J.G. Alessi, E.N. Beebe, M.R. Costanzo, L. DeSanto, S. Ikeda, J.P. Jamilkowski, T. Kanesue, R.F. Lambiase, D. Lehn, C.J. Liaw, D.R. McCafferty, J. Morris, R.H. Olsen, A.I. Pikin, R. Schoepfer, A.N. Steszyn (BNL)**

In March 2014, a Laser Ion Source (LIS) was commissioned which delivers high brightness low charge state heavy ions for the hadron accelerator complex in Brookhaven National Laboratory (BNL). Since then, the LIS has provided many heavy ion species successfully. The induced low charge state (mostly singly charged) beams are injected to the Electron Beam Ion Source (EBIS) where ions are then highly ionized to fit to the following accelerator's Q/M acceptance, like Au^{32+} . Last year, we upgraded the LIS to be able to provide two different beams into EBIS on a pulse-to-pulse basis. Now the LIS is simultaneously providing beams for both the Relativistic Heavy Ion Collider (RHIC) and NASA Space Radiation Laboratory (NSRL). In the conference we present achieved performance and developed new techniques of the LIS.

MOA4I002 Recent Progress in High Intensity Operation of the Fermilab Accelerator Complex16:30 **M.E. Convery, F.G. Garcia, W. Pellico, R.M. Zwaska (Fermilab)**

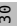
The Proton Improvement Plan is a campaign of upgrades, improvements, and replacements of equipment in the Fermilab Proton Source to enable operation of the machines at higher throughput for an extended period. The Fermilab Proton Source is principally composed of a 400 MeV linac and Booster synchrotron. Now more than half complete, the Fermilab Booster is producing 8 GeV protons at more than twice its previous record rate. Furthermore, this production has been achieved with better reliability and comparable absolute activation as previous running. Several major upgrade to the RF systems, collimation, and beam manipulation have been completed. The remaining upgrades (mostly RF-related) are to improve the operational ability of the Linac and Booster, as well as modernize several original devices.

MOA4C003 Complete Beam Dynamics of the JLEIC Ion Collider Ring Including Imperfections, Corrections, and Detector Solenoid Effects17:00 **G.H. Wei, F. Lin, V.S. Morozov, F.C. Pilat, Y. Zhang (JLab) Y. Nosochkov (SLAC)**

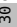
The JLEIC is proposed as a next-generation facility for the study of strong interaction (QCD). Achieving its goal luminosity of up to $10^{34} \text{ cm}^{-2} \text{ s}^{-1}$ requires good dynamical properties and a large dynamic aperture (DA) of $\sim \pm 10$ sigma of the beam size. The limit on the DA comes primarily from non-linear dynamics, element misalignments, magnet multipole components, and detector solenoid effect. This paper presents a complete simulation including all of these effects. We first describe an orbit correction scheme and determine tolerances on element misalignments. And beta beat, betatron tunes, coupling, and linear chromaticity perturbations also be corrected. We next specify the requirements on the multipole components of the interaction region magnets, which dominate the DA in the collision mode. Finally, we take special care of the detector solenoid effects. Some of the complications are an asymmetric design necessary for a full acceptance detector with a crossing angle of 50 mrad. Thus, in addition to coupling, the solenoid causes closed orbit excursion and excites dispersion. It also breaks the figure-8 spin symmetry. We present a scheme with correction of all of these effects.

MOA4C004 Compact Carbon Ion Linac17:15 **P.N. Ostroumov, A. Goel, B. Mustapha, A. Nassiri, A.S. Plastun (ANL) L. Faillace, S.V. Kutsaev, E.A. Savin (RadiaBeam)**

Argonne National Laboratory is developing an Advanced Compact Carbon Ion Linac (ACCIL) in collaboration with RadiaBeam Technologies. The 45-meter long linac is designed to deliver up to 10^9 carbon ions per second with variable energy from 45 MeV/u to 450 MeV/u. To optimize the linac design in this energy range both backward traveling wave and coupled cell standing wave S-band structures were analyzed. To achieve the required accelerating gradients our design uses accelerating structures excited with short RF pulses (~ 500 ns flat-top). The front-end accelerating structures such as the RFQ, DTL and Coupled Cell DTL are designed to operate at lower frequencies to maintain high shunt impedance. In parallel with our design effort ANL's RF test facility has been upgraded and used for the testing of an S-band high-gradient structure designed and built by Radiabeam for high pulsed RF power operation. The 5-cell S-band structure demonstrated 52 MV/m acceleration field at 2 μs 30 Hz RF pulses. A detailed physics design, including a comparison of different accelerating structures and end-to-end beam dynamics simulations of the ACCIL will be presented.

MOB4 — Oral Presentations (MC1)**Chair:** M.A. Palmer (BNL)**MOB4I001 Specifics of Electron Dynamics in High Energy Circular e^+e^- Colliders**16:00  **Q. Qin** (IHEP) *K. Oide* (KEK)


At the energies envisioned for the FCC-ee the synchrotron radiation produces not only closed orbit effects but also some dynamics effects including strong "beta-synchrotron" coupling due to radiation in the final focus quadrupoles. Past experience with LEP and other machines as well as the implications for the new wave of circular electron collider proposals will be discussed.

MOB4I002 Linac-ring and Ring-ring designs for the eRHIC Electron-Ion Collider16:30  **V. Ptitsyn** (BNL)

An overview of the eRHIC project.

MOB4C003 Design of Muon Collider Lattices17:00  **Y.I. Alexahin** (Fermilab)

A Muon Collider promises unique opportunities both as an energy frontier machine and as a factory for detailed study of the Higgs boson and other particles. However, in order to achieve a competitive level of luminosity a number of demanding requirements to the collider optics should be satisfied arising from short muon lifetime and relatively large values of the transverse emittance and momentum spread in muon beams that can realistically be obtained with ionization cooling. Basic solutions which make possible to achieve these goals with Nb3Sn magnet parameters are presented.

MOB4C004 Design of the Room-Temperature Front-End for a Multi-Ion Linac Injector17:15  **A.S. Plastun**, *Z.A. Conway*, *B. Mustapha*, *P.N. Ostroumov* (ANL)

A pulsed multi-ion injector linac is being developed by ANL for Jefferson Laboratory's Electron-Ion Collider (JLEIC). The linac is designed to deliver both polarized and non-polarized ion beams to the booster synchrotron at energies ranging from 135 MeV for hydrogen to 43 MeV/u for lead ions. The linac is composed from a 5 MeV/u fixed velocity room temperature section and a superconducting section with variable velocity profile for different ion species. This paper presents the results of the RF design of the main components and the beam dynamics simulations of the linac with the goal of achieving design specifications at low cost.

MOPOB — Poster Session (MC7)

- MOP0B01 Copper Accelerating Structure Fabrication With Controlled Cu-Ag Joining Conditions**
V. Danielyan, V.S. Avagyan, S.G. Dekhtiarov, A.S. Simonyan (CANDLE SRI)
 The paper is devoted to the development of technological processes of copper accelerating structures fabrication from oxygen-free copper. The experimental set-up for vacuum brazing of long accelerating structures with optimal Cu-Ag joining conditions is described. The experimental results of precise machining and subsequent vacuum brazing of Ag-Cu eutectic are presented.
- MOP0B02 The Electromagnetic Design of a 352.2 MHz RFQ for Proton Accelerator**
C.C. Motta (USP)
 The electromagnetic design of a 352.2 MHz Radio Frequency Quadrupole (RFQ) accelerator has been done for the low energy part of GeV energy proton accelerator, which will accelerate a pulsed proton beam with 10 mA peak current from 50 keV to 2.5 MeV kinetic energy. Three-dimensional cavity studies are performed using computer codes of Ansoft High Frequency Structure Simulator (HFSS) and CST Microwave Studio (MWS). Details of the resonator such as input and output radial matches have been determined as well the vane tips and tuners. The results from both codes have also been compared.
- MOP0B03 Optical Enhancement Cavity Development for Laser-Compton X-Ray Sources**
K. Sakaue (RISE) S. Araki, M.K. Fukuda, Y. Honda, N. Terunuma, J. Urakawa (KEK) M. Washio (Waseda University)
 We have been developing an optical enhancement cavity for laser-Compton X-ray sources as a photon target. The optical enhancement cavity can enhance the laser power in side the cavity more than 100 times regarding with finesse of the cavity. We built bow-tie type 4-mirrors cavity for laser-Compton scattering and invented "burst mode" technique for normal conducting linac based source. The burst mode is a technique using pulsed burst amplifier for injecting laser and temporally increase the laser power at the electron beam timing. In this conference, we will report the introduction of burst mode optical enhancement cavity, recent results of our optical cavity development and future prospective.
- MOP0B04 Design Study of Permanent Magnet Focusing System for Klystrons**
Y. Fuwa, Y. Iwashita (Kyoto ICR)
 Klystron beam focusing system with permanent magnets can reduce power consumption and increase reliability of RF system. Design method of the focusing system and the results of beam simulation with the designed focusing system will be presented.
- MOP0B05 Tokamak Accelerator**
G. Li (ASIPP)
 Tokamak accelerator within plasma is analyzed to be implemented in existing machines for speeding the development of fusion energy with seeding fast particles from high current accelerators - the so-called two-component reactor approach [J. M. Dawson, H. P. Furth, and F. H. Tenney, Phys. Rev. Lett. 26, 1156 (1971)]. All plasma particles are heated at the same time by inductively-coupled power transfer (IPT) within an energy confinement time. This could facilitate the attainment of ignition in tokamak by forming high-gain high-field (HGHF) fusion plasma suggested in [Li. G., Sci. Rep.5, 15790 (2015)]. HGHF mechanism is validated by the flux-conserving process existed in discharges of tokamak plasma at normal operation with long pulses or at compression process within an energy confinement time. Differences between HGHF plasma and former unity-beta plasma are discussed. Tokamak as an accelerator could scale down the design capacity of fusion power plant by simply inserting in-vacuum vertical field coils (IVC) within its vacuum vessel, such as China Fusion Engineering Test Reactor (CFETR).
- MOP0B06 MAX IV and Solaris Linac Magnets Production Series Measurement Results**
M.A.G. Johansson (MAX IV Laboratory, Lund University) K. Karaś (Solaris National Synchrotron Radiation Centre, Jagiellonian University) R. Nietubyć (NCBJ)
 The linacs of the MAX IV and Solaris synchrotron radiation light sources, currently in operation in Lund, Sweden, and Kraków, Poland, use various conventional magnet designs. The production series of totally more than 100 magnets of more than 10 types or variants, which were all outsourced to industry, with combined orders for the types that are common to both MAX IV and Solaris, were completed in 2013 with mechanical and magnetic QA conforming to specifications. This article presents an overview of the different magnet types installed in these machines, and mechanical and magnetic measurement results of the full production series.
- MOP0B07 Off-Orbit Ray Tracing Analysis for the APS-Upgrade Storage Ring Vacuum System**
J.A. Carter, K.C. Harkay, B.K. Stillwell (ANL)
 A numerical method has been developed to maximize photon absorber apertures in the APS-Upgrade storage ring vacuum system design. Synchrotron radiation rays are computed from discretized beam orbit phase space ellipses along the bending magnet paths. The local, extreme phase space ellipses are determined from both expected multi-bend achromat (MBA) lattice parameters and the limiting physical apertures in the future storage ring. Rays are then projected along the horizontal plane and tracked from each point in the discretized ellipse to the locations of downstream absorbers where the shadow they cast towards critical components is evaluated. The absorber apertures are then maximized based on their ability to protect downstream components from all possible rays. The numerical method is conservative as worst case alignment tolerances are added to the global locations of the absorbers and protection limits prior to the projection of synchrotron rays. The ray tracing in the horizontal plane has been verified using geometric construction in a CAD application. Future plans include extending the calculations to include beam trajectories outside of the horizontal plane.
- MOP0B08 Streak Camera Measurements of the APS PC Gun Drive Laser**
J.C. Dooling (ANL) A.H. Lumpkin (Fermilab)
 We report recent pulse-duration measurements of the APS PC Gun drive laser at both second harmonic (SH, 527 nm) and fourth harmonic (FH, 263 nm) wavelengths. The drive laser is a Nd:Glass-based CPA with the IR wavelength (10^{53} nm) twice doubled to obtain UV output for the gun. Pulse-duration data are necessary to characterize the initial photoelectron bunch length for beam dynamics simulations. A Hamamatsu C5680 streak camera and an M5675 synchroscan unit are used for these measurements; the synchroscan unit is tuned to 119 MHz, the 24th subharmonic of the linac operating frequency. Calibration is accomplished both electronically and optically. Electronic calibration utilizes a programmable delay line in the 119 MHz rf path. The optical delay employs an etalon with known spacing between reflecting surfaces; this etalon is coated for the visible, SH wavelength. IR pulse duration is varied with achievable compressor length and monitored with an autocorrelator. Fitting the streak camera image projected profiles with Gaussians, UV rms pulse durations are found to vary from 2.1 ps to 3.5 ps as the IR varies from 2.2 ps to 5.2 ps. Calibration and pulse-duration data will be reported.

- MOP0B09 Thermal and RF Tests of Beamline Higher Order Mode Absorber for APS Upgrade Higher Harmonic Cavity**
S.H. Kim (ANL)
 A superconducting 1.4 GHz (4th harmonic) single-cell cavity is being developed for bunch lengthening in the Advanced Photon Source Upgrade. Higher order modes (HOM) excited by the average 200 mA beam with 15.3 nC max bunch charge and ~50 ps bunch length are damped by a pair of the graphite-direct-sintered silicon carbide (SiC) HOM absorbers located in the room temperature beamline. We measured thermal and RF properties of the finished SiC absorber assemblies. In this talk, we will discuss cooling capacity and HOM damping efficiency.
- MOP0B10 Design of the HGVPV Undulator Vacuum Chamber for LCLS-II**
J.E. Lerch, J.A. Carter, P.K. Den Hartog, G.E. Wiemerslage (ANL)
 A vacuum chamber has been designed and prototyped for the new Horizontal Gap Vertically Polarization Undulator (HGVPV) as part of the LCLS-II upgrade project. Numerous functional requirements for the HGVPV assembly constrained the vacuum chamber design. These constraints included spatial restrictions to achieve small magnet gaps, narrow temperature and alignment specifications, and minimization of wall erosion and pressure drop within the cooling channels. This led to the design of a 3.5-meter length, thin walled, extruded aluminium chamber with interior water cooling. FEA stress analysis was performed to ensure the chamber will not fail under vacuum and water pressure. A cooling scheme was optimized to ensure water flow is sufficient to maintain temperature without the risk of erosion and to minimize pressure drop across the chamber.
- MOP0B11 Research and Development on the Storage Ring Vacuum System for the Advanced Photon Source Upgrade Project**
B.K. Stillwell, B. Brajuskovic, J.A. Carter, H. Cease, J.E. Hoyt, R.M. Lill, R.R. Lindberg, J. R. Noonan, K.J. Suthar, G.E. Wiemerslage, J. Zientek (ANL) M.P. Sangroula (IIT)
 A number of research and development activities are underway at the Advanced Photon Source (APS) to build confidence in the designs for the new storage ring vacuum system required for the Advanced Photon Source Upgrade project (APS-U). The predominant technical risks are: excessive residual gas pressures during operation; excessive heating by induced electrical surface currents; excessive beam impedances; insufficient beam position monitor stability; and insufficient operational reliability. Efforts planned or in progress to mitigate these risks include: a variety of computer simulations, building and studying a full-sector mockup of the vacuum system; mechanical testing of flanges and weld joints needed to attach flanges to chambers; electrical bench measurements of rf liners and beam position monitors; and testing with APS stored beam. Status of these activities and what has been learned to date will be shared.
- MOP0B12 A High Bandwidth Bipolar Power Supply for the Fast Correctors in the APS Upgrade**
J. Wang, G.S. Sprau (ANL)
 The APS Upgrade of a multi-bend achromat (MBA) storage ring requires a fast bipolar power supply for the fast correction magnets. The key performance requirement of the power supply includes a small-signal bandwidth of 10 kHz for the output current. This requirement presents a challenge to the design because of the high inductance of the magnet load and a limited input DC voltage. A prototype DC/DC power supply utilizing a MOSFET H-bridge circuit with a 500 kHz PWM has been developed and tested successfully. The prototype achieved a 10-kHz bandwidth with less than 3-dB attenuation for a signal 0.5% of the maximum operating current of 15 amperes. This paper presents the design of the power circuit, the PWM method, the control loop, and the test results.
- MOP0B13 Post Irradiation Examination Results of the NT-02 Graphite Fins Numi Target**
K. Ammigan, P. Hurh, R.M. Zwaska (Fermilab) D. Asner, A.M. Casella, D.J. Senor (PNNL)
 The NT-02 neutrino target in the NuMI beamline at Fermilab is a 95 cm long target made up of segmented graphite fins. It is the longest running NuMI target, which operated with a 120 GeV proton beam with maximum power of 340 kW, and saw an integrated total proton on target of 6.1×10^{20} . Over the last half of its life, gradual degradation of neutrino yield was observed until the target was replaced. The probable causes for the target performance degradation are attributed to radiation damage, possibly including cracking caused by reduction in thermal shock resistance, as well as potential localized oxidation in the heated region of the target. Understanding the long-term structural response of target materials exposed to proton irradiation is critical as future proton accelerator sources are becoming increasingly more powerful. As a result, an autopsy of the target was carried out to facilitate post-irradiation examination of selected graphite fins. Advanced microstructural imaging and surface elemental analysis techniques were used to characterize the condition of the fins in an effort to identify degradation mechanisms, and the relevant findings are presented in this paper.
- MOP0B14 Experimental Results of Beryllium Exposed to Intense High Energy Proton Beam Pulses**
K. Ammigan, B.D. Hartsell, P. Hurh, R.M. Zwaska (Fermilab) A.R. Atherton (STFC/RAL/ASTeC) M.E.J. Butcher, M. Calviani, M. Guinchard, R. Losito (CERN) O. Caretta, T.R. Davenne, C.J. Densham, M.D. Fitton, P. Loveridge, J. O'Dell (STFC/RAL) V.I. Kuksenkov, S.G. Roberts (University of Oxford) S.G. Roberts (CCFE)
 Beryllium is extensively used in various accelerator beam lines and target facilities as material for beam windows, and to a lesser extent, as secondary particle production targets. With increasing beam intensities of future accelerator facilities, it is critical to understand the response of beryllium under extreme conditions to reliably operate these components as well as avoid compromising particle production efficiency by limiting beam parameters. As a result, an exploratory experiment at CERN's HiRadMat facility was carried out to take advantage of the test facility's tunable high intensity proton beam to probe and investigate the damage mechanisms of several beryllium grades. The test matrix consisted of multiple arrays of thin discs of varying thicknesses as well as cylinders, each exposed to increasing beam intensities. This paper outlines the experimental measurements, as well as findings from Post-Irradiation-Examination (PIE) work where different imaging techniques were used to analyze and compare surface evolution and microstructural response of the test matrix specimens.
- MOP0B15 Electromagnetic Design of Variable Couplers for Testing SRF Cavities**
M.H. Awida, T.N. Khabiboulline (Fermilab)
 Superconducting RF cavities are the corner-stones for building modern particle accelerator machines. Testing SRF cavities is typically done under critical coupling condition on a vertical test stand. Critical coupling is favored in order to reduce the error margins in predicting the quality factor of cavities. Fixed couplers will allow fulfilling the critical coupling condition at only one temperature, while variable couplers offer the advantage of being flexible and can be adjusted during test at various temperatures. In this paper, we present the electromagnetic design of several variable couplers fitted to test various SRF cavities at Fermilab, demonstrating the advantage of using variable coupler, and giving guidelines on how to increase the effective Qext range the coupler.

- MOP0B16 Higher Order Mode Analysis of Fermilab's Recycler Cavity**
M.H. Awida, T.N. Khabiboulline (Fermilab)
 Two recycler cavities are being employed in Fermilab's recycler ring for the purpose of performing slip stacking on the proton bunches, where 6 batches of 8 GeV protons coming from the booster are stacked on top of an additional 6 batches. Slip stacking requires two RF cavities operating at 52.809 and 51.545 MHz. In this paper, we report on the performance of higher order modes inside the recycler cavity, presenting the values for R/Q and shunt impedances. Higher order modes are particularly critical for beam physics and beam instabilities.
- MOP0B17 Resonance Control of Fermilab's PIP-II Injector Test RFQ in Pulsed and CW Modes**
A.L. Edelen, S. Biedron, S.V. Milton (CSU) S. Biedron (University of Ljubljana, Faculty of Electrical Engineering) , D.L. Bowring, B.E. Chase, J.P. Edelen, J. Steimel (Fermilab)
 The RFQ for Fermilab's PIP-II Injector Test program is designed to accelerate a ≤ 10 mA H^- CW beam to 2.1 MeV. The RFQ has a four-vane design, with four modules brazed together for a total of 4.45 m in length. The RF power required is ≤ 130 kW at 162.5 MHz. A 3 kHz limit on the maximum allowable frequency error is imposed by the RF amplifiers. However, as the design does not allow for dynamic tuning, this frequency constraint must be managed entirely through differential cooling of the RFQ's vanes and outer body and associated material expansion. Simulations indicate that the body and vane coolant temperature should be controlled to within 0.1 degrees C. We present the design of the cooling network and the resonant control algorithm for this structure, as well as results from operation in pulsed and in CW mode.
- MOP0B19 Theoretical Dependence of the Vortexes Surface Impedance on the Mean Free Path**
M. Checchin, A. Grassellino, M. Martinello, A. Romanenko (Fermilab) M. Martinello (Illinois Institute of Technology) J. Zasadzinski (IIT)
 One of the main quality factor limitation in SRF cavities is the presence of trapped flux. Magnetic vortexes introduce extra dissipation by their interaction with the time dependent RF currents in the cavity. The model presented explains the dependence of such extra dissipation on the electronic mean free path of the material, increasing the understanding of such dissipation mechanism.
- MOP0B20 Accelerating Field Enhancement in Superconducting Resonators**
M. Checchin, A. Grassellino, M. Martinello, S. Posen, A. Romanenko (Fermilab) M. Martinello (Illinois Institute of Technology) J. Zasadzinski (IIT)
 Superconducting radio-frequency resonators are limited in terms of accelerating gradient by their superconducting nature. Above the field of first penetration the magnetic field is free to penetrate the superconductor increasing abruptly the dissipation and quenching the superconducting state. Ideally, the field of first penetration corresponds to the superheating field, but experimental evidences suggest that only the so-called 120 C baked cavities can reach fields above the lower critical field. Differently from others treatments, the 120 C bake generates a dirty layer at the surface with thickness comparable to the magnetic field penetration depth. Starting from the Ginzburg-Landau equations, I calculated numerically the energy barrier to the flux penetration in presence of a dirty layer at the surface. Such calculation suggests the energy barrier enhancement due to the dirty layer, explaining why 120 C baked cavities can reach higher fields. By N-doping the superficial layer high quality factor at high accelerating gradients should then be possible.
- MOP0B22 Fast Kickers Magnets: Production, Testing and Results**
L. Elementi (Fermilab)
 Fermilab Magnet System has manufactured 18 kicker magnets with 50 Ω impedance and 13 kicker magnets with 25 Ω impedance to be used for the Recycler and Main Injector as part of the NOvA experiments. The 50 Ω kicker magnets required a rise and the fall of the full strength fields in a less than 57 ns and a tight control on the impedance variation to maintain field flatness. These magnets use Sylgard® impregnation which provides the dielectric media for the high voltage capacitors. We have done extensive and precise measurements during productions pre and post potting. Some production methodologies, and the results and statistics of this particular production are herein presented and analyzed.
- MOP0B23 The Radiation Damage In Accelerator Target Environments (RaDIATE) Collaboration R&D Program - Status and Future Activities**
P. Hurh (Fermilab)
 The RaDIATE collaboration (Radiation Damage In Accelerator Target Environments), founded in 2012, has grown to over 50 participants and 11 institutions globally. The primary objective is to harness existing expertise in nuclear materials and accelerator targets to generate new and useful materials data for application within the accelerator and fission/fusion communities. Current activities include post-irradiation examination of materials taken from existing beamlines (such as the NuMI primary beam window from Fermilab) as well as new irradiations of candidate target materials at low energy and high energy beam facilities. In addition, the program includes thermal shock experiments utilizing high intensity proton beam pulses available at the HiRadMat facility at CERN. Status of current RaDIATE activities as well as future plans will be discussed, including special focus on the upcoming RaDIATE irradiation at the Brookhaven Linac Isotope Producer facility (BLIP) in which multiple materials of interest (e.g. beryllium, graphite, silicon, titanium, iridium) will simultaneously be exposed to 120 - 181 MeV proton beam to relevant radiation damage levels.
- MOP0B24 Design of Main Coupler for 650 MHz SC Cavities of PIP-II Project**
S. Kazakov, O.V. Pronitchchev (Fermilab)
 New design of 650 MHz main couplers for superconducting elliptical cavities is presented. Electrical, thermal parameters and mechanical design are reported.
- MOP0B25 The Use of KF Style Flanges in Particle Free Applications**
K.R. Kendziora, J.J. Angelo, C.M. Baffes, D. Franck, R.J. Kellett (Fermilab)
 As SCRF particle accelerator technology advances the need for 'low particulate' and 'particle free' vacuum systems becomes greater and greater. In the course of the operation of these systems there comes a time when various instruments have to be temporarily attached for diagnostic purposes, RGAs, leak detectors, and additional pumps for example. In an effort to make the additions of these instruments easier and more time effective, we propose to use KF style flanges for these types of temporary diagnostic connections. This document will describe the tests used to compare the particles generated during the assembly of the, widely accepted for 'particle free' use, conflat flange to the proposed KF style flange.

MOP0B26 Study of RF Breakdown in 805MHz Pillbox Modular Cavity in Strong Magnetic Field**A.V. Kochemirovskiy (Fermilab)**

RF breakdown has a negative impact on a cavity's performance, especially with the presence of strong magnetic fields. As a part of MTA program at Fermilab, we have tested an 805MHz pillbox "modular" cavity in strong external magnetic fields. Modular structure of the cavity allows for better control over sources of systematic error and enables easy dismounting of flat walls to perform inspection of inner surfaces after each run as well as swapping them to study the effects of various materials on breakdown phenomenon. Results and analysis from high-power test of modular cavity with copper and beryllium flat walls in zero and 3 tesla external magnetic fields will be presented. Surface inspections were performed after each run to track the correlation between damage forming processes and run conditions. Observed variance in damage characteristics between $B=0T$ and $B=3T$ runs indicates different energy deposition mechanisms. Inspection after 3 tesla run revealed near perfect one-to-one correspondence between the breakdown pits on the opposing flat walls which supports our model of breakdown being induced by focused emission currents inside the cavity.

MOP0B27 Superconducting Coil Winding Machine Control System**J.M. Nogiec, S. Kotelnikov, A. Makulski, K. Trombly-Freytag, D.G.C. Walbridge (Fermilab)**

The Spirex magnet coil winder has been equipped with an automation system, which allows operation from both a computer and a remote control unit. This machine is about 6m long with a bridge that moves along a track and supports a rotating boom holding a spool of cable and providing cable tension. The machine control system is distributed between three layers: PC, RTOS, and FPGA providing respectively HMI, operational logic and controls. The PC stores the history of operation, shows the machine positions, status, and their history. Keeping cable tension constant is non-trivial in situations where the length of the cable changes with varying speeds. This has been addressed by a PID controller with feed forward augmentation and low-pass filters. Another challenging problem, synchronizing multiple servo motors, has been solved by designing an innovative decentralized algorithm. Extra attention was given to the safety aspects; a fail-safe, redundant safety system with interlocks has been developed, including protection for the operator and the superconducting cable against such situations as accidental over tension, or fast movement of the cable due to operational errors.

MOP0B28 Progress on the Design of a Perpendicular Biased 2nd Harmonic Cavity for the Fermilab Booster**R.L. Madrak, J.E. Dey, K.L. Duel, J. Kuharik, W. Pellico, J. Reid, G.V. Romanov, M. Slabaugh, D. Sun, C.-Y. Tan, I. Terechkine (Fermilab)**

A perpendicular biased 2nd harmonic cavity is being designed and built for the Fermilab Booster. Its purpose is to flatten the bucket at injection and thus change the longitudinal beam distribution to decrease space charge effects. It can also help with transition crossing. The cavity frequency range is $76 - 10^6$ MHz. It is modeled using CST microwave studio and COMSOL. The power amplifier will use the same tetrode as is used for the fundamental mode cavities in the Fermilab Booster (Y567B). We discuss recent progress on the cavity design, plans for testing the tuner's garnet material, and tests of the power source.

MOP0B29 Measurements of the Properties of Garnet Material for Tuning a 2nd Harmonic Cavity for the Fermilab Booster**R.L. Madrak, W. Pellico, G.V. Romanov, C.-Y. Tan, I. Terechkine (Fermilab)**

A perpendicular biased 2nd harmonic cavity is being designed and built for the Fermilab Booster, to help with injection and transition. The frequency range is $76 - 10^6$ MHz. The garnet material chosen for the tuner is AL800. To reliably model the cavity, its static permeability and loss tangent must be well known. We present our measurements of these properties.

MOP0B30 Development and Comparison of Mechanical Structures for Fermilab's 15 T Nb3Sn Dipole Demonstrator**A.V. Zlobin, I. Novitski (Fermilab)**

Nb3Sn magnets with a nominal operation field of 15-16 T are being considered for the LHC energy upgrade (HE-LHC) and a post-LHC Very High Energy pp Collider (VHEppC). To demonstrate feasibility of 15 T accelerator quality magnets, Fermilab has started the development of a single-aperture Nb3Sn dipole based on a 4-layer graded cos-theta coil with 60 mm aperture and cold iron yoke. Main design challenges for 15 T accelerator magnets include large Lorentz forces at this field level. The large Lorentz forces generate high stresses in the coil and mechanical structure and, thus, need stress control to maintain them below 150 MPa, which is acceptable for brittle Nb3Sn coils. To provide these conditions and achieve the design field in the Fermilab's dipole demonstrator, several mechanical structures have been developed and analyzed. The possibilities and limitations of these designs are discussed in this paper.

MOP0B31 Flanged Joints for Ultra High Vacuum using Aluminum Ring Sealings**M. Parise (Fermilab)**

In order to develop an assembling procedure, that guarantees the sealing of the SSR1 spoke resonator flanges both at room and cryogenic temperature, an experimental characterization of the custom hardware is required. The sealing is obtained through a aluminum ring with an hexagonal cross section flattened using herculoy silicon bronze set screws, stainless steel hex nuts and washers. The characterization is aimed at the determination of an optimal value for the maximum torque applied at the nuts to obtain an ultra high vacuum (UHV) leak tight connection with cleaned hardware and flanges.

MOP0B32 Design and Test of the Prototype Tuner for 3.9GHz SRF Cavity for LCLS II Project**Y.M. Pischalnikov, E. Borissov, J.P. Holzbauer, J.C. Yun (Fermilab)**

Fermilab is responsible for the design of the 3.9GHz cryomodule for the LCLS-II that will operate in continuous wave (CW) mode. Bandwidth of the SRF cavities will be in the range of the XXX. In our tuner design, we adopted as the slow tuner-mechanism slim blade tuner originated by INFN for the European XFEL 3.9GHz. At the same time bandwidth of the SRF cavities for LCLS II will be in the range of the 130Hz and fine/fast tuning of the cavity frequency required. We added to the design fast/fine tuner made with 2 encapsulated piezos. First prototype tuner has been built and went through testing at warm conditions. Details of the design and summary of the tests will be presented in this paper.

MOP0B33 LCLS-II Tuner Assembly for the Prototype Cryomodule at FNAL**Y.M. Pischalnikov, E. Borissov, J.P. Holzbauer, T.N. Khabiboulline, J.C. Yun (Fermilab)**

The tuner design for LCLS-II has been thoroughly verified and fabricated for used in the LCLS-II prototype modules. This paper will present the lessons learned during the installation of these tuners for the prototype modules at FNAL, including installation procedures, best practices, and challenges encountered.

MOP0B34 Mitigating Q0 Degradation in SRF Cavities Through Improved Flux Expulsion**S. Posen, M. Checchin, A.C. Crawford, A. Grassellino, M. Martinello, O.S. Melnychuk, A. Romanenko, D.A. Sergatskov,**

Y. Trenikhina (Fermilab)

For particle accelerators with a substantial dynamic cryogenic heat load from superconducting RF cavities, Q0 optimization is critical to save on cryogenic infrastructure and operational costs. Achieving high Q0 in vertical qualification tests is important, but this Q0 must be achieved also in the cryomodule, which can have much higher background magnetic fields than the vertical test dewar. In this contribution, we demonstrate the impact on Q0 when these remnant fields are trapped in the superconductor during cooldown. We also present new results from a method to prevent degradation by improving the tendency of the superconducting material to expel flux through furnace treatment. Recommended heat treatment recipes for cavities in high Q0 cryomodules are presented.

MOP0B35 **Design of the LBNF Beamline Target Station**

S. Tariq, K. Ammigan, K. Anderson, C.F. Crowley, B.D. Hartsell, P. Hurh, J. Hysten, P.H. Kasper, G.E. Krafczyk, A. Lee, B.G. Lundberg, A. Marchionni, N.V. Mokhov, C.D. Moore, V. Papadimitriou, D. Pushka, I.L. Rakhno, S.D. Reitzner, V.I. Sidorov, A.M. Stefanik, K. Vaziri, K.E. Williams, R.M. Zwaska (Fermilab) C.J. Densham (STFC/RAL)

The Long Baseline Neutrino Facility (LBNF) project will build a beamline located at Fermilab to create and aim an intense neutrino beam of appropriate energy range toward the DUNE detectors at the SURF facility in Lead, South Dakota. Neutrino production starts in the Target Station, which consists of a solid target, magnetic focusing horns, and the associated sub-systems and shielding infrastructure. Protons hit the target producing mesons which are then focused by the horns into a helium-filled decay pipe where they decay into muons and neutrinos. The target and horns are encased in actively cooled steel and concrete shielding in a chamber called the target chase. The reference design chase is filled with air, but nitrogen and helium are being evaluated as alternatives. A replaceable beam window separates the decay pipe from the target chase. The facility is designed for initial operation at 1.2MW, with the ability to upgrade to 2.4MW, and is taking advantage of the experience gained by operating Fermilab's NuMI facility. We discuss here the design status, associated challenges, and ongoing R&D and physics-driven component optimization of the Target Station.

MOP0B36 **Design of the High Beta 650 MHz Cryomodule - PIP II**

V. Roger, T.H. Nicol, Y.O. Orlov (Fermilab) P. Khare (RRCAT)

In this paper the design of the high beta 650 MHz cryomodule will be presented. It has been designed jointly between Fermilab and RRCAT. This cryomodule is composed of six 5-cell 650 MHz elliptical cavities, designed for $\beta=0.92$. These cryomodules are the last elements of the SC linac architecture which is the main component of the Proton Improvement Plan-II (PIP-II) at Fermilab. This paper summarises the design choices which have been done. Mechanical, thermal and cryogenic analysis have been performed to ensure the proper operation. First the concept of having a strong-back at room temperature has been validated. Then the heat loads have been estimated and all the components have been integrated inside the cryomodule by designing especially the supports, the beam line, the thermal shield and the cryogenic lines. All these elements and the calculations leading to the design of this cryomodule will be described in this paper.

MOP0B37 **First Cryogenic AFM and MFM Measurements on Niobium Prepared by Different Surface Treatments**

A. Romanenko (Fermilab)

Cryogenic scanning probe techniques such as atomic force microscopy (AFM) and magnetic force microscopy (MFM) provide invaluable information on both nanoscale surface structure, as well as its superconducting behavior in the vortex state. We present the first results obtained using Fermilab's attoCube scanning probe microscope on niobium samples prepared by state-of-the-art techniques employed for SRF cavities, and discuss the implications for the basic SRF science.

MOP0B38 **Low Field Behavior of Superconducting RF Cavities**

A. Romanenko (Fermilab)

Behavior of the quality factor of SRF cavities at very low fields < 1 MV/m is historically less explored due to the significantly higher gradients used for particle acceleration. Lately however, the low field applications of SRF cavities at the level of single photon per cavity were considered, including quantum computing and dark matter search. These developments emphasized the importance to understand the so-call low field Q slope in SRF cavities, which is also directly related to the understanding of the microwave surface resistance of niobium. In this contribution we present the first low field measurements at < 1 MV/m down to ~ 1 kV/m, which revealed very rich physics in this "low field" frontier of SRF cavities.

MOP0B39 **A 600 Volt Multi-Stage, High Repetition Rate GaN FET Switch**

G.W. Saewert, H. Pfeffer (Fermilab)

Using recently available GaN FETs, a 600 Volt three-stage, multi-FET switch has been developed having 2 nanosecond rise time driving a 200 Ω load with the potential of approaching 30 MHz average switching rates. Possible applications include driving particle beam choppers kicking bunch-by-bunch and beam deflectors where the rise time needs to be custom tailored. This paper reports on the engineering issues addressed, the design approach taken and some performance results of this switch.

MOP0B40 **Quench Training Analysis of Nb3Sn Accelerator Magnets - Strategy and First Results**

S. Stoynev, K.H. Riemer, A.V. Zlobin (Fermilab)

Nb3Sn accelerator magnet technology has made significant progress during the past decades. Thanks to that 11-12 T Nb3Sn dipoles and quadrupoles are planned to be used in accelerators such as LHC in near future for the luminosity upgrade and in longer term for the LHC energy upgrade or a future Very High Energy pp Collider. However, all the state of the art Nb3Sn accelerator magnets show quite long training. This specific feature significantly raises the required design margin or limit the nominal operation field of Nb3Sn accelerator magnets and, thus, increases their cost. To resolve this problem Fermilab has launched a study aiming to analyze the relatively large amount of Nb3Sn magnet training data accumulated at Fermilab magnet test facility. The ultimate goal is to correlate magnet design and manufacturing features and magnet material properties with training performance parameters which will eventually allow us to optimize both the magnet design, fabrication and the training processes. This paper describes the general strategy of the analysis and presents the first results based on partial data processing. Conclusions and further steps are also outlined and discussed.

MOP0B41 **Field Quality Measurements in the FNAL Twin-Aperture 11 T Dipole for LHC Upgrades***

T. Strauss, G. Apollinari, E.Z. Barzi, G. Chlachidze, J. DiMarco, A. Nobrega, I. Novitski, S. Stoynev, D. Turrioni, G. Velev, A.V. Zlobin (Fermilab) B. Auchmann, S. Izquierdo Bermudez, M. Karppinen, L. Rossi, F. Savary, D. Smekens (CERN)

FNAL and CERN magnet groups are developing a twin-aperture Nb3Sn 11 T dipole suitable for installation in the LHC to provide room for additional collimators in the dispersion suppressor (DS) areas. Two of these magnets with a collimator in between

will replace one regular MB dipole. A single-aperture 2-m long dipole demonstrator and two 1-m long dipole models have been assembled and tested at FNAL in 2012-2014. The 1 m long collared coils were then assembled into the twin-aperture configuration and tested in 2015. The first magnet test was focused on the quench performance of twin-aperture magnet configuration including magnet training, ramp rate sensitivity and temperature dependence of magnet quench current. In the second test performed in July 2016 field quality in one of the two magnet apertures has been measured and compared with the data for the single-aperture models. These results are reported and discussed in this paper.

MOP0B42 Design Studies and Optimization of High-Field Nb₃Sn Dipole Magnets for a Future Very High Energy pp Collider
A.V. Zlobin, V.V. Kashikhin, I. Novitski (Fermilab)

Accelerator magnet technology based on the Nb₃Sn superconductor has made significant progress during the past decade. Thanks to that Nb₃Sn dipoles and quadrupoles with a nominal field of 11-12 T are being considered in the near future for the LHC luminosity upgrade (HL-LHC project). In longer term cost-effective 15-16 T Nb₃Sn magnets will be needed for the LHC energy upgrade (HE-LHC) or a future Very High Energy pp Collider (VHEppC). To demonstrate the feasibility of 15 T accelerator quality dipole magnets, Fermilab has started the development of a single-aperture Nb₃Sn dipole for a future hadron collider based on a 4-layer graded cos-theta coil with 60 mm aperture and cold iron yoke. In parallel, to explore the limit of the Nb₃Sn accelerator magnet technology, optimize magnet design and performance parameters, and reduce magnet cost, magnet design studies are also being performed based on 3- and 4-layer 50 mm aperture cos-theta coils with and without stress management elements. Results of these studies are reported and discussed in this paper.

MOP0B43 Models for the Structural Integrity of High-Power Targets, with Application to Sinuous Materials
R.M. Zwaska (Fermilab)

High-power targets are integral components of many hadron facilities, having the role of converting the high-power protons or ions into secondary particles for various experiments. These targets are exposed to very-high energy densities, and subsequently large internal stresses within the materials of the target. In this paper we analyze the problem of pulsed energy deposition from first principles and apply to sinuous materials. We develop several models to quantitatively evaluate the stresses within targets. These models reduce the need for finite-element simulation, and they provide direction toward superior material through broad figures-of-merit. The sinuous target is an engineered material with high strength on the micro-scale, but a very low modulus of elasticity on the meso-scale. The low modulus of elasticity is achieved by constructing the material of spring-like wire segments much smaller than the beam dimension. The intrinsic bends of the wires will allow them to absorb the strain of thermal shock with minimal stress. We apply our models to conceptual materials of sinuous nature, and existing cellular materials that share some of the physical properties.

MOP0B44 Solid-State Thyatron Replacement Switch*

I. Roth, N. Butler, M.P.J. Gaudreau, M.K. Kempkes, M.G. Munderville, R.E. Simpson (Diversified Technologies, Inc.)

Semiconductor thyristors have long been used as a replacement for thyatrons in low power or long pulse RF systems. To date, however, such thyristor assemblies have not demonstrated the reliability needed for installation in short pulse, high peak power RF stations used with many pulsed electron accelerators. The fast rising current in a thyristor tends to be carried in a small region, rather than across the whole device, and this localized current concentration can cause a short circuit failure. An alternate solid-state device, the insulated-gate bipolar transistor (IGBT), can readily operate at the speed needed for the accelerator, but commercial IGBTs cannot handle the voltage and current required. It is, however, possible to assemble these devices in arrays to reach the required performance levels without sacrificing their inherent speed. Diversified Technologies, Inc. (DTI) has patented and refined the technology required to build these arrays of series-parallel connected switches. DTI is currently developing an affordable, reliable, form-fit-function replacement for the klystron modulator thyatrons at SLAC capable of pulsing at 360 kV, 420 A, 6µs, and 120 Hz.

MOP0B45 High Power Resonant Cavity Combined Solid-State Amplifier*

M.P.J. Gaudreau, N. Butler, M.K. Kempkes, J. Kinross-Wright, M.G. Munderville, E.M. Niell, R.E. Simpson (Diversified Technologies, Inc.)

Diversified Technologies, Inc. (DTI) has designed an integrated resonant-cavity combined solid-state amplifier for accelerator applications. The design radically simplifies solid-state transmitters to create straightforward scaling to very high power levels. A crucial innovation is the inherently reliable "soft-failure" mode of operation; a failure in one or several of the transistors has negligible performance impact. In addition, the design couples the transistor drains directly to the cavity without first transforming to 50 Ohms, avoiding the otherwise-necessary multitude of circulators, cables, and connectors. A conventional amplifier has a complete set of electrical and water cooling connections for every stage, resulting in hundreds of connections for a high power transmitter; in some DTI designs, there are as few as four. This construction reduces cost and significantly increases the power level at which it is cost-effective to employ a solid-state transmitter. The prototype has demonstrated multiple-transistor combining from 300 MHz to 1300 MHz, at powers up to 5 kW. This prototype is scalable to several hundred kW at these frequencies.

MOP0B46 Long Pulse Solid-State Pulsed Power Systems Built to ESS Specifications

I. Roth, M.P.J. Gaudreau, M.K. Kempkes, M.G. Munderville, R.E. Simpson (Diversified Technologies, Inc.) J. Domenge (Sigma Phi Electronics) J.L. Lancelot (Sigmaphi)

Diversified Technologies, Inc. (DTI), in partnership with SigmaPhi Electronics (SPE) has built three long pulse solid-state klystron transmitters to meet spallation source requirements. Two of the three units are installed at CEA Saclay and the National Institute of Nuclear and Particle Physics (IN2P3), where they will be used as test stands for the European Spallation Source (ESS). The systems delivered to CEA and IN2P3 demonstrate that the ESS klystron modulator specifications (115 kV, 25 A per klystron, 3.5 ms, 14 Hz) have been achieved in a reliable, manufacturable, and cost-effective design. There are only minor modifications required to support transition of this design to the full ESS Accelerator, with up to 100 klystrons. The systems will accommodate the recently-determined increase in average power (~660 kW), can offer flicker-free operation, are equally-capable of driving Klystrons or MBIOTs, and are designed for an expected MTBCF of over ten years, based on operational experience with similar systems.

MOP0B47 Beam Coupling Impedance Characterization of Third Harmonic Cavities for ALS Upgrade

T.H. Luo, K.M. Baptiste, M. Betz, J.M. Byrd, S. De Santis, S. Kwiatkowski, S. Persichelli (LBNL)

The ALS upgrade to a diffraction-limited light source (ALS-U) depends on the ability to lengthen the stored bunches limiting emittance growth due to intra-beam scattering. In order to achieve lengthening in excess of fourfold necessary to this end we are investigating the use of the same passive 1.5 GHz normal-conducting RF cavities currently used on the ALS. While the upgraded

ring RF parameters and fill pattern make for an easier scenario as the beam-induced phase transient is concerned, the larger lengthening factor and the strongly non-linear lattice require particular attention to the cavities contribution to the machine overall impedance budget. In this paper we present our estimates for longitudinal and transverse short-range wakes based on computer simulations, including the tapers necessary to adapt the ALS cavities to the ALS-U vacuum chamber, and of the narrow-band impedance obtained by careful bench measurements of the cavities' resonant modes.

MOP0B48 **Progress on the Design of Ridge Waveguide HOM Damper for High Current ERL SRF Cavity**

T.H. Luo, D. Li, S. Persichelli, Y. Yang (LBNL)

Energy recovery linac (ERL) superconducting RF (SRF) cavities are proposed for Electron Ion Collider (eRHIC) at BNL. eRHIC consists of 80 5-cell 647 MHz superconducting RF cavities. With the highest total current up to 700 mA, significant amount of HOM power needs to be damped to preserve beam quality and prevent beam-break-up. For the HOMs below the beam pipe cutoff frequency and trapped locally, they are damped through the waveguide couplers on each end of the cavity. In this paper, we present the recent progress on the RF design of HOM damping waveguide for eRHIC ERL SRF cavity.

MOP0B49 **Persistent Current Effects in RHIC Arc Dipole Magnets**

X. Wang, S.A. Gourlay, G.L. Sabbi (LBNL) A.K. Ghosh, R.C. Gupta, A.K. Jain, P. Wanderer (BNL)

The RHIC dipoles are operated at low currents (112 A to 218 A) for low energy Au-Au studies at Brookhaven National Laboratory. At these low currents, significant persistent magnetization of superconducting NbTi filaments leads to strong nonlinear magnetic fields. To understand the field quality at low current, measurements and calculation of the persistent current effect were performed and good agreement was achieved. We report the details of the characterization and calculation of the field errors. The impact of current profile on the persistent currents and the machine operation is discussed.

MOP0B50 **Preparation of LCLS-II 1.3 GHz Prototype Cryomodule Testing at Fermilab**

K. Siorattanakul (Lehigh University) E.R. Harms (Fermilab)

Linac Coherent Light Source II (LCLS-II) is a next generation x-ray free electron laser to be constructed in SLAC National Accelerator Laboratory's existing tunnel. The first prototype 1.3 GHz cryomodule was delivered to Fermilab's Cryomodule Testing Facility (CMTF) from Fermilab's Technical division on July 20, 2016 for testing. In preparation for the testing, we analyze the performance of testing facility's RF system, as well as develop necessary graphical interfaces to monitor the test. Results from test runs using test loads reveal that complete calibrations for power measurements are still needed for multiple cavities. In the meantime, the direct output from the amplifiers are stable with RMS less than 2 percent. It should be possible to make gradient calculations to within 5-10 percent.

MOP0B51 **High-Efficiency 500-W RF-Power Modules for UHF**

F.H. Raab (Green Mountain Radio Research)

GMR has developed solid-state RF-power modules that deliver up to 650 W at frequencies from 325 to 704 MHz. The nominal output of 500 W is delivered with an overall efficiency from 79% at 704 MHz to 83% percent at 325 MHz. In contrast to conventional solid-state power amplifiers, high efficiency is maintained over a wide range of output powers; e.g., 70 percent or better for outputs of 30 W or higher. Each 500-W module contains five 120-W RF power amplifiers (PAs) and a Gysel* splitter and combiner. The class-F** PAs employ GaN FETs and produce over 120 W with efficiencies from 82-86%. A class-S modulator maintains high efficiency over nearly the entire range of amplitudes. Supporting hardware includes a control computer, DSP, low-level RF amplifiers, and drivers. The 500-W modules are intended to be building blocks of a multi-kW RF power source. A system based these modules will consume 1/3 to 1/2 of the prime power required by a system based upon klystrons or conventional solid-state amplifiers and will have significantly lower cooling requirements.

MOP0B52 **Dielectric Loaded High Pressure Gas Filled RF Cavities for Use in Muon Cooling Channels**

B.T. Freemire (IIT) M. Backfish, D.L. Bowring, A. Moretti, D.W. Peterson, A.V. Tollestrup, K. Yonehara (Fermilab) R.P. Johnson (Muons, Inc) A.V. Kochemirovskiy (University of Chicago) Y. Torun (Illinois Institute of Technology)

High brightness muon beams require significant six dimensional cooling. One cooling scheme, the Helical Cooling Channel, employs high pressure gas filled radio frequency cavities, which provide both the absorber needed for ionization cooling, and a means to mitigate RF breakdown. The cavities are placed along the beam's trajectory, and contained within the bores of superconducting solenoid magnets. Gas filled RF cavities have been shown to successfully operate within multi-Tesla external magnetic fields, and not be overcome with the loading resulting from beam-induced plasma. The remaining engineering hurdle is to find a way to fit 325 and 650 MHz single cell pillbox cavities within the bores of the magnets using modern technology. One method to accomplish this is to partially fill the cavities with a dielectric material. Alumina (Al₂O₃) is an ideal dielectric, and the experimental test program to determine its performance under high power in a gas filled cavity has concluded. The final results, and their implications for the design of a muon cooling channel based on gas filled RF cavities will be discussed.

MOP0B53 **Nonlinear Behavior of Multipactor: 3D Simulations**

M. Siddiqi, R.A. Kishek (UMD)

Multipactor is a discharge induced by the impact of electrons on a surface due to radio-frequency (RF) electromagnetic fields and secondary electron emission (SEE). Depending on the impact energy and RF phase of the incident electron, a growth in the electron density is possible. Multipactor can lead to device breakdown in many applications, such as particle accelerator structures and rf systems, satellite communication equipment, and microwave components. Multipactor can also be a precursor for electron cloud effects. Due to the critical need to mitigate multipactor, a more comprehensive theory has been introduced that views multipactor as a global effect that can be analyzed through the concepts of iterative maps and nonlinear dynamics *. In order to test this novel approach, multipactor is simulated in a parallel-plate waveguide using the WARP particle-in-cell code. Different parameters are varied in the simulation to determine the conditions that add to multipactor growth, such as geometry dimensions, electron seeding scenarios, and an applied DC electric field. These computational results and their implications on the further development of this theory will be presented.

MOP0B54 **Superferric arc dipoles for the Ion Ring and Booster of JLEIC**

P.M. McIntyre, J. Breitschopf, J. Gerity, J.N. Kellams, A. Sattarov (Texas A&M University) D. Chavez (DCI-UG)

The JLEIC project requires 3 T superferric dipoles and quadrupoles for the half-cell arcs of its Ion Ring and Booster. A superferric design using NbTi cable-in-conduit conductor is being developed. A mockup winding has been completed, with the objectives to develop and evaluate the coil structure and the winding tooling and methods, and to measure errors in the position of each cable turn in the dipole body. The results of the mockup winding study are presented. The CIC design is now ready for construction and testing of a first model dipole.

- MOP0B55 Room Temperature Magnets in FRIB Driver Linac**
Y. Yamazaki, N.K. Bultman, E.E. Burkhardt, K. Holland, A. Hussain, F. Marti, T. Russo, Q. Zhao (FRIB) W.J. Yang, Q.G. Yao (IMP/CAS)
 The FRIB Driver Linac* is to accelerate all the stable ions beyond 200 MeV/nucleon with a beam power of 400 kW. The linac is unique, being compactly folded twice. In this report, the room temperature magnets, amounting 147 in total, after Front End with a 0.5-MeV RFQ, are detailed, emphasizing the rotating coil field measurements and fiducialization.
- MOP0B56 Frequency Domain Simulations of Co-Linear X-Band Energy Booster (CXEB) RF Cavity Structures and Passive RF Components with ACE3P**
T. Sipahi, S. Biedron, S.V. Milton (CSU)
 Due to their higher intrinsic shunt impedance X-band accelerating structures offer significant gradients with relatively modest input powers, and this can lead to more compact light sources. At the Colorado State University Accelerator Laboratory (CSUAL) we would like to adapt this technology to our 1.3-GHz, L-band accelerator system using a passively driven 11.7 GHz traveling wave X-band configuration that capitalizes on the high shunt impedances achievable in X-band accelerating structures in order to increase our overall beam energy in a manner that does not require investment in an expensive, custom, high-power X-band klystron system. Here we provide the comparisons of the important parameters achieved using SUPERFISH and OMEGA3P for our Co-linear X-band Energy Booster (XCEB) system that will allow us to achieve our goal of reaching the maximum practical net potential across the X-band accelerating structures while driven solely by the beam from the L-band system.
- MOP0B57 Wakefield Excitation in Power Extraction Cavity (PEC) of Co-Linear X-Band Energy Booster (CXEB) in Time Domain (T3P) with ACE3P**
T. Sipahi, S. Biedron, S.V. Milton (CSU)
 We provide the general concept and the design details of our proposed Co-linear X-band Energy Booster (CXEB) in our previous papers. In addition to that we present more advanced 3D simulations of our system with frequency domain modules Omega3P and S3P of ACE3P code suite in another paper at this conference. In here, using the time domain module T3P of ACE3P we provide the single bunch and multiple bunch wakefield excitations with a symmetric Gaussian bunch distribution and related power extraction mechanism in our traveling wave (TW) X-band power extraction cavity (PEC) are discussed further.
- MOP0B58 Eddy Current Calculations for a 1.495 GHz Injection-Locked Magnetron**
S.A. Kahn, A. Dudas, R.P. Johnson, M.L. Neubauer (Muons, Inc) H. Wang (JLab)
 An injection-locked amplitude modulated magnetron is being developed as a reliable, efficient RF source that could replace klystrons used in particle accelerators. The magnetron amplitude is modulated using a trim magnetic coil to alter the magnetic field in conjunction with the anode voltage to suppress the emittance growth due to microphonics and changing beam loads. The rate for microphonic noise can have frequencies in the range 10^{-50} Hz. This is competitive to the inductive decay time of the trim coil. Eddy currents will be induced in the copper anode of the magnetron that will buck the field from the trim coil in the interaction region. This paper will describe the magnetic circuit of the proposed magnetron as well as the calculation and handling of the Eddy currents on the magnetic field.
- MOP0B59 Magnet Design for the Splitter/combiner Regions of the Cornell-Brookhaven Electron-Recovery-Linac Test Accelerator**
J.A. Crittenden, D.C. Burke, C.E. Mayes, K.W. Smolenski (Cornell University (CLASSE), Cornell Laboratory for Accelerator-Based Sciences and Education)
 The Cornell-Brookhaven Electron-Recovery-Linac Test Accelerator (CBETA) will provide a 150-MeV electron beam using four acceleration and four deceleration passes through the Cornell Main Linac Cryomodule housing six 1.3-GHz superconducting RF cavities. The return path of this 6-m-circumference accelerator will be provided by 10^6 fixed-field alternating-gradient (FFAG) cells which carry the four beams of 42, 78, 114 and 150-MeV in a vacuum chamber of 84-mm x 24-mm interior dimensions. Here we describe the splitter and combiner regions which serve to match the on-axis linac beam to the off-axis beams in the FFAG cells, providing the path-length adjustment necessary to energy recovery for each of the four beams. The path lengths of the four beamlines in each of the splitter and combiner regions are designed to be adapted to 1-, 2-, 3-, and 4-pass staged operations. Design specifications and modeling for the 20 dipole and 32 quadrupole electromagnets in each region is presented. The CBETA project will serve as the first demonstration of multi-pass energy recovery using superconducting RF cavities with FFAG cell optics for the return loop.
- MOP0B60 Performance of the Cornell Main Linac Prototype Cryomodule for the CBETA Project**
F. Furuta, N. Banerjee, J. Dobbins, R.G. Eichhorn, G.M. Ge, D. Gonnella, G.H. Hoffstaetter, M. Liepe, T.I. O'Connell, P. Quigley, D.M. Sabol, J. Sears, E.N. Smith, V. Veshcherevich (Cornell University (CLASSE), Cornell Laboratory for Accelerator-Based Sciences and Education)
 The main linac prototype cryomodule (MLC) is a key component for the Cornell-BNL ERL Test Accelerator (CBETA), which is a 4-turn FFAG ERL under construction at Cornell University. The MLC has been designed for high current and efficient continuous wave (CW) SRF cavity operation, and houses six high Q0 7-cell SRF cavities with individual beamline higher order-modes (HOMs) absorbers for strong HOM suppression in high beam current operation. Cavities have achieved specification values of 16.2MV/m with high Q0 of $2.0 \cdot 10^{10}$ at 1.8K in CW operation after cooldown optimizations and RF processing. Damping of the HOMs has been measured in detail, indicating that the loaded quality-factors of all critical modes are low enough to avoid BBU in high current, multi-turn ERL operation. Microphonics measurements have been carried out as well, and vibration sources have been determined and eliminated. Here we report on these cryomodule performance studies.
- MOP0B61 Updates of Vertical Electropolishing Studies at Cornell with KEK and Marui**
F. Furuta, G.M. Ge, T. Gruber, J.J. Kaufman, M. Liepe, J. Sears (Cornell University (CLASSE), Cornell Laboratory for Accelerator-Based Sciences and Education) V. Chouhan, Y.I. Ida, K.N. Nii, T.Y. Yamaguchi (MGH) H. Hayano, S. Kato, T. Saeki (KEK)
 Cornell, KEK, and Marui Galvanizing Co. Ltd (MGI) have started new Vertical Electro-Polishing (VEP) R&D collaboration in 2014. MGI and KEK has developed their original VEP cathode named 'i-cathode Ninja'® which has four retractable wing-shape parts per cell for single-/9-cell cavities. One single cell cavity had processed with VEP using i-cathode Ninja at Cornell. Cornell also performed the vertical test on that cavity. We will present the details of process and RF test result at Cornell.

- MOP0B62 SRF Half Wave Resonator Activities at Cornell for the RAON Project**
G.M. Ge, F. Furuta, T. Gruber, C. Henderson, M. Liepe, T.I. O'Connell, J. Sears, S. Stanley, V. Veshcherevich (Cornell University (CLASSE), Cornell Laboratory for Accelerator-Based Sciences and Education) **J. Joo, J.-W. Kim, W.K. Kim, J. Lee, I. Shin** (IBS)
 The RAON heavy ion accelerator requires ninety-eight 162.5MHz Half-Wave-Resonators (HWR) with a geometrical $\beta=0.12$. Cornell University will test a prototype HWR as well as develop a frequency tuner for this cavity. In this paper we report the progress in designing, fabricating, and commissioning of new HWR preparation and testing infrastructure at Cornell. The HWR infrastructure work includes a new High-Pressure-Rinsing (HPR) setup, and a modified vertical test insert with a 162.5MHz RF system. In addition, we report on the HWR tuner design.
- MOP0B63 Impact of Cooldown Procedure and Ambient Magnetic Field on the Quality Factor of State-of-the-Art Nb3Sn Single-Cell ILC Cavities**
D.L. Hall, J.J. Kaufman, M. Liepe, R.D. Porter (Cornell University (CLASSE), Cornell Laboratory for Accelerator-Based Sciences and Education)
 Single-cell Nb3Sn cavities coated at Cornell University have demonstrated quality factors of $>10^{10}$ at 16 MV/m and 4.2 K in vertical tests, achieving performance requirements of contemporary modern accelerator designs. In this paper, we present results demonstrating the impact of the cooldown procedure on the cavity's ability to achieve these quality factors and accelerating gradients. The impact of the field from thermoelectric currents, generated by thermal gradients across the cavity during the cooldown procedure, is connected to the susceptibility of Nb3Sn to trapped ambient magnetic flux. The dependence of the residual resistance and Q-slope as a function of the thermal gradient across the cavity are given, and conclusions regarding the nature of the cooldown required to ensure satisfactory performance in a cryomodule are drawn.
- MOP0B64 Low Temperature Impurity Doping of Superconducting RF Cavities**
P.N. Koufalas, G.M. Ge, J.J. Kaufman, M. Liepe (Cornell University (CLASSE), Cornell Laboratory for Accelerator-Based Sciences and Education)
 We investigate the effects of low temperature nitrogen doping on the performance of niobium superconducting RF cavities. The doping procedure is done at several temperatures in the range from 120 C to 600 C. Previous studies* have shown that nitrogen doping at high temperatures (i.e. $T \sim 800$ C) leads to the formation of niobium nitride layers on the surface of the niobium and, consequently, diffusion of nitrogen from the nitride layer into the bulk increasing cavity performance. However, at lower temperatures it is not yet clear if diffusion still occurs due to a lack of nitride formation. We seek to find an explanation of the physical mechanism behind low temperature doping in a nitrogen atmosphere and its effect on cavity performance.
- MOP0B65 Investigation of the Origin of the Anti-Q-Slope**
J.T. Maniscalco, D. Gonnella, M. Liepe (Cornell University (CLASSE), Cornell Laboratory for Accelerator-Based Sciences and Education)
 The surface resistance of a superconductor, a property very relevant to SRF accelerators, has long been known to depend on the strength of the surface magnetic field. A recent discovery showed that, for certain surface treatments, microwave cavities can be shown to have an inverse field dependence, dubbed the "anti-Q-slope", in which the surface resistance decreases over an increasing field. Here we present an investigation into what causes the anti-Q-slope in nitrogen-doped niobium cavities and why this phenomenon is not seen in standard bulk niobium.
- MOP0B66 Effectiveness of Chemical Treatments for Reducing the Surface Roughness of Niobium-3 Tin Superconducting Radio-Frequency Cavities**
R.D. Porter, F. Furuta, D.L. Hall, J.J. Kaufman, M. Liepe (Cornell University (CLASSE), Cornell Laboratory for Accelerator-Based Sciences and Education)
 Current Niobium-3 Tin (Nb3Sn) superconducting radio-frequency (SRF) accelerator cavities have rougher surfaces than conventional Niobium accelerator cavities. The surface roughness can cause enhancement of the surface magnetic field pushing it beyond the critical field. If this occurs over a large enough area it can cause the cavity to quench. The surface roughness may cause other effects that negatively impact cavity quality factor (Q) performance. Reducing surface roughness of Nb3Sn cavities may be necessary to achieve higher gradient with high Q. Current chemical treatments for reducing the surface roughness of Niobium are challenging for Nb3Sn: the Nb3Sn layer is only ~ 2 μ m while it is difficult to remove less than 1 μ m uniformly with most chemical treatments; current chemical treatments may preferentially remove Niobium or Tin, changing the ratio of the two. This paper presents measurements of the surface roughness, Nb3Sn thickness, and ratio of Niobium to Tin of Nb3Sn coated sample plates before and after various chemical treatments.
- MOP0B67 Manufacturing of Next-Generation Geometry Superconducting RF Accelerator Structures**
C.H. Boulware, T.L. Grimm, A. Rogacki, J.A. Yancey (Niowave, Inc.)
 The commercialization of superconducting radio-frequency (SRF) accelerators has been accompanied by application of advanced manufacturing techniques to complicated niobium cavities. Two examples from Niowave, Inc. will be discussed in this contribution. The first is the development of crab cavities for the LHC Hi Luminosity upgrade. Two designs, the Double Quarter-Wave (BNL) and RF-Dipole (ODU), are proceeding to testing in the SPS at CERN. Another next-generation cavity project has been the development of photonic bandgap (PBG) accelerators, resonant cavities incorporating an array of rods which confine the fundamental mode in a frequency-specific way. In collaboration with LANL, a set of single PBG cells has been built and tested, followed by a 5-cell elliptical structure with a PBG coupling cell. The construction of these resonant cavities and related RF couplers has pushed forward the industrial state-of-the-art. This contribution will discuss the novel features of these cavity designs and the requirements on cavity manufacture, processing, and cryogenic testing.
- MOP0B68 A New Method for Grain Texture Manipulation in Post-Deposition Niobium Films**
J. Musson, K. Macha, H.L. Phillips (JLab) **W. Cao, H. Elsayed-Ali** (ODU)
 Niobium films are frequently grown using forms of energetic condensation, with modest substrate temperatures to control grain structure. As an alternative, energetic deposition onto a cold substrate results in a dense amorphous film, with a much larger energy density than the re-crystallized state. Re-crystallization is then performed using a pulsed UV (HIPPO) laser, with minimal damage to the substrate. In addition, a graded interface between the substrate and Nb film is created during the early stages of energetic deposition. Experimental approach and apparatus are described.

MOP0B69 Wire Stretching Technique for Measuring RF Crabbing/Deflecting Cavity Electrical Center and a Demonstration Experiment on Its Accuracy

H. Wang (JLab)

The fabrication accuracy of a superconducting RF crab cavity for the Large Hadron Collider High Luminosity Upgrade and the future Electron Ion Collider requires the cavity's electric center line relative to the crabbing plane within sub mm offset and sub degree in rotation. It is very hard for the cavity's niobium sheet formation, high temperature bake and chemistry processes and finally cooling down in cryomodule to satisfy such tight tolerance. A new wire stretching technique combining with the RF measurement in the deflecting modes has been demonstrated on the bench to detect less than 10um resolution on the RF signal when the wire is moving away from the ideal electric center line. The foundation of this technique and its difference from the use in other applications will be reviewed. Based on this principle, the possible implementations for detecting RF leakage to the higher order mode couplers, cavity string alignment and cryomodule assembly will be discussed.

MOP0B70 Plasma Etching of Superconducting Radio Frequency Cavity

J. Upadhyay, S. Popović, L. Vušković (ODU) A.D. Palczewski, H.L. Phillips, A-M. Valente-Feliciano (JLab)

We are developing plasma processing technology of superconducting radio frequency (SRF) cavities. The formation of dc self-biases due to surface area asymmetry in this type of plasma and its variation on the pressure, rf power and gas composition was measured. Enhancing the surface area of the inner electrode to reduce the asymmetry was studied by changing the contour of the inner electrode. The optimized contour of the electrode based on these measurements was chosen for SRF cavity processing. To test the effect of the plasma etching on the cavity rf performance, a 1497 MHz single cell SRF cavity is used, which previously mechanically polished, buffer chemically etched afterwards and rf tested at cryogenic temperatures for a baseline test. Plasma processing was accomplished by moving axially the inner electrode and the gas flow inlet in a step-wise manner to establish segmented plasma processing. The cavity is rf tested afterwards at cryogenic temperatures. The rf test and surface condition results are presented.

MOP0B71 Consideration on Determination of Coupling Factors of Waveguide Iris Couplers

S.W. Lee, M.S. Champion, Y.W. Kang (ORNL)

Waveguide iris couplers are frequently used for powering accelerating cavities in low beta sections of ion accelerators. In ORNL SNS, six drift tube linac (DTL) cavity structures have been operating. Each cavity is fed by a tapered ridge waveguide iris input coupler with a waveguide ceramic disk window. The original couplers and cavities have been in service for more than a decade. Since all DTL cavity structures are fully utilized for neutron production, none of the cavity structure is available as a test cavity or a spare. Maintaining spares for operations and for future system upgrade, test setup of the iris couplers for precision tuning is considered. A smaller single cell cavity may be used for iris pretuning of the coupling iris as the test cavity and RF conditioning of the iris couplers as the bridge waveguide. In this paper, study of using a single cell cavity for the iris tuning and the conditioning is presented with 3D simulations. A single cell test cavity has been built and used for bench measurement with the iris couplers to show the design and pretuning of the coupling irises.

MOP0B72 Development of L-Band Combiners for Klystron Replacement

A.V. Smirnov, S. Boucher (RadiaBeam Systems) R.B. Agustsson, D.I. Gavryushkin, J.J. Hartzell, K.J. Hoyt, A.Y. Murokh, T.J. Villabona (RadiaBeam)

The JLAB upgrade program requires a ~8 kW, 1497 MHz amplifier operating at more than 55-60% efficiency, and 8 kW CW power to replace 340 klystrons. One of possibilities of the klystron replacement is usage of high electron mobility packaged GaN transistors applied in array of highly efficient amplifiers using precise in-phase, low-loss, combiners-dividers. Design features and challenges related to radial multi-way dividers/combiners are discussed including HFSS simulations and cold measurements.

MOP0B73 Thermal Analysis for the Higher Order Mode Waveguide and Fundamental Power Coupler for the 647 MHz Accelerating Cavity for the Electron Ion Collider

D. Ravikumar, R. Than, C. Xu (BNL)

The work focuses on the thermal analysis for the cryogenically cooled waveguide for the Higher Order Mode RF energy dampers and Fundamental mode Power Coupler [FPC] for the 647 MHz 5-cell accelerating cavities being proposed for the Electron Ion Collider's Linear Accelerator. We develop a model to execute thermal analysis for the aforementioned waveguide/power coupler using SLAC's multiphysics program ACE3p running on NERSC computing facility or using the ANSYS multiphysics program running on a workstation. The goal would be to complete a thermal design optimized for either a 2 or 3 thermal intercept configuration.

MOP0B74 A Permanent Magnet Quadrupole Magnet for CBETA

H. Witte, M. Anerella, J.S. Berg, J. Schmalzle (BNL)

Recently a collaboration between Brookhaven National Laboratory and Cornell University was established, aiming to build the CBETA accelerator. CBETA is a 150 MeV electron test accelerator, which prototypes essential technologies of eRHIC, which is a proposed upgrade to the existing Relativistic Heavy Ion Collider (RHIC) hadron facility at Brookhaven National Laboratory. Similar to eRHIC, CBETA employs an FFAG lattice for the arcs. The arcs require short, large aperture quadrupole magnets, which are located close together. BNL has been working on a design employing permanent magnets; we show the concept and the engineering design of these magnets. Prototype magnets have been constructed recently; we report on magnetic field quality measurements and their agreement with computer simulations.

MOP0B75 Halbach Magnets for CBETA and eRHIC

H. Witte, J.S. Berg (BNL)

At Brookhaven National Laboratory two design efforts are underway: eRHIC and CBETA. eRHIC is a proposed upgrade to the existing Relativistic Heavy Ion Collider (RHIC), which would allow collisions of up to 21 GeV polarized electrons with protons or heavy ions. CBETA is a 150 MeV electron accelerator, aiming to demonstrate essential technology necessary for eRHIC. Both machines employ FFAG arcs and are designated to use permanent magnet material for the required quadrupole magnets. One proposed design is a Halbach magnet; this paper investigates the feasibility of this approach.

MOP0B76 Field Emission Dark Current Simulation for eRHIC ERL

C. Xu, I. Ben-Zvi, Y. Hao, V. Pritsyn, K.S. Smith, W. Xu, A. Zaltsman (BNL)

The eRHIC project will be a electron and proton collider proposed in BNL. These high repetition rates will require Super-Conducting Radio-Frequency cavities with fundamental frequency of 650MHZ for high current applications. Each with a string of two of those cavities. The strong electromagnetic fields in the SRF cavities will extract electrons from the cavity walls and will accelerate those. Most dark current will be deposited locally, although some electrons may reach several neighbor cryomodules, thereby gaining

substantial energy before they hit a collimator or other aperture. Simulation of these effects is therefore crucial for the design of the machine. Track3P code was used to simulate field-emission electrons from different SRF cavities setup to optimize the field emission dark current characterizes.

MOP0B77 Surface Chemistry of Niobium Involving Oxygen, Hydrogen, and Nitrogen Relevant to the Performance of Superconducting RF Accelerator Cavities

R.D. Veit, N.A. Kautz, S.J. Sibener (*The University of Chicago*) A. Romanenko, A. Romanenko (*Fermilab*)

Superconducting radio frequency (SRF) technology enables high-efficiency high-gradient accelerators. Performance of SRF cavities is characterized by their quality factor, Q_0 , and the maximum accelerating gradient, E_{acc} . Chemical and structural defects at the surface and in the near-surface region of niobium SRF cavities can negatively or positively affect cavity performance. We investigate the surface structure, chemistry, and oxidative state of single-crystal niobium samples as well as technical grade polycrystalline SRF cavity samples using scanning tunneling microscopy (STM), Auger electron spectroscopy (AES), and x-ray photoelectron spectroscopy (XPS). We report results on the kinetics of the reduction and dissolution of the native pentoxide overlayer, the affect of the underlying crystal orientation on surface monoxide structure, the oxidation and dissolution of oxygen through the NbO-(100) ladder structures, and an XPS depth-profiling study of nitrogen-doped niobium SRF cavities. Inspired by recent discoveries at the Fermi National Accelerator Laboratory, we also explore the possible relationship between nitrogen-doping and nanoscale hydride surface precipitation.

MOP0B78 Design of RAON Vacuum System

T. Ha, H.S. Choi (*PAL*) D. Jeon, J.H. Kim, H.J. Son (*IBS*)

RAON is a rare isotope heavy-ion accelerator for diverse research fields including exploration of new isotopes, new materials and applied medical research in Korea. The technical design of RAON vacuum system is scheduled to be finished in 2016, with completion of the construction in 2021 as the goal. RAON consists of 20 subsystems of which vacuum levels are from 10^{-11} mbar to 10^{-6} mbar depending on the vacuum requirements for each subsystem. Normal vacuum chambers will be made of stainless steel whose outgassing rate is assumed as $3 \cdot 10^{-11}$ mbar l/s cm^2 for base pressure calculations. A test-particle Monte-Carlo simulator (MolFow) is used to calculate the vacuum profile of the system and to determine the quantity, pumping speeds and the positions of the vacuum pumps. In this presentation, we report status of the design of RAON vacuum system focusing on the superconducting linac section.

MOP0B79 Pulsed-Power Supply for Fast Kicker System


J. Prager, K.E. Miller, T.M. Ziemba (*EHT*)

Short-pulse dielectric Two-Beam Accelerators (TBAs) can produce high accelerating gradients near GV/m at significantly lower cost and complexity over traditional superconducting accelerators, which could significantly reduce the overall cost of accelerators. The development of a high voltage fast kicker system is critical for the staged dielectric TBA. Kickers are electromagnetic devices that create very fast fields to deflect charged particles to divert a portion of the beam away from the accelerator for use. Kicker systems require fast rise times and precision flat-top for uniform beam deflection. The requirements for the fast kicker system for dielectric short-pulse TBA are very demanding, and there is currently no power supply that can meet the all the necessary requirements. Eagle Harbor Technologies, Inc. has developed unique high voltage nanosecond pulse technology that can be utilized to meet the requirement for future TBA systems. EHT has demonstrated an 80 kV modular power supply system with fast rise time capability (~ 16 ns). To reach the desired output voltage of 160 kV EHT proposes to combine two of the 80 kV systems to enable the fast kicker power supply.


MOP0B80 MAX IV and Solaris 1.5 GeV Storage Rings Magnet Block Production Series Measurement Results

M.A.G. Johansson (*MAX IV Laboratory, Lund University*) K. Karaś (*Solaris National Synchrotron Radiation Centre, Jagiellonian University*) R. Nietubýć (*NCBJ*)

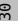
The magnet design of the MAX IV and Solaris 1.5 GeV storage rings replaces the conventional support girder + discrete magnets scheme of previous third-generation synchrotron radiation light sources with an integrated design having several consecutive magnet elements precision-machined out of a common solid iron block, with mechanical tolerances of ± 0.02 mm over the 4.5 m block length. The production series of 12+12 integrated magnet block units, which was totally outsourced to industry, was completed in the spring of 2015, with mechanical and magnetic QA conforming to specifications. This article presents mechanical and magnetic field measurement results of the full production series.

TUA1 — Oral Presentations (MC4)**Chair:** F.C. Pilat (JLab)**TUA1I001 Status of FRIB**08:30 **G. Pozdeyev, M. Ikegami, J. Wei (FRIB)**


The Facility for Rare Isotope Beams (FRIB) is based on a continuous-wave superconducting heavy ion linac to accelerate all the stable isotopes to above 200 MeV/u. The anticipated beam power is 400 kW, being approximately two-to-three orders of magnitude higher than those of operating heavy-ion facilities. The FRIB Project entered into full construction phase recently. This report summarizes the current design and construction status.

TUA1I002 Status Report on the SPIRAL2 Facility at GANIL09:00 **E. Petit (GANIL)**


Presentation of the status report of the SPIRAL2 facility at the GANIL laboratory. The status report will concern the construction of the facility and the first beam commissioning results

TUA1I003 Technological Challenges in the Path to 3.0 MW at the SNS Accelerator09:30 **K.W. Jones, M.A. Plum (ORNL)**


This talk discusses the design and anticipated challenges associated with upgrading the SNS beam power from the original 1.4 MW baseline design to the upgrade goal of 3 MW.

TUA1C004 Simulation of Beam Dynamics in a Strong-Focusing Cyclotron10:00 **P.M. McIntyre, J. Gerity, A. Sattarov (Texas A&M University) S. Assadi (HiTek ESE LLC) , K.E. Badgley (Fermilab) N. Pogue (LLNL)**

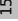
The strong-focusing cyclotron is an isochronous sector cyclotron in which slot-geometry superconducting half-cell cavities are used to provide sufficient energy gain per turn to fully separate orbits and superconducting quadrupoles are located in the aperture of each sector dipole to provide strong focusing and control betatron tune. The SFC offers the possibility to address the several effects that most limit beam current in a CW cyclotron: space charge, bunch-bunch interactions, resonance-crossing, and wake fields. Simulation of optical transport and beam dynamics entails several new challenges: the combined-function fields in the sectors must be properly treated in a strongly curving geometry, and the strong energy gain induces continuous mixing of horizontal betatron and synchrotron phase space. We present a systematic simulation of optical transport using modified versions of MAD-X and SYNERGIA. We report progress in introducing further elements that will set the stage for studying dynamics of high-current bunches.

TUA1C005 Design of a Compact Ring for Pulse Structure Manipulation of Heavy Ion Beams at the NSCL10:15 **A.N. Pham, R. Ready (NSCL) M.J. Syphers (Northern Illinois University)**


The Reaccelerator (ReA) Facility at the Michigan State University (MSU) National Superconducting Cyclotron Laboratory (NSCL) offers the low-energy nuclear science community unique capabilities to explore wider ranges of nuclear reactions and structures of exotic nuclei. Designed to provide a pulse repetition rate of 80.5 MHz, ReA fulfills the requirements of a broad class of nuclear experiments. However, future sensitive time-of-flight experiments will require the widening of pulse separation for the temporal resolution of single bunch detection while minimizing loss of rare isotope beams. In this contribution, we introduce a design of a compact heavy ion ring that will address the task of bunch compression, bunch separation enhancement, satellite bunches elimination, beam loss mitigation, and improvement of beam transmission.

TUB1 — Tutorial (MC9) / Oral Presentation (MC2)**Chair:** L.K. Spentzouris (Illinois Institute of Technology)**TUB1TU01 A Discussion on Phase Space and Beam Emittance**08:30  **R. Li, C. Tennant (JLab)**


The use of the term 'beam emittance' as a description of beam performance often has a contextual meaning, which may not be obvious to the reader. This tutorial presents a general discussion on the topic of beam emittance to differentiate between the various descriptions and definitions and where they are best applied. The tutorial begins with an overview of Hamiltonian dynamics and Liouville's Theorem to define the beam emittance based on canonical coordinates. The goal in accelerators is often to preserve the beam emittance. Discussion is therefore given to phenomena causing emittance non-conservation. We conclude with a statistical analysis of beam emittance, often calculated with beam tracking simulation codes, and how they are practically measured in particle accelerators. Examples demonstrate the subtleties of various definitions, particularly to reveal the many contributors to the emittance in a space-charge dominated and magnetized electron bunch.

TUB1C002 Operating Synchrotron Light Sources with a High Gain Free Electron Laser10:00  **S. Di Mitri, M. Cornacchia (Elettra-Sincrotrone Trieste S.C.p.A.)**


The peak current required by a high gain free electron laser (FEL) is not deemed to be compatible with the multi-bunch filling pattern of synchrotrons. We show that this problem can be overcome by virtue of magnetic bunch length compression in a ring section and that, after lasing, the beam returns to equilibrium conditions without beam quality disruption*. As a consequence of bunch length compression, the peak current stimulates a high gain FEL emission, while the large energy spread makes the beam less sensitive to the FEL heating and to the microwave instability. The beam large energy spread is matched to the FEL energy bandwidth through a transverse gradient undulator. Feasibility of lasing at 25 nm is shown for the Elettra synchrotron light source (SLS) at 1 GeV. Viable scenarios for the upgrade of existing or planned SLSs to the new hybrid insertion devices-plus-FEL operational mode are discussed, while ensuring little impact on the standard beamlines functionality.

TUB1C003 ALS-U: A Soft X-Ray Diffraction Limited Light Source10:15  **C. Steier, K. Chow, D. Robin, M. Venturini (LBNL)**


Improvements in brightness and coherent flux of about two orders of magnitude over operational storage ring based light sources are possible using multi bend achromat lattice designs. These improvements can be implemented as upgrades of existing facilities, like the proposed upgrade of the Advanced Light Source (ALS-U). The upgrade proposal will reuse much of the existing infrastructure, thereby reducing cost and time needed to reach full scientific productivity on a large number of beamlines. We will report on the accelerator design progress as well as the details of the ongoing R+D program.

TUA2 — Oral Presentations (MC3)**Chair:** V. Yakimenko (SLAC)**TUA2I001 AWAKE - a Proton Driven Plasma Wakefield Acceleration Experiment at CERN****11:00**  **A. Caldwell** (MPI-P) **P. Muggli** (MPI)


The AWAKE experiment at CERN will be the first of a kind experiment to demonstrate the potential of proton beam driven plasma wakefield acceleration. AWAKE will use the stored energy in the 450 GeV SPS beam at CERN to drive large amplitude wakefield in a 10 meter long plasma through the self modulation instability. Phase 1 experiments will excite the instability and Phase 2 will inject an external electron beam and use the wakefield to boost the electron beam energy by 1 GeV. Status of the AWAKE experiment, results from the 2016 commissioning runs and first data will be discussed along with plans for the future.

TUA2I002 Staging Results at the Argonne DLA facility**11:30**  **M.E. Conde**, **W. Gai**, **C.-J. Jing**, **J.G. Power** (ANL)


Present recent results on staging with dielectric accelerators as well as outline plans for experiments towards a e^-/e^+ , DLA-based collider

TUA2C003 A Novel Technique of Power Control in Magnetrons**12:00**  **G.M. Kazakevich**, **R.P. Johnson**, **M.L. Neubauer** (Muons, Inc) **V.A. Lebedev**, **W. Schappert**, **V.P. Yakovlev** (Fermilab)

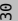
A novel technique for dynamic control of RF phase and power in high-power magnetrons is presented. Magnetrons controlled with this technique have sufficient bandwidth to suppress the parasitic modulation caused by beam loading as well as detuning due to microphonics and/or the Lorentz force in the case of superconducting RF cavities. Magnetron transmitters utilizing this technique also provide significantly higher efficiency and lower power unit cost than any other currently available high-power RF sources. The technique has been demonstrated using 2.45 GHz, 1kW magnetrons operating in both pulsed and CW regimes. The results of these experiments are presented and discussed. A concept for high-power magnetron transmitters suitable for powering future accelerators is outlined.

TUA2C004 Vacuum Breakdown Research at 110 GHz**12:15**  **S.C. Schaub** (MIT) **M.A. Shapiro**, **R.J. Temkin** (MIT/PSFC)

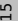
A 1.5 MW, 110 GHz gyrotron produces a linearly polarized quasioptical beam in 3 microsecond pulses. The beam is concentrated in vacuum to produce strong electric fields on the surfaces of dielectric and metallic samples, which are being tested for breakdown threshold at high gradient. Dielectrics are tested in the forms of both windows, with electric fields parallel to the surface, and sub-wavelength dielectric rod waveguides, with electric fields perpendicular to the surface. Visible light emission, absorbed/scattered microwave power, and Faraday cups are used to detect discharges on dielectric surfaces. Dielectrics to be tested include crystal quartz, fused quartz, sapphire, high resistivity float-zone silicon, and alumina with purities ranging from 96 to 99.9 percent. Metallic accelerator structures fabricated at SLAC will also be tested. These tests will require shortening of the pulse length to the nanosecond scale.

TUB2 — Oral Presentations (MC2)**Chair:** A. Zholents (ANL)**TUB2I001 Accelerator Physics Challenges in the Design of Multi Bend Achromat Based Storage Rings****11:00**  **M. Borland** (ANL) *R.O. Hettel (SLAC) S.C. Leemann (MAX IV Laboratory, Lund University) D. Robin (LBNL)*


With the recent success in commissioning of MAX IV, the multi-bend achromat (MBA) lattice has begun to deliver on its promise to usher in a new generation of higher-brightness synchrotron light sources. In this paper, we begin by reviewing the challenges, recent success, and lessons learned of the MAX-IV project. Drawing on these lessons, we then describe the physics challenges in even more ambitious rings and how these can be met. In addition, we touch on engineering issues and choices that are tightly linked with the physics design.

TUB2I002 Advanced Concepts for Seeded FELs**11:30**  **E. Ferrari, E. Allaria** (Elettra-Sincrotrone Trieste S.C.p.A.)

The use of an external laser to seed an electron beam at the beginning of the Free Electron Laser process has been proposed as a way to improve temporal coherence of modern short wavelength FELs. More recent studies and experiments have shown that electron beam manipulation through interaction with a seed laser can be exploited for tailoring FEL properties to specific user's requests. Recently, experiment for phase control, multi-color emission and coherent control have been reported.

TUB2C003 Fokker-Planck Analysis of Transverse Collective Instabilities in Electron Storage Rings**12:00**  **R.R. Lindberg** (ANL)

We analyze single bunch transverse instabilities due to wakefields using a Fokker-Planck model. We expand on the work of Suzuki*, writing out the linear matrix equation including chromaticity, both dipolar and quadrupolar transverse wakefields, and the effects of damping and diffusion due to the synchrotron radiation. The eigenvalues and eigenvectors determine the collective stability of the beam, and we show that the predicted threshold current for transverse instability and the profile of the unstable agree well with tracking simulations. In particular, we find that predicting collective stability for high energy electron beams at moderate to large values of chromaticity requires the full Fokker-Planck analysis to properly account for the effects of damping and diffusion due to synchrotron radiation.

TUB2C004 Corrugated Structure Insert to Extend SASE Bandwidth Up to 3% at the European XFEL**12:15**  **I. Zagorodnov, G. Feng, T. Limberg** (DESY)

The usage of x-ray free electron laser (XFEL) in femtosecond nanocrystallography involves sequential illumination of many small crystals of arbitrary orientation. Hence a wide radiation bandwidth could be useful in order to obtain and to index a larger number of Bragg peaks used for determination of crystal orientation. Considering the baseline configuration of the European XFEL in Hamburg, and based on beam dynamics simulations, we demonstrate here that usage of corrugated structures allows for a considerable increase in radiation bandwidth. It allows for data collection with a 3% bandwidth, a few microule radiation pulse energy, a few fs pulse duration, and a photon energy 4.1 keV.

- TUPOA01 Application of Accelerators in the Measurement of Reaction Cross-Section Data**
M.K. Sharma (*Aligarh Muslim University, Accelerator Laboratory*)
 In recent years there is an interest for development of high-energy and high-current accelerators due to the potential of accelerator-driven sub-critical reactor systems (ADS). The experimental cross-section data is required in the basic research for nuclear reaction mechanism as well as in the applied research for designing the energy generation devices such as the ADS reactors. In ADS systems, a high energy proton beam (GeV) is used to produce spallation neutrons from some heavy target. In such systems, light heavy charged particles such as like ^8Be , ^{12}C , ^{14}N , ^{16}O , ^{19}F etc., are also produced as a result of spallation. As such, information regarding the cross-section for reactions initiated by these particles produced in such devices is required for modeling of the system. In view of the above cross-section data for a large number of reactions produced in $^{12}\text{C}+^{128}\text{Te}$, $^{13}\text{C}+^{159}\text{Tb}$, $^{16}\text{O}+^{159}\text{Tb}$, $^{16}\text{O}+^{169}\text{Tm}$ and $^{16}\text{O}+^{181}\text{Ta}$ systems have been measured. The analysis of data within the framework of statistical model indicates reaction mechanisms such as complete fusion, incomplete fusion, direct reaction and pre-equilibrium emission involved in these systems.
- TUPOA02 Gold Nanoparticles Production Using Reactor and Cyclotron Based Methods in Assessment of ^{196}Au and ^{198}Au Production Yields by ^{197}Au Neutron Absorption for Therapeutic Purposes**
A. Khorshidi (*Gerash Research Institute, Gerash University of Medical Sciences*)
 Medical nano-gold radioisotopes is produced regularly using high-flux nuclear reactors, and an accelerator-driven neutron activator can turn out higher yield of $^{197}\text{Au}(n,\gamma)^{198}\text{Au}$ and $^{197}\text{Au}(n,2n)^{196}\text{Au}$ reactions. Here, nano-gold production via radiative/neutron capture was investigated using irradiated Tehran Research Reactor flux and also simulated proton beam of Karaj cyclotron in Iran. The production yield was examined using 30 MeV proton beam via simulated new neutron activator containing beryllium target, bismuth moderator around the target, and PbF_2 reflector enclosed the moderator region. Transmutation in ^{197}Au nano-solution samples were explored at 15 and 25 cm distances. The transport of fast neutrons inside bismuth material as heavy nuclei by a lesser lethargy can be contributed in enhanced nano-gold transmutation with long duration time than the water moderator in reactor-based method. Cyclotron-driven production of β -emitting radioisotopes for brachytherapy applications can complete the nano-gold production technology as a cheaper and safer approach as compared to the reactor-based method.
- TUPOA03 What Are the Most Important Factors for Startups Success?**
R. Geometrante (*KYMA*)
 Start-ups are enterprises with great ideas, enthusiasm and people but, despite that, more than 90% of them fails. Why? What factors account the most for start-up success or failure? The key ingredients for a successful start-up company will be discussed, considering the most critical steps to overtake in crucial moments such as technology transfer, growth in the market, creation of a world wide business. Kyma Srl, a spin-off company of Elettra-Sincrotrone Trieste, will be presented as a case study of a successful start-up.
- TUPOA04 Study on THz Imaging by Using the Coherent Cherenkov Radiation**
M. Nishida, M. Brameld, M. Washio (*Waseda University*) **R. Kuroda, Y. Taira** (*AIST*) **K. Sakaue** (*Waseda University, Waseda Institute for Advanced Study*)
 THz frequency is a special electromagnetic wave which is categorized between a radio wave and a light wave. It can pass through the various materials like a radio wave and can be transported with optical components like a light wave. Thus, it's suitable for imaging application of materials. At Waseda University, it's possible to generate a high-quality electron beam using Cs-Te photocathode RF-Gun and the electron beam is applied to several application researches. As an application of this electron beam, we generate a coherent Cherenkov radiation, and succeed in observing a high power THz light. The successful results of high power THz radiation encourage us to perform the THz imaging with transmission and reflection imaging using some materials, cross-section imaging using a simple material. On studying the THz imaging, it is necessary to clarify the spatial resolution. So, we tried to evaluate the spatial resolution in our device. Furthermore, our target is to get the three-dimensional THz images. We will introduce the CT technique in order to obtain the clear cross-section image. In this conference, we report the recent results of the THz imaging and future prospective.
- TUPOA05 Development of a Fiber Laser for Improving the Pulse Radiolysis System**
Y. Saito (*Waseda University*)
 When material is irradiated by the ionizing radiation, short-lived and highly reactive substance intermediate active species are made and then react with substances. The chemical reaction is determined by intermediate active species in early process. Proving the behavior of intermediate active species is important for understanding and controlling radiation chemical reaction. In Waseda university we been developing a Pulse Radiolysis System, a method to measure the behavior of intermediate species, for radiation chemical analysis with RF electron gun. Currently we are developing a Supercontinuum ray(SC ray) as a probe ray to improve Pulse Radiolysis System. We have introduced a SC ray using Yb fiber laser and PCF(Photonic Crystal Fiber). But this type of prove light isn't stable enough in the visible light region. Therefore we started to study Er fiber laser oscillator as new prove ray source. We have succeeded to oscillate a Er fs laser pulse, second harmonic generation and measurement of hydrated electron in ns time resolution. In this presentation we will report current research about generation of SC ray, Er fiber laser system and dose rate effect against the hydrated electron.
- TUPOA06 The Research and Analysis of the Electro&-Mechanical Interactions in the Crymodule of C-ADS Proton Linac Injector I**
X. Huang (*IHEP*)
 The LLRF System has been successfully used in the ADS Proton Linac injector I test facility built in IHEP. In order to improve the reliability and availability of the system, some measurements and analyses have been done during operation, such as the Lorentz transfer function and several mechanical fast tuner experiments. This article describes the implements of the experiments, analyzes the results and provides effective solutions.
- TUPOA07 IoT Application in the Control System of the BEPCII Power Supplies**
C.H. Wang (*IHEP*)
 In recent years in the development of Internet technology, the Internet of things (IoT) has begun to apply to each domain. The paper introduces the idea how to apply IoT to the accelerator control system and take the existing control system of the BEPCII power supplies as an example for IoT application. It not only introduce the status of the control system of the BEPCII power

supplies, but also present a solution how to apply IoT to the existing control system. The purpose is to make the control system more intelligent and automatically identify what and where problem when the alarm of the control system of the power supplies. That means that IoT can help to automatically identify which crate and which PSC board inserted in the crates and which PSI sitting in the power supply crates as well as the optic fiber cables between the PSCs and the PSIs. It is great convenient for the maintainer to use a mobile phone to diagnose faults and create the electronic maintenance record.

TUPOA08 **High Reliability LLRF System for High Beam Current Proton Accelerator**

Q. Chen (IMP/CAS) *J.M. Byrd, L.R. Doolittle, G. Huang (LBNL)*

High beam current proton accelerator need a high stability, flexibility, reliability low level radio frequency (LLRF) control system for future manufacture produce. Separated the RF front-ended, AD/DA converter, FPGA digital control board for LLRF control system into three modules. Each module can upgrade independently. With the industry standard connectors, they can design individually. Considering high reliability, imported hardware and software interlock protection, monitoring, protection and redundancy circuits are also designed for cavity and equipment protection. For high accuracy measurements and data acquisition, analog differential signals also be chosen for common noise rejection.

TUPOA09 **Installation of the Double Bend Achromat Magnets Blocks in the 1.5 GeV Storage Ring at Synchrotron Solaris and MAX IV**

J.J. Wiechecki, M. Boruchowski, P. Król (Solaris) *M.A.G. Johansson, L. Th'nell (MAX IV Laboratory, Lund University)*
K. Karaś, R. Nietubyć (Solaris National Synchrotron Radiation Centre, Jagiellonian University)

National Radiation Center Solaris is the first synchrotron built in Poland. It replicates the 1.5 GeV storage ring of MAX IV Laboratory. In these storage rings, all magnet elements of each double bend achromat are precision-machined out of a common 4.5 m long solid iron block. Following paper presents the magnet block installation sequence, with focus on canceling sag under own weight to achieve correct straightness in final installed state, and observed long-term deformations.

TUPOA10 **Cyclotrons for Accelerator-Driven Systems**

T.-Y. Lee, H.-S. Lee, J. Lee, S. Shin (PAL) *C.U. Choi, M. Chung (UNIST)*

Accelerator-Driven system (ADS) can transmute long lived nuclear waste to short lived species. For this system to be fully realizable, a very stable high energy and high power proton beam (typically, 1 GeV beam energy and 10 MW beam power) is required, and preparing such a powerful and stable proton beam is very costly. Currently, the most promising candidate is superconducting linear accelerators. However, high power cyclotrons may be used for ADS particularly at the stage of demonstrating proof of principle of ADS. This paper discusses how cyclotrons can be used to demonstrate ADS.

TUPOA11 **Power Positron Beams as a Novel Road for Apply Physics**

V.V. Gorev (NRC)

After more then 60 years of intensive study, it is clear now that some apply problems have no solution within framework of the present day technical level. Especially, this concerns high velocity acceleration of macroparticles* and extremaly short wave lasers. In this talk I will discuss to day situation in power positron beams and usage of this simplest form of antimatter for above-mentioned problems

TUPOA12 **The Updated of LLRF Control System for the TLS LINAC**

C.Y. Wu, Y.-S. Cheng, P.C. Chiu, K.T. Hsu, K.H. Hu, D. Lee, C.Y. Liao (NSRRC)

The performance of linear accelerator (LINAC) affects beam stability of injector directly. The amplitude and phase of the RF field at LINAC will decide the quality of the extracted beam. In order to improve and study performance of the linac system for the Taiwan Light Source (TLS), the new design of low-level radio frequency (LLRF) control system are developed and setup for the TLS LINAC. The main component of LLRF control system equip with I/Q modulator, Ethernet-based waveform generator, I/Q demodulator and LLRF timing/interlock circuit which are essential part of LLRF feedforward control. This paper will present the efforts for improving of LLRF control system. A feasibility of the LLRF feed-forward control will be studied at the linear accelerator of TLS.

TUPOA13 **Planned High Density Material Imaging Experiments Using Relativistic Electron Beam at the Argonne Wakefield Accelerator**

Y.R. Wang (AAI/ANL) *M.E. Conde, D.S. Doran, W. Gai, W. Liu, J.G. Power, J.Q. Qiu, C. Whiteford, E.E. Wisniewski (ANL)*
Z.M. Zhang (IMP/CAS)

A test facility, AWA, has been commissioned and in operation since last year. It can provide beam of several bunches in a train of nano-seconds and 10s of nC with energy up to 70 MeV. In addition, the AWA can accommodate various beamlines for experiments. One of the proposed experiments is to use the AWA beam as a diagnostics for time resolved high density material, typically a target with high Z and time dependent, imaging experiments. When electron beam scatters after passing through the target, and the angular and energy distribution of beam will depend on the density and thickness of the target. A small aperture is used to collimate the scattered electron beam for off axis particles, and the target image will be detected by imaging plate. By measuring the scattered angle and energy at the imaging plate would yield information of the target. In this paper, we will report on the planned experiments setup, which consist of a target, imaging optics and 4 meters of beam transport. The imaging beamline is currently under installation and experiment will be performed soon. This work will have implication on the high energy density physics and even future nuclear fusion studies.

TUPOA14 **An Internet Rack Monitor-Controller for APS LINAC RF Electronics Upgrade**

H. Ma, A. Nassiri, T.L. Smith, Y.-E. Sun (ANL) *L.R. Doolittle, A. Ratti (LBNL)*

To support the current research and development in APS LINAC area, the existing LINAC rf control performance needs to be much improved, and thus an upgrade of the legacy LINAC rf electronics becomes necessary. The proposed upgrade plan centers on the concept of using a modern, network-attached, rack-mount digital electronics platform 'Internet Rack Monitor-Controller (or IRMC)' to replace the existing analog ones on the legacy crate/backplane-based hardware. The system model of the envisioned IRMC is basically a 3-tier stack with a high-performance processor in the mid- layer to handle the general digital signal processing (DSP). The custom FPGA IP's in the bottom layer handle the high-speed, real-time, low-latency DSP tasks, and provide the interface ports. A network communication gateway, in conjunction with an embedded event receiver (EVR), in the top layer merges the Internet Rack Monitor-Controller device into the networks of the accelerator controls infrastructure. Although the concept is very much in trend with today's Internet-of-Things (IoT), this implementation has actually been used in accelerators for over two decades.

TUPOA15 **Design and Operation of a Multi-slit Emittance Station at the FAST Facility**

D.J. Crawford (Fermilab)

The Fermilab Accelerator Science and Technology (FAST) facility has accelerated electrons to 50 MeV. A diagnostic station was developed to utilize the multi-slit method for transverse emittance measurement. We report on the design and first beam measurements.

TUPOA16 A VME and FPGA Based Data Acquisition System for Intensity Monitors

J.S. Diamond, A. Ibrahim, N. Liu, A. Semenov, R. Tokarek (Fermilab)

A universal data acquisition front end supporting Toroids, DCCTs, Faraday Cups, Scrapers and other types of intensity monitors has been developed for reporting beam intensity measurements to the Fermilab accelerator controls system (ACNET). Instances of this front end, supporting dozens of intensity monitor devices, have been deployed throughout the Fermilab accelerator complex in the Main Injector, Recycler, Fermilab Accelerator Science and Technology (FAST) facility and the PIP-II Injector Experiment (PXIE). Each front end consists of a VME chassis containing a single board computer (SBC), timing and clock module and one or more 12-channel data acquisition modules. The data acquisition modules are based on the Cyclone V FPGA with firmware developed in-house allowing a wide range of flexibility and digital signal processing (DSP) capability. The front end data acquisition software adds a list of new features to the previous generation allowing users to: take beam intensity measurements at custom points in the acceleration cycle, access waveform data, control machine protection system (MPS) parameters and calculate beam energy loss.

TUPOA17 A Longitudinal Digital Mode Damper System for the Fermilab Booster

N. Eddy (Fermilab)

The Fermilab Booster accelerates bunches and accelerates proton beams from 400 MeV to 8 GeV. During the acceleration the Radio Frequency (RF) cavities are swept from 38MHz to 52.8MHz and requires crossing through transition where accelerating phase is shifted 90 degrees. In order to keep the beam stable and minimize losses and emittance growth a longitudinal damping system is required. This has traditionally been done by dedicated analog electronics designed to operate on specific beam modes for frequencies of instabilities. A complete digital implementation has been developed for this same purpose. The new digital system features and performance are detailed.

TUPOA18 Low level RF Control for the PIP-II Injector Test RFQ and Bunching Cavity

J.P. Edelen, B.E. Chase, E. Cullerton, J. Einstein, P. Varghese (Fermilab)

The PIP-II injector test radio frequency quadrupole (RFQ) arrived at Fermilab in the fall of 2015. The RFQ is a 162.5MHz H⁺ accelerator with a nominal drive power of 100kW which yields a beam energy of 2.1MeV. In this paper we discuss operational issues and optimization of the low level RF (LLRF) control system for both the RFQ and bunching cavity. We will begin by describing the general system configuration used during pulsed operations and discuss briefly the CW commissioning of the bunching cavity. We will then highlight temperature related issues in the high power RF system, which necessitate active control over the phase and amplitude balance of the two amplifiers. Results of this controller show a greater degree of stability in the RF system over time and improve the overall performance of the machine. Additionally we demonstrate performance of the RF feedback and feed-forward compensation needed to produce a flat RF field during 20 microsecond beam pulses in both the RFQ and in the bunching cavity.

TUPOA19 The 50-MeV Run in the FAST Electron Accelerator

D.R. Edstrom, C.M. Baffes, C.I. Briegel, D.R. Broemmelsiek, K. Carlson, B.E. Chase, D.J. Crawford, E. Cullerton, J.S. Diamond, N. Eddy, B.J. Fellenz, E.R. Harms, M.J. Kucera, J.R. Leibfritz, A.H. Lumpkin, D.J. Nicklaus, E. Prebys, P.S. Prieto, J. Reid, J. Ruan, J.K. Santucci, T. Sen, V.D. Shiltsev, G. Stancari, J.C.T. Thangaraj, R.M. Thurman-Keup, A. Valishev, A. Warner, S.J. Wesseln (Fermilab) A. Halavanau, D. Mihalcea, P. Piot (Northern Illinois University) J. Hyun (Sokendai) P. Kobak (BYU-I) W.D. Rush (KU)

The low-energy section of the photoinjector-based electron linear accelerator at the Fermilab Accelerator Science & Technology (FAST) facility was recently commissioned to an energy of 50 MeV. This linear accelerator relies primarily upon pulsed SRF acceleration and an optional bunch compressor to produce a stable beam within a large operational regime in terms of bunch charge, total average charge, bunch length, and beam energy. Various instrumentation was used to characterize fundamental properties of the electron beam including the intensity, stability, emittance, and bunch length. While much of this instrumentation was commissioned in a 20 MeV running period prior, some (including a new Martin-Puplett interferometer) was in development or pending installation at that time. All instrumentation has since been recommissioned over the wide operational range of beam energies up to 50 MeV, intensities up to 4 nC/pulse, and bunch structures from ~1 ps to more than 50 ps in length.

TUPOA20 3D Hall Probe Calibration for Mu2e Experiment

L. Elementi (Fermilab)

Fermilab Magnet System is readying to calibrate 3-D hall probe sensors to high accuracy with the intended purpose of characterizing the Detector Solenoid Field for the Mu2e experiment currently under construction. In order to achieve few tens of ppm simultaneously in the three Cartesian coordinates we are using a temperature and current regulated calibration magnet with a known geometry and designed special purpose equipment. Simulation of the effect of specific geometrical and constructive deviation have been simulated with the goal of perfecting the Calibration Equipment one order of magnitude above the accuracy required by the experiment. The equipment in use, process and results are herein presented and analyzed.

TUPOA21 NM4 South Labyrinth Dose Rate Measurement

M.G. Geelhoed (Fermilab)

The prompt dose rate from a labyrinth in an enclosure has been on going with multiple measurements. The source of the radiation in the service building has been difficult to locate based on its low dose rate, and complex experimental hall shielding geometry. Currently the measurements that have been calculated in the past have been in a parking lot outside, both upstream and downstream labyrinth exits of the enclosure, and penetrations leading from the enclosure. This latest measurement focused primarily on the south labyrinth, where dose rates can't be confirmed from the labyrinth as a single source.

TUPOA22 Multiharmonic RF Gun for Industrial Electron Accelerator

I.V. Gonin, R.D. Kephart, T.N. Khabiboulline, N. Solyak, V.P. Yakovlev (Fermilab)

We will present our current activity in the development of compact RF-Gun. The goal of design is to optimize the RF-Gun and 1.3 GHz cavity assembly to minimize the power losses in the cavity walls as well as in cathode due to backward bombardment. Low energy part simulations has been done by SMASON code. High energy part beam simulations and analysis of beam distribution at accelerator exit has been done by MatLab script.

TUPOA23 Search for X-Ray Channeling Radiation at FAST

P. Hall (Fermilab)

Channeling Radiation (CR) is generated by charged beams (typically electrons or positrons) passing through a crystal parallel with a crystallographic plane*. Electrons may oscillate perpendicular to the plane and generate CR which propagates in the same direction as the incident beam**. Electron beams with moderate energy ranging from 4 to 50 MeV can be used to produce x-rays through Channeling Radiation. The x-ray spectrum from electron beams extends up to 140 keV, and this range covers the demand for most practical applications***. The beam experiment at the Fermilab Accelerator Science and Technology (FAST) facility will have a beam energy of 50 MeV, and offers the possibility of a precise, tunable X-ray source. This poster will give a brief overview of FAST's channeling radiation experiment, and the progress made in achieving x-ray channeling radiation.

TUPOA24 **The Beam Intensity Monitoring System for the PIP-II Injector Test Accelerator**

N. Liu, N. Eddy (Fermilab)

The PIP-II injector test accelerator is an integrated systems test for the front-end of a proposed CW-compatible, pulsed H⁻ superconducting RF linac. This linac is part of Fermilab's Proton Improvement Plan II (PIP-II) upgrade. This injector test accelerator will help minimize the technical risk elements for PIP-II and validate the concept of the front-end. Major goals of the injector accelerator are to test a CW RFQ and H⁻ source, a bunch-by-bunch MEBT beam chopper and stable beam acceleration through low-energy superconducting cavities. Operation and characterization of this injector places stringent demands on the types and performance of the accelerator beam diagnostics. This paper discusses the beam intensity monitor systems as well as early commissioning measurements of beam transport through the Medium-Energy Beam Transport (MEBT) beamline.

TUPOA25 **Initial Demonstration of 9-MHz Framing Camera Rates on the FAST UV Drive Laser Pulse Trains***

A.H. Lumpkin, D.R. Edstrom, J. Ruan (Fermilab)

Although beam centroid information at the MHz-micropulse-repetition rate has routinely been achieved at various facilities with rf BPMS, the challenge of recording beam size information at that rate is more daunting. The Integrable Optics Test Accelerator (IOTA) ring being planned at Fermilab has ~8 MHz revolution rates. To simulate the IOTA synchrotron radiation source temporal structure, we have used the UV component of the drive laser of the Fermilab Accelerator Science and Technology (FAST) Facility. This laser is normally set at 3 MHz, but has also been run at 9 MHz. We have configured our Hamamatsu C5680 streak camera in a framing camera mode using a slow vertical sweep plugin unit with the dual axis horizontal sweep unit**. A two-dimensional array of images sampled at the MHz rate can then be displayed on the streak tube phosphor and recorded by the CCD readout camera at up to 10 Hz. As an example, by using the 10 microsecond vertical sweep with the 100 microsecond horizontal sweep ranges, 49 of the 300 micropulses at 3 MHz are displayed for a given trigger delay in each of six images. Example 2D image arrays with profiling examples will be presented.

TUPOA26 **Observations of Bunch Elongation of Electron Beams in a SCRF Accelerator***

A.H. Lumpkin, D.R. Edstrom, J. Ruan, J.K. Santucci, R.M. Thurman-Keup (Fermilab)

Commissioning at the SCRF accelerator at the Fermilab Accelerator Science and Technology (FAST) Facility has included the implementation of a versatile bunch-length monitor located after the 4-dipole chicane bunch compressor for electron beam energies of 20-50 MeV and integrated charges in excess of 10 nC. The team has initially used a Hamamatsu C5680 synchroscan streak camera. An Al-coated Si screen was used to generate optical transition radiation (OTR) resulting from the beam's interaction with the screen. The chicane bypass beamline allowed the measurements of the bunch length without the compression stage at the downstream beamline location using OTR and the streak camera. The UV component of the drive laser had previously been characterized with a Gaussian fit sigma of 3.5-3.7 ps**. However, the uncompressed electron beam is expected to elongate due to space charge forces in an initial 1.5-m drift from the gun to the first SCRF accelerator cavity. We have observed electron beam bunch lengths from 5 to 14 ps (sigma) for micropulse charges of 60 pC to 800 pC, respectively. Commissioning of the system and initial results with uncompressed and compressed beam will be presented.

TUPOA27 **From Relativistic Electrons to X-ray Phase Contrast Imaging**

A.H. Lumpkin (Fermilab) M.A. Anastasio, A.B. Garson (Washington University in St. Louis)

X-ray phase contrast (XPC) imaging is an emerging technology that holds great promise for biomedical applications due to its ability to provide information about soft tissue structure *. The need for high spatial resolution at the boundaries of the tissues is noted for this process. Based on results from imaging of relativistic electron beams with single crystals **, we proposed transferring single-crystal imaging technology to this bio-imaging issue. Using a microfocus x-ray tube (17 kVp) and the exchangeable phosphor feature of the camera system, we compared the point spread function (PSF) of the system with the reference P43 phosphor to that with several rare earth garnet single crystals of varying thickness. Based on single Gaussian peak fits to the collimated x-ray images, we observed a four times smaller system PSF (21 microns (FWHM)) with the 25-mm diameter single crystals than with the reference polycrystalline phosphor's 80-micron value. Initial images of 33-micron diameter carbon fibers have also been obtained with small crystals installed. Tests with a full-scale 88-mm diameter single crystal (patent-pending configuration) are being planned.

TUPOA28 **Feasibility of Optical Transition Radiation Imaging for Laser-Driven Plasma Accelerator Electron-Beam Diagnostics**

A.H. Lumpkin (Fermilab) M. Downer (The University of Texas at Austin) D.W. Rule (Private Address)

Recent measurements of betatron x-ray emission from quasi-monoenergetic electrons accelerating to 500 MeV within a laser plasma accelerator (LPA) enabled estimates of normalized transverse emittance well below 1 mm-mrad and divergences of order 1/gamma [1]. Such unprecedented LPA beam parameters can, in principle, be addressed by utilizing the properties of linearly polarized optical transition radiation (OTR) that provide additional beam parameter sensitivity. We propose a set of complementary measurements of beam size and divergence with near-field and far-field OTR imaging, respectively, on LPA electron beams ranging in energy from 100 MeV [2] to 2 GeV [3]. The feasibility is supported by analytical modeling for beam size sensitivity and divergence sensitivity. In the latter case, the calculations indicate that the parallel polarization component of the far-field OTR pattern is sensitive to divergences from 0.1 to 0.4 mrad (sigma) at 2 GeV, and it is similarly sensitive to divergences from 1 to 5 mrad (sigma) at 100 MeV. We anticipate the signal levels from charges of 100 pC will require a 16-bit cooled CCD camera. Other practical challenges in the LPA will also be discussed.

TUPOA29 **The Beam Position Monitoring System for the PIP-II Injector Test Accelerator**

N. Patel, J.S. Diamond, N. Eddy, B.J. Fellenz, J. Fitzgerald, V.E. Scarpine (Fermilab)

The PIP-II injector test accelerator is an integrated systems test for the front-end of a proposed CW-compatible, pulsed H⁻ superconducting RF linac. This linac is part of Fermilab's Proton Improvement Plan II (PIP-II) upgrade. This injector test accelerator will help minimize the technical risk elements for PIP-II and validate the concept of the front-end. Major goals of the injector

accelerator are to test a CW RFQ and H⁻ source, a bunch-by-bunch MEBT beam chopper and stable beam acceleration through low-energy superconducting cavities. Operation and characterization of this injector places stringent demands on the types and performance of the accelerator beam diagnostics. This paper discusses the beam position monitors system as well as early commissioning measurements of beam transport through the Medium-Energy Beam Transport (MEBT) beamline.

TUPOA30 **Fermilab Switchyard Resonant BPM Electronics Upgrade**

T.B. Petersen (*Fermilab*)

The readout electronics for the resonant beam position monitors (BPMs) in the Fermilab Switchyard have been upgraded, utilizing a low noise amplifier transition board and Fermilab designed digitizer boards. Beam intensities range from 10⁷ protons/bunch and a stripline BPM is used to detect the charge. The BPM has an estimated average signal output of between -110 dBm and -80 dBm, with an estimated peak output of -70 dBm. An external resonant circuit which uses the plate capacitance and a tuned coil to the SY machine frequency of 53.10348 MHz. Both the digitizer and transition boards have variable gain in order to accommodate the large dynamic range and irregularity of the resonant extraction spill. These BPMs will aid in auto-tuning of the SY beamline as well as enabling operators to monitor beam position through the spill.

TUPOA31 **Fermilab Cryomodule Test Stand Interlocks System**

T.B. Petersen (*Fermilab*)

An interlock system has been designed for the Fermilab Cryomodule Test Stand (CMTS), a test bed for the cryomodules to be used in the upcoming Linac Coherent Light Source 2 (LCLS-II) project at SLAC. The interlock system features 8 independent subsystems, consisting of a superconducting RF cavity, a coupler, and solid state amplifier (SSA). Each system monitors several devices to detect fault conditions such as arcing in the waveguides or quenching of the SRF system. Additionally each system can detect fault conditions by monitoring the RF power seen at the cavity coupler through a directional coupler. In the event of a fault condition, each system is capable of removing RF signal to the amplifier (via a fast RF switch) as well as turning off SSA. Additionally, each input signal is available for remote viewing and recording via a Fermilab designed digitizer board.

TUPOA32 **Mars15-Based Fermicord Code System for Calculation of the Accelerator-Induced Residual Dose**

V.S. Pronskikh, A.F. Leveling, N.V. Mokhov (*Fermilab*) **A.V. Grebe** (*MIT*) **T. Lu** (*IMSA*)

FermiCORD is a set of codes based on the MARS15 Monte-Carlo code system that calculates the accelerator-induced residual doses at experimental facilities of arbitrary configurations. FermiCORD has been written in C++ and runs under Linux. The algorithm consists of two stages: 1) Simulation of residual doses on contact with the surfaces surrounding the studied location and of radionuclide inventories in the structures surrounding those locations using MARS15, and 2) simulation of the emission of the nuclear decay photons by the residuals in the activated structures and scoring the prompt doses of these photons at arbitrary distances from those structures. FermiCORD has been validated using similar algorithms based on other code systems and showed a good agreement. It has been applied for calculation of the residual dose of the target station for the Mu2e experiment and the results have been compared to existing approximate approaches.

TUPOA33 **Thermal Analysis of Energy Production Demonstrator for Megawatt Proton Beams**

V.S. Pronskikh, N.V. Mokhov, I. Novitski (*Fermilab*) **S.I. Tyutyunnikov** (*JINR*)

A preliminary study of the Energy Production Demonstrator (EPD) concept - a solid heavy metal target irradiated by GeV-range intense proton beams and producing more energy than consuming - is carried out. Neutron production, fission, energy deposition, energy gain, testing volume and helium production are simulated with the MARS15 code for tungsten, thorium, and natural uranium targets in the proton energy range of 0.5 to 120 GeV. This study shows that proton energies from 2 to 4 GeV are optimal for both a natU EPD and the tungsten-based testing station that would be the most suitable for proton accelerator facilities. Conservative estimates of the beam power sufficient for energy production, not including breeding and fission of plutonium, based on the simulations are made. Using as an input the MARS15-calculated energy maps, the ANSYS thermal analysis shows that the concept considered has a problem due to a possible core meltdown. A number of approaches are suggested to mitigate the issue.

TUPOA34 **Value Analysis of Accelerator-Driven System Options**

V.S. Pronskikh (*Fermilab*) **B. Taebi** (*Harvard University, Belfer Center for Science and International Affairs*)

Nuclear energy brings a number of large benefits but it also presents certain risks and concerns, which are to be reduced if nuclear energy is to be considered a viable option in the future energy mix. Accelerator-driven systems (ADS), i.e. systems including accelerator and subcritical reactor capable of both nuclear energy production and incineration of nuclear wastes with little greenhouse gas productions are often considered an alternative to conventional nuclear power stations. We perform a comparative analysis of several ADS designs (Pb+Bi target/MOX blanket, Pb+Bi target/Minor Actinide (MA) blanket, and MA molten salt on the one hand and Fast Breeder Reactors (FBR) on the other, based on an underlying set of values that associate with the burdens and benefits of each cycle. We derive our set of values from the notion of sustainability, including environmental friendliness, public safety, security, safeguards, resource durability, and economic viability. We will investigate which alternative allows a more equitable distribution of both benefits from energy production and burdens imposed by it on present and future generations.

TUPOA35 **A Non-Invasive Beam Profile Measurement for the Fermilab Booster**

R. Tesarek (*Fermilab*)

Measurements of the beam profile allow for the determination of the phase space occupied by the beam and predictions of possible beam loss patterns. Measurement of accelerator losses are used as a diagnostic tool to understand aperture restrictions and confirm predictions noted above. It is seldom that the two measurements may be made using the same instrumentation. We present here the first measurements of the Fermilab booster horizontal beam profile using fast loss monitors. The profiles are measured after injection by observing the scattering of protons from the H⁻ stripping foils. We show that the beam profile measurements may be calibrated in situ and thus relax requirements for a detailed calibration and detector stability. Finally, we compare these profile measurements with those from other techniques.

TUPOA36 **Computed Tomography of Transverse Phase Space**

A.C. Watts, C. Johnstone, J.A. Johnstone (*Fermilab*)

Two computed tomography techniques are explored to reconstruct beam transverse phase space using both simulated beam and multi-wire profile data in the Fermilab Muon Test Area ("MTA") beamline. Both Filtered Back-Projection ("FBP") and Simultaneous Algebraic Reconstruction Technique ("SART") algorithms are considered and compared. Errors and artifacts are compared as a function of each algorithm's free parameters, and it is shown through simulation and MTA beamline profiles that SART is advantageous for reconstructions with limited profile data.

TUPOA37 Long-Term Performance and Autopsies of the NuMI Hadron Monitor**R.M. Zwaska** (*Fermilab*)

The hadron monitor is an device within the secondary beam of the NuMI neutrino facility at Fermilab, critical in commissioning and beam-based alignment. The hadron monitor rests at the end of the decay region, 700 m downstream of the particle-production target. The hadron monitor measures the spatial distribution of the surviving proton beam after interaction with the target. The hadron monitor signals are directly related with the amount of material the proton beam traversed, essentially radiographing the target and other components near the beamline axis. Since first beam in 2004, the hadron monitor has been the central tool for aligning the target. It is exposed to high-radiation (> 1 GRad / year), and is designed to be robust; it is composed of an array of helium ionization chambers. Two hadron monitors have failed during beam operation, with degrading signal quality and increased leakage current. A third is in present operation. Autopsies of the first two devices were performed. We report on in-beam performance data of these devices, the results of the autopsies, and prescriptions for future devices.

TUPOA38 Real-Time Magnetic Electron Energy Spectrometer for Use With Medical Linear Accelerators**P.E. Maggi, H.R. Hogstrom, K.L. Matthews II** (*LSU*) **R.L. Carver** (*Mary Bird Perkins Cancer Center, Our Lady of the Lake*)

Accelerator characterization and quality assurance is an integral part of electron linear accelerator (linac) use in a medical setting. The current clinical method for radiation metrology of electron beams (dose deposition versus depth in water) only provides a surrogate for the underlying performance of the accelerator, and does not provide direct information about the electron energy spectrum. We have developed an easy to use real-time magnetic electron energy spectrometer for characterizing the electron beams of medical linacs. Our spectrometer uses a 0.54 T permanent magnet block as the dispersive element, and scintillating fibers coupled to a CCD camera as the position sensitive detector. The goal is to have a device capable of 0.3 MeV energy resolution (which corresponds to a range shift of approximately 1 mm), with a minimum readout rate of 1 Hz, over an energy range of 3 to 25 MeV. This work describes the real-time spectrometer system, the detector response model, and the spectrum unfolding method. Measured energy spectra from multiple electron beams are presented.

TUPOA39 Plans for Synchronization of the HiRES Ultrafast Electron Diffraction Facility at LBNL**J.M. Byrd, L.R. Doolittle, Q. Du, D. Filippetto, G. Huang, R.B. Wilcox** (*LBNL*)

The HiRES facility is a new development at LBNL of a high repetition rate, high brightness electron source for electron scattering. HiRES is based on the APEX gun, producing femtosecond relativistic pulses, capable of running with repetition rates up to 186 MHz at beam energies of under 1 MeV, with an average flux in excess of 10^{13} electrons/s. The electron source has successfully tested at LBNL and a dedicated diffraction beamline (HiRES) is now under commissioning. The electron flux will benefit the S/N ratio in stroboscopic experiments. Femtosecond synchronization between the electron beam and pump laser is critical for time-resolved pump-probe experiments. The high repetition rate will provide a unique opportunity to combine jitter reduction techniques on individual systems with beam-based feedback to reach the highest level of synchronization. We plan to combine high precision RF control, laser-RF synchronization, laser-laser synchronization, and beam-based feedback to reach this goal. This paper will outline our plans to implement this synchronization for the near future.

TUPOA40 Low Noise Digitizer Design for LCLS-II LLRF**G. Huang, L.R. Doolittle, Y.L. Xu, J. Yang** (*LBNL*) **Y.L. Xu, J. Yang** (*TUB*)

Modern accelerators use a digital low level RF controller to stabilize the fields in accelerator cavities. The noise in the receiver chain and analog to digital conversion (ADC) for the cavity probe signal is critically important. Within the closed-loop bandwidth, it will eventually become part of the field noise seen by the beam in the accelerator. Above the open-loop cavity bandwidth, feedback processes transfer that noise to the high power drive amplifiers. The LCLS-II project is expected to use an undulator to provide soft X-rays based on a stable electron beam accelerated by a superconducting linac. Project success depends on a low noise, low crosstalk analog to digital conversion. We developed a digitizer board with 8 ADC channels and 2 DAC channels. The broadband phase noise of this board is measured at < -151 dBc/Hz, and the adjacent channel crosstalk is measured at < -80 dB. In this paper we describe the digitizer board design, performance test procedures, and bench-test results.

TUPOA41 FPGA Control in Laser Pulse Stacking**Y.L. Xu, J.M. Byrd, L.R. Doolittle, Q. Du, G. Huang, R.B. Wilcox, Y. Yang** (*LBNL*)

Laser pulse stacking (LPS) is a new time-domain coherent addition technique that stacking several optical pulses into a single output pulse, enabling high average power and kHz repetition rate. Due to advantages of precise timing and fast processing, FPGA processes digital signals and does feedback control so as to realize the stacking-cavity stabilization. We develop a hardware and firmware design platform to support the laser pulse stacking application. Bias control module for the modulator is implemented to stabilize the bias operating point at the minimum of its transfer function. Cavity control module ensures that each optical cavity is kept at a certain individually-prescribed and stable round-trip phase in this pulse stacking system.

TUPOA42 4-Cavity Pulse Stacking Using Herriott Cell**Y. Yang, G. Huang, Q. Qiang, R.B. Wilcox** (*LBNL*) **Y.L. Xu** (*TUB*)

Coherent Pulse Stacking provides a promising way to generate a single high energy pulses from a sequence of phase and amplitude modulated laser pulses using a set of optical cavities. Herriot cell can be used as the cavities for its transverse stability. Experiment have shown that 4 Herriot cell cavities can generate a peak power enhancement factor of 7 and near 95% efficiency. This can provide a new path for the tens of J KHz laser pulse for the future kHz laser-drive plasma accelerator facility.

TUPOA43 Artificial Intelligence Based Control Toolkits for Accelerators**S. Biedron, A.L. Edelen, S.V. Milton** (*Element Aero*)

Element Aero is developing adaptive, artificial intelligence-based tools specifically to address control challenges found in complex systems such as high-power lasers, directed energy systems, and particle accelerators. We will discuss the opportunities and challenges, especially for future compact, mobile sources that will not necessarily be co-located with expert operators. We also discuss our plans to develop a portable AI toolbox for use in particle accelerators that will link directly to larger control systems such as EPICS.

TUPOA44 Future Prospects of RF Hadron Beam Profile Monitors for Intense Neutrino Beam**Q. Liu** (*Case Western Reserve University*) **M. Backfish, A. Moretti, V. Papadimitriou, A.V. Tollestrup, K. Yonehara, R.M. Zwaska** (*Fermilab*) **M.A.C. Cummings, R.P. Johnson, G.M. Kazakevich** (*Muons, Inc*) **B.T. Freemire, Y. Torun** (*IIT*)

A novel beam monitor based on a gas-filled RF resonator is proposed to measure the precise profile of secondary particles downstream of a target in the LBNF beam line at high intensity. The RF monitor is so simple that it promises to be radiation robust

in extremely high-radiation environment. When a charged beam passes through a gas-filled microwave RF cavity, it produces electron-ion pairs in the RF cavity. The induced plasma changes the gas permittivity in proportion to the beam intensity. The permittivity shift can be measured by the modulated RF frequency and quality factor. The beam profile can thus be reconstructed from the signals from individual RF cavity pixels built into the beam profile monitor. A demonstration test is underway, and the current results has shown technical feasibility. The next phase consists of two stages, (1) to build and test a new multi-cell 2.45 GHz RF cavity that can be used for the NuMI beamline, and (2) to build and test a new multi-cell 9.3 GHz RF cavity that can be put in service in a future beamline at the LBNF for spatial resolution. These two resonant frequencies are chosen since they are the standard frequencies for magnetron RF source.

TUP0A45 **Multi-Electrode Sensors to Quantify Moments of a Non Relativistic Beam**

B. Beaudoin, H. Baumgartner, S. Bernal, I. Haber, R.A. Kishek, T.W. Koeth, K.J. Ruisard, D.F. Sutter (UMD)

The use of multi-electrode beam sensors with eight or more elements is not well developed, even though theoretical studies have indicated that eight or more sensors may be able to provide better resolution of a beam's second and higher order moments. Accelerator applications where the preservation of beam emittance, matching and spot size at final focus are critical, and will be substantially impacted by the availability of an inexpensive and reliable means of measuring beam second moments. This is particularly true for medical applications, materials processing, certain light sources and low energy front end optics of research facilities for high energy and nuclear physics. While a destructive means for measuring beam intensity and position are very well developed, there is still a need to develop a non-destructive and inexpensive means for determining beam cross section and its evolution over multiple turns of an intense particle beam. This paper details the initial work on evaluating the second moments from Beam Position Monitor (BPM) data of the University of Maryland Electron Ring (UMER) beam as well as data from bench tests of a prototype multi-element wall current sensor.

TUP0A46 **Development of Automated Beam Emittance Measurement System via the Quadrupole Scan Technique at the Fermilab Accelerator Science and Technology (FAST) Facility**

A.T. Green (Northern Illinois University) Y.-M. Shin (Fermilab) Y.-M. Shin (Northern Illinois University)

Beam emittance is an important characteristic which helps to describe a charged particle beam. In linear accelerators (linac), it is critical to characterize the beam phase space parameters and, in particular, to precisely measure transverse beam emittance. The quadrupole scan (quad-scan) is a well established technique used to characterize transverse beam parameters in four-dimensional phase space. Quad-scans are very time consuming and off-line analysis is needed to extrapolate the beam phase space parameters. We have developed a computational algorithm with Python scripts to automatically estimate beam parameters, in particular beam emittance, using the quadrupole scan technique in the electron linac of Fermilab Accelerator Science and Technology (FAST) facility. These Python scripts have decreased the time it takes to perform a single quad scan from a few hours to a few minutes. From the experimental data, the emittance calculator quickly delivers various results including: transverse emittance, Courant-Snyder parameters, and Beam Size (squared) vs Quadrupole field strength plots, among others.

TUP0A47 **Development of Short Undulators for Electron-Beam-Radiation Interaction Studies**

P. Piot (Fermilab), M.B. Andorf (Northern Illinois University)

Interaction of an electron beam with external field or its own radiation has widespread applications ranging from coherent radiation generation, phase space cooling or formation of time-structured beam. An efficient coupling mechanism between an electron beam and radiation field relies on the use of a magnetic undulator. In this contribution we detail the construction and magnetic measurements of short (11 period) undulators with 7-cm period built using parts of the ALADDIN U3 undulator*. Possible use of these undulators at two accelerator test facilities to support experiment relevant to cooling techniques and radiation sources are discussed.

TUP0A48 **A High-Level Python Interface to Fermilab ACNET Control System**

P. Piot (Fermilab), A. Halavanau (Northern Illinois University)

This paper discusses the implementation of a PYTHON-based high-level interface to the Fermilab ACNET control system. We will especially present examples of applications which include the interfacing of an ELEGANT beam-dynamics model to assist lattice matching and an automated emittance measurement via the quadrupole-scan method.

TUP0A49 **A General Model of Vacuum Arcs in Linacs**

J. Norem (Nano Synergy, Inc.) Z. Insepov (Purdue University)

We are developing a general model of breakdown and gradient limits that applies to accelerators, along with other high field applications such as power grids and laser ablation. Our recent efforts have considered failure modes of integrated circuits, sheath properties of dense, non-Debye plasmas and applications of capillary wave theory to rf breakdown in linacs. In contrast to much of the rf breakdown effort that considers one physical mechanism or one experimental geometry, we are finding that there is an enormous volume of relevant material in the literature that helps to constrain our model and suggest experimental tests.

TUP0A51 **Machine Learning and Artificial Intelligence Based Controls for Particle Accelerators**

A.L. Edelen, S. Biedron, S.V. Milton (CSU) D.L. Bowring, B.E. Chase, J.P. Edelen, J. Steimel (Fermilab)

Particle accelerators have nonlinear and complex physical phenomena. They involve a multitude of interacting systems, are subject to tight performance demands, and should be able to run for extended periods of time with minimal interruptions. Machine learning and artificial intelligence constitutes a versatile set of techniques that are particularly well-suited to modeling, control, and diagnostic analysis of complex, nonlinear, and time-varying systems, as well as systems with large parameter spaces. Consequently, the use of adaptive, machine learning and artificial intelligence-based modeling and control techniques could be of significant benefit to particle accelerators and the scientific endeavors that they support. Recently, we have developed and tested a set of neural network-based control systems at Fermilab for the PXIE RFQ. The control systems - based on model predictive control and reinforcement learning - regulate the resonant frequency of the RFQ by adjusting the temperature of the water in the wall and vane cooling circuits. Results of our tests and description of the systems are presented herein, along with the results of test cases conducted on various machines.

TUP0A52 **Updates to the Low-Level RF Architecture for Fermilab**

J. Einstein, S. Biedron, S.V. Milton (CSU) B.E. Chase, J. Einstein (Fermilab)

Fermilab has teamed with Colorado State University on several projects in LLRF controls and architecture. These projects include new LLRF hardware, updated controls techniques, and new system architectures. Here we present a summary of our work to date.

- TUP0A53 Preliminary Results of Electro-Optic Longitudinal Bunch Profile**
J.E. Williams, S. Biedron, S.V. Milton (CSU) S.V. Benson, S. Zhang (JLab)
 Development of the next generation FEL light sources requires improving emittance measurement techniques to best correlate the input beam with its respective output. With output requirements pushing past operating longitudinal bunch sizes, accurate measurement in this degree of freedom is important for optimal input analysis. The use of electro optic diagnostics to measure the longitudinal bunch size had been employed previously to sub-100s of femtosecond accuracy at various machines, however this work explores implementation on a high average current light source. The initial results and crystal status post operation are presented in the following paper.
- TUP0A54 Examination of Out-of-Field Dose and Penumbra Width of Flattening Filter Free Beams in Medical Linear Accelerators**
L.C. Bennett, O. N. Vassiliev (M.D.A.C.C.)
 Medical linear accelerators (LINACS) have traditionally used a flattening filter to ensure that the photon spectrum entering the patient was homogeneous within a given field size. Recently, leading manufacturers of medical accelerators have begun including an option for Flattening Filter Free (FFF) beams on their accelerators. These beams are characterized by a softer spectrum (lower average energy), peaked profiles, and less side scatter. Previous work with Monte Carlo models has shown that the elimination of the flattening filter from the beam path has the potential to greatly reduce scatter in regions immediately adjacent to the primary field (Kry 2010); however, systematic in-depth investigation of these effects has yet to be done using actual measurements from a linac equipped with FFF beams. We have examined and compared measurements of different energy pairings of FFF and FF beams from the Varian TrueBeam accelerators and found reductions of peripheral dose at upwards of 30% for the FFF beams and nearly 5% reduction in penumbral width at nearly all depths and field sizes; reductions were greatest for shallow depths and small field size.
- TUP0A56 MuSTAR - SRF Linacs Driving Subcritical GEM*STAR Small Modular Systems**
R.P. Johnson, R.J. Abrams, M.A.C. Cummings, M.L. Neubauer, T.J. Roberts (Muons, Inc)
 Mu*STAR Inc., promoting high-power superconducting accelerators driving subcritical GEM*STAR small modular systems, has been created to support a consortium of private companies, universities, and national laboratories to design, build, and exploit this new approach to carbon-free energy. This team is uniquely ready to carry out these tasks by virtue of their complimentary skills, experience, assets and leadership.
- TUP0A57 Using High Precision Beam Position Monitors at the Cornell Electron Storage Ring (Cesr) to Measure the One Way Speed of Light Anisotropy**
W.F. Bergan, M.J. Forster, N.T. Rider, D. L. Rubin (Cornell University (CLASSE), Cornell Laboratory for Accelerator-Based Sciences and Education) B.A. Schmookler (MIT) B. Wojtsekhowski (CMU)
 The Cornell Electron Storage Ring (CESR) has been equipped with a number of high-precision beam position monitors, which are capable of measuring the orbit of a circulating beam with a precision of a few microns. Using this technology to measure the orbits of electrons and positrons, we will be able to make a precision measurement of deviations in the one-way speed of light. An anisotropic speed of light will alter the beam momentum as it travels through the ring, resulting in a change of orbit over the course of a sidereal day. Using counter-circulating electron and positron beams, we will be able to suppress many of the systematics such as those relating to variations in RF voltage or magnet strength. We show here initial feasibility studies to measure the stability of our beam position monitors and the various systematic effects which may hide our signal and discuss ways in which we can minimize their impact.
- TUP0A58 Minimization of Emittance at the Cornell Electron Storage Ring With Sloppy Models**
W.F. Bergan, A.C. Bartnik, I.V. Bazarov, H. He, D. L. Rubin (Cornell University (CLASSE), Cornell Laboratory for Accelerator-Based Sciences and Education) J.P. Sethna (Cornell University)
 Our current method to minimize the vertical emittance of the beam at the Cornell Electron Storage Ring (CESR) involves measurement and correction of the dispersion, coupling, and orbit of the beam and lets us reach emittances of 10 pm, but is limited by finite dispersion measurement resolution.* For further improvement in the vertical emittance, we propose using a method based on the theory of sloppy models.** The storage ring lattice permits us to identify the dependence of the dispersion and emittance on our corrector magnets, and taking the singular value decomposition of the Jacobian of the dispersion/corrector matrix gives us the combinations of these magnets which will be effective knobs for emittance tuning, ordered by singular value. These knobs will permit us to empirically tune the emittance based on direct measurements of the vertical beam size. Simulations show that when starting from a lattice with realistic alignment errors which has been corrected by our existing method to have an emittance of a few pm, this new method will enable us to reduce the emittance to nearly the quantum limit, assuming that vertical dispersion is the primary source of our residual emittance.
- TUP0A59 Successful Laboratory-Industrial Partnerships: the Cornell-Friatec Segmented Insulator for High Voltage DC Photocathode Guns**
K.W. Smolenski, B.M. Dunham (Cornell University (CLASSE), Cornell Laboratory for Accelerator-Based Sciences and Education)
 High voltage DC photocathode guns currently offer the most reliable path to electron beams with high current and brightness. The performance of a gun is directly dependent on its vacuum and high voltage capabilities, determined in large part by the ceramic insulators. The insulator must meet XHV standards, bear the load of pressurized SF6 on its exterior, support the massive electrode structures as well as holding off DC voltages up to 750kV. Construction of UHV and high voltage capable insulators require high purity ceramics and metal components proven to minimize thermal stress between the brazed ceramic rings and metal guard rings. The use of replaceable guard rings is a critical way of controlling manufacturing costs while extending the life cycle of the insulator. Successful fabrication requires proven manufacturing methods in flatness, parallelism, and maintaining alignment of many parts during the brazing process. Taking a scalable, modular approach, the insulator design can be applied to a variety of gun voltages and can be used by other projects. The Cornell-Friatec insulator was designed collaboratively and has now been produced in quantity for Cornell and elsewhere.
- TUP0A60 The Use of Graphene as Stripper Foils in the Siemens Eclipse Cyclotron**
S. Korenev, R. Dishman, A. Martin Yebra (Siemens Medical Solutions Molecular Imaging) N.D. Meshcheryakov, I.B. Smirnov (Siemens Healthcare) I. Pavlovsky (ANI)

This paper presents the results of an experimental study for the use of graphene foils as an extractor (stripper) foil in the 11-MeV Siemens Eclipse Cyclotron. The main advantage of graphene foils compared with carbon and graphite foils is its very high thermal conductivity. The graphene also has significant mechanical strength for atomically thin carbon layers. The life time of these foils is more than 18,000 $\mu\text{A}\cdot\text{H}$. The graphene foils showed a significant increase in the transmission factor (the ratio of the beam current on the stripper foil to the current on the target), which was approximately 90%. The technology in fabricating these graphene foils is shown. The pros and cons of using the graphene material as a stripper foil in cyclotrons are analyzed.

TUP0A61 **Integrated Control System for an X-Band-Based Laser-Compton X-Ray Source**

D.J. Gibson, G.G. Anderson, C.P.J. Barty, R.A. Marsh (LLNL)

LLNL's compact, tunable, laser-Compton x-ray source has been built around an advanced X-band photogun and accelerator sections and two independent laser systems. In support of this source, the control system has evolved from a minimal, isolated control points to an integrated architecture that continues to grow to simplify operation of the system and to meet new needs of this research capability. In addition to a PLC-based machine protection component, a custom, LabView-based suite of control software monitors systems including low level and high power RF, vacuum, magnets, and beam imaging cameras. This system includes a comprehensive operator interface, automated arc detection and rf processing to optimize rf conditioning of the high-gradient structures, and automated quad-scan-based emittance measurements to explore the beam tuning parameter space. The latest upgrade to the system includes a switch from real-time OS to FPGA-based low-level RF generation and arc detection. This offloads processing effort from the main processor allowing for arbitrary expansion of the monitored points. It also allows the possibility of responding to arcs before the pulse is complete.

TUP0A62 **Klynac (Combined Klystron and Linac)**

A. Malyzhenkov, B.E. Carlsten, K.E. Nichols (LANL)

We present the new type of a compact linear accelerator: resonant Klynac device, which is a combined linear accelerator and its power supply - klystron[*,**]. The intended purpose of a Klynac device is to provide a compact and inexpensive alternative to a conventional 1 to 6 MeV accelerator requiring a separate RF source, accelerator itself and all the associated hardware. Because the Klynac is a single structure, it has the potential to be much less sensitive to temperature variations than a system with a separate klystron and linac. We introduce the simplified theoretical model for Klynac-type device. We demonstrate particle-in-cell simulation results for mono-resonant and two bi-resonant types of such a device. We discuss the different design options from the stability point of view and the required input RF power. We compare the simulation results for the actual built bi-resonant design (type-2) with experimental results from testing a prototype in July 2016.

TUP0A63 **Preliminary Study of Advanced LLRF Controls at LANSCE for Beam Loading Compensation in the MaRIE X-FEL**

A. Scheinker, J.T. Bradley III, L.J. Castellano, D.J. Knapp, S. Kwon, J.T.M. Lyles, M.S. Prokop, D. Rees, P.A. Torrez (LANL)
The analog low level RF (LLRF) control system of the Los Alamos Neutron Science Center is being upgraded to a Field Programmable Gate Array (FPGA)-based digital system (DLLRF). In this paper we give an overview of the FPGA design and the overall DLLRF system. We also present preliminary performance measurements including results utilizing model-independent iterative feedforward for beam-loading transient minimization, which is being studied for utilization in the future MaRIE X-FEL, which will face difficult beam loading conditions.

TUP0A64 **Effects of Low Frequency Buncher Field Variation on an H^- Beam Phase-Space**

P.K. Roy, Y.K. Batygin, R.C. McCrady (LANL)

Beam bunching optimization at low energy (750keV) before injecting into a DTL (100MeV) is essential for beam transport, emittance reduction, and focusing on to a target. The LANSCE simultaneously utilizes H^+ and H^- beam (with a timing variation) for many important national security sciences. In addition to quadrupole, several bunchers are utilized in the transport. A technique with pre-bunching at lower frequency and main bunching at higher frequency is utilized for beam injection into the linac. The buncher parameters (voltage and frequency) are well established for operations. However, there is the possibility that the parameters vary with time due to electrical malfunction or adverse tuning during a beam development activity. Some effort is needed to correct the parameters as a non-optimized pre-bunching setup can alter the beam phase space and the nominal beam intensity at a desired location. Here, we examine emittance and phase space distribution variation for H^- beam due to variation of the low frequency (16 MHz) buncher voltage, which typically operates at 25 kV peak. Beam phase dynamics with buncher voltage variation is also examined using the beam transport code Parmila.

TUP0A67 **Helium Pressure Vessel Jacketing of the Fermilab SSR1 Single Spoke SC Cavities**

E.C. Bonnema (Meyer Tool & MFG)

Meyer Tool recently completed the welding of the liquid helium pressure vessel jackets around ten (10) superconducting single spoke niobium cavities for Fermilab. The SSR1 cavities are intended for use in the PIP-II Injector Experiment Cryomodule. Meyer Tool's scope of supply included review of the Fermilab Pressure Rating Analysis Document and the development of fabrication details and a fabrication sequence to meet that document's requirements, while minimizing the effects of jacketing cavity frequency, and the actual jacketing of the cavities. This paper will focus on the development of the fabrication details and sequence and how the details and sequence evolved over the course of welding and final machining of the ten (10) jackets. As the frequency of these cavities is critical the fabrication sequence accommodated numerous in process frequency checks, a frequency tuning step prior to the final weld, the use of thermal cameras to monitor weld heat input into the cavity, and post welding final machining of critical features. Lessons learned from this fabrication will be discussed.

TUP0A68 **Design, Simulations and Experimental Demonstration of an Intra-Pulse Ramped-Energy Travelling Wave Linac for Cargo Inspection**

S.V. Kutsaev, R.B. Agustsson, A. Arodzero, K. Beck, R.D.B. Berry, S. Boucher, Y.C. Chen, J.J. Hartzell, B.T. Jacobson, A. Laurich, A.Y. Murokh, E.A. Savin, A.Yu. Smirnov, A. Verma (RadiaBeam)

Novel radiographic imaging techniques [1] based on adaptive, intra-pulse ramped-energy short X-ray packets of pulses, a new type of fast X-ray detectors, and advanced image processing are currently some of the most promising methods for real-time cargo inspection systems. RadiaBeam Technologies is currently building the high-speed Adaptive Railroad Cargo Inspection System (ARCIS), which will enable better than 5 mm line pair resolution, penetration greater than 450 mm of steel equivalent, material discrimination over the range of 6 mm to 250 mm, 100% image sampling rate at speed 45 km/h, and minimal average dose. One of the core elements of ARCIS is a new S-band travelling wave linac with a wide range of energy control that allows energy ramping from 2 to 9 MeV within a single 16 μs RF pulse using the beam loading effect. In this paper, we will discuss the linac design approach

and its principal components, as well as engineering and manufacturing aspects. The results of the experimental demonstration of intra-pulse energy ramping will be presented.

TUP0A69 Extereme Ultraviolet Transition Radiation Beam Profile Monitor

A.Y. Murokh, M. Ruelas, H.L. To (RadiaBeam) P. Naulleau (LBNL) G. Stupakov (SLAC)

We propose a method of measuring transverse profile of high quality photo-injector generated electron beams, using a backscattered transition radiation from multilayer mirrors at the extreme ultraviolet (EUV) spectral region. The motivation for such a short wavelength is twofold: first, the method mitigates parasitic coherent effects (COTR), which are expected to be negligible at EUV band, while proven to be highly detrimental to the beam profile measurements at optical and near-optical wavelengths. In addition, with 10 nm light it should be straight forward to achieve sub-micron resolution for high precision applications such as those requiring electron beam matching into photonic structures, i.e. in dielectric laser accelerators. The specific wavelength of 13.5 nm was selected to take advantage of high quality optics availability, resulting from two decades of development for EUV lithography. A design of the EUV TR beam profile monitor is discussed and its performance estimated for the case of a LCLS beam. The design of a recently constructed proof of concept prototype is presented, including experimental plans and possibly results of the prototype commissioning.

TUP0A70 Multipacting Behaviour Study for the 112 MHz Superconducting Photo-Electron Gun

I. Petrushina (SUNY SB)

Superconducting 112 MHz quarter-wave resonator (QWR) photo-electron gun is used as a source of electron beam for the Coherent electron Cooling experiment (CeC PoP) at BNL. During the CeC commissioning, numerous multipacting zones were encountered in the cavity. It was also observed that introduction of CsK₂Sb photocathode creates additional multipacting zone. This paper presents experimental study of the multipactor discharge in the QWR along with possible ways of crossing the multipacting levels. The results of numerical simulations of multipactor discharge are discussed and compared with the experimental data.

TUP0A71 Beam Stability During Top Off Operation at NSLS-II Storage Ring

W.X. Cheng (BNL)

NSLS-II storage ring started top off operation since Oct 2015. User operation current has been gradually increased to 250mA. Observations of beam stabilities during top-off operations will be presented. Total beam current was typically maintained within $\pm 0.5\%$ and bunch to bunch current variation was less than 20%. Injection transition during top-off was measured bunch by bunch digitizer, and BPM to analyze the orbit motion at various bandwidths (turn by turn, 10kHz and 10Hz rate). Coupled bunch unstable motions were monitored. As the vacuum pressure improves, fast-ion instability is not as severe compared to early stage of commissioning/operation, but still observed as the dominant instability. Resistive wall instability is noticed as more in-vacuum-undulator (IVU) gaps closed. xBPM measured photon stability and electron beam stability at top off injection have been evaluated. Short term and long term orbit stabilities will be reported.

TUP0A72 Expanded Diagnostic Capability With an X-Band Deflector Cavity at the BNL Accelerator Test Facility

M.G. Fedurin, K. Kusche, C. Swinson (BNL) G. Andonian (RadiaBeam) V. Wacker (DESY)

An X-band Deflector Cavity (XDC) has recently been commissioned at the Accelerator Test Facility (ATF) at Brookhaven National Laboratory. The 11.424 GHz XDC was designed and constructed at RadiaBeam Technologies to perform longitudinal characterization of the sub-picosecond ultra-relativistic electron beams available at the ATF. The device is optimized for operation with a 100 MeV electron beam and is scalable to higher energies. Key features include short filling time, femtosecond resolution, and a small footprint. This new diagnostic tool enables longitudinal bunch length measurements with a resolution of 10 fs. The XDC has been installed in front of a spectrometer arm at the end of one of ATF's experimental beam lines. In this location it allows characterization of the e-beam longitudinal phase space for a range of experiments being conducted at the ATF.

TUP0A73 Commissioning and First Results From a Channeling-Radiation Experiment at FAST

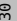
J. Hyun (Sokendai) D.R. Broemmelsiek, D.R. Edstrom, T. Sen (Fermilab) D. Mihalcea, P. Piot (Northern Illinois University) W.D. Rush (KU)

X-rays have widespread applications in science. Developing compact and high-quality X-ray sources, easy to disseminate, has been an on going challenge. Our group has explored the possible use of channeling radiation driven by a 50 MeV low-emittance electron beam to produce narrowband hard X-rays (photon energy from 40 keV to 140 keV). In this contribution we present the simulated X-ray spectrum including the background bremsstrahlung contribution, and optimization of the relevant electron-beam parameters required to maximize the X-ray brilliance. The results of experiments carried out at Fermilab's FAST facility – which include a 50 MeV superconducting linac and a high-brightness photoinjector – are also discussed. The average brilliance in our experiment is expected to be about one order of magnitude higher than that in previous experiments.

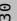
TUP0A74 The Design and Construction of a Resonance Control System for the IOTA Storage Ring

G.M. Bruhaug (Fermilab)


The IOTA ring will be an advanced storage ring used for non-linear beam dynamics experiments to assist in the construction of future accelerators. This ring is being built in conjunction with the FAST electron LINAC and the HINS RFQ proton source, at Fermilab, for injection into the ring. These accelerators will generate +150 MeV electron beams and 2.5 MeV proton beams respectively. As the beams are injected into the IOTA storage ring their longitudinal profile will begin to smear out and become more uniform. This will prevent detection of beam position with a Beam Position Monitoring system (BPM). To combat this a ferrite loaded bunching cavity is being constructed. This paper details the design and construction of an automatic resonance control system for this bunching cavity.

TUA3 — Oral Presentations (MC3)**Chair:** P. Muggli (MPI)**TUA3I001 Possible Road Maps for High-Energy Collider Based on Advanced Acceleration Techniques**14:00  **S. Nagaitsev** (*Fermilab*)


In February 2016, DOE organize a closed workshop to discuss possible roadmaps toward future high-energy linear colliders. Three accelerations techniques were discussed. The purpose of this paper is to summarize the outcome of this workshop.

TUA3I002 FACET Results and FACET II Perspective14:30  **V. Yakimenko**, *M.J. Hogan* (*SLAC*)

Very short summary of the FACET results followed by plans for FACET II, the facility and the science towards a e^-/e^+ PWEA- based collider

TUA3C003 Compact Ring-Based X-Ray Source With on-Orbit and on-Energy Laser-Plasma Injection15:00  **M. Turner** (*CERN*) *J.R. Cheatham, A.L. Edelen (CSU) J. Gerity (Texas A&M University) A. Lajoie, C.Y. Wong (NSCL) G. Lawler (UCLA) O. Lishilin (DESY Zeuthen) K. Moon (UNIST) A. A. Sahai, A. Seryi (JAI) K. Shih (SBU) B. Zerbe (MSU)*

We report here the results of one week long investigation performed during June 2016 USPAS class "Unifying physics..." on conceptual design of an X-ray source based on a compact ring with on-orbit and on-energy laser-plasma acceleration injection (mini-project 10.4 from [1]). We describe three versions of the light source, based on 1 GeV normal conducting and superconducting bending magnets, and 3 GeV superconducting. We describe the design choices, present the tables of parameters of the machines, and describe possible next steps of the design and optimization of the considered machines.

TUA3C004 Kinetic Limits to Average Power in Plasma Wakefield Accelerators15:15  **S.D. Webb** (*RadiaSoft LLC*)

We present the effects of beam loading and plasma kinetics on the length of the wake in a beam-driven plasma wakefield accelerator in the blowout regime. This allows us to estimate the limits to the average beam power available to a plasma wakefield accelerator.

TUB3 — Oral Presentations (MC2)**Chair:** C. Steier (LBNL)**TUB3I001 Commissioning of Max-IV, the First Light Source Using a Multi Bend Achromat**

14:00

**P.F. Tavares, S.C. Leemann** (*MAX IV Laboratory, Lund University*)

MAX IV is the first light source based on a multibend achromat lattice design to achieve much smaller emittance and therefore higher brightness in a relatively compact circumference. In addition to the new lattice concept, the ring design also includes other innovative solutions, particularly in vacuum and magnet technology. The talk will give an overview of the facility design, describe the major steps along the construction and installation phase and conclude with highlights of the commissioning run that started in 2015.

TUB3I002 Overview of Electron Source Development for High Repetition Rate FEL Facilities

14:30

**F. Sannibale** (*LBNL*)

Overview of world-wide development of sources (normal conducting RF, superconducting RF, electrostatic) that can be used for high repetition rate FEL facilities, including recent experimental results.

TUB3C003 Demonstration of fresh slice self seeding in a hard X-ray free electron laser

15:00

**C. Emma, C. Pellegrini** (*UCLA*) **M.W. Guetg, A.A. Lutman, A. Marinelli, T.J. Maxwell, C. Pellegrini, J. Wu** (*SLAC*)

We discuss the first demonstration of fresh slice self seeding (FSSS) in a hard X-ray Free Electron Laser (XFEL). The FSSS method utilizes a single electron beam to generate a strong seed pulse and amplify it with a small energy spread electron slice. This extends the capability of self seeded XFELs by producing short pulses, not limited by the duration set by the self-seeding monochromator system, with high peak intensity. The scheme relies on using a parallel plate dechirper to impart a spatial chirp on the beam, and appropriate orbit control to lase with different electron beam slices before and after the self-seeding monochromator. The performance of the FSSS method is analyzed with start-to-end simulations for the Linac Coherent Light Source (LCLS). The simulations include the effect of the parallel plate dechirper and propagation of the radiation field through the monochromator. We also present results of the first successful demonstration of FSSS at LCLS. The radiation properties of FSSS X-ray pulses are compared with the Self-Amplified Spontaneous Emission (SASE) mode of FEL operation for the same electron beam parameters.

TUB3C004 A New Thermionic RF Electron Gun for Synchrotron Light Sources

15:15

**S.V. Kutsaev, A.Y. Murokh, E.A. Savin, A.V. Smirnov** (*RadiaBeam Systems*) **R.B. Agustsson, J.J. Hartzell, A. Verma** (*RadiaBeam*) **A. Nassiri, Y.-E. Sun, G.J. Waldschmidt, A. Zholents** (*ANL*) **E.A. Savin** (*MEPhI*)

A thermionic RF gun is a compact and efficient source of electrons used in many practical applications. RadiaBeam Systems and the Advanced Photon Source of Argonne National Laboratory collaborate in developing of a reliable and robust thermionic RF gun for synchrotron light sources which would offer substantial improvements over existing thermionic RF guns and allow stable operation with up to 1A of beam peak current at a 100 Hz pulse repetition rate and a 1.5 μ s RF pulse length. In this paper, we discuss the electromagnetic and engineering design of the cavity, and report the progress towards high power tests of the cathode assembly of the new gun.

TUA4 — Oral Presentations (MC3)

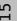
Chair: A. Caldwell (MPI-P)

TUA4I001 **Staging Results at BELLA and Plans for BELLA**16:00  **S. Steinke** (LBNL)


Summary of the staging results obtained at BELLA as well as perspective on facility experiments towards a e^-/e^+ , LWFA-based collider

TUA4I002 **Eupraxia: A Compact European Plasma Accelerator With Superior Beam Quality**16:30  **U. Dorda** (DESY)


Plasma wakefield accelerators can sustain multi-GeV/m fields that may allow much smaller accelerators that could be used for a wide range of fundamental and applied research applications. 3 M€ of funding have been awarded to 16 laboratories and universities from 5 EU member states within the European Union's Horizon 2020 programme. They will be joined by 18 associated partners that make additional in-kind commitments. The goal of this ambitious project is to produce a conceptual design report for the worldwide first high energy plasma-based accelerator that can provide industrial beam quality and user areas. It is the important intermediate step between proof-of-principle experiments and ground-breaking, ultra-compact accelerators for science, industry, medicine or the energy frontier. Major elements of the project and the expected timeframe will be discussed.

TUA4C003 **Loading of Wakefields in a Plasma Accelerator Section Driven by a Self-Modulated Proton Beam**17:00  **V.K.B. Olsen**, *E. Adli* (University of Oslo) *P. Muggli* (MPI-P) *J. Vieira* (Instituto Superior Tecnico)

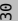
Using parameters from the AWAKE project and particle-in-cell simulations we investigate beam loading of a plasma wake driven by a self-modulated proton beam. Addressing the case of injection of an electron witness bunch after the drive beam has already experienced self-modulation in a previous plasma, we optimise witness bunch parameters of size, charge and injection phase to maximise energy gain and minimise relative energy spread and emittance of the accelerated bunch.

TUA4C004 **High-Power Tunable THz Generation in Corrugated Plasma Waveguides**17:15  **C.M. Miao**, *T.M. Antonsen* (UMD) *J. Palastro* (NRL)

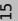
Intense, short laser pulses propagating through inhomogeneous plasmas generate terahertz (THz) radiation. We consider the excitation of THz radiation by the interaction between an ultra short laser pulse and a miniature plasma waveguide. Such corrugated plasma waveguides support electromagnetic (EM) channel modes with subluminal phase velocities, thus allowing the phasing matching between the generated THz modes and the ponderomotive potential associated with laser pulse, making significant THz generation possible. Full format PIC simulations and theoretical analysis are conducted to investigate this slow wave phase matching mechanism. We find the generated THz is characterized by lateral emission and a coherent, narrow band spectrum. A range of realistic laser pulse and plasma profile parameters are considered with the goal of increasing the conversion efficiency of optical energy to THz radiation. As an example, a fixed driver pulse (1.66 J) with spot size of $15\ \mu\text{m}$ and pulse duration of $50\ \text{fs}$ excites approximately $83.7\ \mu\text{J}$ of THz radiation in a $500\text{-}\mu\text{m}$ -long corrugated waveguide with on axis average density of $10^{18}\ \text{cm}^{-3}$.

TUB4 — Oral Presentations (MC2)**Chair:** R.M. Zwaska (Fermilab)**TUB4I001 Status of the MaRIEProject****16:00**  **J.L. Erickson, C.W. Barnes, R.L. Sheffield (LANL)**

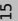
The Matter-Radiation Interactions in Extremes (MaRIE) project will provide capability that will address the control of performance and production of materials at the mesoscale. MaRIE will characterize the behavior of interfaces, defects, and microstructure between the spatial scales of atomic structures and those of the engineering continuum where there is a current capability gap. The mission need is well-met with an x-ray source, coherent to optimize disordered imaging capability, brilliant and high-rep-rate to provide time-dependent information, and high enough energy to see into and through the mesoscale of materials of interest. It will be designed for time-dependence from electronic motion (picosecond) through sound waves (nanosecond) through thermal diffusion (millisecond) to manufacturing (seconds and above). The mission need, the requirements, a plausible alternative reference design of a 12-GeV linac-based 42-keV x-ray free-electron laser, and the status of the project will be described.

TUB4I002 Accelerator Technical Progress and First Commissioning Results from the European XFEL**16:30**  **R. Wichmann (DESY)**

The construction of the European XFEL is coming to an end. The linac tunnel will be closed and commissioning of the main linac will start. The status of the construction project is reviewed. Commissioning of the injector of the European XFEL was already performed in 2016 while construction of the main linac was continuing. The commissioning goals and achievements for the XFEL injector will be reviewed.

TUB4C003 Optimization of Compton source Performance through Electron Beam Shaping**17:00**  **A. Malyzhenkov, N.A. Yampolsky (LANL)**

We investigate a novel scheme for significantly increasing the brightness of x-ray light sources based on inverse Compton scattering (ICS) - scattering laser pulses off relativistic electron beams. The brightness of these sources is limited by the electron beam quality since electrons traveling at different angles, and/or having different energies, produce photons with different energies. Therefore, the spectral brightness of the source is defined by the 6d electron phase space shape and size, as well as laser beam parameters. The peak brightness of the ICS source can be maximized then if the electron phase space is transformed in a way so that all electrons scatter off the x-ray photons of same frequency in the same direction. We describe the x-ray photon beam quality through the Wigner function (6d photon phase space distribution) and derive it for the ICS source when the electron and laser rms matrices are arbitrary. We find the optimal electron beam phase space distribution resulting in the highest brightness of the ICS source. We demonstrate a potential electron beamline which transforms a given electron beam into the beam with optimal distribution.

TUB4C004 Progress on the Magnetic Performance of Planar Superconducting Undulators**17:15**  **M. Kasa, C.L. Doose, J.D. Fuerst, E. Gluskin, Y. Ivanyushenkov (ANL)**

One of the primary goals of the superconducting undulator (SCU) program at the Advanced Photon Source (APS) is to achieve a high quality undulator magnetic field without the need for magnetic shimming to tune the device. Over the course of two years, two SCUs were designed, manufactured, assembled, and tested at the APS. Both SCUs were one meter in length with a period of 1.8 cm. After magnetic measurements of the first undulator were completed, several design changes were made in order to improve the quality of the undulator magnetic field. The design modifications were implemented during construction and assembly of the second SCU. The details of the design modifications along with a comparison of the magnetic measurement results will be described.

TUPOB01 Lattice Calibration at Duke Storage Ring Using Directly Measured Beta-Functions**W. Li, W.W. Gao (USTC/NSRL) W.W. Gao (Fujian University of Technology) H. Hao, Y.K. Wu (FEL/Duke University)**

A storage ring lattice is designed with a number of advantages for physics research and high performance for light sources. However, due to the focusing errors from the devices or surrounding environment, linear optics in the real circular accelerator are usually different from the designed, leading to beta beatings in the real machine. To reduce this perturbation, lattice modeling and compensation is commonly performed using model and orbit response matrix based techniques like LOCO. However, the LOCO technique can not be applied in the DSR in any straight forward manner. Therefore, we developed a compensation technique to correct the lattice for the Duke storage ring using directly measured beta-functions. The development of this technique will be present. This technique was applied at the Duke storage ring to reduce the beta beatings. The compensation result will be present and the residual lattice discrepancy will be discussed.

TUPOB02 Development of the Method for Evaluation of a Traveling Wave Cavity With Feedback Waveguide.**R.A. Kostin (LETI) P.V. Avrakhov, A. Kanareykin (Euclid TechLabs, LLC) N. Solyak, V.P. Yakovlev (Fermilab)**

Euclid Techlabs is developing a superconducting traveling wave cavity with feedback waveguide [1,2,3] and demonstrated traveling wave at room temperature in a 3-cell cavity [4]. A special method described in the paper was developed for the cavity evaluation. It is based on S-matrix approach. The cavity tuning procedure is described based on this method.

TUPOB03 3-Cell SC Traveling Wave Cavity Test in Liquid Helium**R.A. Kostin (LETI) P.V. Avrakhov, A. Kanareykin (Euclid TechLabs, LLC) T.N. Khabiboulline, A.M. Rowe, N. Solyak, V.P. Yakovlev (Fermilab)**

Superconducting traveling wave cavity (SCTW) with the feedback waveguide may allow higher average acceleration gradient compared to conventional standing wave cavities [1]. Euclid Techlabs in collaboration with Fermilab has demonstrated high accelerating gradient in a single cell cavity with a feedback waveguide [2], i.e. the waveguide does not limit the cavity performance. The next step is high gradient traveling wave demonstration in superconducting cavity. 3 cell SCTW cavity was proposed and developed [3] for that purpose. Two Nb cavities have been built by Spring 2016. This paper presents the results of 3 cell SC traveling wave cavity testing in liquid Helium at Fermilab.

TUPOB04 A More Compact Design for the JLEIC Ion Pre-Booster Ring**B. Mustapha, P.N. Ostroumov (ANL) B. Erdelyi (Northern Illinois University)**

The original design of the JLEIC pre-booster was a 3-GeV figure-8 shaped synchrotron with a circumference of about 240 m. In the current baseline design, the 3-GeV pre-booster was converted into an 8-GeV booster of the same shape and size but using super-ferric magnets with fields up to 3 Tesla. In order to limit the foot-print of the JLEIC ion complex and reduce its total cost, we have designed a more compact and cost-effective octagonal 3-GeV ring about half the size of the original one. At 3 GeV, the figure-8 shape is not required to preserve ion polarization; Siberian snakes with reasonable magnetic fields can be used for spin correction. As the ion collider ring requires an injection energy of at least 8 GeV, we propose to use the existing electron storage ring, which is part of the electron complex, as a large booster for the ions up to 11 GeV. The design optimization of the pre-booster ring will be presented leading to the final octagonal ring design. Preliminary beam simulations will also be presented and discussed.

TUPOB05 An Alternative Approach for the JLEIC Ion Accelerator Complex**B. Mustapha, P.N. Ostroumov (ANL) Y.S. Derbenev, V.S. Morozov, Y. Zhang (JLab)**

The current baseline design for the JLab EIC (JLEIC) ion accelerator complex is based on a pulsed superconducting linac, an 8-GeV booster followed by a dual function 20-100 GeV booster and collider ring. Both the 8-GeV booster and collider ring will use super-ferric magnets with fields up to 3 Tesla. We here propose an alternative cost-effective and low-risk design where the 8-GeV booster is replaced with a more compact 3-GeV booster using room-temperature magnets. The electron storage ring, which is part of the electron complex, will also serve as large booster for the ions, up to 11 GeV. We also propose two stages for the JLEIC. A first low-energy stage up to 60 GeV, where room-temperature magnets (up to 1.6 Tesla) will be used for the ion collider ring, to be later replaced with 6 Tesla superconducting magnets in a second stage of the project providing up to 200 GeV energy. In this second stage, the 1.6 T room-temperature magnets will replace the PEP-II magnets in the electron storage ring to boost the ions to higher energies (25 GeV or higher) for appropriate injection into the higher energy collider. Details and feasibility of the proposed plan will be presented and discussed.

TUPOB06 Accomplishments of the Heavy Electron Particle Accelerator Program**D.V. Neuffer, D. Stratakis (Fermilab) M.A.C. Cummings (Muons, Inc) M.A. Palmer (BNL) D.J. Summers (UMiss)**

The Muon Accelerator Program has completed a four-year study on the feasibility of muon colliders and on using stored muon beams for neutrinos. That study was broadly successful in its goals, establishing the feasibility of lepton colliders from the 125 GeV Higgs Factory to more than 10 TeV, as well as exploring using μ storage rings for neutrinos. The key components of the muon collider scenarios are a high-intensity proton source, a multi MW target and transport system for π capture, a front end system for bunching, energy compression and initial cooling of μ 's, muon cooling systems to obtain intense μ^+ and μ^- bunches, acceleration up to multi-TeV energies, and a collider ring with detectors for high luminosity collisions. For a neutrino factory a similar system could be used but with a racetrack storage ring for ν production and without the cooling needed for high luminosity collisions. Feasible designs and detailed simulations of all of these components have been obtained, including some initial hardware component tests, setting the stage for future implementation where resources are available and clearly associated physics goals become apparent.

TUPOB07 Considerations on Energy Frontier Colliders After LHC**V.D. Shiltsev (Fermilab)**

The future of the world-wide HEP community critically depends on the feasibility of possible post-LHC colliders. The concept of the feasibility is complex and includes at least three factors: feasibility of energy, feasibility of luminosity and feasibility of cost. The talk will give an overview of all current options for post-LHC colliders from such perspective (ILC, CLIC, Muon Collider, plasma colliders, CEPC, FCC, HE-LHC, etc) and discuss major challenges and accelerator R&D required to claim these machines feasible.

TUPOB08 Beam Extraction from the Recycler Ring to P1 Line at Fermilab**M. Xiao (Fermilab)**

The transfer line for beam extraction from the Recycler ring to P1 line provides a way to deliver 8 GeV kinetic energy protons

from the Booster to the Delivery ring, via the Recycler, using existing beam transport lines, and without the need for new civil construction. It was designed in 2012. The kicker magnets at RR520 and the lambertson magnet at RR522 in the RR were installed in 2014 Summer Shutdown, the elements of RR to P1 Stub (permanent quads, trim quads, correctors, BPMs, the toroid at 703 and vertical bending dipole at V703 (ADCW)) were installed in 2015 Summer Shutdown. On Tuesday, June 21, 2016, beam line from the Recycler Ring to P1 line was commissioned. The detailed results will be presented in this report.

TUPOB09 **Stripline Kicker Solid-State Pulse Generator***

N. Butler, M.P.J. Gaudreau, M.K. Kempkes, J. Kinross-Wright, M.G. Munderville, R.E. Simpson (*Diversified Technologies, Inc.*)

Diversified Technologies, Inc. (DTI) has designed, built, and demonstrated a prototype pulse amplifier for stripline kicker service capable of less than 5 ns rise and fall times, 5 to 90 ns pulse lengths, peak power greater than 13.7 MW at pulse repetition rates exceeding 100 kHz, and measured jitter under 100 ps. The resulting pulse is precise and repeatable, and will be of great interest to accelerator facilities requiring electromagnetic kickers. The pulse generator is based on the original specifications for the NGLS fast deflector. DTI's planar inductive adder configuration uses compensated-silicon power transistors in low inductance leadless packages with a novel charge-pump gate drive to achieve unmatched performance. The unit was brought to LBNL, compared with other researcher's efforts, and was judged very favorably. A number of development prototypes have been constructed and tested, including a successful 18.7 kV, 749 A unit. The modularity of this design will enable configuration of systems to a wide range of potential applications in both kickers and other high speed requirements, including high performance radars, directed energy systems, and excimer lasers.

TUPOB10 **Fast and Accurate Calculations of Dynamical Friction for Magnetized Electrons**

D.L. Bruhwiler, C.C. Hall, S.D. Webb (*RadiaSoft LLC*)

Relativistic magnetized electron cooling in untested parameter regimes is essential to achieve the ion luminosity requirements of proposed electron-ion collider (EIC) designs. Therefore, accurate calculations of magnetized dynamic friction are required, with the ability to include all relevant physics that might increase the cooling time, including space charge forces, field errors and complicated phase space distributions of imperfectly magnetized electron beams. Advances in the understanding of unmagnetized dynamic friction were achieved through semi-analytic treatment of individual electron-ion collisions [1]. We are generalizing this previous work to the case of magnetized friction, which is only possible due to recent work [2] that shows how to correctly handle perturbative treatment of Vlasov systems over long times. The new semi-analytic treatment of dynamic friction is Hamiltonian and momentum conserving, and effectively exploits the perturbative nature of the problem.

TUPOB11 **Quantification of Octupole Magnets for the University of Maryland Electron Ring**

H. Baumgartner, B. Beaudoin, I. Haber, T.W. Koeth, D.B. Matthew, K.J. Ruisard, M.R. Teperman (*UMD*)

The intensity frontier is limited by the ability to propagate substantial amounts of beam current without resulting in particle scraping and/or losses from resonant growth and halo formation. Modern accelerators are based on the theories developed in the 1950's that assume particle motion is bounded and subject to linear forces. Recent theoretical developments have demonstrated that a strongly nonlinear lattice can be used to stably transport an intense beam has resulted in a fundamental rethinking of the conventional wisdom. A lattice composed of strong nonlinear magnets is predicted by theory to damp resonances while maintaining dynamic aperture. Results of rotating coil measurements, magnetic field scans and simulations will be presented, quantifying the multi-pole moments and fringe fields in the 1st generation Printed Circuit Board (PCB) octupoles for UMER's nonlinear lattice experiments.

TUPOB12 **Early Results and Experimental Plans for Single-Channel Strong Octupole Fields at the University of Maryland Electron Ring**

K.J. Ruisard, B. Beaudoin, I. Haber, T.W. Koeth (*UMD*)

Nonlinear quasi-integrable optics is a promising development on the horizon of high-intensity ring design. Large amplitude-dependent tune spreads, driven by strong nonlinear magnet inserts, lead to decoupling from incoherent tune resonances. This reduces intensity-driven beam loss while quasi-integrability ensures a well-contained beam. In this paper we discuss on-going work to install and interrogate a long-octupole channel at the University of Maryland Electron Ring (UMER). This is a discrete insert that occupies 20 degrees of the ring, consisting of independently powered printed circuit octupole magnets. Transverse confinement is obtained with quadrupoles external to this insert. Operating UMER as a non-FODO lattice, in order to meet the beam-envelope requirements of the quasi-integrable lattice, is a challenge. We discuss efforts to match the beam and optimize steering solutions. We also discuss our experiences operating a distributed strong octupole lattice.

TUPOB13 **Simulations of Space Charge Neutralization in a Magnetized Electron Cooler**

J. Gerity, P.M. McIntyre (*Texas A&M University*) **D.L. Bruhwiler, C.C. Hall** (*RadiaSoft LLC*) **V. Moens** (*EPFL*) **C.S. Park, G. Stancari** (*Fermilab*)

Magnetized electron cooling at relativistic energies and Ampere scale current is essential to achieve the proposed ion luminosities in a future electron-ion collider (EIC). Neutralization of the space charge in such a cooler can significantly increase the magnetized dynamic friction and, hence, the cooling rate. The Warp framework is being used to simulate magnetized electron beam dynamics during and after the build up of neutralizing ions, via ionization of residual gas in the cooler. The design follows previous experiments at Fermilab as a verification case. We also discuss the relevance to EIC designs.

TUPOB14 **An Accurate and Efficient Numerical Integrator for Pair-Wise Interaction**

A.A. Al Marzouk, B. Erdelyi (*Northern Illinois University*) **B. Erdelyi** (*ANL*)

We are developing a new numerical integrator based on Picard iteration method for Coulomb collisions. The aim is to achieve a given prescribed accuracy most efficiently. The integrator is designed to have adaptive time stepping, variable order, and dense output. It also has an automatic selection of the order and the time step. We show that with a good estimation of the radius of convergence of the expansion, we can obtain the optimal time step size. We also show how the optimal order of the integration is chosen to maintain the required accuracy. For efficiency, particles are distributed over time bins, and propagated accordingly with the use of parallelization.

TUPOB15 **Implementing the Fast Multipole Boundary Element Method With High-Order Elements**

A.J. Gee, B. Erdelyi (*Northern Illinois University*) **B. Erdelyi** (*ANL*)

The next generation of beam applications will require high-intensity beams with unprecedented control. For the new system designs, simulations that model collective effects must achieve greater accuracies and scales than conventional methods allow. The

fast multipole method is a strong candidate for modeling collective effects due to its linear scaling. It is well known the boundary effects become important for such intense beams. We implemented a constant element fast boundary element method (FMBEM) * as our first step in studying the boundary effects. To reduce the number of elements and discretization error, our next step is to allow for high-order elements using differential algebraic methods. In this paper we will present the theory and status of the implementation using high-order boundary elements.

TUPOB16 Simple Method for Measuring the Electron-Beam Magnetization

A. Halavanau, P. Piot (Northern Illinois University) **P. Piot** (Fermilab)

There are a number of projects that require magnetized beams for applications, such as electron cooling or aiding in flat beam transforms. Here we explore a simple technique to characterize the magnetization, observed through angular momentum, of magnetized beams. These beams are produced through photoemission, the generating drive laser first passed through a microlens arrays (fly-eye light condensers) to form a transversely modulated pulse incident on the photocathode surface. The resulting charge distribution accelerated from the photocathode, we explore the evolution of the pattern with the relative shearing of the beamlets providing information on the angular momentum. This method is illustrated through numerical simulation and preliminary measurements carried out at the Fermilab Accelerator Science & Technology (FAST) facility are presented.

TUPOB17 Simulations in Support of Wire Beam-Beam Compensation Experiment at the LHC

A.S. Patapenka (Northern Illinois University) **R. De Maria, Y. Papaphilippou** (CERN) **A. Valishev** (Fermilab)

The compensation of long-range beam-beam interaction with current wires is considered as a possible technology for the HL-LHC upgrade project. A demonstration experiment is planned in the present LHC machine starting in 2018. This paper summarizes the tracking studies of long range beam-beam effect compensation in the LHC aimed to aid in planning the demonstration experiment. The impact of wire compensators is demonstrated on the tune footprints, dynamic aperture, beam emittance and beam intensity degradation. The simulations are performed with SIXTRACK code. The symplectic transport map for the wire element, its verification and implementation into the code are also discussed.

TUPOB18 Beam Test of Masked-Chicane Micro-Buncher

Y.-M. Shin (Northern Illinois University) **D.R. Broemmelsiek, D.J. Crawford, A.H. Lumpkin, R.M. Thurman-Keup** (Fermilab) **A.T. Green** (Northern Illinois University)

Masking a dispersive beamline such as a dogleg or a chicane [1, 2] is a simple way to shape a beam in the longitudinal and transverse space. This technique is often employed to generate arbitrary bunch profiles for beam/laser-driven accelerators and FEL undulators or even to reduce a background noise from dark currents in electron linacs. We have been investigating a beam-modulation of a slit-masked chicane, which was deployed for crystal-channeling experiments at the injector beamline of the Fermilab Accelerator Science and Technology (FAST) facility. With a nominal beam of 3 ps bunch length, Elegant simulations showed that a slit-mask with slit period 900 μm and aperture width 300 μm induces a modulation with bunch-to-bunch space of about 187 μm (0.25 nC), 270 μm (1 nC) and 325 μm (3.2 nC) with 3 ~ 6% correlated energy spread: An initial energy modulation pattern has been observed in the electron spectrometer downstream of the masked chicane using a micropulse charge of 260 pC and 40 micropulses. Investigations of the beam longitudinal modulation are planned with a Martin-Puplett interferometer and a synchro-scan streak camera at a station between the chicane and spectrometer.

TUPOB19 FEL Wiggler Bussbar Field Compensation

B. Li, H. Hao, Y.K. Wu (FEL/Duke University) **J.Y. Li** (USTC/NSRL)

Abstract The Duke storage ring is a dedicated driver for the storage ring based free-electron laser (FEL) and the High Intensity Gamma-ray Source (HIGS). The high intensity gamma-ray beam is produced using Compton scattering between the electron and FEL photon beams. The beam displacement and angle at the collision point need to be maintained constant in the gamma-ray beam production. The magnetic field of the copper bussbars carrying the current to the FEL wigglers can impact the beam orbit. The compensation scheme ingeneral is complicated. In this work, we report preliminary results of a bussbar compensation scheme for one of the wiggler and power supply configurations. Significant reductions of the orbit distortions have been realized using this compensation.

TUPOB20 Spin-Orbit Correlations and Nonlinear Muon Beam Dynamics for Precision g-2 Measurements

D. Tarazona (MSU)

The main goal of the Muon g-2 Experiment (g-2) at Fermilab is to measure the muon anomalous magnetic moment to unprecedented precision. This new measurement will allow to test the completeness of the Standard Model (SM) and to validate other theoretical models beyond the SM. Unique to this experiment is the roughly 3 km muon delivery system as muons produced from pion decays at the target station will pass through several sections permeated by various configurations of magnetic fields along the beamlines of g-2, promoting the development of interplays between spin polarization and orbit distributions of the muon beam. Since spin-orbit correlations have the potential effect to influence the main measurement of g-2 inside the Storage Ring, we are elaborating analytical studies and computational simulations using COSY INFINITY from Michigan State University to deepen the understanding of this problem. Furthermore, we are paying special attention to spin-orbit correlations in the multi-pass Delivery Ring.

TUPOB21 MuSim, a Graphical User Interface for Multiple Simulation Codes

T.J. Roberts (Muons, Inc)

MuSim is a user-friendly program designed to interface to many different particle simulation codes, regardless of their data formats or geometry descriptions. It presents the user with a compelling graphical user interface that includes a flexible 3-D view of the simulated world plus powerful editing with drag-and-drop capabilities. All aspects of the design can be parameterized so that parameter scans and optimizations are easy. MuSim is particularly well suited to accelerator-driven subcritical reactors, as one code can be used to model the accelerator, and a completely different code for the reactor, or multiple codes for each, all from a single description of the system (geometry, materials, sources, fields, and instrumentation). It is simple to create plots and display events in the 3-D viewer (with a slider to vary the transparency of solids). Many simulation tools and beam optics codes were written long ago, with primitive user interfaces by today's standards [–] MuSim is specifically designed to make it easy to interface to all such codes.

TUPOB22 Dependence of the Coupling of Dipole Motion From Bunch to Bunch Caused by Electron Clouds at CsrTA Due to Variations in Bunch Length and Chromaticity

M.G. Billing, L.Y. Bartnik, M.J. Forster, N.T. Rider, J.P. Shanks (Cornell University (CLASSE), Cornell Laboratory for

Accelerator-Based Sciences and Education) R. Holtzapple (CalPoly)

The Cornell Electron-Positron Storage Ring Test Accelerator (CesrTA) has been utilized to probe the interaction of the electron cloud with a 2.1 GeV stored positron beam. Recent experiments have characterized any dependence of beam-electron cloud (EC) interactions on the bunch length (or synchrotron tune) and the vertical chromaticity. The measurements were performed on a 30-bunch positron train with a 14 ns spacing, at a fixed current of 0.75mA/bunch. The dynamics of the stored beam, in the presence of the EC, was quantified using: 10 turn-by-turn beam position monitors in CESR to measure the correlated bunch-by-bunch dipole motion and an x-ray beam size monitor to record the bunch-by-bunch, turn-by-turn vertical size of each bunch within the trains. In this paper we report on the observations from these experiments and analyze the coupling of dipole motion from bunches within the train to subsequent bunches caused by the EC.

- TUP0B23 Electron Cloud Simulations for the CHESS-U Upgrade at the Cornell Electron Storage Ring**
J.A. Crittenden, S. Poprocki, J.E. San Soucie (Cornell University (CLASSE), Cornell Laboratory for Accelerator-Based Sciences and Education)

The Cornell Electron Storage Ring operations group is studying a major upgrade of the storage ring performance as an X-ray user facility. The principal modification foresees replacing the former e^+e^- interaction region with six double-bend achromats, reducing the emittance by a factor of four. The beam energy will increase from 5.3 to 6.0 GeV and single-beam operation will replace the present two-beam operation with pretzel orbits in a common beam pipe. The initial phase of the project will use a single positron beam, so electron cloud buildup can be expected to dominate performance limitations. This work describes a synchrotron radiation analysis of the new ring, and employs its results to provide ring-wide estimates of cloud buildup and consequences for the lattice optics and beam dynamics.

- TUP0B24 Effect of Energy Variation on the Performances of Linear Induction Radiography Accelerator**
Wu, Y.H. Wu, Y.J. Chen, L. Ellsworth (LLNL)

The current interest for the next generation linear induction accelerator (LIA) is to generate multiple electron beam pulses with high peak currents. The beam energy and current may vary from pulse to pulse. Consequently, the transport and control of multi-pulsing intense electron beams through a focusing lattice over a long distance on such machine becomes challenging. In this study, we are developing an optimization method for tuning the transport system for beams with energy and current variations. Our simulation studies of multi-pulse LIAs using AMBER and BREAKUP Code are described. These include optimal beam focusing magnetic tune for minimization of emittance growth and steering correction for corkscrew motion.

- TUP0B25 Unfolding of Electron Beam Parameters using AMBER PIC Code**
Wu, Y.H. Wu, Y.J. Chen, L. Ellsworth (LLNL)

The FXR linear induction accelerator at Lawrence Livermore National Laboratory produces x-ray bursts for radio-graphs. The machine is able to deliver a stable electron beam to the bremsstrahlung target with spot sizes less than 2mm. We have done magnet scanning at the downstream of the accelerator. Using the spot sizes obtained from the magnet scanning, the authors unravelled the beam parameters at the exit of accelerating modules by modelling the FXR LINAC with the simulation code Amber [1]. In this study, we present the most recent spot size measurement results and techniques that used to extract the beam parameters.

- TUP0B26 Dynamics of Intense Beam in Quadrupole-Duodecapole Lattice Near Sixth Order Resonance**
Y.K. Batygin, T.T. Fronk (LANL)

The presence of duodecapole components in quadrupole focusing field results in excitation of sixth-order single-particle resonance if the phase advance of the particles transverse oscillation is close to 60 deg. This phenomenon results in intensification of beam losses. We present analytical and numerical treatment of particle dynamics in the vicinity of sixth-order resonance. The topology of resonance in phase space is analyzed. Beam emittance growth due to crossing of resonance islands is determined. Halo formation of intense beams in presence of resonance conditions is examined.

- TUP0B27 Reconciling Common Transport Line to Support Two Experimental Facilities**
J.S. Kolski, T.T. Fronk, R.C. McCrady, P.K. Roy (LANL)

The Proton Radiography (pRAD) and Ultra-cold Neutron (UCN) experimental facilities at the Los Alamos Neutron Science Center (LANSCE) share a common transport line in Line X. Before the results of our work, Line X operated with different machine tunes (focusing lattice and beam steering) for production beam to pRad and UCN, preventing the facilities from operating at the same time. We discuss efforts to reconcile the Line X tune to support beam operations to pRad and UCN without changing the Line X focusing lattice and beam steering. We use a combination of beam measurements (wire scan and phosphor screen imaging) and beam line modeling using TRANSPORT to derive and verify the reconciled Line X tune.

- TUP0B28 Entrance and Exit CSR Impedance for Non-ultrarelativistic Beams**
R. Li (JLab) C.-Y. Tsai (Virginia Polytechnic Institute and State University)

As a high-brightness electron bunch being transported through magnetic bending system such as bunch compression chicane or recirculating arcs, the bunch phase space quality could be degraded by the microbunching instability resulting from the coherent synchrotron radiation (CSR) effect. The frequency domain Vlasov analysis of microbunching instability requires the expression of the CSR impedance for both the steady-state and the transient interaction including the entrance and exit of a magnetic dipole. Of particular interest is the energy dependence of the CSR impedance at very short microbunching wavelength. The transient CSR wakefield for non-ultrarelativistic regime has been well studied [1] and the results are widely applied in time-domain particle trackings. In this paper, we extend our earlier analysis of the non-ultrarelativistic steady-state CSR impedance [2] to the entrance and exit cases. This result is shown to be useful for the more complete and accurate Vlasov analysis of the high-gain microbunching instability in recirculating arcs.

- TUP0B29 Simulations of Nonlinear Beam Dynamics in the JLEIC Electron Collider Ring**
F. Lin, Y.S. Derbenev, V.S. Morozov, F.C. Pilat, G.H. Wei, Y. Zhang (JLab) Y. Cai, Y. Nosochkov, M.K. Sullivan (SLAC)

The short lengths of colliding bunches in the proposed Jefferson Lab Electron-Ion Collider (JLEIC) allow for small beta-star values at the interaction point (IP) yielding a high luminosity. The strong focusing associated with the small beta-star values results in high natural chromaticities and potentially a beam smear at the IP. Rapid growth of the electron equilibrium emittances and momentum spread with energy further complicates the situation. We developed a nonlinear dynamics correction scheme that overcomes these problems and allows for stable beam dynamics and sufficient beam lifetime at the highest electron energy. In this paper, we present simulations of the momentum acceptance and dynamic aperture optimizing and validating the developed scheme.

- TUP0B30 Spin Flipping System in the JLEIC Collider Ring**
V.S. Morozov, Y.S. Derbenev, F. Lin, Y. Zhang (JLab) Y. Filatov (MIPT) A.M. Kondratenko, M.A. Kondratenko (Science and Technique Laboratory Zaryad)
 The figure-8 JLEIC collider ring opens wide possibilities for manipulating proton and deuteron spin directions during an experiment. Using 3D spin rotators, one can, at the same time, efficiently control the polarization direction as well as the spin tune value. The 3D spin rotators allow one to arrange a system for reversals of the spin direction in all beam bunches during an experiment, i.e. a spin-flipping system. To preserve the polarization, one has to satisfy the condition of adiabatic change of the spin direction. When adjusting the polarization direction, one can stabilize the spin tune value, which completely eliminates resonant beam depolarization during the spin manipulation process. We provide the results of numerical modeling of a spin-flipping system in the JLEIC ion collider ring. The presented results demonstrate the feasibility of organizing a spin-flipping system using a 3D rotator. The figure-8 JLEIC collider provides a unique capability of doing high-precision experiments with polarized ion beams.
- TUP0B31 Compensation of Chromaticity in the JLEIC Electron Collider Ring**
Y. Nosochkov, Y. Cai, M.K. Sullivan (SLAC) Y.S. Derbenev, F. Lin, V.S. Morozov, F.C. Pilat, G.H. Wei, Y. Zhang (JLab)
 The Jefferson Lab Electron-Ion Collider (JLEIC) is being designed to achieve a high luminosity of up to $10^{34} \text{ 1/(cm}^2\text{*sec)}$. The latter requires a small beam size at the interaction point demanding a strong final focus (FF) quadrupole system. The strong beam focusing in the FF unavoidably creates a large chromaticity which has to be compensated in order to avoid a severe degradation of momentum acceptance. This has to be done while preserving sufficient dynamic aperture. An additional design requirement for the chromaticity compensation optics in the electron ring is preservation of the low beam emittance. This paper reviews the development and selection of a chromaticity correction scheme for the electron collider ring.
- TUP0B32 Theory of Skew Parametric-Resonance Ionization Cooling**
A. Afanasev (GWU) Y.S. Derbenev, V.S. Morozov, A.V. Sy (JLab) R.P. Johnson (Muons, Inc)
 We develop a theoretical description of muon beam optics in a muon cooling channel that implements a half-integer (parametric) resonance in order to provide periodic beam focusing for ionization cooling. This approach named Skew Parametric-Resonance Ionization Cooling (PIC) uses skew quads to couple horizontal and vertical betatron oscillations. We demonstrate both analytically and using numerical examples that introduction of coupling results in modified betatron tunes and prevents a betatron resonance from arising for the periodic beam focusing designed for PIC. We also analyze the properties of beam dispersion and effects of nonlinear periodic fields. The developed semi-analytical approach provides guidance for full-scale simulation of Skew PIC transport channel, including compensation for chromatic and geometrical aberrations.
- TUP0B33 The Beam-Beam Effect and its Consequences for the Jefferson Lab EIC**
E.W. Nissen (JLab)
 In this work we address the effect of beam jitter on emittance growth as caused by the beam-beam effect on the Jefferson Lab Electron Ion Collider (JLEIC). This proposed collider would collide 100 GeV proton beams with up to 10 GeV electron beams. Due to the asymmetric rigidities of the beams the nonlinear lensing action of the beams on each other during a collision can cause collective effects that limit beam storage times. Using analytical methods as well as simulations we can predict the lifetime of the proton and electron beams in JLEIC, and determine how best to maximize the useable store time of the beam.
- TUP0B34 The Effects of Space Charge on the Dynamics of the Booster Synchrotron in the Jefferson Lab EIC**
E.W. Nissen, S.A. Bogacz (JLab)
 We examine the effects of space charge on the dynamics of the booster synchrotron with imaginary transition gamma for the proposed JLEIC electron ion collider. This booster will inject and accumulate protons and heavy ions at some reasonably low energy and then engage in a process of acceleration and electron cooling to bring it to its extraction energy of approximately 7 GeV. This would then be sent into the ion collider ring portion of JLEIC chain. In order to examine the effects of space charge on the dynamics of these processes we use the SYNERGIA particle tracking package. In particular, we address halo generation and emittance degradation due to resonance crossing in the presence of space-charge.
- TUP0B35 Progress on Skew Parametric Resonance Ionization Cooling Channel Design and Simulation**
A.V. Sy, Y.S. Derbenev, V.S. Morozov (JLab) A. Afanasev (GWU) Y. Bao (UCR) R.P. Johnson (Muons, Inc)
 Skew Parametric-resonance Ionization Cooling (Skew PIC) is an extension of the Parametric-resonance Ionization Cooling (PIC) framework that has previously been explored as the final 6D cooling stage of a high-luminosity muon collider. The addition of skew quadrupoles to the PIC magnetic focusing channel induces coupled dynamic behavior of the beam that is radially periodic. The periodicity of the radial motion allows for the avoidance of unwanted resonances in the horizontal and vertical transverse planes, while still providing periodic locations at which ionization cooling components can be implemented. Progress on aberration compensation in the coupled correlated optics channel is presented and discussed.
- TUP0B36 Simulation Study on JLEIC High Energy Bunched Electron Cooling***
H. Zhang, S.V. Benson, Y.S. Derbenev, Y. Roblin, Y. Zhang (JLab)
 In the JLab Electron Ion Collider (JLEIC) project the traditional electron cooling technique is used to reduce the ion beam emittance at the booster ring, and to compensate the intrabeam scattering effect and maintain the ion beam emittance during the collision at the collider ring. Different with other electron coolers using DC electron beam, the proposed electron cooler at the JLEIC ion collider ring uses high energy bunched electron beam, provided by an ERL. In this paper, we report some recent simulation study on how the electron cooling rate will be affected by the bunched electron beam properties, such as the correlation between longitudinal position and momentum spread, bunch shape and size, and the Larmor radius of the electrons.
- TUP0B37 Diffusion Measurement From Transverse Echoes**
Y.S. Li (Carleton College) T. Sen (Fermilab)
 Beam diffusion is an important measure of stability in high intensity beams. Traditional methods of diffusion characterization (e.g. beam scraping) can be very time-consuming. In this study, we investigated transverse beam echoes as a novel technique for measuring beam diffusion. With aid of both analytical and numerical solutions, we analyzed variations in maximum echo amplitude with and without diffusion. We performed a self-consistent measurement of linear diffusion coefficient via a parameter scan over delay time τ . We also demonstrated the effectiveness of pulsed quadrupoles as a means to boost echo amplitude. Results from this study will support the planned echo experiments in the IOTA proton ring under construction at Fermilab.
- TUP0B38 Implementation of MAD-X into MuSim**
Y. Bao (UCR) T.J. Roberts (Muons, Inc)

MuSim is a new and innovative graphical system that allows the user to design, optimize, analyze, and evaluate accelerator and particle systems efficiently. It is designed for both students and experienced physicists to use in dealing with the many modeling tools and their different description languages and data formats. G4beamline and MCNP have been implemented into MuSim in previous studies. In this work, We implement MAD-X into MuSim so that the users can easily use the graphical interface to design beam lines and compare the modeling results of different codes.

- TUP0B39 Mechanical Design and Manufacturing of a Two Meter Precision Non-Linear Magnet System**
J.D. McNevin (*RadiaBeam Systems*) **R.B. Agustsson, F.H. O'Shea** (*RadiaBeam*)
 RadiaBeam Technologies is currently developing a non-linear magnet insert for Fermilab's Integrable Optics Test Accelerator (IOTA), a 150 MeV circulating electron beam storage ring designed for investigating advanced beam physics concepts. The physics requirements of the insert demand a high level of precision in magnet geometry, magnet axis alignment, and corresponding alignment of the vacuum chamber geometry within the magnet modules to maximize chamber aperture size. Here we report on the design and manufacturing of the vacuum chamber, magnet manufacturing, and kinematic systems.
- TUP0B40 Fundamental Properties of a Novel, Metal-Dielectric, Tubular Structure with Magnetic RF Compensation**
A.V. Smirnov, S.V. Kutsaev (*RadiaBeam Systems*) **E.A. Savin** (*MEPhI*)
 A number of electron beam vacuum devices such as small radiofrequency (RF) linear accelerators (linacs) and microwave traveling wave tubes (TWTs) utilize slow wave structures which are usually rather complicated in production and may require multi-step brazing and time consuming tuning. Fabrication of these devices becomes challenging at centimeter wavelengths, at large number of cells, and when a series or mass production of such structures is required. A hybrid, metal-dielectric, periodic structure for low gradient, low beam current applications is introduced here as a modification of Andreev's disk-and-washer (DaW) structure. Compensated type of coupling between even and odd TE₀₁ modes in the novel structure results in negative group velocity with absolute values as high as 0.1c-0.2c demonstrated in simulations. Sensitivity to material imperfections and electrodynamic parameters of the disk-and-ring (DaR) structure are considered numerically using a single cell model.
- TUP0B41 Bi-Complex Toolbox Applied to Gyromagnetic Beam Break-Up**
A.V. Smirnov (*RadiaBeam*)
 Transverse instability of a multi-bunch beam in the presence of a longitudinal magnetostatic field and hybrid dipole modes is considered analytically within a single-section model. It incorporates resonant interaction with beam harmonics and eigenmodes, degenerated waves of different polarizations, and the Lorentz RF force contribution. The analysis is performed in a very compact form using a bi-complex i,j-space including four-component collective frequency of the instability. Rotating polarization of the collective field is determined by ImiImj part of the bi-complex collective frequency in agreement with available data. The other three components represent detuning of the collective frequency ReiRej, the left-hand, and right-hand increments ImiRej±ReilImj of the gyro-magnetic BBU effect. The scalar hyper-complex toolbox can be applied to spin transport analysis and for characterization of complex transverse dynamics in gyro-devices such as Gyro-TWTs.
- TUP0B42 Non-Linear Inserts for the IOTA Ring**
F.H. O'Shea, R.B. Agustsson, P.S. Chang (*RadiaBeam*) **J.D. McNevin** (*RadiaBeam Systems*)
 RadiaBeam Technologies is building the non-linear insert for the proof of concept of integrable optics at the Integrable Optics Test Accelerator at Fermilab. Herein we describe the device as delivered to Fermilab. In particular, we present the magnetic performance of the magnet sections, including alignment and briefly discuss the vacuum chamber performance.
- TUP0B43 Magnetic Cloaking of Charged Particle Beams**
K.G. Capobianco-Hogan (*SBU*)
 In order to measure the momentum of particles produced by asymmetric collisions in the proposed Electron Ion Collider, a magnetic field must be introduced perpendicular to the path of the beam without bending or depolarizing it. A magnetic cloak consisting of a superconducting magnetic shield surrounded by a ferromagnetic layer is capable of shielding the interior from a magnetic field – thereby protecting the beam – without distorting the field outside of the cloak – permitting detector coverage at high pseudorapidity.
- TUP0B44 Final 6d Muon Ionization Cooling Using Strong Focusing Quadrupoles**
T.L. Hart, J.G. Acosta, L.M. Cremaldi, S.J. Oliveros, D.J. Summers (*UMiss*) **D.V. Neuffer** (*Fermilab*)
 Low emittance muon beam lines and muon colliders are potentially a rich source of BSM physics for future experimenters. A normalized transverse muon emittance of 280 microns has been achieved in simulation with short solenoids and a betatron function of 3 cm. Here we use ICOOL, G4Beamline, and MAD-X to explore using a flat 400 MeV/c muon beam and strong focusing quadrupoles to achieve a normalized transverse emittance of 100 microns and finish 6D cooling. The low beta regions, as low as 5 mm, produced by the quadrupoles are occupied by dense, low Z absorbers, such as lithium hydride or beryllium, that cool the beam. Equilibrium transverse emittance is linearly proportional to the beta function. Reverse emittance exchange with septa and/or wedges is then used to decrease transverse emittance from 100 to 25 microns at the expense of longitudinal emittance for a high energy lepton collider. Cooling challenges include chromaticity correction, momentum passband overlap, quadrupole acceptance, and staying in phase with RF.
- TUP0B45 A Model to Simulate the Effect of a Transverse Feedback System on Single Bunch Instability Thresholds**
G. Bassi, A. Blednykh, V.V. Smaluk (*BNL*)
 A model to simulate the effect of a transverse feedback system is implemented in SPACE, a parallel, self-consistent code for collective effects. As an application, we discuss single bunch instability thresholds in the NSLS-II storage ring and compare the numerical results with measurements.
- TUP0B46 A Study of the Low-Frequency Impedance Induced by the NSLS-II In-Vacuum Undulators**
G. Bassi, A. Blednykh, V.V. Smaluk (*BNL*)
 We present a study of the dipole and quadrupole impedance induced by the NSLS-II In-vacuum Undulators in the low-frequency regime. The calculated complex frequency shifts are compared with measurements. In order to enhance the impedance effects, lattices with local beta bumps and lowered fractional betatron tune are used in the studies.
- TUP0B48 Low-Frequency Impedance of Undulators and Wigglers**
A. Blednykh, G. Bassi, Y. Hidaka, V.V. Smaluk (*BNL*) **G. Stupakov** (*SLAC*)
 An analytical expression of the low-frequency quadrupole impedance for undulatory and wigglers is derived and benchmarked

against beam-based impedance measurements, done at the 3GeV NSLS-II storage ring. The adopted theoretical model, valid for an arbitrary number of electromagnetic layers with parallel geometry, allows to calculate the quadrupole impedance for arbitrary values of the magnetic permeability. In the comparison of the analytical results with the measurements for variable magnet gaps, two limit cases of the permeability have been studied: the case of perfect magnets ($\mu \rightarrow \infty$), and the case in which the magnets are fully saturated ($\mu=1$).

TUP0B49 Muti-Bunch Intensity Dependent Tune Shift in NSLS-II

A. Blednykh, G. Bassi, Y. Hidaka, V.V. Smaluk (BNL)

The tune shifts dependence on the average current has been studied in the NSLS-II storage ring. The vertical and horizontal tune slopes have opposite signs and merges with increase of the average current. Their slopes depend on the local betatron functions, the magnet gaps and the magnetic properties of the magnet at low-frequency. Low-frequency quadrupole impedance of Insertion Devices, dipole magnets and multipole magnets have been considered and its effect on the tune shifts have been discussed.

TUP0B50 Beam-Induced Heating of the Kicker Ceramics Chambers at NSLS-II

A. Blednykh, B. Bacha, G. Bassi, C. Hetzel, T.V. Shafan, V.V. Smaluk (BNL)

Experience with the beam-induced heating of the ceramics chambers in the NSLS-II storage ring has been discussed. Four ceramic chambers with 2 microns titanium coating are installed in the injection kickers and one same chamber is installed in the pinger. Beam studies showed that the ceramic chambers are heated up by the coherent beam energy loss caused by beam-chamber interaction. The maximum temperature reached 100 degree C and this was considered as a serious problem of upcoming 500 mA operations. Visual inspection of the most problematic chamber, which has been removed from the ring during the shutdown, showed a damage of the titanium coating. This chamber replaced by the pinger chamber, which in turn has been replaced by a spare one. To improve the heat removal, a forced air cooling is implemented to the kicker units. The latest experiments show significant decrease of the chamber temperatures when the cooling is on.

TUP0B51 A Comparison of Collective Effects Codes

A. Blednykh, G. Bassi, V.V. Smaluk (BNL) R.R. Lindberg (ANL)

In this paper we compare the results obtained by simulations with measured data. Bunch lengthening effect and energy spread vs beam intensity using the computed longitudinal wakefield by the GdfidL code. Stabilizing effect of positive chromaticity on the single-bunch threshold current and on the coupled bunch instabilities applying the transverse dipole and quadrupole wake fields computed for a 1mm bunch length.

TUP0B52 Linear Optics Characterization and Correction Method Using Turn-by-Turn BPM Data Based on Resonance Driving Terms with Simultaneous BPM Calibration Capability

Y. Hidaka, B. Podobedov (BNL) J. Bengtsson (J B Optima, LLC)

A fast new linear lattice characterization/correction method based on turn-by-turn (TbT) beam position monitor (BPM) data in storage rings has been recently developed and experimentally demonstrated at NSLS-II. This method performs least-square fitting iteratively on the 4 frequency components extracted from TbT data and dispersion functions. The fitting parameters include the errors for normal/skew quadrupole strength and 4 types of BPM errors (gain, roll, and deformation). The computation of the Jacobian matrix for this system is very fast as it utilizes analytical expressions derived from the resonance driving terms (RDT), from which the method name DTBLOC (Driving-Terms-Based Linear Optics Characterization/Correction) originates. At NSLS-II, a lattice corrected with DTBLOC was estimated to have beta-beating of <1%, dispersion errors of ~1 mm, and emittance coupling ratio on the order of 10⁻⁴. In addition, a novel method is proposed to assess the confidence level on the fit estimates obtained from DTBLOC or any other method by making a systematic comparison of TbT- and Twiss-derived RDTs.

TUP0B53 Transverse and Longitudinal Beam Dynamics Studies for an Energy-Recovery Experiment at CEBAF

P. Korysko, F. Méot, G. Robert-Demolaize (BNL)

A proposal for a multiple-pass, high energy, energy-recovery experiment using CEBAF is under preparation within a JLab-BNL collaboration. In order to prepare for beam dynamics studies and in addition to the existing Elegant model, a version of the CEBAF lattice is developed for MAD-X. In the following, results from numerical simulations are presented, with the focus being transverse and longitudinal beam dynamics, in particular issues related to the longitudinal matching over the course of multiple-pass tracking.

TUP0B54 Using Square Matrix to Realize Phase Space Manipulation and Dynamic Aperture Optimization

Y. Li, L. Yu (BNL)

We introduce a new method of using square matrix to realize phase space manipulation and dynamic aperture optimization in storage rings. Both the tracking simulation and the experimental observation in the NSLS-II ring lattice are presented.

TUP0B55 Optimize the Algorithm for 10 Hz Orbit Feedback at Fixed Energies and During Acceleration

C. Liu, R.L. Hulsart, K. Mernick, R.J. Michnoff, M.G. Minty (BNL)

The 10 Hz global orbit feedback system is in routine operation for RHIC programs at fixed energies and during acceleration, to combat the beam oscillation introduced by triplets vibrations. The optimization of the feedback performance by cutting eigenvalues of the response matrix will be presented. With updated lattice for proton beam in 2015, the performance of the feedback system during acceleration was jeopardized by the corrector current transients. Tikhonov regulation was employed to solve the problem. The experimental results will be shown.

TUP0B56 The eRHIC Ring-Ring Design

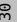
C. Montag, G. Bassi, J. Beebe-Wang, J.S. Berg, M. Blaskiewicz, A.V. Fedotov, W. Fischer, Y. Hao, A. Hershcovitch, Y. Luo, R.B. Palmer, B. Parker, S. Peggs, V. Ptitsyn, V.H. Ranjbar, S. Seletskiy, T.V. Shafan, V.V. Smaluk, S. Tepikian, E.J. Willeke, H. Witte, Q. Wu (BNL)

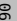
The ring-ring version of the eRHIC electron-ion collider design aims at providing electron-proton collisions with a center-of-mass energy ranging from 32 to 141 GeV at a luminosity reaching 10³³ cm⁻² sec⁻¹. This design of the double-ring collider also supports electron-ion collisions with similar electron-nucleon luminosities, and is upgradeable to 10³⁴ cm⁻² sec⁻¹ using bunched beam electron cooling of the hadron beam. The baseline luminosities are achievable using existing technologies and beam parameters that have been routinely achieved at RHIC in hadron-hadron collisions or elsewhere in e⁺e⁻ collisions. This minimizes the risk associated with the challenging luminosity goal and is keeping the technical risk of the e-RHIC electron-ion collider low. The latest design status will be presented.

- TUP0B57 The Role of Adami Information in Beam Cooling**
V.H. Ranjbar (BNL)
 We re-consider stochastic cooling as type of information engine using the Adami* definition of information. Following the spirit of Adami we define information as data which can permit the cooling system to predict the individual trajectories better than purely random prediction and then act on that data to modify the trajectories of an ensemble of particles. In this study we track the flow of this type of information through the closed system and consider the limits based on sampling and correction as well as the role of the underlying model.
- TUP0B58 Dependence of LEReC Beam Energy Spread on Photocathode Laser Modulation**
S. Seletskiy, M. Blaskiewicz, A.V. Fedotov, D. Kayran, J. Kewisch, M.G. Minty, B. Sheehy, Z. Zhao (BNL) *C.M. Gulliford (Cornell University (CLASSE), Cornell Laboratory for Accelerator-Based Sciences and Education)*
 Present requirements to the photocathode DC gun of the low energy RHIC electron cooling (LEReC) project is to produce 100 ps long bunch of electrons with 130 pC charge. The laser pulse of required length will be produced with the stacking of multiple few picosecond long sub-pulses. Depending on the choice of the laser sub-pulse length and on the relative delay between these sub-pulses one can obtain laser pulse with various longitudinal intensity modulations. The longitudinal modulation of laser intensity creates longitudinal modulation of electron bunch charge. Such modulation is known to cause the growth of e-beam uncorrelated energy spread in photoinjectors' the effect we would like to avoid. In this paper we estimate growth of e-beam energy spread due to its initial density modulation and set requirements to the maximum allowable depth of longitudinal modulation of photocathode laser intensity.
- TUP0B59 Simulation of Beam-Beam Noise Effect in Linac-Ring Scheme eRHIC**
K. Shih, Y. Hao (BNL)
 The linac-ring scheme eRHIC promises higher luminosity and versatile upgradability than its ring-ring counterpart. However the fresh electron beam may heat up the ion beam in the ring through beam-beam interaction. The noise effect of the electron beam had been studied theoretically, while detailed simulation is needed to explore the effect beyond linear theories. In this paper, we will present the simulation results of the electron beam noise effect to the ion beam considering the nonlinearity of the beam-beam force and effect of the finite bunch length.
- TUP0B60 Permanent Magnets for High Energy Nuclear Physics Accelerators***
N. Tsoupas, S.J. Brooks, A.K. Jain, G.J. Mahler, F. Méot, V. Ptitsyn, D. Trbojevic (BNL)
 The proposed eRHIC accelerator¹ will collide 20 GeV polarized electrons with 250 GeV polarized protons or 100 GeV/n polarized ³He ions or other unpolarized heavy ions. The electron accelerator of the eRHIC will be based on a 1.665 GeV Energy Recovery Linac (ERL) placed in the RHIC tunnel and two Fixed Field Alternating Gradient (FFAG) recirculating rings placed alongside the RHIC accelerator. The electron bunches reach the 20 GeV energy after passing 12 times through the ERL by recirculation in the FFAG rings. The FFAG rings consist of FODO cells comprised of one focusing and one defocusing quadrupoles made of permanent magnet material. Similarly other sections of the electron accelerator will utilize permanent magnets. In this presentation we will discuss details on the design of these magnets and their advantages over the current-excited magnets.
- TUP0B61 Recent Improvements to TAPAs, the Android Application for Accelerator Physics and Engineering**
M. Borland (Private Address)
 The Android application TAPAs, the Toolkit for Accelerator Physics on Androids, was released in 2012 and at present has over 300 users. TAPAs provides over 50 calculations, many of which are coupled together. Updates are released about once a month and have provided many new capabilities. Calculations for electron storage rings are a particular emphasis, and have expanded to include CSR threshold, ion trapping, Laslett tune shift, and emittance dilution. Other additions include helical superconducting undulators, rf cavity properties, Compton backscattering, and temperature calculations for mixing water.
- TUP0B62 Benchmark Strong-Strong Simulation of the Kink Instability in an Electron-Ion Collider Design**
J. Qiang, R.D. Ryne (LBNL) *Y. Hao* (BNL)
 The kink instability limits the performance of a potential linac-ring based electron-ion collider design. In this paper, we report on the simulation study of the kink instability using a self-consistent strong-strong beam-beam model.
- TUP0B63 Electron Cloud Build Up simulation for Main Injector and Recycler at Fermilab Using POSINST**
Y. Ji (IIT) *L.K. Spentzouris (Illinois Institute of Technology) R.M. Zwaska (Fermilab)*
 E-cloud effect could be a limiting factor for Fermilab accelerator operation. A potential E-cloud related instability was observed at 2014. To study this instability, simulation on E-cloud build up in the Main injector and Recycler was performed.
- TUP0B64 Beam Measurements at the PIP-II Injector Test Low Energy Beam Transport**
J.-P. Carneiro, B.M. Hanna, L.R. Prost, A.V. Shemyakin (Fermilab)
 This paper presents the main results obtained during a series of beam measurements performed on the Proton Improvement Plan II (PIP-II) Injector Test Low Energy Beam Transport from November 2014 to June 2015. The measurements which focus on beam transmission, beam size and emittance at various locations along the beam line are compared with the beam dynamics codes TRACK and TRACEWIN. These studies were aimed at preparing the beam for optimal operation of the RFQ, while evaluating simulation tools with respect to experimental data.
- TUP0B66 Beam Alignment in the PIP-II Injector Test Radio-Frequency Quadrupole**
J.-P. Carneiro, L.R. Prost, A.V. Shemyakin, J. Steimel (Fermilab)
 The Proton Improvement Plan II (PIP-II) Injector Test Radio-Frequency Quadrupole (RFQ) has been in operation with beam at Fermilab since March 2016. The RFQ is capable of accelerating a negative hydrogen ion beam from 30 keV to 2.1 MeV at a maximum current of 10 mA both in pulse and CW modes. Simulations with the beam dynamics code TRACK predict that a misalignment of the beam at the RFQ entrance can deteriorate the transverse and longitudinal emittance at the RFQ exit without necessarily impacting the beam transmission. The paper discusses the procedure to align the beam injected into the RFQ with respect to the RFQ electrical axis and compares experimental results with TRACK predictions.


WEA1 — Oral Presentations (MC5)

Chair: A. Seryi (JAI)


- WEA1I001 08:30  Demonstration of Energy-Chirp Control in Relativistic Electron Bunches at LCLS Using a Corrugated Structure**
T.J. Maxwell (SLAC)
 An experimental study is presented of a corrugated structure that uses wakefields to remove linear energy correlation in a high energy (4.4 - 13.3 GeV) electron beam (a dechirper). Time-resolved measurements of both longitudinal and transverse wakefields of the device are presented and compared with simulations. We demonstrate flexible control of the LCLS FEL bandwidth and present novel uses of the device in addition to energy chirp control.
- WEA1I002 09:00  Computation of Electromagnetic Fields Generated by Relativistic Beams in Complicated Structures**
I. Zagorodnov (DESY)
 We discuss recent developments of numerical methods for computation of wakefields excited by short bunches in accelerators. They include a low-dispersive computational algorithm, conformal approximation of the boundaries, surface conductivity, and indirect wake potential integration. The implementation of these methods in the electromagnetic code ECHO for 2D and 3D problems are presented with a special emphasis on a new ECHO2D code for fast calculations of wakefields in rectangular geometries. Several examples of application of the code to calculation of wakefields for the European Free Electron Laser project and in the Linac Coherent Light Source (LCLS) project are considered.
- WEA1C003 09:30  Simulations of Booster Injection Efficiency for the APS-Upgrade**
J.R. Calvey, K.C. Harkay, R.R. Lindberg, C. Yao (ANL)
 The APS-Upgrade will require the injector chain to provide high single bunch charge for swap-out injection. One possible limiting factor to achieving this is an observed reduction of injection efficiency into the booster synchrotron at high charge. We have simulated booster injection using the particle tracking code elegant, including a model for the booster impedance and beam loading in the RF cavities. The simulations point to two possible causes for reduced efficiency: energy oscillations leading to losses at high dispersion locations, and a vertical beam size blowup caused by ions in the particle accumulator ring. We also show that the efficiency is much higher in an alternate booster lattice with smaller vertical beta function and zero dispersion in the straight sections.
- WEA1C004 09:45  Hollow Electron Beam Collimation for HL-LHC - Effect on the Beam Core**
M. Fitterer, G. Stancari, A. Valishev (Fermilab)
 Collimation with hollow electron beams is currently one of the most promising concepts for active halo control in HL-LHC. In previous studies it has been shown that the halo can be efficiently removed with an hollow electron lens. Equally important as an efficient removal of the halo, is also to demonstrate that the core stays unperturbed. In this paper, we present simulations of the beam core for different electron lens parameters and modes of operation.
- WEA1C005 10:00  Microwave Instability Studies in NSLS-II**
A. Blednykh, B. Bacha, G. Bassi, Y. Chen-Wiegart, W.X. Cheng, O.V. Chubar, A.A. Derbenev, V.V. Smaluk (BNL)
 The microwave instability in the NSLS-II has been studied for the current configuration of insertion devices, 9 In-Vacuum Undulators (IVU's), 3EPU's, 3 Damping Wigglers. The energy spread as a function of single bunch current has been measured based on the frequency spectrum of IVU for X-Ray Spectroscopy (SRX) beam line. The results for two lattices, bare lattice with nominal energy spread 0.0005 and a lattice with one DW magnet gap closed (nominal energy spread 0.0007) are compared. In addition we used a Spectrum Analyzer to measure the beam spectrum. The instability thresholds for two different lattices cross-checked numerically using the particle tracking code SPACE and longitudinal impedance.
- WEA1C006 10:15  Analytical theory for McMillan map**
T. Zolkin, S. Nagaitsev (Fermilab)
 McMillan map is an important discrete time model of 1D transverse nonlinear accelerator lattice. We provide a full analytical theory based on parametrization of individual canonical biquadratic curves*. Using the normal forms provided in* we were able to generalize this result to entire phase-plane of finite trajectories and calculate mechanical action-angle coordinates. The bifurcation map for canonical McMillan map including stability of fixed points is provided. In addition, we discuss the connection of these results with possible 2D generalizations - axially symmetric and 2D-magnetostatic McMillan lenses.

WEB1 — Tutorial & Oral Presentation (MC7)**Chair:** J.R. Delaysen (ODU)**WEB1TU01 Superconducting Accelerators Magnets****08:30**  **S. Prestemon, P. Ferracin (LBNL)**


Based on the US PAS class "Superconducting Accelerators Magnets" by Soren Prestemon / Paolo Ferracin

WEB1C002 Investigation of Structure and Composition Development in the Two-Step Diffusion Coating of Nb₃Sn on Niobium**10:00**  **U. Pudasaini, M.J. Kelley (The College of William and Mary) G.V. Eremeev, M.J. Kelley, C.E. Reece (JLab) M.J. Kelley, J. Tuggle (Virginia Polytechnic Institute and State University)**

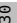
The potential for higher operating temperatures and increased accelerating gradient has attracted SRF researchers to Nb₃Sn coatings on niobium or other substrates for nearly 50 years. Its seeming simplicity has made the two-step tin vapor diffusion process the leading candidate, despite the almost universal finding of quality factor of coated cavities falling with increasing gradient. We have undertaken a fundamental materials study of the nucleation and deposition steps. Nucleation was accomplished within the usual parameter range: 400oC-500oC, 1-5 hours duration, 5 mg to 1 g SnCl₂ and 1-3 g Sn. The resulting deposit consists of a low (< 10%) coverage of micron-sized tin particles by SEM/EDS and a high (> 50%) coverage of few nm thick tin film by XPS and Scanning Auger Microscopy. The crystallography by EBSD and the topography of the substrate by AFM and SEM had no evident effect on the nucleation or the final film.

WEB1C003 Surface Impurity Content Optimization to Maximize Q-factors of Superconducting Resonators**10:15**  **M. Martinello (Fermilab)**


The superconducting properties of niobium RF cavities are enhanced when nitrogen impurities are dissolved as interstitial in the material. In this paper we study how the surface resistance is affected by this impurities introduction, in comparison with standard surface treatment for niobium resonators. A variety of 1.3 GHz cavities with different surface treatments are studied in order to cover a large range of interstitial impurities content: from few to thousand of nanometers of mean free path. Different contributions of the surface resistance are studied in this paper, focusing on the BCS and the trapped flux surface resistance. We found that interstitial impurities help to lower the BCS resistance contribution, allowing to obtain mean free path close to the predicted minimum of BCS resistance as a function of mean free path. Also we found that the trapped flux surface resistance follow a bell-shaped trend as a function of the mean free path. Adding these results together we show that optimal Nitrogen doping (N-doping) treatment allows to maximize Q-factor at 2 K and 16 MV/m as long as the magnetic field fully trapped during the cavity cooldown stays below 10 mG.

WEA2 — Oral Presentations (MC5)**Chair:** M. Blaskiewicz (BNL)**WEA2I001 Calculating Spin Lifetime**11:00  **V.H. Ranjbar** (BNL)


In polarized proton colliders there are continuous losses in polarization over the course of a several hour physics store. Recently, appropriate algorithms and sufficient computer power became available to address this problem. The techniques are summarized and applied to the RHIC collider.

WEA2I002 Proposed Experimental Validation of Hamiltonian Perturbation Theory in IOTA11:30  **D.L. Bruhwiler**, N.M. Cook, C.C. Hall, R.A. Kishek, S.D. Webb (*RadiaSoft LLC*) K.E. Badgley, S. Nagaitsev, E. Prebys, A.L. Romanov, G. Stancari, A. Valishev (*Fermilab*)


The Integrable Optics Test Accelerator (IOTA) is a small ring under construction to explore advanced concepts in beam dynamics, initially with electron pencil beams to emulate single-particle dynamics and later with low-energy proton beams including significant space charge tune depression. Hamiltonian perturbation theory and simulations with Synergia, Warp and other codes are being used to develop an experimental program for beam dynamics, including the highly nonlinear 'elliptic' magnet originally proposed by Danilov and Nagaitsev. The results suggest a number of experiments that could be performed at IOTA. For example, small changes in the linear tune and the strength of the elliptic magnet can be used to control dynamic aperture. Both electron and proton beams can be used to measure the tune spread as a function of the elliptic magnet strength, for comparison with theory. Space charge driven halo formation due to envelope oscillations can be measured over a range of elliptic magnet strengths. Theoretical and computational results will be presented to guide future decisions regarding experimental diagnostics for IOTA.

WEA2C003 Incoherent Vertical Emittance Growth from Electron Cloud at CEsrTA12:00  **S. Poprocki**, J.A. Crittenden, S.N. Hearsh, J.D. Perrin, D. L. Rubin, S. Wang (*Cornell University (CLASSE), Cornell Laboratory for Accelerator-Based Sciences and Education*)

We report on measurements of electron cloud (EC) induced tune shifts and emittance growth at the Cornell Electron-Positron Storage Ring Test Accelerator (CesrTA) with comparison to tracking simulation predictions. Experiments were performed with 2.1 GeV positrons in a 30 bunch train with 14 ns bunch spacing and 9 mm bunch length, plus a witness bunch at varying distance from the train to probe the cloud as it decays. Complementary data with an electron beam were obtained to distinguish EC effects from other sources of tune shifts and emittance growth. The simulations are based on a weak-strong model of the interaction of the positron beam (weak) with the electron cloud (strong), using high resolution electric field maps in the small region around the beam as the bunch passes through the cloud, computed with EC buildup simulation codes (ECLLOUD). Tracking simulations through the full lattice with electron cloud elements in the dipole and field-free regions predict vertical emittance growth, and tune shifts in agreement with the measurements.

WEA2C004 Vlasov Analysis of Microbunching Gain for Magnetized Beams12:15  **C.-Y. Tsai** (*Virginia Polytechnic Institute and State University*) Y.S. Derbenev, D. Douglas, R. Li, C. Tennant (JLab)

For a high-brightness electron beam with low energy and high bunch charge traversing through a recirculation beamline, coherent synchrotron radiation and space charge effect may result in the microbunching instability (MBI). Both tracking simulation and Vlasov analysis for an early design of Circulator Cooler Ring* of Jefferson Lab Electron Ion Collider reveal serious MBI. It is envisioned such MBI could be substantially suppressed by using a magnetized beam. In this work, we extend the existing Vlasov analysis, originally developed for a non-magnetized beam, to the description of transport of a magnetized beam including relevant collective effects. The new formulation will be further employed to confirm prediction of microbunching suppression for a magnetized beam transport in a recirculating beamline.

WEB2 — Oral Presentations (MC7)**Chair:** M.S. Champion (ORNL)**WEB2I001 Development of Higher Harmonic Superconducting Cavity for Light Sources**11:00  **M.P. Kelly** (ANL)

A new bunch lengthening cryomodule using a single-cell "higher-harmonic" superconducting cavity (HHC) operating at the 4th harmonic (1408 MHz) of the main RF is under development at Argonne. The system will be used to improve the Touschek lifetime and increase the single-bunch current limit in the upgraded multibend achromat lattice of the Advanced Photon Source electron storage ring. The system will use a pair of moveable 20 kW (each) CW RF power couplers to adjust the loaded Q and extract power from the beam. This will provide the flexibility to adjust the impedance presented to the beam and run at various beam currents. Higher-order modes (HOMs) induced by the circulating electron beam will be extracted along the beam axis and damped using a pair of room temperature beam line absorbers. The prototyping of the cavity, power couplers and HOM absorbers are discussed.

WEB2I002 Compact Crabbing Cavity Systems for Particle Colliders11:30  **S.U. De Silva** (ODU)

In circular or ring-based particle colliders, crabbing cavities are used to increase the luminosity. The first superconducting crabbing cavity system was successfully implemented at KEKB electron-positron collider that have demonstrated the luminosity increase with overlapping bunches. Crabbing systems are an essential component in the future colliders with intense beams, such as the LHC high luminosity upgrade and proposed electron-ion colliders. Novel compact superconducting cavity designs with improved rf properties, at low operating frequencies have been prototyped successfully that can deliver high operating voltages. We present single cavity and multi-cell crabbing cavities proposed for future particle colliders and addresses the challenges in those cavity systems.

WEB2C003 High Power Production Target for FRIB12:00  **F. Pellemoine** (FRIB)

This talk will discuss the Facility for Rare Isotope Beams (FRIB) target development including thermo-mechanical challenges, challenges due to radiation damage in material, and prototyping in order to validate the concept.

WEB2C004 Nb3Sn SRF Coatings at Fermilab12:15  **S. Posen, M. Merio, A. Romanenko, Y. Trenikhina** (Fermilab)

Nb3Sn coatings on superconducting RF cavities can substantially improve performance compared to niobium. Substantially improved cryogenic efficiency has been demonstrated, and theoretical predictions suggest substantially improved accelerating gradients are possible. A Nb3Sn SRF program has begun at Fermilab, beginning with the design and fabrication of a Nb3Sn coating system. In this contribution, we present the design, assembly, and commissioning efforts related to this system.

- WEPOA01 Affects of Changes in the Initial Proton Bunch Parameters on the Phase of the driven Wakefield in AWAKE**
N. Savard (University of Victoria) , **P. Muggli** (MPI) **E. Öz** (MPI-P) **J. Vieira** (IPFN)
 In AWAKE, long proton bunches propagate through a plasma, generating wakefields through the self-modulation instability (SMI). The phase velocity of these wakefields changes during the first 4 m of propagation and growth of the SMI, after which it stabilizes at the proton bunch velocity. This means that the ideal injection point for electrons to be accelerated is after 4 m into the plasma. Using the PIC code OSIRIS, we study how small changes in the initial proton bunch parameters (such as charge, radial and longitudinal bunch length, etc) to be expected in the experiment affect the phase velocity of the wakefields, primarily by looking at the difference in the phase of the wakefields at the point of injection (along the bunch and along the plasma) when changing these parameters by a small amount ($\pm 5\%$). We also look for the region of optimal acceleration/focusing for electron injection. Ultimately, it is found that small changes in the initial proton bunch parameters are not expected to significantly impact electron injection experiments in the future.
- WEPOA02 Progress Toward an Experiment at AWAKE***
P. Muggli (MPI)
 The AWAKE experimental program is scheduled to start at the end of 2016. The aim of the first experiments is to detect and study the self-modulation instability (SMI) of the long proton bunch ~ 12 cm in a plasma with wakefields of period of ~ 1.2 mm. The occurrence of SMI results in the formation of a charge core surrounded by a halo in the time-integrated images of the proton bunch transverse profile. Transverse profiles are obtained from scintillator screens and from optical transition radiation (OTR). The OTR is time resolved using a ps-resolution streak camera to determine the start of the wakefields along the bunch on a slow time scale (\sim ns), i.e., the location of the seeding of the SMI generated by the ionizing laser pulse. The modulation period is measured using the faster time scale (\sim ps). Coherent transition radiation (CTR) is analyzed by a heterodyne system to also yield the modulation frequency. Later experiments will sample the wakefields generated by externally injecting low-energy (~ 15 MeV) electrons expected to be accelerated to the GeV energy level over the 10 m-long plasma. Progress toward the completion of the experimental set-up will be presented.
- WEPOA03 Synchrotron Oscillation Derived From Three Components Hamiltonian**
K. Jimbo (Kyoto University) **H. Souda** (Gunma University, Heavy-Ion Medical Research Center)
 The Hamiltonian, which was composed of coasting, synchrotron and betatron motions, clarified the synchro-betatron resonant coupling mechanism in a storage ring*. The equation for the synchrotron motion was also obtained from the Hamiltonian. It shows that the so-called synchrotron oscillation is an oscillation around the revolution frequency as well as of the kinetic energy of the on-momentum particle. The detectable synchrotron oscillation is a horizontal oscillation on the laboratory frame.
- WEPOA04 Design of RFQ for RF Synchronized Short Pulse Laser Ion Source**
Y. Fuwa, **Y. Iwashita** (Kyoto ICR)
 A short pulse laser ion source is under development. In this ion source, ions are produced by femto-second laser in RF electric field and produced ion bunch with a few nanosecond pulse length. This feature can eliminate bunching section of RFQ and beam can be accelerated from the first cell of RFQ. In this presentation, results of design study for the RFQ without bunching section will be presented.
- WEPOA05 EBIS Charge Breeder for RAON Facility**
S.A. Kondrashev, **J.-W. Kim**, **Y.K. Kwon**, **Y.H. Park**, **H.J. Son** (IBS)
 New large scale accelerator facility called RAON is under design in Institute for Basic Science (IBS, Daejeon, Korea). Both techniques of rare isotope production Isotope Separation On-Line (ISOL) and In-Flight Fragmentation (IF) will be combined within one facility for the first time to provide wide variety of rare isotope ion beams for nuclear physics experiments and applied research. Electron Beam Ion Source (EBIS) charge breeder will be used to prepare rare isotope ion beams produced by ISOL method for efficient acceleration. Beams of different rare isotopes will be charge-bred by an EBIS charge breeder to a charge-to-mass ratio ($q/A \geq 1/4$) and accelerated by linac post-accelerator to energies of 18.5 MeV/u. RAON EBIS charge breeder will provide the next step in the development of breeder technology by implementation of electron beam with current up to 3 A and utilization of wide (8') warm bore of 6 T superconducting solenoid. The design of RAON EBIS charge breeder and results of dumping of high power DC and pulsed electron beam into collector will be presented and discussed.
- WEPOA06 New Coolers for Ion Ion Colliders**
V.V. Parkhomchuk (BINP SB RAS)
 2016 Robert R. Wilson Prize for Achievement in the Physics of Particle Accelerators Recipient: Vasili Parkhomchuk. For crucial contributions in the proof of principle of electron cooling, for leading contribution to the experimental and theoretical development of electron cooling, and for achievement of the planned parameters of coolers for facilities in laboratories around the world. New future coolers for ion*ion collider will be discussed.
- WEPOA07 Neutrons and Photons Fluences in the DTL Section of the ESS Linac**
L. Lari, **R. Bevilacqua**, **R. Miyamoto**, **C. Pierre**, **L. Tchelidze** (ESS) **F. Cerutti**, **L.S. Esposito**, **A. Mereghetti** (CERN) **L.S. Esposito** (ADAM)
 The last section of the normal conducting front end of the ESS accelerator is composed by a train of 5 DTL tanks. They accelerate the proton beam from 3.6 until 90 MeV. The evaluation of the radiation field around these beam elements gives a valuable piece of information to define the layout of the electronic devices to be installed in the surrounding tunnel area. Indeed the risk of SEE and long term damage has to be considered in order to maximize the performance of the ESS accelerator and to avoid possible long down time. A conservative loss distribution is assumed and a comparison of MCNPX and FLUKA results in term of neutrons and photon fluence is presented.
- WEPOA08 Betatron Tune Characterisation of the Rutgers 12-Inch Cyclotron**
C. Hernalsteens (CERN) **B. Beaudoin**, **T.W. Koeth**, **K.J. Ruisard** (UMD) **M. Miller** (Brown University) **T.S. Ponter** (IBA)
 The Rutgers cyclotron is a 12-Inch, 1.2 MeV proton cyclotron. Sets of magnet pole-tips were designed to demonstrate different cyclotron focusing options: weak focusing, radial sector focusing and spiral sector focusing. The focus of this paper is on the experimental characterization of the transverse dynamics provided by these different focusing options. Magnetic field measurement

results providing insight into the as-built properties of these magnetic poles configurations are reported. First measurements of the axial betatron tune as a function of the beam energy along the machine radius are discussed in detail and are shown to be in excellent agreement with the values expected from measured magnetic data. Turn-by-turn betatron envelope oscillation measurements are also reported and compared with the tune measurements. Excellent agreement is once again found.

WEPOA09 **Proton Beam Defocusing as a Result of Self-Modulation in Plasma**

M. Turner, *E. Gschwendtner, A.V. Petrenko (CERN) K.V. Lotov, A. Sosedkin (Budker INP & NSU)*

The AWAKE experiment, currently under construction at CERN, will use a 400 GeV/c proton beam with a longitudinal bunch length of $\sigma_{\text{az}} = 12$ cm to create and sustain GV/m plasma wakefields over meters. A 12 cm long bunch can only drive strong wakefields in a plasma with $n_p = 7 \cdot 10^{14}$ atoms/cm³ after the self-modulation instability (SMI) developed, and microbunches -spaced at the plasma wavelength- formed. The fields present during SMI focus and defocus the protons in the transverse plane. By inserting two imaging screens downstream the plasma, we can measure the angle of the defocused protons. Measuring maximum defocusing angles around 1 mrad indirectly proves that SMI developed successfully and that GV/m plasma wakefields were created. In this paper we present numerical studies on how and when the wakefields defocus protons in plasma, the expected measurement results of the two screen diagnostics and the physics we can deduce from it.

WEPOA10 **Crunch-in Regime - Non-linearly driven hollow-channel plasma**

A. A. Sahai (JAI), *M. Turner (CERN)*

Plasma wakefields driven inside a hollow-channel plasma are significantly different from those driven in a homogeneous plasma. We investigate the scaling laws of the accelerating and focusing fields in the novel "crunch-in" regime [1] [2]. This regime is excited due to the collapse of the electron-rings from the channel walls onto the propagation axis of the energy-source in its wake. This regime is thus the non-linearly driven hollow channel, since the electron-ring displacement is of the order of the channel radius [3]. We present the properties of the coherent structures in the "crunch-in" regime where the channel radius is matched to the beam properties such that channel-edge to on-axis collapse time has a direct correspondence to the energy source intensity. We also investigate the physical mechanisms that underlie the "crunch-in" wakefields by tuning the channel radius. Using a theoretical framework and results from PIC simulations the possible applications of the "crunch-in" regime for acceleration of positron beams with collider-scale parameters is presented.

WEPOA11 **Frequency Manipulation of Half-Wave Resonators During Fabrication and Processing**

Z.A. Conway, *M. Kedzie, M.P. Kelly, S.H. Kim, P.N. Ostroumov, T. Reid (ANL)*

Argonne National Laboratory is developing a superconducting cavity cryomodule for the acceleration of 1 mA H⁻ beams from 2.1 to 10.3 MeV for Fermi National Accelerator Laboratory's Proton Improvement Project-II. The cryomodule contains 9 superconducting niobium half-wave resonators operating at 162.5 MHz with a 120 kHz tuning window. This paper reviews the half-wave resonator fabrication techniques used to manipulate the resonant frequency to the design goal of 162.5 MHz at 2 K. The target frequency at select stages of the cavity construction and processing, how these frequencies were determined and the physical measurements are discussed.

WEPOA12 **Interleaving Lattice Design for APS Linac Advanced Accelerator R&D**

Y.-E. Sun, *S. Shin, A. Zholents (ANL)*

In order to realize and test advanced accelerator concepts and hardware, the existing beamline with both old and new components are being reconfigured in Linac Extension Area (LEA) of APS linac. Photo injector, which had been installed in the beginning of APS linac, will provide low emittance electron beam into the LEA. The thermionic RF gun beam for storage ring and photo-cathode RF gun beam for LEA will be operated though the LINAC in an interleaved fashion. In this presentation, technical issues as well as beam dynamics on the design for interleaving operation will be described.

WEPOA13 **RF Design and Simulation of a Non-Periodic Lattice Photonic Band Gap (PBG) Accelerating Structure**

N. Zhou (ANL)

Photonic Band Gap (PBG) structures (metallic and or dielectric) have been proposed for accelerators. These structures act like a filter, allowing RF field at some frequencies to be transmitted through, while rejecting RF fields in some (unwanted) frequency range as well as supporting selective field patterns (modes) in a resonator or waveguide. In this paper, we will report on the RF design and simulation results of an X-band PBG structure including lattice optimization to improve its RF performance.

WEPOA14 **Resistive Wall Growth Rate Measurements in the Fermilab Recycler**

R. Ainsworth, *P. Adamson, A.V. Burov, I. Kourbanis (Fermilab)*

Impedance could represent a limitation of running high intensity beams in the Fermilab recycler. With high intensity upgrades foreseen, it is important to quantify the impedance. To do this, studies have been performed measuring the growth rate of presumably the resistive wall instability. The growth rates at varying intensities and chromaticities are shown. The measured growth rates are compared to ones calculated with the resistive wall impedance.

WEPOA15 **Progress at That PIP-II Injector Test at Fermilab**

C.M. Baffes, *R. Andrews, A.Z. Chen, P. Derwent, B.M. Hanna, B.D. Hartsell, L.R. Prost, V.E. Scarpine, A.V. Shemyakin, J. Steimel (Fermilab)*

A CW-compatible, pulsed H⁻ superconducting linac is envisaged as a possible path for upgrading Fermilab's injection complex. To validate the concept of the front-end of such a machine, a test accelerator (The PIP-II Injector Test, formerly known as "PXIE") is under construction. The warm part of this accelerator comprises a 10 mA DC, 30 keV H⁻ ion source, a 2m-long LEBT, a 2.1 MeV CW RFQ, and a 10-m long MEBT that is capable of creating a large variety of bunch structures. The paper will report on the installation and commissioning of the RFQ and the first sections of the MEBT.

WEPOA16 **Fermilab Recycler Collimation System Design**

B.C. Brown, *P. Adamson, R. Ainsworth, D. Capista, K.J. Hazelwood, I. Kourbanis, N.V. Mokhov, D.K. Morris, V.I. Sidorov, E.G. Stern, I.S. Tropin, M.-J. Yang (Fermilab)*

To provide 700 kW proton beams for neutrino production in the NuMI facility, we employ slip stacking in the Recycler with transfer to the Main Injector for recapture and acceleration. Slip stacking with 12 Booster batches per 1.33 sec cycle of the Main Injector has been implemented and extensive operation with 8 batches and 10 batches per MI cycle has been demonstrated. Operation in this mode since 2013 shows that loss localization is an essential component for long term operation. Beam loss in the Recycler will be localized in a collimation region with design capability for absorbing up to 2 kW of lost protons in a pair of 20-Ton collimators (absorbers). This system will employ a two stage collimation with a thin Mo scattering foil to define the bottom edge of both the

injected and decelerated-for-slipping beams. Optimization and engineering design of the collimator components and radiation shielding are based on comprehensive MARS15 simulations predicting high collimation efficiency as well as tolerable levels of prompt and residual radiation. The system installation during the Fermilab 2016 facility shutdown will permit commissioning in the subsequent operating period.

WEPOA17 On the Possibility of Using Nonlinear Elements for Landau Damping in High-Intensity Beams

Y.I. Alexahin, A.V. Burov, E. Gianfelice-Wendt, V.A. Lebedev, A. Valishev (Fermilab)

Direct space-charge force shifts the incoherent tunes down from the coherent ones switching off Landau damping of coherent oscillations at high beam intensity. To restore it the nonlinear elements can be employed which move back tunes of large amplitude particles. In the present report we consider the possibility of creating a "nonlinear integrable optics" insertion in the Fermilab Recycler to host either octupoles or hollow electron lens for this purpose. For comparison we also consider the classic scheme with distributed octupole families. It is shown that for the Proton Improvement Plan II parameters the required nonlinear tunes shift can be created without destroying the dynamic aperture.

WEPOA18 Experimental Studies of Beam Collimation System in the Fermilab Booster

V.V. Kapin, S. Chaurize, N.V. Mokhov, W. Pellico, M. Slabaugh, T. Sullivan, R. Tesarek, A.K. Triplett (Fermilab)

A two-stage collimation (2SC) system was installed in Fermilab Booster around 2004 and consists of 2 primary collimators (PrC), one for each of the horizontal and vertical planes and 3 secondary collimators (SC) each capable of acting in both planes. Presently, only SC are used as the single-stage collimation (1SC). Part of the Fermilab Proton Improvement Plan (PIP) includes a task to test 2SC for Booster operations. In this paper we describe preparatory steps to fix SC motion issues and installation of a 380um thick aluminum foil PrC and post-processing software for beam orbit and beam loss measurements. The initial experimental results for 2SC in the vertical plane are also presented. The tuning of 2SC system has been performed using fast loss monitors allowing much higher time-resolution than existing BLMs. The results of post-processing for measured data are presented and a feasibility of 2SC system are discussed. Plans for future experimental studies aimed for comparison of 1SC and 2SC schemes are suggested.

WEPOA19 Analysis of Beam Collimation in the Fermilab Booster

V.V. Kapin, V.A. Lebedev (Fermilab)

A two-stage collimation (2SC) system installed in Fermilab Booster ~12 years ago has never been used in operations. Instead, its secondary collimators are used as a single-stage collimators (1SC). Presently, a feasibility of the 2SC system is under studies. In this paper, the factors limiting collimation efficiency of Booster 2SC system are discussed. They include both non-optimal locations of collimators forced by available spaces in Booster and by small aperture in dipoles and RF cavities. The combination of MADX and MARS15 codes was used in simulations. In particular, the simulations include proton tracking in the Booster with accounting proton scattering on collimators. Alternative collimation schemes are also considered. Their efficiency is evaluated for comparisons with existing 1SC and 2SC systems. These schemes require a location of the primary collimator in close vicinity of the first secondary collimator and include replacement of existing thin-foil primary collimators either by rather thick foil or by electrostatic septum. Moreover, a possible usage of momentum collimation is also considered.

WEPOA20 Numerical Simulations of Collimation Efficiency for Beam Collimation System in the Fermilab Booster

V.V. Kapin, V.A. Lebedev, N.V. Mokhov, S.I. Striganov, I.S. Tropin (Fermilab)

A two-stage beam collimation (2SC) system has been installed in the Fermilab Booster more than 10 years ago. It consists of two primary collimators for horizontal and vertical planes and three 1.2m-long secondary collimators. The two-stage collimation mode has never been used in Booster operations due to variations of the beam orbit under conditions of the momentum coggling. Instead, secondary collimators were used in the single-stage collimation (1SC) mode. The conditions for implementation of the 2SC scheme have recently been improved as a result of stabilization of the beam orbit via magnetic coggling. In this paper, evaluation of the 2SC mode performance is done in comparison to that of the existing 1SC mode. Several parameters which characterize a collimation efficiency are calculated in order to compare both schemes. The bundle of the MADX and MARS15 codes is used for proton tracking in the Booster lattice with their scattering on collimators. The efficiency dependence on the primary collimators copper foil thickness is presented. The efficiency dependence on the proton energy is also obtained for the optimal foil. The feasibility of the 2SC scheme for the Booster is discussed.

WEPOA21 High-Efficiency 2 MeV Linear Accelerator

V.E. Teryaev (Omega-P, Inc.) , J.L. Hirshfield (Yale University, Physics Department) S. Kazakov (Fermilab)

A novel multi-beam electron accelerator is described. This device, which we have dubbed Electron Voltage Transformer (EVT), falls into the broad class of two-beam accelerators, but differs significantly from other configurations in that the RF source and accelerator are built into the same vacuum envelope. Multiple drive beamlets and the beam to be accelerated receive RF modulation in a set of RF buncher cavities, from which the beams pass into the accelerating structure. The latter structure comprises decoupled, inductively-tuned cavities, wherein energy is transferred from the drive beams to the accelerated beam. Correct phasing to achieve initial RF bunching followed by acceleration is achieved by appropriate spacing of the cavity gaps. Preliminary results of numerical simulations are presented for a prototype EVT, operating at L-band, in which a 6 A 110 kV beam is accelerated to 2 MeV with an overall efficiency of 60%. This unusually-high efficiency, high average power electron beam source should be attractive for a range of industrial applications.

WEPOA22 nuPIL - Neutrinos from a Plon Beam Line

A. Liu (Fermilab)

The Fermilab Deep Underground Neutrino Experiment (DUNE) was proposed to determine the neutrino mass hierarchy and demonstrate leptonic CP violation. The current design of the facility that produces the neutrino beam (LBNF) uses magnetic horns to collect pions and a decay pipe to allow them to decay. In this paper, a design of a possible alternative for the conventional neutrino beam in LBNF is presented. In this design, a magnetic beam line is used to collect the pions from the downstream face of a horn, bend them by ~5.8 degrees and then transport them in a straight beam line or a decay pipe where they decay to produce neutrinos. The idea of using neutrinos from the Plon beam Line (nuPIL) provides flavor pure neutrino beams that can be well understood by implementing standard beam measurement technology. The neutrino flux and the resulting δ_{CP} sensitivity from nuPIL are also presented in the paper.

WEPOA23 The Status of Muon Accelerator R&D for Future High Energy Accelerators

M.A. Palmer, D.V. Neuffer (Fermilab)

Muon accelerators offer unique potential for high energy physics applications. Muon storage rings can provide intense, pure, and

precisely measured neutrino beams for short- and long-baseline neutrino oscillation studies. Since the discovery of the Higgs boson, there has been an active discussion on the most effective route to deploying lepton collider capabilities for its detailed study - a muon collider offers one interesting option. Since muon beams are not subject to the synchrotron radiation and beamstrahlung limits imposed on electron-positron colliders, they can be efficiently accelerated to energies of several TeV and stored in collider rings where the beams can be brought into repeated collision for $\sim 10^3$ revolutions. For center-of-mass energies in the multi-TeV range, muon colliders can be shown to provide the most power efficient route to providing a high luminosity lepton collider. The status of the the R&D towards these capabilities is described.

- WEPOA24 Installation and Commissioning of an Ultrafast Electron Diffraction Facility as Part of the ATF-II Upgrade**
M.A. Palmer, M. Babzien, M.G. Fedurin, M. Fulkerson, K. Kusche, J.J. Li, R. Malone, T.V. Shafan, L. Snydstrup, C. Swinson, E.J. Willeke (BNL)
 The Accelerator Test Facility (ATF) at Brookhaven National Laboratory (BNL) is presently carrying out an upgrade, ATF-II, which will provide significantly expanded experimental space and capabilities for its users. One of the new capabilities being integrated into the ATF-II program is an Ultrafast Electron Diffraction (UED) beam line, which was originally deployed in the BNL Source Development Laboratory. Inclusion of the UED in the ATF-II research portfolio will enable ongoing development and extension of the UED capabilities for use in materials research. We discuss the design, installation and commissioning of the UED beam line at ATF-II as well as plans for future upgrades.
- WEPOA25 Fermilab Accelerator R&D Program Toward Intensity Frontier Machines: Status and Progress**
V.D. Shiltsev (Fermilab)
 Fermilab actively carries out broad R&D program toward future Intensity Frontier accelerators which includes novel beam physics approaches tests in IOTA ring at FAST, research on cost-effective SRF and development of multi-MW beam targets. This presentation gives a high level overview of the program, motivation, status and progress.
- WEPOA26 Fermilab Muon Campus as a Potential Probe for Studying Neutrino Physics**
D. Stratakis, Z. Pavlovic (Fermilab) J.M. Grange (ANL) , S-C. Kim (Cornell University (CLASSE), Cornell Laboratory for Accelerator-Based Sciences and Education) J.A. Zennaro (Enrico Fermi Institute, University of Chicago)
 In the next decade the Fermilab Muon Campus will host two world class experiments dedicated to the search for signals of new physics. The Muon g-2 experiment will determine with unprecedented precision the anomalous magnetic moment of the muon. The Mu2e experiment will improve by four orders of magnitude the sensitivity on the search for the as-yet unobserved Charged Lepton Flavor Violation process of a neutrinoless conversion of a muon to an electron. In this paper, we will discuss the possibility for extending the Muon Campus capabilities for neutrino research. With the aid of numerical simulations, we estimate the number of produced neutrinos at various locations along the beamlines as well along the Small Baseline Neutrino Detector which faces one of the straight sections of the delivery ring. Finally, we discuss diagnostics required for realistic implementation of the experiment.
- WEPOA27 Operational Performance of the Upgraded NuMI Target & Facility**
R.M. Zwaska (Fermilab)
 The NuMI beam was upgraded to be capable of 700 kW in 2013, including a completely new design for the target. The Fermilab accelerators first achieved 700 kW in June of 2016. This paper describes the operational experience of the target and facility in this higher-power regime. The target performed well, accumulating 110^{20} protons on the first of the series - well beyond the design lifetime. At the end if its operations run, the performance remained stable to within several percent of its original production efficiency; a significant helium leak in the primary containment eventually led to its replacement. An autopsy is planned, and the next target will include several beryllium target elements to test that material. One of the upgraded horns failed prematurely due to vibration-enhanced fatigue - prompting cooling upgrades to an old-style horn, and modifications to the new-style horn to reduce vibration and improve fatigue endurance. Management of the heat, chemical, isotope byproducts are challenges to facility operation; notable examples are described.
- WEPOA28 Lattice Design for Recirculating Proton Linac**
K. Huang, J. Qiang (LBNL)
 The acceleration efficiency of the recirculating RF linac was demonstrated by operating electron machines. The acceleration concept of recirculating proton beam was recently proposed and is currently under study. In this paper, we present a 6D lattice design and beam dynamics tracking for a two-pass recirculating proton linac from 150 MeV to 500 MeV, which is the first section of the three acceleration steps proposed earlier. Issues covered are optimization of simultaneous focusing of two beams passing the same structure and achromatic condition under space-charge potential.
- WEPOA29 Recent Experiments at NDCX-II: Irradiation of Materials Using Short, Intense Ion Beams**
P.A. Seidl, E. Feinberg, Q. Ji, B.A. Ludewigt, A. Persaud, T. Schenkel, M.S. Silverman, A.A. Sulyman, W.L. Waldron (LBNL) J.J. Barnard, A. Friedman, D.P. Grote (LLNL) E.P. Gilson, I. Kaganovich, A.D. Stepanov (PPPL) M. Zimmer (TU Darmstadt)
 We present an overview of the performance of the Neutralized Drift Compression Experiment-II (NDCX-II) accelerator at Berkeley Lab, and summarize recent studies of material properties created with nanosecond and millimeter-scale ion beam pulses. The scientific topics being explored include the dynamics of ion induced damage in materials, materials synthesis far from equilibrium, warm dense matter and intense beam-plasma physics. We summarize the improved accelerator performance, diagnostics and results of beam-induced irradiation of thin samples of, e.g., tin and silicon. Bunches with over 3×10^{10} ions, 1-mm radius, and 2-30 ns FWHM duration have been created. To achieve these short pulse durations and mm-scale focal spot radii, the 1.2 MeV He^+ ion beam is neutralized in a drift compression section which removes the space charge defocusing effect during final compression and focusing. Quantitative comparison of detailed particle-in-cell simulations with the experiment play an important role in optimizing accelerator performance; these keep pace with the accelerator repetition rate of $\sim 1/\text{minute}$.
- WEPOA30 High-Performance Modeling of Plasma-Based Acceleration and Laser-Plasma Interactions.**
J.-L. Vay, G. Blaclair, R. Lehe, M. Lobet, H. Vincenti (LBNL) B.B. Godfrey (UMD) M. Kirchen (University of Hamburg) P. Lee (Laboratoire de Physique des Gaz et des Plasmas, Universite Paris-Sud)
 Large-scale numerical simulations are essential to the design of plasma-based accelerators and laser-plasma interactions for ultra-high intensity (UHI) physics. The electromagnetic Particle-In-Cell (PIC) approach is the method of choice for self-consistent simulations, as it is based on first principles, and captures all kinetic effects, and also scales easily (for uniform plasmas) to many cores on supercomputers. The standard PIC algorithm relies on second-order finite-difference discretizations of the Maxwell and

Newton-Lorentz equations. We present here novel PIC formulations, based on the use of very high-order pseudo-spectral Maxwell solvers, which enable near-total elimination of the numerical Cherenkov instability and increased accuracy over the standard PIC method. We also present the latest implementations in the PIC modules Warp-PICsAR and FBPIC on the Intel Xeon Phi and GPU architectures. Examples of applications will be given on the simulation of laser-plasma accelerators and high-harmonic generation with plasma mirrors.

WEPOA31 Nonlinear Dynamics, Dispersive, and Chromatic Considerations in the IOTA Lattice

N.M. Cook, D.L. Bruhwiler, C.C. Hall, R.A. Kishek, S.D. Webb (*RadiaSoft LLC*) A.L. Romanov, A. Valishev (*Fermilab*)

Tune spread with amplitude suppresses intensity-driven parametric instabilities such as beam halo. Conventional approaches to achieving high tune spreads, such as the use of octupoles, can reduce the single-particle dynamic aperture. The nonlinear integrable optics promise to introduce large tune spreads with amplitude without introducing resonances that limit the dynamic aperture. The idealized zero-current dynamics is constrained by two integrals of the motion, but remain susceptible to perturbations driven by energy spread. To study this concept, Fermilab is building the Integrable Optics Test Accelerator (IOTA). Simulations using the accelerator simulation package Synergia have demonstrated higher order effects to the ideal lattice, including effects due to finite phase advance across the nonlinear magnet as well as nonlinear dispersive and chromatic effects. We present evidence for these higher-order effects, and illustrate the sensitivity of the dynamics to sextupole fields, showing that their proper pairing can preserve integrability and reduce beam loss.

WEPOA32 Simulations of High-Gradient Dielectric Laser Acceleration

B.M. Cowan (*Tech-X*) R.L. Byer, E.A. Peralta, K. Soong (*Stanford University*) R.J. England, I.V. Makasyuk, K.P. Wootton, Z. Wu (*SLAC*) A. Hanuka (*Technion*)

Recently, dielectric laser-driven accelerator structures based on dual grating configurations have been demonstrated to achieve gradients in excess of 0.6 GV/m*. The particle dynamics in these experiments are complicated because a significant fraction of the beam passes through the structure material, and because the structure is driven with a single laser pulse, particles can be driven transversely into and out of the material. In this presentation, we describe full scale simulations, using the Vorpil simulation engine, that include these phenomena and match experimental parameters. We show how the simulation data confirm the high gradients inferred from experimental measurements, as well as the optical phase dependence of the acceleration. We discuss the computational methods used for the key material interactions, namely bremsstrahlung and energy straggling. We show the results, including comparison with experimental energy spectra. We discuss the contributions to the spectrum from particles traversing the vacuum gap and those passing through the material.

WEPOA33 Novel Metallic Structures for Wakefield Acceleration

X.Y. Lu, M.A. Shapiro, R.J. Temkin (*MIT/PSFC*)

Three novel ideas for wakefield acceleration (WFA) of electrons with metallic periodic subwavelength structures will be presented. The first idea is a deep corrugation structure for collinear WFA. A design for the Argonne Wakefield Accelerator is shown. An analytical model is developed and it agrees with the CST wakefield solver. A scaling study has been performed, and ways to increase the gradient will be discussed. The deep corrugation structure can generate a higher gradient than a dielectric tube with the same beam aperture when excited by the same bunch. The second idea is an elliptical structure for two-beam acceleration (TBA). The unit cell is an elliptical cavity, and the drive beam hole and the witness beam hole are located around the two focal points. The TBA process has been calculated and will be presented. The third idea is a metamaterial 'wagon wheel' structure for a power extractor design. The fundamental mode is a TM mode with a negative group velocity. A power extractor at 11.7 GHz based on the structure can reach a GW power level when a train of 40 nC bunches with 1.3 GHz rep rate are sent in.

WEPOA34 Progress on Beam-Plasma Effect Simulations in Muon Ionization Cooling Lattices

J.S. Ellison (*IIT*) P. Snopok (*Fermilab*) P. Snopok (*Illinois Institute of Technology*)

New computational tools are essential for accurate modeling and simulation of the next generation of muon-based accelerators. One of the crucial physics processes specific to muon accelerators that has not yet been simulated in detail is beam-induced plasma effect in liquid, solid, and gaseous absorbers. We report here on the progress of developing the required simulation tools and applying them to study the properties of plasma and its effects on the beam in muon ionization cooling channels.

WEPOA35 Wedge Absorbers for Muon Cooling with a Beam Test at MICE

D.V. Neuffer (*Fermilab*) , T.A. Mohayai (*IIT*) P. Snopok (*Illinois Institute of Technology*) D.J. Summers (*UMiss*)

Emittance exchange mediated by wedge absorbers is required for longitudinal ionization cooling and for final transverse emittance minimization for a muon collider. A wedge absorber within the MICE beam line could serve as a demonstration of the type of emittance exchange needed for 6-D cooling, including the configurations needed for muon colliders. Parameters for this test are explored in simulation and possible experimental configurations with simulated results are presented.

WEPOA36 Simulated Measurements of Beam Cooling in Muon Ionization Cooling Experiment

T.A. Mohayai (*IIT*) D.V. Neuffer, D.V. Neuffer, P. Snopok (*Fermilab*) C.T. Rogers (*STFC/RAL/ASTeC*) P. Snopok (*Illinois Institute of Technology*)

Cooled muon beams are essential to enable future Neutrino Factory and Muon Collider facilities. The international Muon Ionization Cooling Experiment (MICE) aims to demonstrate muon beam cooling through ionization energy loss in material. A figure of merit for muon beam cooling in MICE is the transverse root-mean-square (RMS) emittance reduction and to measure this, the individual muon positions and momenta are reconstructed using two scintillating-fiber tracking detectors housed in spectrometer solenoid modules. The reconstructed positions and momenta before and after a low-Z absorbing material are then used for constructing the covariance matrix and measuring normalized transverse RMS emittance of MICE muon beam. However, RMS emittance is sensitive to nonlinear effects in beam optics. In this study, the direct measurement of phase-space density as an alternative approach to measuring the muon beam cooling using the novel Kernel Density Estimation (KDE) method, is described.

WEPOA37 Hybrid Methods for Simulation of Muon Ionization Cooling Channels

J.D. Kunz, P. Snopok (*IIT*) J.D. Kunz (*Anderson University*)

COSY Infinity is an arbitrary-order beam dynamics simulation and analysis code. It uses high-order transfer maps of combinations of particle optical elements of arbitrary field configurations. New features have been developed and implemented in COSY to follow charged particles through matter. To study in detail the properties of muons passing through a material, the transfer map approach alone is not sufficient. The interplay of beam optics and atomic processes must be studied by a hybrid transfer map-Monte Carlo approach in which transfer map methods describe the average behavior of the particles including energy loss, and Monte

Carlo methods are used to provide small corrections to the predictions of the transfer map, accounting for the stochastic nature of scattering and straggling of particles. This way the vast majority of the dynamics is represented by fast application of the high-order transfer map of an entire element and accumulated stochastic effects. The gains in speed simplify the optimization of muon cooling channels which are usually very computationally demanding. Progress on the development of the required algorithms is reported.

WEPOA38 **Optically Based Diagnostics for Optical Stochastic Cooling**

M.B. Andorf (Northern Illinois University) V.A. Lebedev, P. Piot, J. Ruan (Fermilab)

An Optical Stochastic Cooling (OSC) experiment of electrons will take place at Fermilab in the IOTA ring soon. OSC requires timing the arrival of an electron and its radiation generated from the upstream pickup undulator into the downstream kicker undulator to a precision on the order of a few femtoseconds. The interference of the pickup and kicker radiation suggest a way to diagnose the arrival time to the required precision and furthermore provides a way to tune the sextupoles in the bypass chicane.

WEPOA39 **Theoretical and Numerical Study on Plasmon-Assisted Channeling Interactions in Nano-Structures**

Y.-M. Shin (Northern Illinois University) A.T. Green (Northern Illinois University)

A plasmon-assisted channeling acceleration can be realized with a large channel possibly in a nanometer scale. Carbon nanotubes are the most typical example of nano-channels that can confine a large amount of channeled particles and confined plasmon in a coupling condition. This paper presents theoretical and numerical study on the concept of the laser-driven surface-plasmon (SP) acceleration in a carbon nanotube (CNT) channel. Analytic description of the SP-assisted laser acceleration is detailed with practical acceleration parameters, in particular with specifications of a typical tabletop femto-second laser system. The maximally achievable acceleration gradients and energy gains within dephasing lengths and CNT lengths are discussed with respect to laser-incident angles and CNT-filling ratios.

WEPOA40 **Construction Status of a RF-Injector with a CNT-Tip Cathode for High Brightness Field-Emission Tests**

Y.-M. Shin, G. Fagerberg, M. Figora (Northern Illinois University) A.T. Green (Northern Illinois University)

We have been constructing a S-band RF-injector system for field-emission tests of a CNT-tip cathode. A pulsed Sband klystron is installed and fully commissioned with 5.5 MW peak power in a 2.5 microsecond pulse length and 1 Hz repetition rate. A single-cell RFgun is designed to produce with 0.5 - 1 pC electron bunches in a photo-emission mode within a 50 fs - 3 ps at 0.5- 1 MeV. The measured RF system jitters are within 1 % in magnitude and 0.2° in phase, which would induce 3.4 keV and 0.25 keV of energy jitters, corresponding to 80 fs and 5 fs of temporal jitters, respectively. Our PIC simulations indicate that the designed bunch compressor reduces the TOAjitter by about an order of magnitude. Emission current and beam brightness of the field-emitted beam are improved by implanting CNT tips on the cathode surface, since they reduce the emission area, while providing high current emission. Once the system is completely commissioned in field-emission mode, the CNT-tip cathode will be tested in terms of klystron-power levels to map out its I-V characteristics under pulse emission condition.

WEPOA41 **Delivery Ring Lattice Modifications for Transitionless Deceleration**

M.J. Syphers (Northern Illinois University) J.A. Johnstone, M.J. Syphers (Fermilab)

A portion of the remnant Tevatron program infrastructure at Fermilab is being reconfigured to be used for the generation and delivery of proton and muon beams for new high-precision particle physics experiments. The Mu2e* experiment will receive 8.9 GeV/c bunched beam slow spilled from the Delivery Ring (DR) |— a refurbished debuncher ring from Tevatron antiproton production. For Muon g-2**, the DR will be tuned to 3.1 GeV/c to capture muons off of a target before sending them to this experiment's Storage Ring. To provide further flexibility in the operation of the DR for future possible low-energy, high-intensity particle physics experiments (REDTOP***, for example) and detector development, the feasibility of decelerating beams from its maximum 8 GeV level to lower energies, down to 1-2 GeV, is being studied. In this paper we look at possible lattice modifications to the DR to avoid a transition crossing during the deceleration process. Hardware requirements and other operational implications of such schemes will also be discussed.

WEPOA42 **Design of a High Average Beam-Power SRF Electron Source**

N. Sipahi, S. Biedron, S.V. Milton (CSU) S. Biedron (University of Ljubljana, Faculty of Electrical Engineering)

There is a significant interest in achieving high-average power electron sources particularly in the area of electron sources integrated with Superconducting Radio Frequency (SRF) systems. For these systems, the electron gun and cathode parts are critical components for stable intensity and high-average powers. In this initial design study, we will present the design of 9-cell accelerator cavity having 1.3-GHz frequency and field optimization studies by comparing simulation results.

WEPOA43 **Magnetic Force and Parameter Evaluation for the High Current Striplines of Magnetic Horns at Fermilab**

T. Sipahi, S. Biedron, S.V. Milton (CSU) J. Hylen, R.M. Zwaska (Fermilab)

Both the NuMI (Neutrinos and the Main Injector) beam line, that has been providing intense neutrino beams for several Fermi National Accelerator Laboratory (Fermilab) experiments (MINOS, MINERvA, NOvA), and the newly proposed LBNF (Long Base-line Neutrino Facility) beam line which plans to produce the highest power neutrino beam in the world for DUNE (the Deep Underground Neutrino Experiment) need pulsed magnetic horns to focus the mesons which decay to produce the neutrinos. The high current horn and stripline design has been evolving as NuMI reconfigures for higher beam power and as LBNF produces designs for even higher beam power and horn current. In this paper, we present the EM interaction simulation results for the stripline plates of the NuMI horns at critical stress points using the Poisson and ANSYS Maxwell 3D codes. In addition, we give the electrical simulation results using the ANSYS Electric code. These results are being used to support the development of evolving horn stripline designs to handle increased electrical current and higher beam power for NuMI upgrades and for LBNF.

WEPOA44 **Acceleration System of Beam Brightness Booster**

V.G. Dudnikov (Muons, Inc) A.V. Dudnikov (BINP SB RAS)

The brightness and intensity of a circulating proton beam now can be increased up to space charge limit by means of charge exchange injection or by an electron cooling but cannot be increased above this limit. Significantly higher brightness can be produced by means of the charge exchange injection with the space charge compensation [1]. The brightness of the space charge compensated beam is limited at low level by development of the electron-proton (e-p) instability [2]. Fortunately, e-p instability can be self-stabilized at a high beam density. A beam brightness booster (BBB) for significant increase of accumulated beam brightness is discussed. Accelerating system with a space charge compensation is proposed and described. The superintense beam production can be simplified by developing of nonlinear nearly integrable focusing system with broad spread of betatron tune and the broadband feedback system for e-p instability suppression.

- WEPOA45 Positive and Negative Ions Radio Frequency Sources with Solenoidal Magnetic Field**
V.G. Dudnikov, R.P. Johnson (Muons, Inc) G. Dudnikova (ICT SB RAS) B. Han, S. Murrey, C. Stinson (ORNL RAD) T.R. Pennisi, C. Piller, M. Santana, M.P. Stockli, R.F. Welton (ORNL)
 Operation of Radio Frequency surfaces plasma sources (RF SPS) with a solenoidal magnetic field are described. RF SPS with solenoidal and saddle antennas are discussed. Dependences of beam current and extraction current on RF power, gas flow, solenoidal magnetic field and filter magnetic field are presented.
- WEPOA46 The Muon Injection Simulation Study for the Muon g-2 Experiment at Fermilab**
S.-C. Kim (Cornell University (CLASSE), Cornell Laboratory for Accelerator-Based Sciences and Education) N.S. Froemming (University of Washington, CENPA) D. L. Rubin (Cornell University) D. Stratakis (Fermilab)
 The new experiment, under construction at Fermilab, to measure the muon magnetic moment anomaly, aims to reduce measurement uncertainty by a factor of four to 140 ppb. The required statistics depend on efficient production and delivery of the highly polarized muon beams from production target into the g-2 storage ring at the design "magic"-momentum of 3.094 GeV/c, with minimal pion and proton contamination. We have developed the simulation tools for the muon transport based on G4Beamline and BMAD, from the target station, through the pion decay line and delivery ring and into the storage ring, ending with detection of decay positrons. These simulation tools are being used for the optimization of the various beam line guide field parameters related to the muon capture efficiency, and the evaluation of systematic measurement uncertainties. We describe the details of the model and some key findings of the study.
- WEPOA47 A High Intensity Positron Source Based on a Superconducting Electron Linac for Nuclear Physics Research**
J.L. McCarter, C.H. Boulware, D. Gorelov, T.L. Grimm, J.L. Hollister, M. Mamtimin, V.N. Starovoitova (Niowave, Inc.) T.A. Forest (ISU) S.A. Maloy, E.R. Olivas, K.A. Woloshun (LANL)
 Positron sources are essential components of next-generation colliders and have important applications in industry and government research where they are used to probe stress, vacancies, and fatigue in materials at the microstructure level. However, there is a lack of inexpensive, reliable, high intensity positron sources. Niowave is developing a positron production target that can be used in conjunction with a high-power superconducting electron accelerator (linac). The liquid metal target will be capable of converting a 10 MeV, 100 kW electron beam into a high flux positron source. Thin lead-bismuth eutectic targets create positrons as efficient as conventional solid targets and have superior thermomechanical properties. The beamline was simulated and optimized for positron creation and capture. Preliminary experimental results of the performance of the accelerator and target system indicate the production and detection of positrons. Because of the power handling properties of the liquid metal, the target is capable of scaling positron production to the CW power levels need for next generation lepton accelerators (CLIC, ILC, JLEIC, eRHIC, Super KEK B).
- WEPOA48 Simulation of a 25 GeV Plasma Wakefield Accelerator for Electrons with Plasma Ion Motion**
W. An, C. Chandrashekar, W.B. Mori (UCLA)
 Plasma based accelerator is being considered as the basis for building a future linear collider. The nonlinear plasma wake field accelerator have ideal properties for focusing and accelerating electrons. However, for nano Coulomb beams with nanometer scale matched spot sizes, the large space charge forces around the beam can pull the plasma ions inwards and generate nonlinear focusing force inside the wake. As a result, the beam emittance cannot be preserved. We find that although the ion density becomes 100 times larger than the initial density on the axis, the width of the ion density peak is around 1/10 of the beam spot size and the emittance growth of the beam is only 20% in a lithium plasma. We then simulate a plasma wake field accelerator for 25 GeV energy gain while enabling the ion motion. The tolerance of hosing in the acceleration process is also studied.
- WEPOA49 Using Quasi-3D OSIRIS Simulations of LWFA to Study Generating High Brightness Electron Beams Using Ionization and Density Downramp Injection**
T.N. Dalichaouch, A.W. Davidson, W.B. Mori, X.L. Xu, P. Yu (UCLA) R.A. Fonseca, J. Vieira (Instituto Superior Tecnico) F. Li, W. Lu, C.J. Zhang (TUB)
 In the past few decades, there has been much progress in theory, simulation, and experiment towards using Laser wakefield acceleration (LWFA) as the basis for designing and building compact x-ray free-electron-lasers (XFEL) as well as a next generation linear collider. Recently, ionization injection and density downramp injection have been proposed and demonstrated as a controllable injection scheme for creating higher quality relativistic electron beams using LWFA. However, full-3D simulations of plasma-based accelerators are computationally intensive, sometimes taking millions of core-hours on today's computers. A quasi-3D algorithm was developed and implemented into OSIRIS using a particle-in-cell description with a charge conserving current deposition scheme in r-z and a gridless Fourier expansion in ϕ . Due to the azimuthal symmetry in LWFA, quasi-3D simulations are computationally more efficient than Full-3D simulations since only the first few harmonics are needed ϕ to capture the 3D physics of LWFA. Using the quasi-3D approach, we present preliminary results of ionization and down ramp triggered injection and compare the results against Full-3D LWFA simulations.
- WEPOA50 High Quality Electron Beam Injection and Acceleration Using a Longitudinal Density-Tailored Plasma-Based Accelerator in the Blowout Regime**
X.L. Xu, C. Joshi, W.B. Mori (UCLA) F. Li, W. Lu (TUB)
 We studied the generation of high quality electron beams (high brightness and low energy spread) from a plasma-based accelerator in the blowout regime using self-injection in tailored plasma density profiles. The underlying physical mechanism that leads to the generation of high quality electrons is uncovered by tracking the particle trajectories of the electrons as they cross the sheath and are trapped by the wake. Details on how the intensity of the driver and the density scale length controls the ultimate beam quality are described. Three-dimensional particle-in-cell simulations indicate that this concept has the potential to produce beams with ~ 0.5 nC of charge, peak brightnesses of 0.5×10^{20} A/m²/rad² and with absolute projected energy spreads of < 0.5 MeV using existing lasers or electron beams to drive nonlinear wakefields.
- WEPOA51 Photonic Band Gap Structure With Improved Design**
J. Upadhyay (ODU) E.I. Simakov (LANL)
 Photonic band gap (PBG) structures have great potential in filtering higher order modes (HOMs) without perturbing the fundamental mode and in suppressing the wakefields. An efficient PBG structure would help a lot in terms of beam quality for high beam current future free-electron lasers (FEL). An improved design of X-band normal conducting PBG accelerating structure with elliptical rods will be presented. A comparison of cavity parameters between cylindrical and elliptical shape rod PBG structures will

be shown. This new optimized PBG structure would be fabricated and tested at Argonne Wakefield Accelerator (AWA) test facility. The status of the test will be reported.

WEPOA52 Modeling and Simulation of RFQs for Analysis of Fields and Frequency Deviations with Respect to Internal Dimensional Errors

S.W. Lee, Y.W. Kang (ORNL)

Performance of radio frequency quadrupole (RFQ) is sensitive to the changes in internal dimensions like other high Q cavities used for charged particle acceleration and other beam interactions. The changes in dimensions can affect the resonance frequency and the field distribution on the beam axis along the structure. The dimensional changes can come from various sources of disturbances such as physical distortions, thermal expansion, even sometimes coolant pressure changes etc. During 15 years of continuous operation, the SNS RFQ has been re-tuned few times to compensate the deviations in frequency and field flatness with suspected dimensional changes. In order to predict and understand the performance degradation, full 3-D models of SNS RFQs were generated and simulated. Field and frequency errors from transverse vane perturbations, and potential vane erosions and metallic deposition (such as Cesium introduced by the ion source operation) at the low energy ends are discussed along with proper field retuning.

WEPOA53 Intense Low-Energy Muon Beam Production and Collection

Y. Bao (UCR) D.V. Neuffer (Fermilab)

The phase rotation technology for collecting muon beams has been developed for high energy muon accelerators. We adapt this technique to effectively collect low-energy muons, which can be used in muon rare decay experiments. The muons are produced by a short bunched proton beam, and after a drift channel, the muon beam form a time-momentum correlation. A series of rf cavities is used to bunch the muons and then phase rotate the bunches so that all the bunches reaches a momentum around 100 MeV/c. Then another group of rf cavities is used to decelerate the muon bunches to low-energy. Such a concept has been outlined in Ref[1]. In this work, we use a lower-energy proton driver such as the 800 MeV PIP-II proton beam. We optimize the production target and update the collection channel to maximize the yield of low-energy muons. The intensity of the low-energy muons is significantly increased and such a beam would provide the possibility for the next generation rare decay searches and other muon beam applications. [1] D. Neuffer, Y. Bao and G. Hanson, "PHASE ROTATION OF MUON BEAMS FOR PRODUCING INTENSE LOW-ENERGY MUON BEAMS ". Proceeding of IPAC2016, Busan, Korea

WEPOA54 Simulation of a Skew Parametric Resonance Ionization Cooling Channel

Y. Bao (UCR) A. Afanasev (GWU) Y.S. Derbenev, V.S. Morozov, A.V. Sy (JLab) R.P. Johnson (Muons, Inc)

Skew Parametric-resonance Ionization Cooling (Skew-PIC) is designed for the final 6D cooling of a high-luminosity muon collider. Tracking of muons in such a channel has been modeled in MAD-X in previous studies. However, the ionization cooling process has to be simulated with a code that can handle matter dominated beam lines. In this paper we present the simulation of a Skew-PIC channel using G4beamline. We implemented the required magnetic field components into G4beamline and compare the tracking of muons by the two different codes. We optimize the cooling channel and present the muon cooling effect in the Skew-PIC channel for the first time.

WEPOA55 Modulator Simulations for Coherent Electron Cooling

J. Ma (SBU) V. Litvinenko, V. Samulyak, G. Wang (BNL) V. Litvinenko (Stony Brook University) V. Samulyak (SUNY SB)

Cooling high-energy hadron beams is one of major challenges in modern accelerator physics. Coherent electron cooling (CEC) is a novel technique for rapidly cooling high-energy, high-intensity hadron beams. CEC consists of three sections: a modulator, where the ion imprints a density wake on the electron distribution, an amplifier, where the density wake is amplified, and a kicker, where the amplified wake interacts with the ion, resulting in dynamical friction for the ion. In this work, we perform highly resolved numerical simulations based on modulator, the first section of CEC. SPACE, a 3D electromagnetic particle-in-cell code is used. The beam parameters for simulations are relevant to the Relativistic Heavy Ion Collider (RHIC) at Brookhaven National Laboratory. Kappa-2 velocity distribution is used to model the electron temperature. We calculate the number density modulation and energy modulation of a longitudinal slice of electrons, induced by a single ion. Various moving velocities for ion are studied and compared with theoretical results. Our simulations are consistent with theoretical values in number density modulation and energy modulation.

WEPOA56 Design of RFQ Linac to Accelerate High Current 7Li^{3+} Beam from Laser Ion Source for Compact Neutron Source

S. Ikeda, T. Kanesue, M. Okamura (BNL)

Accelerator-driven compact neutron sources have been developed to conduct nondestructive inspection more conveniently and/or on the spot with lower cost than other neutron sources, such as spallation sources and nuclear reactors. In typical compact source, proton or deuteron are injected into Li or Be. To develop a higher flux source than conventional ones, we propose a source with 7Li beam generated by laser ion source using direct injection scheme (DPIS) into RFQ linac. Because of the higher velocity of center of mass than that in the case of proton beam injection, generated neutrons are more collimated. In addition, laser ion source with DPIS is expected to accelerate mA class fully ionized 7Li beam stably with simple setup, while it is difficult for conventional ion sources. The high collimation and high current are expected to lead to higher neutron flux. In this presentation, we present a design of RFQ linac optimized to accelerate such a high current beam with shorter distance.

WEPOA57 Stabilized Operation Mode of Laser Ion Source Using Pulsed Magnetic Field

S. Ikeda, M.R. Costanzo, T. Kanesue, R.F. Lambiase, C.J. Liaw, M. Okamura (BNL)

A laser ion source (LIS) provides several types of singly charged ions into an electron beam ion source (EBIS) followed by linear accelerator injectors for the Relativistic Heavy Ion Collider (RHIC) and the NASA Space Radiation Laboratory (NSRL) at Brookhaven National Laboratory. In the present set-up of the LIS, beam current shape varies with time drastically. It is expected that the present current shape is not optimal for the ion trap of the EBIS. However, there are no knobs to modify the shape flexibly. Therefore, as an upgrade of the LIS, we install a coil and a pulsed circuit* that generates a fast-rising pulsed magnetic field to tailor the beam current shape. In this presentation, the effect of the magnetic field on the beam profile from the LIS and the performance of the injectors, such as the transmission and the charge injected into an accelerator downstream, are described.

WEPOA58 Project Towards CO₂-Laser-Driven Wake-Field Accelerator With External Injection

V. Litvinenko, M. Babzien, M.G. Fedurin, Y.C. Jing, K. Kusche, I. Pogorelsky, M.N. Polyanskiy, C. Swinson (BNL) C. Chandrashekar, W.B. Mori, N. Vafaei (UCLA) M. Downer, R. Zgadzaj (The University of Texas at Austin) H. Li (Stony Brook University) W. Lu, C.J. Zhang (TUB) J.R. Welch (Cornell University)

The project will explore a large (e.g. psec or 0.5 mm) length of 'bubble' in CO₂-laser driven plasma wake-field accelerator. Injecting of an external high quality electron bunch with duration ~ 10 fsec synchronized with the "bubble" would allow us to accelerate high quality electron beams with energy stability and spread reaching towards 10^{-4} . We rely on CO₂-laser power upgrades that are in progress at BNL. We present our considerations for visible diagnostics, plasma source with ramp-up and ramp-down density profiles and the electron bunch compressor to 10 fsec with emittance preservation. We present current status of the project and results of first experiments.

WEPOA59 Progress with Coherent Electron Cooling at RHIC

V. Litvinenko (BNL)

Vladimir N Litvinenko for CeC team (list to be filled) A Coherent-electron Cooling (CeC) based on the FEL and micro-bunching instability had been proposed few years ago. Being a very flexible version of stochastic cooling, the CeC approach promises significant increase in the bandwidth and, therefore, significant shortening of cooling time in high-energy hadron colliders. In principle, it also can be considered as a possible final-stage cooling technique for muon colliders. In this paper we present our progress in simulating and testing the key aspects of this proposed techniques using the coherent-electron-cooling proof-of-principle experiment at BNL. We present current status of the project, first results of its commissioning and plans for the future.

WEPOA60 Design Considerations for the Fermilab PIP-II 800 MeV Superconducting Linac

A. Saini (Fermilab)

Proton Improvement Plan (PIP) -II is a proposed upgrade of existing proton accelerator complex at Fermilab. It is primarily based on construction of a superconducting linear accelerator that would be capable to operate in the continuous wave and pulsed modes. It will accelerate the 2mA H⁺ ion beam up to 800 MeV. In this paper we discuss design considerations of PIP-II SC linac that have determined the machine design. Among the various technical and beam optics issues associated with high beam power the beam mismatch, uncontrolled beam losses, halo formation and possible element's failures are the most critical elements that largely affect performance and reliability of the linac. This paper reviews these issues in the framework of PIP-II SC linac and discusses experience accumulated in the course of this work.

WEPOA61 New ERL with NS-FFAG Arcs at Cornell University

C.E. Mayes, I.V. Bazarov, J.A. Crittenden, J. Dobbins, B.M. Dunham, R.G. Eichhorn, G.H. Hoffstaetter, Y. Li, W. Lou, J.R. Patterson, K.W. Smolenski (Cornell University (CLASSE), Cornell Laboratory for Accelerator-Based Sciences and Education) **J.S. Berg, M. Blaskiewicz, S.J. Brooks, G.J. Mahler, F. Méot, R.J. Michnoff, M.G. Minty, S. Peggs, V. Ptitsyn, T. Roser, P. Thieberger, D. Trbojevic, N. Tsoupas, J.L. Tuozzolo, H. Witte** (BNL) **D. Douglas** (JLab)

We will use a novel Fixed Field Alternating Gradient beam line (FFAG) to replace multiple beam lines in existing ERLs (4-pass at Novosibirsk, ERL of CEBAF, ERL at KEK, etc.) with a single FFAG beam line connected with spreaders and combiners to the linac. We present Cornell University Brookhaven National Laboratory (BNL) Electron Test Accelerator (CBETA) an energy Recovery Linac with a total of 8 passes through the linac: four during acceleration and four during the energy recovery. The project is expected to be funded by the New York State. This is the proof of principle electron accelerator for the future Electron Ion Collider to be built at BNL: "eRHIC". The FFAG arc made of permanent magnets is to be built at Cornell University Wilson Hall where there are already available injector, superconducting linac accelerator and the dump. There are very new developments in the FFAG design never accomplished before: arc-to straight adiabatic matching with merged multiple orbits into one, permanent magnet design for the arc and straights with ability of four times in energy, etc.


WEPOA62 An Approach to Increasing Beam Brightness

J.R. Patterson, G.H. Hoffstaetter (Cornell University (CLASSE), Cornell Laboratory for Accelerator-Based Sciences and Education) **Y.K. Kim** (University of Chicago)

We present a strategy for increasing electron beam brightness using an interdisciplinary approach. It augments the capabilities of accelerator physicists with those of physical chemists, materials scientists, condensed matter physicists, plasma physicists, and mathematicians. This approach has the potential to increase the brightness of electron sources through better photocathodes, the efficiency and gradient of SRF cavities through deeper understanding of superconducting compounds and their surfaces, and better understanding of beam storage and transport and the associated optics by using new mathematical techniques.

WEA3 — Oral Presentations (MC5)**Chair:** V. Litvinenko (BNL)**WEA3I001 Emittance Growth from Modulated Focusing in Bunched Beam Cooling**14:00  **M. Blaskiewicz** (BNL)


Electron cooling at high enough energies can only be accomplished with bunched electron beams. Using bunched beams for electron cooling can lead to dynamically generated emittance growth since the electron bunches are typically shorter than the ion bunches, and, due to the synchrotron motion, interact with the electron bunches in some turns, and not in others. The effect of these interactions on the ion beam emittance has been evaluated for the RHIC Low Energy cooling Project.

WEA3I002 Start-to-End Beam Dynamics Optimization of X-Ray FEL Light Source Accelerators14:30  **J. Qiang** (LBNL)

State-of-the-art tools have been developed that allow start-to-end modeling of the beam formation at the cathode, to its transport, acceleration, and delivery to the undulator. Algorithms are based on first principles, enabling the capture of detailed physics such as shot-noise driven micro-bunching instabilities. The most recent generation of the IMPACT code, using multi-level parallelization on massively parallel supercomputers, now enables multi-objective parametric optimization. This is facilitated by recent advances such as the unified differential evolution algorithm*. The most recent developments will be described, together with applications to the modeling of LCLS-II**.

WEA3C003 Efficiency of Feedbacks for Suppression of Transverse Instabilities of Bunched Beams15:00  **A.V. Burov** (Fermilab)


Which gain and phase have to be set for a bunch-by-bunch transverse damper, and at which chromaticity it is better to stay? How high are the remaining growth rates for the given gain and beam parameters? These questions are addressed by means of two Vlasov solvers: for high energy beams, the Nested Head Tail solver is used, while for strong space charge case, a new SChargeV code is exploited.

WEA3C004 Impedance Characterization and Collective Effects in the MAX IV 3 GeV Ring15:15  **G. Skripka**, Å. Andersson, P.F. Tavares (MAX IV Laboratory, Lund University), F.J. Cullinan, R. Nagaoka (SOLEIL)

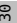
Collective instabilities in the MAX IV 3 GeV storage ring are enhanced by the combination of high beam current, ultralow emittance and small vacuum chamber aperture. To mitigate instabilities by Landau damping and improve lifetime three passive harmonic cavities are installed to introduce synchrotron tune spread and bunch lengthening respectively. We present the results of studies of collective effects driven by the machine impedance. Bunch lengthening and detuning were measured to characterize the effective impedance and estimate the effect of the harmonic cavity potential. Investigations of collective effects as a function of parameters such as beam current and chromaticity are discussed.

WEB3 — Oral Presentations (MC7)


Chair: I. Ben-Zvi (BNL)

WEB3I001 Superconducting Cryomodule Development and Production for the FRIB Linac14:00  **T. Xu, T. Xu (FRIB)**


The Facility for Rare Isotope Beams' heavy ion continuous-wave (CW) linac extends superconducting RF to low beam energy of 500 keV/u. 332 low-beta cavities are housed in 48 cryomodules. The resonators (at 2 K temperature) and magnets (at 4.5 K) supported from the bottom to facilitate alignment and the cryogenic headers suspended from the top for vibration isolation. High performance subsystems including resonator, coupler, tuner, mechanical damper, solenoid and magnetic shielding are necessary. In 2015, the first innovatively designed FRIB 'bottom-up' prototype cryomodule was tested meeting all FRIB specifications. In 2016, the first full production cryomodule is constructed and tested. The preproduction and production cryomodule procurements and in-house assembly are progressing according to the project plan.

WEB3I002 First Test Results of the 150 mm Aperture IR Quadrupole Models for the High Luminosity LHC14:30  **G. Ambrosio (Fermilab)**

The High Luminosity upgrade of the LHC at CERN will use large aperture (150 mm) quadrupole magnets to focus the beams at the interaction points. The high field in the coils requires Nb₃Sn superconductor technology, which was brought to maturity by the LHC Accelerator Research Program (LARP) over the last 10 years. The key design targets for the new IR quadrupoles were established in 2012, and fabrication of model magnets started in 2014. This paper reports on the test results from the first short quadrupole models, and those of individual short and long coils assembled in a magnetic mirror structure. Feedback to the design and fabrication, and the status of preparations toward series production, are also described.

WEB3C003 650 MHz Elliptical Superconducting RF Cavities for PIP-II Project15:00  **V. Jain, I.V. Gonin, C.J. Grimm, T.N. Khabiboulline, C.S. Mishra, D.V. Mitchell, T.H. Nicol, Y.M. Pischalnikov, A.M. Rowe, N.K. Sharma, V.P. Yakovlev (Fermilab)**


Proton Improvement Plan-II at Fermilab has designed an 800MeV superconducting pulsed linac which is also capable of running in CW mode. The high energy section from 185MeV to 800MeV instigated using 650MHz elliptical cavities. The low beta (LB) $\beta G = 0.61$ portion would accelerate proton from 185MeV-500MeV, while high beta (HB) $\beta G = 0.92$ portion of the linac would accelerate from 500 to 800 MeV. The development of both LB and HB cavities is going on under the umbrella of the Indian Institutions Fermilab Collaboration (IIFC) project. The design of LB cavity is being jointly carried out between Fermilab and VECC. The design of the HB cavity is done by Fermilab and the cavity is being jointly developed at RRCAT and at Fermilab. This paper presents design methodology adopted for both low beta and high beta cavities design starting from RF design to get mechanical dimensions of the cavity cells and then converting it to the workable dressed cavity design. A common end group, helium vessel, coupler and tuner designs are being developed for both the cavities. The design, analysis and integration of the dressed cavity are presented in details.

WEB3C004 Preliminary Tests of Plasma Cleaning as an in-Situ Superconducting RF Cavity Cleaning Technique15:15  **B.R. Barber (University of Chicago)**

Oxygen plasmas have shown promise for removing surface hydrocarbons from niobium in superconducting RF cavities. These techniques are candidates for in-situ cleaning techniques for installed accelerating cavities. The goal is to improve the performance of cavities that have degraded over time, without removing them from their cryomodule. By varying the governing parameters of the plasma, the primary cleaning method can be varied between a primarily physical process (sputtering) and a primarily chemical process. We extend this work from organic contaminants to more general contaminants, including metallic species. These preliminary tests are primarily concerned with characterizing the cleaning power of various plasma compositions. A variety of gas species are used to create different plasma compositions, including Ar, Ne, O₂, N₂, H₂, and He. Cleaning power is determined by performing surface characterization analysis on room-temperature niobium samples before and after plasma treatment. Samples are maintained in a clean environment between characterization and treatment, to prevent surface recontamination. Measurements of surface contamination and surface character are presented.

WEA4 — Oral Presentations (MC5)


Chair: M. Steck (GSI)

WEA4I001 **Dynamics of Beams With Canonical Angular Momentum in Non-Axisymmetric Optical Elements**16:00  **C.Y. Wong** (NSCL) *S.M. Lund (FRIB)*


Magnetized beams emerging from electron cyclotron resonance (ECR) ion sources have large statistical canonical angular momentum that substantially alters the beam dynamics. This paper examines the single-particle dynamics of such beams in non-axisymmetric lattice elements. The work supports commissioning activities at the FRIB Front End by illustrating how xy projections of the components of a multi-species beam become tilted due to dipoles and quadrupoles, which can complicate charge state selection with slits. The results help guide simulations performed using the PIC code WARP to achieve better optimization of the collimation in the charge selection system (CSS). Beam statistical angular momentum also evolves in the CSS which in turn changes the x- and y-plane emittances. Possible implications of this effect on the final thermalized beam emittances delivered by the Front End are discussed.

WEA4C002 **Impact of Space Charge on Beam Dynamics and Integrability in the IOTA Ring**16:30  **C.C. Hall**, *D.L. Bruhwiler, N.M. Cook, R.A. Kishek, S.D. Webb (RadiaSoft LLC) A.L. Romanov, A. Valishev (Fermilab)*


Modern hadron accelerators such as spallation sources and neutrino factories must push the intensity limits to meet increasingly challenging goals. The Integrable Optics Test Accelerator (IOTA) is a small ring, currently under construction at Fermilab, which will explore advanced concepts in beam dynamics with low-energy proton beams with high space charge tune depression. Through use of a special nonlinear magnet insertion, large tune spread with amplitude can be achieved while preserving two integrals of motion for the single particle behavior. The tune shift and spread induced by space charge can disrupt the stability of these invariants. In this work we examine the behavior of these invariants in the presence of space charge. Simulations of a modified IOTA lattice that accounts for the space charge tune depression are shown, and the behavior of the invariants is examined.

WEA4C003 **Intrinsic Landau Damping of Bunched Beams at Transverse Coupling Resonance**16:45  **A. Macridin**, *J.F. Amundson, A.V. Burov, P. Spentzouris, E.G. Stern (Fermilab)*

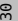
Using Synergia accelerator modeling package and Dynamic Mode Decomposition technique, the properties of the first transverse dipole mode in Gaussian bunches with space charge are compared at transverse coupling resonance and off-resonance. The Landau damping at coupling resonance and in the strong space charge regime is a factor of two larger, while the mode's tune and shape are nearly the same. While the damping mechanism in the off-resonance case fits well with the classical Landau damping paradigm, the enhancement at coupling resonance is due to a higher order mode-particle coupling term which is modulated by the amplitude oscillation of the resonance trapped particles.

WEA4C004 **Suppression of Half-Integer Resonance in FNAL Booster and Space Charge Losses at Injection**17:00  **A. Valishev**, *V.A. Lebedev (Fermilab)*

The particle losses at injection in the FNAL Booster are one of the major factors limiting the machine performance. The losses are caused by motion non-linearity due to direct space charge and due to non-linearity introduced by large values of chromaticity sextupoles required to suppress transverse instabilities. The report aims to address the former - the suppression of incoherent space charge effects by reducing deviations from the perfect periodicity of linear optics functions. It should be achieved by high accuracy optics measurements with subsequent optics correction and by removing known sources of optics perturbations. The study shows significant impact on half-integer stop band with subsequent reduction of particle loss. We use realistic Booster lattice model to understand the present limitations, and investigate the possible improvements which would allow high intensity operation with PIP-II parameters.

WEA4C005 **Accelerator Physics Design and Challenges of RF Based Electron Cooler LEReC**17:15  **A.V. Fedotov**, *M. Blaskiewicz, W. Fischer, D. Kayran, J. Kewisch, S. Seletskiy, J.E. Tuozzolo (BNL)*


A Low Energy RHIC electron Cooler (LEReC) is presently under construction at BNL to improve the luminosity of the Relativistic Heavy Ion Collider (RHIC). The required electron beam will be provided by a photoemission electron gun and accelerated by a RF linear accelerator. As a result, LEReC will be first bunched beam electron cooler. In addition, this will be the first electron cooler to cool beams under collisions. The achievement of very tight electron beam parameters required for cooling is very challenging and is being addressed by a proper beam transport and engineering design. In this paper, we describe accelerator physics requirements, design considerations and parameters, as well as associated challenges of such electron cooling approach.

WEB4 — Oral Presentations (MC7)**Chair:** S.A. Belomestnykh (Fermilab)**WEB4I001 Advanced High Gradient, High Efficiency RF Technology**16:00  **S.G. Tantawi** (SLAC)

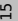
Recent advances in rf structure design, material choices and power distribution technology promise to enable high gradient (100s MV/m), highly efficient compact accelerator implementations for a variety of applications.

WEB4I002 CLIQ: a New Quench Protection Technology for Superconducting Accelerator Magnets16:30  **E. Ravaoli** (LBNL)

Protection against the effects of a magnet quench is a crucial challenge for superconducting accelerators. In order to avoid overheating and damage, the energy stored in the quenching magnets needs to be quickly and uniformly distributed in the winding pack while maintaining a safe voltage distribution among components. The recently-developed Coupling-Loss-Induced Quench (CLIQ) system is an advantageous alternative to traditional quench protection systems based on quench heaters. CLIQ utilizes inter-filament coupling loss as an effective intra-wire heat deposition mechanism, which by principle is faster than thermal diffusion. Being based on simple and robust electrical components, CLIQ reduces the risk of failure and electrical breakdown. However, its integration in an accelerator magnet circuit requires careful consideration of several interdependent systems, including powering, electrical distribution and cryogenics. We review the principles of the CLIQ method, the validation tests carried out in accelerator magnets so far, its planned use in the high luminosity LHC, and the general outlook for application to future accelerators.

WEB4C003 Phase Shift Calibration of CEBAF Linac Cavities17:00  **A. Carpenter**, *J. F. Benesch, C.J. Slominski* (JLab)

CEBAF relied on a null balance method for cavity momentum gain calibration for its first two decades of operation. The highest energy gain cavity in a linac was calibrated using the following arc as a magnetic spectrometer. It was then set to the lower limit of RF control system stability and increased to maintain constant momentum in the arc when other cavities in the linac were sequentially lowered to the stability limit. Allowed momentum excursions limited precision of the measurement to ~7%. This abstract describes a new method of cavity gain calibration based on varying the cavity phase. This allows for larger range of momentum excursions. Monte Carlo simulations suggest that a calibration precision of 1-3% could be achieved. During the commissioning of the upgraded CEBAF, 876 measurements were performed on 375 of the 400 CEBAF linac cavities Fall 2015 and applied December 2015. Linac optics appears to be closer to design as a result. The calibration ensemble proved to be 2% over the value needed to get the desired energy in the arcs. Continued offline analysis of the data has allowed for error analysis and better understanding of the process.

WEB4C004 100 kW Very Compact Pulsed Solid-State RF Amplifier. Development and Tests17:15  **G.B. Sharkov**, *A.A. Krasnov, S.A. Polikhov* (NIITFA) , *R.J. Patrick* (TMD Technologies)

A high power solid-state RF amplifier system has been developed and tested. The modular scalable architecture of the system allows to build megawatt-range compact, robust, cost effective RF amplifiers/generators with high plug efficiency. Using a special designed technology of RF power on-board combination for several LDMOS transistors and very compact high power RF combiners, the amplifier with output power of 100 kW and duty cycle of 5% has been fit into a single 19" cabinet. The system has been tested at the output power up to 104 kW with 3.5 ms pulses. The overview of the technologies, the design of the machine, and its main subsystems is given in this talk. The test results and the market perspectives are also presented.

WEPOB — Poster Session (MC2)

WEPOB01 Lower Emittance Lattice for the Advanced Photon Source Upgrade Using Reverse Bending Magnets**M. Borland**, V. Sajaev, Y.P. Sun (ANL)

The Advanced Photon Source (APS) is pursuing an upgrade to the storage ring to a hybrid seven-bend-achromat design*. The nominal design provides a natural emittance of 67 pm. By adding reverse dipole fields to several quadrupoles**, we can reduce the natural emittance to 41 pm while simultaneously providing more optimal beta functions in the insertion devices. The improved emittance results from a combination of increased energy loss per turn and a change in the damping partition. At the same time, the nonlinear dynamics performance is very similar, thanks in part to increased dispersion in the sextupoles. This paper describes the properties, optimization, and performance of the new lattice.

WEPOB02 Simulation of Swap-Out Reliability for the Advance Photon Source Upgrade**M. Borland** (ANL)

The proposed upgrade of the Advanced Photon Source (APS) to a multibend achromat lattice relies on the use of swap-out injection to accommodate the small dynamic acceptance, allow use of unusual insertion devices, and minimize collective effects at high single-bunch charge. This, combined with the short beam lifetime, will make injector reliability even more important than it is for top-up operation. We used historical data for the APS injector complex to obtain probability distributions for injector up-time and down-time durations. Using these distributions, we simulated several years of swap-out operation for the upgraded lattice for several operating modes. The results indicate that obtaining very high availability of beam in the storage ring will require improvements to injector reliability.

WEPOB03 Magnetic Measurements of Storage Ring Magnets for the APS Upgrade Project***R.J. Dejus**, H. Cease, J.T. Collins, G. Decker, A.T. Donnelly, C.L. Doose, W.G. Jansma, M.S. Jaski, J. Liu (ANL) A.K. Jain (BNL)

Extensive prototyping of storage ring magnets is ongoing at the Advanced Photon Source (APS) in support of the APS Multi-Bend Achromat upgrade (APS-U) project. As part of the R&D activities 4 quadrupole magnets with slightly different geometries and pole tip materials, and one sextupole magnet with vanadium permendur pole tips were designed, built and tested. Magnets were measured individually using a rotating coil and a Hall probe for detailed mapping of the magnetic field. Magnets were then assembled and aligned relative to each other on a steel support plate and concrete plinth using precision machined surfaces to gain experience with the alignment method chosen for the APS-U storage ring magnets. The required alignment of magnets on a common support structure is 30 micron rms. Measurements of magnetic field quality, strength and magnet alignment after subjecting the magnets and assemblies to different tests will be presented.

WEPOB04 Beamline-Controlled Steering of Source-Point Angle at the Advanced Photon Source**L. Emery**, G.I. Fystro, H. Shang, M.L. Smith (ANL)

An EPICS-based steering software system has been implemented for beamline personnel to directly steer the angle of the synchrotron radiation sources at the Advanced Photon Source. A script running on a workstation monitors "start steering" beamline EPICS records, and effects a steering by the value of "angle request" EPICS records that beamlines have set. The new system effectively bypasses floor coordinators and MCR operators, and makes the steering process much faster than before, although these older protocols can still be used. As with the original steering there are EPICS alarm limits that prevent large steering from occurring and avoid other problems. Error messages and statuses, OPI windows and alarm configurations are provided to the beamlines and the accelerator operators. Underpinning this new steering protocol is the recent refinement of the global orbit feedback process whereby feedforward of dipole corrector set points and orbit set points are used to create a local steering bump in a rapid and seamless way. In principle and in practice, many simultaneous steering commands from many beamlines are possible. We report on a complete 3-month run of experience.

WEPOB05 Operational Experience With Beam Abort System for Superconducting Undulator Quench Mitigation**K.C. Harkay**, J.C. Dooling, V. Sajaev, J. Wang (ANL)

A beam abort system has been implemented in the Advanced Photon Source storage ring. The abort system works in tandem with the existing machine protection system (MPS), and its purpose is to control the beam loss location and, thereby, minimize beam loss-induced quenches at the two superconducting undulators (SCUs). The abort system consists of a dedicated horizontal kicker designed to kick out all the bunches in a few turns after being triggered by MPS. The abort system concept was developed on the basis of single- and multi-particle tracking simulations using elegant and bench measurements of the kicker pulse. Performance of the abort system—kick amplitudes and loss distributions of all bunches—was analyzed using beam position monitor (BPM) turn histories, and agrees reasonably well with the model. Beam loss locations indicated by the BPMs are consistent with the fast fiber-optic beam loss diagnostics described elsewhere [1]. Operational experience with the abort system, various issues that were encountered, limitations of the system, and quench statistics are described.

WEPOB06 Parameterization of Superconducting Helical Undulator Magnetic Field***S.H. Kim** (ANL)

A scaling law [1, 2] shows that when the undulator dimensions are scaled according to a period ratio, the magnetic field distribution remains unchanged for a constant value of coil current density times the period. Using this scaling law, the magnetic fields of superconducting helical undulators (SCHUs) for a period range of 8 mm to 50 mm were parameterized by using the field calculations of one SCHU with a period of 30 mm. The field calculations included the on-axis fields at the coil critical current densities of NbTi and Nb₃Sn superconductors, as well as at different values of the inner coil radius. The parameterized on-axis fields for the period range are expressed in terms of the period and inner radius of the helical coils. The corresponding critical current densities and coil maximum fields are also included. Detailed calculation procedures and results will be presented. [1] NIM A546 (2005) 604. [2] NIM A584 (2008) 266.

WEPOB07 Dielectrically-Loaded Waveguide as a Short Period Superconducting Microwave Undulator**R. Kustom**, A. Nassiri, K.J. Suthar, G.J. Waldschmidt (ANL)

The HEM12 mode in a cylindrical, dielectrically-loaded waveguide provides E and H fields on the central axis that are significantly higher than the fields on the conducting walls. The waveguide is designed to operate near its cutoff frequency where the wavelength and phase velocity vary significantly to enable tuning of the equivalent undulator wavelength. The operating frequency would range from 18 - 24 GHz. It would be possible to generate coherent, high-energy 45 - 65 KeV x-rays from the fundamental mode

which are tunable over a 20% energy range by changing the source frequency while maintaining constant field strengths. The x-ray brilliance of the microwave undulator would be 3 times higher at 56-KeV and 7 times higher at 66 KeV than what is available with the APS 1.8 cm period Superconducting Wire Undulator. Since the loss factor of sapphire is very low at cryogenic temperatures, it is possible to consider a superconducting microwave undulator, although resistive losses of ~200 to 700 W/m may be a bit too high for CW operation.

WEPOB08 Collective Effects at Injection for the APS-U MBA Lattice

R.R. Lindberg, M. Borland (ANL) A. Blednykh (BNL)

The Advanced Photon Source has proposed an upgrade to a multi-bend achromat (MBA) with a proposed timing mode calls for 48 bunches of 15 nC each. In this mode of operation we find that phase space mismatch from the booster can drive large wakefields that in turn may limit the current below that of the nominal collective instability threshold. We show that collective effects at injection lead to emittance growth that makes usual off-axis accumulation very challenging. On-axis injection ameliorates many of these issues, but we find that transverse feedback is still required. We explore the role of impedance, feedback, and phase-space mismatch on transverse instabilities at injection.

WEPOB09 Field Quality Impact from Tolerance Stack Up in Quadrupoles for the Advanced Photon Source Upgrade*

J. Liu, M. Borland, R.J. Dejus, A.T. Donnelly, C.L. Doose, J.S. Downey, M.S. Jaski (ANL) A.K. Jain (BNL)

The Advanced Photon Source (APS) at Argonne National Laboratory (ANL) is considering upgrading the current double-bend, 7-GeV, 3rd generation storage ring to a 6-GeV, 4th generation storage ring with a Multibend Achromat (MBA) lattice. In this study, a novel method is proposed to determine fabrication and assembly tolerances through a combination of magnetic and mechanical tolerance analyses. Mechanical tolerance stackup analyses using Teamcenter Variation Analysis are carried out to determine the part and assembly level fabrication tolerances. Finite element analyses using OPERA are conducted to estimate the effect of fabrication and assembly errors on the magnetic field of a quadrupole magnet and to determine the allowable tolerances to achieve the desired magnetic performance. Finally, results of measurements in R&D quadrupole prototypes are compared with the analysis results.

WEPOB10 Simulation Study of the Helical Superconducting Undulator Installation at the Advanced Photon Source

V. Sajaev, Y.P. Sun, A. Xiao (ANL)

A helical superconducting undulator is planned for installation at the APS. Such an installation would be first of its kind [–] helical devices were never installed in synchrotron light sources before. Due to its reduced horizontal aperture, a lattice modification is required to accommodate for large horizontal oscillations during injection. We describe the lattice change details and show the new lattice experimental test results. To understand the effect of the undulator on single-particle dynamics, first, its kick maps were computed using different methods. We have found that often-used Elleaume formula* for kick maps gives wrong results for this undulator. We then used the kick maps obtained by other methods to simulate the effect of the undulator on injection and lifetime.

WEPOB11 Tuning of the APS Linac Accelerating Cavities After Structural Re-Alignment

T.L. Smith, G.J. Waldschmidt (ANL)

A new S-band LCLS type Photo-cathode (PC) gun was recently installed in the APS linac. As a consequence, it was recognized that many of the linac accelerating structures were out of their 1mm straightness tolerances. In order to reduce the effects of wakefield on the beam, several of the misaligned structures were straightened. This paper discusses the bead-pull RF measurements, the effect of the straightening efforts on rf and the cell to cell retuning efforts that were performed.

WEPOB12 Multi-Objective Online Optimization of Beam Lifetime at APS

Y.P. Sun (ANL)

In this paper, online optimization of beam lifetime at the APS (Advanced Photon Source) storage ring is presented. A general genetic algorithm (GA) is developed and employed for some online optimizations in the APS storage ring. Sextupole magnets in 40 sectors of the APS storage ring are employed as variables for the online nonlinear beam dynamics optimization. The algorithm employs several optimization objectives and is designed to run with topup mode or beam current decay mode. Up to 50% improvement of beam lifetime is demonstrated, without affecting the transverse beam sizes and other relevant parameters. In some cases, the top-up injection efficiency is also improved.

WEPOB13 Online Minimization of Vertical Beam Sizes at APS

Y.P. Sun (ANL)

In this paper, online minimization of vertical beam sizes along the APS (Advanced Photon Source) storage ring is presented. A genetic algorithm (GA) is developed and employed for the online optimization in the APS storage ring. A total of 59 families of skew quadrupole magnets are employed as knobs to adjust the coupling and the vertical dispersion in the APS storage ring. Starting from initially zero current skew quadrupoles, small vertical beam sizes along the APS storage ring are achieved in a short optimization time of one hour. The optimization results from this method is briefly compared with the one from LOCO (Linear Optics from Closed Orbits) response matrix correction.

WEPOB14 APS-U Lattice Design for Off-Axis Accumulation

Y.P. Sun, M. Borland, R.R. Lindberg, V. Sajaev (ANL)

A 67-pm hybrid-seven-bend achromat (H7BA) lattice is being proposed for a future Advanced Photon Source (APS) multi-bend-achromat (MBA) upgrade project. This lattice design pushes for smaller emittance and requires use of a swap-out (on-axis) injection scheme due to limited dynamic acceptance. Alternate lattice design work has also been performed for APS upgrade to achieve better beam dynamics performance than the nominal APS MBA lattice, in order to allow off-axis accumulation. One of such alternate H7BA lattice designs, which still targets a low emittance of 90 pm, is discussed in details in this paper. Although the single-particle-dynamics performance is good, simulations of collective effects indicate that surprising difficulty would be expected accumulating high single-bunch charge in this lattice. The brightness of the 90-pm lattice is also a factor of two lower than the 67-pm H7BA lattice.

WEPOB15 Comparison of nonlinear dynamics optimization methods for APS-U

Y.P. Sun, M. Borland (ANL)

Many different objectives and genetic algorithm have been proposed for storage ring nonlinear dynamics performance optimization. These optimization objectives include nonlinear chromaticities and driving/detuning terms, on-momentum and off-momentum dynamic acceptance, chromatic detuning, local momentum acceptance, variation of transverse invariant, etc. In this paper, the effectiveness of several different optimization methods and objectives are compared for the nonlinear beam dynamics optimization

of the Advanced Photon Source upgrade (APS-U) lattice. The optimized solutions from these different methods are compared in terms of the dynamic acceptance, local momentum acceptance, chromatic detuning, and other performance measures.

WEPOB16 **Simulation Studies of a Prototype Stripline Kicker for the APS-MBA Upgrade***

X. Sun, C. Yao (ANL)

A prototype dual blade stripline kicker for the multi-bend achromat (MBA) at the APS has been designed and developed. It was modeled and simulated using 3D CST Microwave Studio to verify its 2D design. The high voltage (HV) feedthrough and air-side connector were optimized. Deflecting angle and maximum electric fields are calculated when 15kV differential pulse voltage is applied to the kicker blades. Beam impedance and the power dissipation on the different parts of the kicker and external loads are studied for MBA 48-bunch fill pattern. Our results show that the prototype of the kicker with its HV feedthroughs meet the specified requirements.

WEPOB17 **Integrated Approach to Optimize the Design of Vacuum Chamber Combining Responsible Physics in Finite Element Analysis**

K.J. Suthar, P.K. Den Hartog, B.K. Stillwell (ANL) D.L. Bruhwiler (RadiaSoft LLC)

The next generation of synchrotron light sources require much more compact vacuum chambers, greatly increasing performance requirements which are already numerous, demanding, complex, and coupled. For example, in the proposed APS-U multibend achromat storage ring, ~10 kW of synchrotron radiation will be generated in each of the 40 sectors. Most of the residual gas in the vacuum system will result from photon-stimulated desorption, so the location and shape of photon absorbers will determine residual gas pressures. Strong wakefields near such structures will perturb the beam dynamics and deposit energy within the chamber. Heating of vacuum system components can cause material damage and reduce the accuracy of beam position monitors. We present an integrated approach to vacuum chamber design that can simultaneously account for all these effects and thus correctly optimize performance. This paper discusses preliminary results from a coupled finite element analysis of synchrotron radiation, non-ideal electron beam trajectories and the resultant surface heating. The codes COMSOL Multiphysics and SynRad are both used to enable benchmarking during the development of new capabilities.

WEPOB18 **Bend Magnet Head Loads and Out of Orbit Scenarios**

T.T. Valicenti, J.A. Carter, K.J. Suthar (ANL)

This paper presents an analytical calculation of the spatial power spectrum emitted from relativistic electrons passing through a series of bend magnets. Using lattice files from the software Elegant, both the ideal and missteered trajectories taken by the beam are considered in determination of the power profile. Calculations were performed for the Advanced Photon Source Upgrade multi-bend-achromat storage-ring. Results were validated with Synrad, a monte-carlo based program designed at CERN. The power distribution and integrated total power values are in agreement with Synrad's results within one percent error. The analytic solution used in this software gives a both quick and accurate tool for calculating the heat load on a photon absorber. The location and orientation can be optimized in order to reduce the peak intensity and thus the maximum thermal stress. This can be used with any optimization or FEA software and gives rise to a versatile set of uses for the developed program.

WEPOB19 **Photocathode Performance and Improvements in the High-Gradient, High-Charge AWA Drive Gun**

E.E. Wisniewski, S.P. Antipov, M.E. Conde, D.S. Doran, W. Gai, C.-J. Jing, J.G. Power, C. Whiteford (ANL) S.P. Antipov, C.-J. Jing (Euclid TechLabs, LLC)

The AWA L-band, high-charge photoinjector for the 70 MeV drive beamline has been operating for almost 3 years at the Argonne Wakefield Accelerator (AWA) facility. at Argonne National Laboratory (ANL). The gun operates at high-field (85 MV/m peak field on the cathode) and has a high quantum efficiency (QE) Cesium telluride photocathode with a large area (30 mm diameter). It produces high-charge, short pulse, single bunches ($Q > 100$ nC) as well as long bunch-trains ($Q > 600$ nC) for wakefield experiments (high peak current). During the first two years of operation, photocathode performance was evaluated and areas of improvement were identified. After study, consideration and consultation, steps were taken to improve the performance of the photocathode. So far, in total, three photocathodes have been fabricated on-site, installed and operated in the gun. Improvements made to the photocathode plug, vacuum system, and gun operation are detailed. The results include vastly improved conditioning times, better cathode performance, and QE above 4% for over 7 months.

WEPOB20 **Multiple Scattering Effects on a Short Pulse Electron Beam Travelling Through Thin Beryllium Foils**

E.E. Wisniewski, S.P. Antipov, M.E. Conde, D.S. Doran, W. Gai, C.-J. Jing, W. Liu, J.G. Power, C. Whiteford (ANL) S.P. Antipov, C.-J. Jing (Euclid TechLabs, LLC) G. Ha (POSTECH)

The Argonne Wakefield Accelerator beamlines have stringent vacuum requirements (100 picotorr) necessitated by the Cesium telluride photoinjector. In direct conflict with this, the structures-based wakefield accelerator research program sometimes includes worthy but complex experimental installations with components or structures unable to meet the vacuum standards. A proposed chamber to sequester such experiments safely behind a thin beryllium (Be) window is described and the results of a study of beam-quality issues due to the multiple scattering of the beam through the window are presented and compared to GEANT4 simulations via G4beamline as well as analytical calculations incorporated into GPT. Three thicknesses of Be foil were used: 30, 75 and 127 micron, probed by electron beams of three different energies: 25, 45, and 65 MeV. Multiple scattering effects were evaluated by comparing the measured transverse rms beam size for the scattered vs. unscattered beam. The experimental results are presented and compared to simulations. Results are discussed along with the implications and suggestions for the future sequestered vacuum chamber design.

WEPOB21 **Benchmarking of Touschek Beam Lifetime Calculations for the Advanced Photon Source**

A. Xiao, B.X. Yang (ANL)

Particle loss from Touschek scattering is one of the most significant issues faced by present and future synchrotron light source storage rings. For example, the predicted, Touschek-dominated beam lifetime for the Advanced Photon Source (APS) Upgrade lattice in 48-bunch, 200-mA timing mode is only ~2 h. In order to understand the reliability of the predicted lifetime, a series of measurements with various beam parameters was performed on the present APS storage ring. This paper first describes the entire process of beam lifetime measurement, then compares measured lifetime with the calculated one by applying the measured beam parameters. The results show very good agreement.

WEPOB22 **Beam Loss Simulation and Collimator System Configurations for the Advanced Photon Source Upgrade**

A. Xiao, M. Borland (ANL)

The proposed multi-bend achromat lattice for the Advanced Photon Source upgrade (APS-U) has a design emittance of less than 70

pm. The Touschek loss rate is high: compared with the current APS ring, which has an average beam lifetime ~ 10 h, the simulated beam lifetime for APS-U is only ~ 2 h when operated in the high flux mode ($I = 200$ mA in 48 bunches). An additional consequence of the short lifetime is that injection must be more frequent, which provides another potential source of particle loss. In order to provide information for the radiation shielding system evaluation and to avoid particle loss in sensitive locations around the ring (for example, insertion device straight sections), simulations of the detailed beam loss distribution have been performed. Several possible collimation configurations have been simulated and compared.

WEPOB23 Performance of the Full-Length Vertical Polarizing Undulator Prototype for LCLS-II

N.O. Strelnikov, E. Gluskin, I. Vasserman, J.Z. Xu (ANL)

As part of the LCLS-II R&D program, a novel 3.4-meter long undulator prototype with horizontal main magnetic field and dynamic force compensation - called the horizontal gap vertical polarization undulator (HGVPU) - has recently been developed at the Advanced Photon Source (APS). Initial steps of the project included designing, building, and a testing 0.8-meter long prototype. Extensive mechanical testing of the HGVPU has been carried out. The magnetic tuning was accomplished by applying a set of magnetic shims. As a result, the performance of the HGVPU meets all the stringent requirements for the LCLS-II insertion device, which includes limits on the field integrals and phase errors for all operational gaps, as well as the reproducibility and accuracy of the gap settings. The HGVPU has been included in the baseline of the LCLS-II project for the hard x-ray undulator line.

WEPOB24 Preliminary Test Results of a Prototype Fast Kicker for APS MBA Upgrade

C. Yao, J. Carwardine, A.R. Cours, F. Lenkszus, L.H. Morrison, X. Sun, J. Wang, F. Westferro (ANL)

The APS multi-bend achromatic (MBA) upgrade storage ring plans to support two bunch fill patterns: a 48-bunch and a 324-bunch. A 'swap out' injection scheme is required. In order provide the required kick to injected beam, to minimize the beam loss and residual oscillation of injected beam, and to minimize the perturbation to stored beam during injection, the rise, fall, and flat-top parts of the kicker pulse must be within a 16.9-ns interval. Stripling-type kickers are chosen for both injection and extraction. We developed a prototype kicker that support a ± 15 kV differential pulse voltage. We performed high voltage discharge, TDR measurement, high voltage pulse test and beam test of the kicker. We report the design of the fast kicker and the test results.

WEPOB25 Analytical Modeling of Electron Back-Bombardment Induced Current Increase in Un-Gated Thermionic Cathode Rf Guns

J.P. Edelen (Fermilab) J.R. Harris (Directed Energy Directorate, Air Force Research Laboratory) J.W. Lewellen (LANL) Y.-E. Sun (ANL)

In this paper we derive analytical expressions for the output current of an un-gated thermionic cathode RF gun in the presence of back-bombardment heating. We provide a brief overview of back-bombardment theory and show comparisons between the analytical back-bombardment predictions and simulation models. We then derive an expression for the output current as a function of the RF repetition rate and discuss relationships between back-bombardment, field-enhancement, and output current. We discuss in detail the relevant approximations and then provide predictions about how the output current should vary as a function of repetition rate for some given system configurations.

WEPOB26 Observation of Repetition-Rate Dependent Emission From an Un-Gated Thermionic Cathode Rf Gun

J.P. Edelen (Fermilab) J.R. Harris (Directed Energy Directorate, Air Force Research Laboratory) J.W. Lewellen (LANL) Y.-E. Sun (ANL)

Thermionic cathodes are well known as a robust source of electrons that have a long lifetime and produce beams with low thermal emittance. In electron accelerators these cathodes are often used in either a DC gun or a gated RF gun. In some cases electron emission is regulated only by the time varying fields in the cavity. A consequence of emission not being regulated to a narrow RF phase range is that electrons emitted late in the RF period will not gain enough energy to exit the gun. These electrons accelerate back to the cathode and deposit their energy on the cathode surface. Recent work at Fermilab in collaboration with the Advanced Photon Source and members of other national labs, designed an experiment to attempt to observe the predicted increase in the average current per RF pulse driven by an increase in the RF repetition rate. Contrary to our existing theoretical models, we observed a decrease in the average current per RF pulse as we increased the repetition rate. These observations shed new light on the challenges and fundamental limitations associated with scaling an un-gated thermionic cathode RF gun to high average current machines.

WEPOB27 Modification of 3rd Harmonic Cavity for CW Operation in LCLS-II Accelerator

T.N. Khabiboulline, M.H. Awida, I.V. Gonin, S. Kazakov, A. Lunin, V.P. Yakovlev (Fermilab)

3.9 GHz 3rd harmonic cavity developed at FNAL is used in FLASH accelerator at DESY in order to improve FEL operation. XFEL accelerator in Hamburg also adapted same design. LCLS-II accelerator planning using of this cavity in CW regime. CW operation and higher average current in LCLS-II results to power load to coupler and HOM couplers. Some cavity design modification was proposed and investigated. Results of design review and modification will be presented.

WEPOB29 Modeling of Dark Current Generation and Transport Using the IMPACT-T Code

J. Qiang, K. Hwang (LBNL)

Dark current from unwanted electrons in photoinjector can present significant danger to the accelerator operation by causing damage to photocathode and power deposition onto conducting wall. In this paper, we present numerical models of dark current generation from the field emission and from the electron impact ionization of the residual gas that were recently developed in the IMPACT-T code. We also report on the application of above numerical model to an LCLS-II like photoinjector.

WEPOB30 Simulation of the Shot-Noise Driven Microbunching Instability Experiment at the LCLS

J. Qiang (LBNL) Y. Ding, P. Emma, Z. Huang, D.F. Ratner, T.O. Raubenheimer (SLAC)

The shot-noise driven microbunching instability can significantly degrade electron beam quality in next generation light sources. Experiments were carried out at the Linac Coherent Light Source (LCLS) to study this instability. In this paper, we will present start-to-end simulation of the shot-noise driven microbunching instability experiment at the LCLS.

WEPOB31 Dark Current Simulation of a Standing Wave Disk-Loaded Waveguide Structure at 17 GHz

H. Xu, B.J. Munroe, M.A. Shapiro, R.J. Temkin (MIT/PSFC)

We present calculations of the dark current in a high gradient accelerator with the intent of understanding its role in breakdown. The initial source of the dark current is the field emission of electrons from the surfaces where the electric field is maximum. For a 17 GHz single-cell standing wave disk-loaded waveguide structure, the 3-d particle-in-cell simulation shows that only a small portion of the charge emitted is reaching the current monitors at the ends of the structure, while most of the current collides on the

structure inner surfaces, causing secondary electron emission. In the simulation, a two-point multipactor process is observed on the side wall of cell due to the low electric field on the surface. The multipactor reaches a steady state within nanoseconds when the electric field is suppressed by the electron cloud formed so that the average secondary electron yield equals to unity. In the steady state when operating at 80 MV/m, the multipactor current on the side wall goes up to 100'1000 A with an average electron energy of around 30 eV. This multipactor current can cause the ionization of the metal material and surface outgassing, leading to breakdown.

WEPOB32 Performance of a Combined System Using an X-Ray FEL Oscillator and a High-Gain FEL Amplifier

L. Gupta (University of Chicago) *K.-J. Kim, R.R. Lindberg (ANL)*

The LCLS-II at SLAC will feature a 4 GeV CW superconducting (SC) RF linac [1] that can potentially drive a 5th harmonic X-Ray FEL Oscillator to produce fully coherent, 1 MW photon pulses with a 5 meV bandwidth at 14.4 keV [2]. The XFEL output can serve as the input seed signal for a high-gain FEL amplifier employing fs electron beams from the normal conducting SLAC linac, thereby generating coherent, fs x-ray pulses with ~TW peak powers using a tapered undulator after saturation [3]. Coherent, intense output at several tens of keV will also be feasible if one considers a harmonic generation scheme. Thus, one can potentially reach the 42 keV photon energy required for the MaRIE project [4] by beginning with an XFEL operating at the 5th harmonic to produce 8.4 keV photons using a 3.1 GeV SCRF linac, and then subsequently using the high-gain harmonic generation scheme to generate and amplify the 5th harmonic at 42 keV [5]. We report extensive GINGER simulations that determine an optimized parameter set for the combined system. [1] "Linac Coherent Light Source-II Conceptual Design Report," SLAC-R-978 (2011)

WEPOB33 Second Harmonic Generation in Nonlinear Crystal Using Extracted FEL Beam on the Duke Storage Ring

J. Yan, H. Hao, T. He, S.F. Mikhailov, V. Popov, Y.K. Wu (FEL/Duke University)

A new pulsed FEL operational mode using an rf frequency switching technique is developed for the Duke storage ring FEL system. With this operational mode, the peak FEL power is enhanced by two to three orders of magnitude. Taking advantage of this substantial enhancement of peak FEL power, we have experimentally achieved the second harmonic generation (SHG) in a BBO crystal with an extracted FEL beam around 530 nm. The nonlinear optical effect of the FEL beam in the crystal is investigated in terms of its wavelength tunability and the SHG conversion efficiency. The wavelength dependency of the crystal phase-matching angle is also examined.

WEPOB34 Simulation of an Extraction System for a Compact Microtron

R.J. Abrams, M.A.C. Cummings, R.P. Johnson, S.A. Kahn, G.M. Kazakevich (Muons, Inc)

A microtron is an efficient electron accelerator that can be used as a copious source of gamma rays and neutrons. The electron beam is held inside the microtron in circular orbits by a uniform magnetic field. The beam can be extracted passively from the microtron shielding the beam from the field with a soft steel tube placed inside the microtron. The magnetic field inside the microtron will be perturbed by the presence of the extraction tube. To operate properly the microtron requires a high degree of field uniformity. The next-to-last orbit before entering the extraction shield is greatly affected and the field along its path must be corrected. In this paper we study how to modify the extraction shielding for the microtron to minimize the effects of the field non-uniformity. We then simulate the microtron with a particle tracking code to study the performance of the optimized extraction system.

WEPOB35 Characterization of Laser-Compton X-Rays at LLNL

Y. Hwang, T. Tajima (UCI) *G.G. Anderson, C.P.J. Barty, D.J. Gibson, R.A. Marsh (LLNL)*

Laser-Compton X-rays have been produced at LLNL using the unique compact X-band accelerator at LLNL operated in a novel multibunch mode, and results agree very well with modeling predictions. Flux, source size and bandwidth of the 30 keV X-ray beam were measured using an X-ray CCD camera and image plates. K-edge absorption images using thin foils confirm the narrow bandwidth of the source and offer electron beam diagnostics through matched imaging simulation. Future plans for medically relevant imaging will be discussed with facility upgrades to enable 100 keV x-ray production.

WEPOB36 Chess-U: Upgrade of the Cornell Electron Storage Ring (CESR) as a Synchrotron Light Source

D. L. Rubin, J.P. Shanks, S. Wang (Cornell University (CLASSE), Cornell Laboratory for Accelerator-Based Sciences and Education)

The planned upgrade of the Cornell Electron Storage Ring as an x-ray source for CHESS will include: increase in beam energy and decrease in emittance from 100nm-rad at 5.3 GeV to 30 nm-rad at 6Gev, four new zero dispersion insertion straights that can each accommodate a pair of canted undulators, increase in beam current from 120 to 200mA, and continuous top-off injection of the single circulating beam. The existing sextant of the storage ring arc that is the source for all of the CHESS x-ray beam lines will be replaced with 6 double-bend achromats, consisting of two pairs of horizontally focusing quadrupoles, and a single pair of combined function gradient bend magnets. The chromaticity will be compensated by the existing sextupoles in the legacy FODO arcs. We describe details of the linear optics, sextupole distribution to maximize dynamic aperture and injection efficiency, and characterization of magnetic field and alignment error tolerance. We also discuss beam instrumentation, including beam position monitors and feedback, and the proposed optics correction and emittance tuning strategy.

WEPOB37 Backbombardment-Free Thermionic Cathode Electron Gun for High Average Current

J.L. McCarter, C.H. Boulware, D. Gorelov, T.L. Grimm, A.B. Schnepp, V.N. Starovoitova (Niowave, Inc.)

One key advantage of superconducting electron accelerators is their ability to operate at high duty cycle and therefore at very high average beam powers. These machines are good candidates for many applications, including the irradiation treatment of municipal solid waste at high throughput ' an application requiring MWs of beam power and an ampere-class electron source. For high-current operation, small transverse emittances are needed to keep the beam losses low, particularly the losses to cryogenically-cooled surfaces. To fulfill these requirements, Niowave is developing a new normal conducting RF 350 MHz thermionic electron gun, with electron emission gated via a novel combination of both DC and second harmonic biasing of the cathode. Unlike many conventional implementations, the gating design does not intercept any part of the electron beam, and as such allows for a higher brightness beam at extremely high currents. Presented here are preliminary results for an electron source optimized to produce high current, high brightness beams. These electron sources can also drive accelerators for extremely high power free-electron lasers and high power beam-driven RF sources.

WEPOB38 LLNL Mark I X-Band RF Gun Results

R.A. Marsh, G.G. Anderson, C.P.J. Barty, D.J. Gibson (LLNL) *Y. Hwang (UCI)*

An X-band test station and laser-Compton x-ray source has been built and commissioned at LLNL. The electron beam source is a

unique 5.59 cell RF photoinjector, which is described in detail, including: quantum efficiency, emittance measurements, energy spread and jitter, final focus spot size and stability, laser profile and final transport, and consistency with expectations based on beam dynamics simulations. Various jitter sources will be discussed and are distinguished in an effort to produce the lowest emittance and tightest final focus possible.

WEPOB39 Photo-Injector Optimization and Validation Study with the OPAL Beam Simulation Code

L.D. Duffy, K. Bishofberger, J.W. Lewellen, S.J. Russell, D.Y. Shchegolkov (LANL)

A 42 keV x-ray free electron laser (XFEL) is a plausible technology alternative for the Matter Radiation Interactions in Extremes (MaRIE) experimental project, a concept developed by Los Alamos National Laboratory. An early pre-conceptual design for such an XFEL calls for 100 pC electron bunches with very low emittance and energy spread. High fidelity simulations that capture all beamline physics will be required to ensure a successful design. We expect to use the beam simulation code OPAL as one of the tools in this process. In this study, we validate OPAL as a photo-injector design tool by comparing its performance with published PITZ experimental data and simulations.

WEPOB40 High Efficiency Energy Extraction Results from the Nocibur Experiment

N.S. Sudar, J.P. Duris, P. Musumeci (UCLA)

We present results from the Nocibur experiment recently performed at Brookhaven National Laboratory's Accelerator Test Facility. Using a 54 cm long strongly tapered undulator to couple a 65 MeV beam to a 200 GW CO₂ laser seed we are able to decelerate 45% of the electrons to a final energy of 35 MeV, extraction 30% of the electron beams initial energy. These results demonstrate a great improvement in electro-optical conversion efficiencies for an electron beam-undulator interaction, serving as an important step in the further development of high peak and average power coherent radiation sources.

WEPOB41 Measurement of Internal Quality Factor in Cryogenic Copper Accelerators at High Power

A.D. Cahill, J.B. Rosenzweig (UCLA) V.A. Dolgashev, S.G. Tantawi (SLAC)

Recent SLAC experiments with cryogenically cooled X-band standing wave copper accelerating cavities have shown that these structures can operate with accelerating gradients of ~250 MV/m and low breakdown rates. To better understand what is happening in the copper structure we would like to measure the internal Q factor during a pulse of 1-10 MW of power in an X-Band accelerating structure. This work is to verify previous work measuring Q at low power, and to discover if rf pulse heating will have effects on the internal Q during a single pulse, if there is any time-dependence to the internal Q. These measurements are part of studies with the goal of reaching very high operating accelerating gradients in normal conducting rf structures*.

WEPOB42 High Gradient S-Band Cryogenic Accelerating Structure for RF Breakdown Studies

A.D. Cahill, A. Fukasawa, J.B. Rosenzweig (UCLA) G.B. Bowden, V.A. Dolgashev, S.G. Tantawi (SLAC)

Operating accelerating gradient in normal conducting accelerating structures is often limited by rf breakdowns. The limit depends on multiple parameters, including input rf power, rf circuit, cavity shape, cavity temperature, and material. Experimental and theoretical study of the effects of these parameters on the breakdown limit is ongoing at SLAC. Most of the data is obtained at 11.4 GHz. We are extending this research to S-band. We have designed a single cell accelerating structure, based on the extensively tested X-band cavities. The setup uses matched TM₀₁ mode launcher to feed rf power into the test cavity. Our ongoing study of the physics of rf breakdown in cryogenically X-band accelerating cavities shows improved breakdown performance. Therefore, this S-band experimental setup is designed so that the cavity can be cooled to cryogenic temperatures. We present the rf design and discuss the experimental setup.

WEPOB43 Recent Developments and Plans to Get Two Bunches with up to 1 us Separation at LCLS

F.-J. Decker, W.S. Colacho, S. Gilevich, Z. Huang, J.R. Lewandowski, A.A. Lutman, J.C. Sheppard, J.L. Turner, S. Vetter (SLAC)

To get two electron bunches with a separation of up to 1 us at LCLS is important for LCLS-II developments. Two lasing bunches up to 35 ns have been demonstrated. Many issues have to be solved to get that separation increased by a factor of 30. The typical design and setup for one single bunch has to be questioned for many devices. RF pulse widths have to be widened, BPMs diagnostic can see only one bunch, feedbacks have to be doubled up, the main Linac RF needs to run probably un-SLEDeD, and special considerations have to be done for the Gun and LIX RF.

WEPOB44 JLab New Injector Cryomodule Design, Fabrication and Testing

G. Cheng, J.F. Fischer, K. Macha, H. Wang (JLab)

A new Injector Cryomodule (INJ CM) aimed to replace the existing Quarter Cryomodule in CEBAF tunnel has been developed and scheduled to be first tested in the Cryomodule Test Facility (CMTF) for module performance then the Upgraded Injector Test Facility (UITF) with electron beam at Jefferson Lab (JLab). This new cryomodule, hosting a 2-cell and 7-cell cavities, is designed to boost the electron energy from 200 keV to 5 MeV and permit 380 μ A - 1.0 mA beam current. The 2-cell cavity is a new design whereas the 7-cell cavity is refurbished from a previous low loss cavity for the JLab's Renaissance Cryomodule. The INJ CM adopts quite a few designs from the JLab 12 GeV Upgrade Cryomodule (C100), such as the cold mass is hung from a spaceframe structure by use of axial and transverse Nitronic rods, cavities to be tuned by scissor-jack style tuners and the end cans are actually modified from C100 style end cans. However, this new INJ CM is not a quarter of the C100 Cryomodule. This paper focuses on the major design features, fabrication and alignment process and testing of the module and its components.

WEPOB45 Compact Compton Light Source

K.E. Deitrick, J.R. Delaysen, G.A. Krafft (ODU) J.R. Delaysen, G.A. Krafft (JLab)

We present a compact Compton light source using an electron linear accelerator, which includes a low emittance superconducting radiofrequency quarter wave gun and double spoke cavities. Evaluation of this design is done by end-to-end simulation, producing results which make this design a strong choice for producing high flux, narrow-band X-ray beams.

WEPOB46 High Duty Cycle Inverse Compton Scattering X-Ray Source

A.Y. Murokh, R.B. Agustsson, T.J. Campese, A.G. Ovodenko (RadiaBeam) M. Babzien, M.G. Fedurin, I. Pogorelsky, M.N. Polyanskiy, T.V. Shafitan, C. Swinson (BNL) J.B. Rosenzweig, Y. Sakai (UCLA)

An important challenge in the development of practical X-ray sources based on Inverse Compton Scattering is the implementation of a reliable, increased-repetition-rate operation cycle. To this end, we report the first demonstration of an actively re-amplified CO₂ laser intra-cavity ICS source, which matches the electron linac pulse structure at 40 MHz repetition rate. Multi-bunch interaction with 5- and 15-pulse trains was demonstrated, and near linear photon yield gain from multi-pulse interaction was demonstrated. The system shows noticeably higher operational reliability than several contemporary single shot systems, as well as a great potential for future scalability.

- WEPOB47 Development of a Short Period Cryogenic Undulator at RadiaBeam**
F.H. O'Shea, R.B. Agustsson, Y.C. Chen, A. J. Palmowski, E. Spranza (RadiaBeam)
 RadiaBeam Technologies has developed a 7-mm period length cryogenic undulator prototype to test fabrications techniques in cryogenic undulator production. We present here our first prototype, the production techniques used to fabricate it, its magnetic performance at room temperature and the temperature uniformity after cool down.
- WEPOB48 THz and Sub-THz Capabilities of a Table-Top Radiation Source Driven by an RF Thermionic Electron Gun**
A.V. Smirnov, R.B. Agustsson, S. Boucher, T.J. Campese, Y.C. Chen, J.J. Hartzell, B.T. Jacobson, A.Y. Murokh, F.H. O'Shea, M. Ruelas, E. Spranza (RadiaBeam) W. Berg, J.C. Dooling, L. Erwin, R.R. Lindberg, S.J. Pasky, N. Sereno, Y.-E. Sun, A. Zholents (ANL)
 Design features and experimental results are presented for a sub-mm wave source [1] based on APS RF thermionic electron gun. The source upgrade to generate frequencies beyond 1 THz is discussed. The table-top layout consists of alpha-magnet, four quadrupoles, radiators, and a THz beamline. The Sub-THz radiator is composed of a planar, oversized structure with gratings. The THz radiator under construction uses a short-period undulator having about 1 T field amplitude, 20 cm length and integrated with a low-loss oversized waveguide. The radiators are integrated with a miniature horn antenna and a small $\sim 90^\circ$ -degree in-vacuum bending magnet. The electron beamline is designed to form different shapes including a flat beam interacting efficiently with the radiator. Holographic imaging of micro-structured objects is considered among the THz source applications. The experiment demonstrated a good potential of compact and robust, laser-free, table-top system for generation of a narrow bandwidth THz radiation. This setup can be considered as a prototype of a relatively compact, laser-free, THz-sub-THz source capable to operate in a long-pulse multi-bunch mode of operation.
- WEPOB49 LCLS Injector Laser Profile Shaping Using Digital Micromirror Device**
S. Li (Stanford University) S.C. Alverson, D.K. Bohler, A.R. Fry, S. Gilevich, Z. Huang, A. Miahnahri, D.F. Ratner, J. Robinson, F. Zhou (SLAC)
 In the Linear Coherent Light Source (LCLS) at SLAC, the injector laser plays an important role as the source of the electron beam for the Free Electron Laser (FEL). The emittance of the beam is highly related to the transverse shape of the injector laser. Currently the LCLS injector laser has hot spots that degrade the FEL performance. The goal of this project is to use adaptive optics to modulate the transverse shape of the injector laser, in order to produce a desired shape of electron beam. With a more controllable electron transverse profile, we can achieve lower emittance for the FEL, improve the FEL performance, and operation reliability. We use a digital micromirror device (DMD) to achieve the laser's transverse profile shaping. In this paper, we demonstrate the experiment set up to shape and transport the beam in the LCLS injector laser lab. We present testing results of the device damage threshold, pulse front tilt correction, and demonstration of beam shaping.
- WEPOB50 Emittance Measurements in 112 MHz Superconducting SRF Electron Gun with CsK2Sb Photo-Cathode**
K. Mihara (Stony Brook University) V. Litvinenko, I. Pinayev (BNL)
 The proof principle experiment to test a coherent electron cooling (CeC) is currently ongoing the commissioning phase. A 112 MHz superconducting radio frequency gun with CsK2Sb photocathode is generating CW electron beam with kinetic energy of 1.2 MeV and charges per bunch from 100 pC to 3 nC. In this paper we present experimental result of beam emittance measurement from our gun at various charges per bunch. We compare these measurements with simulations.
- WEPOB52 Synthesis and X-Ray Characterization of Sputtered Bi-Alkali Antimonide Photocathodes**
M. Gaowei, K. Attenkofer, J. Smedley, J. Walsh (BNL) H. Bhandari, M. S. J. Marshall (Radiation Monitoring Devices) Z. Ding, E.M. Muller, J. Sinsheimer (SBU) H.J. Frisch (Enrico Fermi Institute, University of Chicago) H.A. Padmore, S.G. Schubert (LBNL) J. Xie (ANL)
 Alkali antimonide photocathodes are appealing candidates for the next-generation photon sources, for it has been shown to have high quantum efficiency in green and low thermal emittance. Traditional sequential growth method of alkali antimonide photocathodes are optimized with QE performance. However, the inherently high roughness of these cathode materials will lead to a relatively high emittance of the emitted electrons. In this paper we report the results of the study on the growth and crystallography of sputter deposition of bi-alkali antimonide photocathodes from a K2CsSb sputter target, using in situ, in operando x-ray fluorescence spectroscopy, x-ray reflectivity and x-ray diffraction measurements. We found that the sputtered cathode material has sub nanometer roughness and an adequate green QE of over 3%.
- WEPOB53 Computation of Synchrotron Radiation**
D.A. Hidas (BNL)
 This presentation introduces a new open-source software development for the computation of radiation from charged particles and beams in magnetic and electric fields. The computations are valid in the near-field regime for both relativistic and non-relativistic scenarios. This project is being developed, and is currently in use, at Brookhaven National Laboratory's National Synchrotron Light Source II. Primary applications include, but are not limited to, the computation of spectra, photon flux densities, and power density distributions from undulators, wigglers, and bending magnets on arbitrary shaped surfaces in 3D making possible detailed study of sensitive accelerator and beam-line equipment. Application interfaces are available in Python, Mathematica, and C. Practical use cases are demonstrated and benchmarked. Additionally, future upgrades will be elaborated on.
- WEPOB54 DC Photogun Gun Test for RHIC Low Energy Electron Cooler (LEReC).**
D. Kayran, Z. Altinbas, D.R. Beavis, S. Bellavia, D. Bruno, M.R. Costanzo, A.V. Fedotov, D.M. Gassner, J. Halinski, K. Hamdi, J.P. Jamilkowski, J. Kewisch, C.J. Liaw, G.J. Mahler, T.A. Miller, S.K. Nayak, T. Rao, S. Seletskiy, B. Sheehy, J.E. Tuozzolo (BNL)
 Non-magnetized bunched electron cooling of low energy RHIC requires electron beam energy in range of 1.6-2.6 MeV, with average current at 30 mA, very small energy spread, and low emittance [1]. A 400kV DC gun equipped with photocathode and laser delivery system will serve as a source of high quality electron beam. Acceleration will be achieved by an SRF 704MHz booster cavity and other RF components that are scheduled to be operational in early 2018. The DC gun testing in its installed location in RHIC will start in early 2017. During this stage we plan to test the critical equipment in close to operation conditions: laser beam delivery system, cathode QE lifetime, DC gun, beam instrumentation, high power beam dump system, and controls. In this paper we describe the gun test set up, major components, and parameters to be achieved and measured during the gun beam test.
- WEPOB55 Simulation of Stray Electrons in the RHIC Low Energy Cooler**
J. Kewisch (BNL)

The Low Energy RHIC electron Cooler, under construction at BNL, accelerates electrons with a 400 kV DC gun and a 2.2 MeV SRF booster cavity. Electrons which leave the cathode at the wrong time will not be accelerated to the correct energies and will not reach the beam dump at the end of the accelerator. They may impact the beam pipe after incorrect deflection in dipoles or after being slowed down longitudinally in the booster while the transverse momentum is not affected. In some cases their direction is reversed in the booster and they will impact the cathode. We simulated the trajectories of these electrons using the GPT tracking code. The results are qualitative, not quantitative, since the sources and numbers of the stray electrons are unknown.

WEP0B56 Beam Optics for the RHIC Low Energy Electron Cooler (LEReC)

J. Kewisch, A.V. Fedotov, D. Kayran, S. Seletskiy (BNL)

A Low-energy RHIC Electron Cooler (LEReC) system is presently under construction at Brookhaven National Laboratory. This device shall enable gold ion collisions at energies below the design injection energy with sufficient luminosity. Electron beam with energies between 1.6, 2.0 and 2.6 MeV are necessary. This machine will be the first to attempt electron cooling using bunched electron beam, using a 703 MHz SRF cavity for acceleration. Special consideration must be given to the effect of space charge forces on the transverse and longitudinal beam quality. We will present the current layout of the cooler and beam parameter simulations using the computer codes PARMELA and GPT.

WEP0B57 Magnetic Optimization of Long EPU's at NSLS-II

C.A. Kitegi, P.L. Cappadoro, O.V. Chubar, H.C. Fernandes, D.A. Harder, D.A. Hidas, W. Licciardi, M. Musardo, J. Rank, C. Rhein, T. Tanabe (BNL)

At National Synchrotron Light Source II (NSLS-II), the production of high brilliant photon beams with adjustable polarization, in the VUV soft X-Ray range, is often achieved by means of Advanced Planar Polarized Light Emitter-II (APPLE-II) undulators. Following the request of two beamlines under construction, the Soft Inelastic X-ray scattering (SIX) and the Electron-Spectro-Microscopy (ESM), for a source providing circularly and vertically polarized radiation, a 3.5 m and 2.8m long APPLE-II type undulators were designed. The magnetic optimization of these long devices was performed NSLS-II. The magnetic and mechanical design of the two undulators is summarized and their achieved magnetic performances are reviewed.

WEP0B58 Cathode Puck Insertion System Design for the LEReC Photoemission DC Electron Gun

C.J. Liaw, V. De Monte, L. DeSanto, K. Hamdi, M. Mapes, T. Rao, A.N. Steszyn, J.E. Tuozzolo, J. Walsh (BNL) K.W. Smolenski (Cornell University (CLASSE), Cornell Laboratory for Accelerator-Based Sciences and Education)

The operation of LEReC is to provide an electron cooling to improve the luminosity of the RHIC heavy ion beam at lower energies in a range of 2.5-25 GeV/nucleon. The electron beam is generated in a DC Electron Gun (DC gun) designed and built by the Cornell High Energy Synchrotron Source Group. This DC gun will operate around the clock for at least two weeks without maintenance. This paper presents the design of a reliable cathode puck insertion system, which includes a multi-pucks storage device, a transfer mechanism, a puck insertion device, a vacuum/control system, and a transport scheme.

WEP0B59 Performance of CEC Pop Gun During Commissioning

I. Pinayev, W. Fu, Y. Hao, M. Harvey, T. Hayes, J.P. Jamilkowski, Y.C. Jing, P. K. Kankiya, D. Kayran, R. Kellermann, V. Litvinenko, G.J. Mahler, M. Mapes, K. Mernick, K. Mihara, T.A. Miller, G. Narayan, M.C. Paniccia, W.E. Pekrul, T. Rao, F. Severino, B. Sheehy, J. Skaritka, K.S. Smith, J.E. Tuozzolo, E. Wang, G. Wang, W. Xu, A. Zaltsman, Z. Zhao (BNL) I. Petrushina (SUNY SB)

The Coherent Electron Cooling Proof-of-Principle (CeC PoP) experiment employs a high-gradient CW photo-injector based on the superconducting RF cavity. Such guns operating at high accelerating gradients promise to revolutionize many sciences and applications. They can establish the basis for super-bright monochromatic X-ray and gamma ray sources, high luminosity hadron colliders, nuclear waste transmutation or a new generation of microchip production. In this paper we report on our operation of a superconducting RF electron gun with a high accelerating gradient at the CsK2Sb photo-cathode (i.e. ~ 20 MV/m) generating a record-high bunch charge (above 4 nC). We give short description of the system and then detail our experimental results.

WEP0B60 Commissioning of CeC PoP Accelerator

I. Pinayev, Z. Altinbas, J.C.B. Brutus, A.J. Curcio, A. Di Lieto, C. Folz, W. Fu, D.M. Gassner, Y. Hao, M. Harvey, T. Hayes, R.L. Hulsart, J.P. Jamilkowski, Y.C. Jing, P. K. Kankiya, D. Kayran, R. Kellermann, V. Litvinenko, G.J. Mahler, M. Mapes, K. Mernick, R.J. Michnoff, K. Mihara, T.A. Miller, G. Narayan, P. Orfin, D. Phillips, T. Rao, F. Severino, B. Sheehy, J. Skaritka, L. Smart, K.S. Smith, V. Soria, Z. Sorrell, R. Than, J.E. Tuozzolo, E. Wang, G. Wang, B. P. Xiao, W. Xu, A. Zaltsman, Z. Zhao (BNL) I. Petrushina (SUNY SB)

Coherent electron cooling is new cooling technique to be tested at BNL. Presently we are in the commissioning stage of the accelerator system. In this paper we present status of various systems and achieved beam parameters as well as operational experience. Near term future plans are also discussed.

WEP0B61 Magnetic Shielding of LEReC Cooling Section

S. Seletskiy, A.V. Fedotov, D.M. Gassner, D. Kayran, G.J. Mahler, W. Meng (BNL)

The transverse angle of the electron beam trajectory in the low energy RHIC Electron Cooling (LEReC) accelerator cooling section (CS) must be much smaller than 100 urad. This requirement sets 2.3 mG limit on the ambient transverse magnetic field. The maximum ambient field in the RHIC tunnel along the cooling section was measured to be 0.52 G. In this paper we discuss the design of the proposed LEReC CS magnetic shielding, which is capable of providing required attenuation.

WEP0B62 Absolute Energy Measurement of the LEReC Electron Beam

S. Seletskiy, M. Blaskiewicz, A.V. Fedotov, D. Kayran, J. Kewisch, T.A. Miller, P. Thieberger (BNL)

The goal of future operation of the low energy RHIC Electron Cooling (LEReC) accelerator is to cool the RHIC ion beams. To provide successful cooling, the velocities of the RHIC ion beam and the LEReC electron beam must be matched with E-4 accuracy. While the energy of ions will be known with the required accuracy, the e-beam energy can have an initial offset as large as 5%. The final setting of the e-beam energy will be performed by observing either the Schottky spectrum or the recombination signal from debunched ions co-traveling with the e-beam. Yet, to start observing such signals one has to set the absolute energy of the electron beam with an accuracy better than E-2, preferably better than $5 \cdot 10^{-3}$. In this paper we discuss how such accuracy can be reached by utilizing the LEReC 180 degree bend as a spectrometer.

WEP0B63 In Situ X-Ray Analysis of Thin-Film Photocathodes

J. Smedley (BNL)

The alkali antimonides are a novel class of semiconductors best known for photocathode applications in photomultipliers and

image intensifiers. While recipes exist to grow films with high quantum efficiency, these recipes are largely empirical, and result in films with very rough surfaces. In situ x-ray tools at NSLS and CHESS have enabled the development of ultrasmooth (sub nm) versions of these materials required for accelerator applications, with peak QE over 30%, and allowed new deposition methods to be investigated. In the future, these tools open the possibility of controlled doping and the creation of complex heterojunctions ' potentially leading to this class of materials becoming the next big thing in photovoltaics.

WEPOB64 **Precise Sextupole Magnets Alignment Using Vibrating Wire Technique and Beam Based Local Bump Method at NSLS-II**

G.M. Wang, A.K. Jain, T.V. Shafan, F.J. Willeke (BNL)

Modern synchrotron light source had very tight tolerances on magnet alignment to reach high performance. A new method, vibrating wire technique, was used in NSLS-II to reach magnet to magnet alignment specification, <30 μm . It is to align several magnets on a girder based on magnetic measurements in the lab. After tunnel installation, further survey and alignment relies on the girder, not individual magnet, by assuming that magnets relative to girder shift are neglectable. In this paper, we described a beam based sextupoles alignment using local bump method and compared the result with magnetic measurements. This will be helpful to verify the vibrating wire alignment result, track the long term drift and any unknown reasons caused magnet misalignment.

WEPOB65 **Experiments of Lossless Crossing - Resonance With Tune Modulation by Synchrotron Oscillations**

G.M. Wang, Y. Li, J. Rose, T.V. Shafan, V.V. Smaluk (BNL)

It had become a standard practice to constrain particle's tune footprint while designing the storage ring lattice so that the tunes fit between harmful resonances that limit ring dynamic aperture (DA). However, in recent ultra-bright light source design, the nonlinearities of storage ring lattices are much enhanced as compared with the 3rd generation light source one. It is becoming more and more difficult to keep the off-momentum tune footprint confined and even more, the solution cannot be found to confine off-energy tune footprint in certain cases. The questions have been asked whether crossing of a resonance stopband from off-momentum particle will necessarily lead to particle loss. In NSLS-II, we modified the lattice working point to mimic machine tune footprint crossing half integer with beam synchrotron oscillation excitation and demonstrated that beam can cross a resonance without loss with control of stopband width and high order chromaticity.

WEPOB66 **NSLS-II Post Mortem Function Development and Data Analysis of Beam Dump**

G.M. Wang (BNL)

The National Synchrotron Light Source II (NSLS-II) is a state of the art 3 GeV third generation light source at Brookhaven National Laboratory. The storage ring was commissioned in 2014 and transitioned to routine operations in the December of the same year. At this point the facility hosts 14 operating beam lines with beam current upto 250 mA. During beamline operation, various sources (protection system or subsystem malfunction) may cause beam dump. To identify the beam trip sources and improve the operation reliability, post mortem function was developed in NSLS-II to capture the sub-systems status and beam information prior and after beam dump, including RF system, power supply, BPMs and active interlock system. Most of the trip events have been identified and related source was improved. In this paper, we'll present the post mortem function and data application.

WEPOB67 **K2CsSb Photocathode Performance in QWR SRF Gun**

E. Wang, Y. Hao, Y.C. Jing, D. Kayran, V. Litvinenko, I. Pinayev, T. Rao, G. Wang (BNL) V. Litvinenko (Stony Brook University)

In 2016 run of Coherent Electron Cooling, we have successfully tested the performance of a number of K2CsSb cathodes. These cathodes with QE of 6%-10% were fabricated in Instrumentation Division, a few miles away, transported to RHIC tunnel under UHV conditions, attached to the CeC gun, kept in storage, and inserted in the gun as needed. A maximum bunch charge of 4.6 nC was generated in the gun when the QE was 1.8 %. With careful conditioning at increasing accelerating fields, it was possible to maintain the QE of several cathodes for more than a week. For the cathodes that experienced degradation, the primary cause was multipacting when the power into the gun was increased. In the initial runs, the entire 20 mm substrate face was coated with the cathode material causing cathode induced multipacting. For subsequent measurements, the substrate was masked to coat only the central 9 mm of the substrate. By optimizing the procedure for boosting the power to the gun and covering all viewports to minimize dark current, we were able to minimize QE degradation. In this paper we discuss the cathode preparation, transfer to the gun and operational experience with the cathodes in 112 MHz gun.

WEPOB68 **Optimization of Multi-Slit Design for LEReC Emittance Measurement**

C. Liu, A.V. Fedotov, J. Kewisch, M.G. Minty (BNL)

To improve the luminosity of beam energy scan of low energy Au-Au collision, a electron machine is under construction to cool ion beams in both RHIC rings with pulsed electron beam. Over the course of the project, a multi-slit device is needed to characterize the transverse beam emittance of three energies, 0.4, 1.6 and 2.6 MeV. This report shows the optimization and compromise of the design, which include the slit width, slit spacing, and drift space from the multi-slit to the downstream profile monitor.

WEPOB69 **Impedance Simulation for LEReC Booster Cavity Transformed from ERL Gun Cavity**

C. Liu (BNL)

Wake impedance induced energy spread is a concern for the electron beam to be used for electron cooling of the low energy ion beams in RHIC. The impedance simulation of the booster cavity for the Low Energy RHIC electron cooling (LEReC) project is presented in this report. The simulation is done for both non-relativistic and ultra-relativistic cases. The space charge impedance in the first case is discussed. For an impedance budget consideration of the electron machine only a simulation of the geometrical impedance in the latter case is necessary since space charge is considered separately.

WEPOB70 **Mechanical Straightening of the 3m Accelerating Structures at the Advanced Photon Source**

D.J. Bromberek, W.G. Jansma, T.L. Smith, G.J. Waldschmidt (ANL)

A project is underway at the Advanced Photon Source to mechanically straighten the thirteen 3 meter accelerating structures in the Linac in order to minimize transverse wakefield, and improve charge transport efficiency and beam quality. Flexure supports allow positioning of the structures in the X & Y directions. Mechanical design of the flexure support system, straightening techniques, mechanical measurement methods, and mechanical & RF results will be discussed.

THA1 — Oral Presentations (MC7)

Chair: S.A. Gourlay (LBNL)

THA1I001 **Progress in High Q SRF cavities development: from Single Cell to Cryomodule**08:30 ³⁰ **A. Grassellino** (*Fermilab*)

This talk will present the summary of the latest progress in nitrogen doping and magnetic flux reduction strategies, starting from the knowledge of the basic phenomena developed via single cell cavities studies in vertical and horizontal cryogenic dewars and via advanced surface studies of samples, to the implementation in an actual large scale cryomodule. Results of studies of the quality factors as a function of cooldown details though critical temperature for the first LCLS2 prototype cryomodule will be presented.

THA1I002 **Results of the 2015 Helium Processing of CEBAF Cryomodules**09:00 ³⁰ **M.A. Drury, F. Humphry, L.K. King, M.D. McCaughan, A.D. Solopova** (*JLab*)

The CEBAF accelerator at Jefferson Lab consists of an injector and two linacs connected by arcs. Each linac contains 25 cryomodules and are designed to deliver an integrated energy of 1.1 GeV per pass to an electron beam in order to meet 12 GeV energy requirements. Helium processing is a processing technique that is used to reduce field emission in SRF cavities. Helium processing of the 50 installed linac cryomodules was seen as necessary to meet the 12 GeV energy requirements. This paper will outline performance of the cryomodules as measured both before and after processing and the establishment of operating gradients following processing. Notice: Authored by Jefferson Science Associates, LLC under U.S. DOE Contract No. DE-AC05-06OR23177. The U.S. Government retains a non-exclusive, paid-up, irrevocable, world-wide license to publish or reproduce this manuscript for U.S. Government purposes.

THA1C003 **MAX IV and Solaris 1.5 GeV Storage Rings Magnet Block Production Series Measurement Results**09:30 ¹⁵ **M.A.G. Johansson** (*MAX IV Laboratory, Lund University*) **K. Karaś** (*Solaris National Synchrotron Radiation Centre, Jagiellonian University*) **R. Nietubýć** (*NCBJ*)

The magnet design of the MAX IV and Solaris 1.5 GeV storage rings replaces the conventional support girder + discrete magnets scheme of previous third-generation synchrotron radiation light sources with an integrated design having several consecutive magnet elements precision-machined out of a common solid iron block, with mechanical tolerances of ± 0.02 mm over the 4.5 m block length. The production series of 12+12 integrated magnet block units, which was totally outsourced to industry, was completed in the spring of 2015, with mechanical and magnetic QA conforming to specifications. This article presents mechanical and magnetic field measurement results of the full production series.

THA1C004 **Persistent Current Effect in 15-16 T Nb₃Sn Accelerator Dipoles and its Correction**09:45 ¹⁵ **A.V. Zlobin, V.V. Kashikhin** (*Fermilab*)

Coil magnetization effects in superconducting accelerator magnets degrade the magnet field quality and, thus, reduce the accelerator dynamic aperture, decrease the operation field range and complicate the field correction system. In a new generation of accelerator magnets based on the Nb₃Sn superconductor it is significantly larger than in traditional Nb-Ti magnets due to higher critical current density and larger superconductor filament size. Commercially produced Nb₃Sn composite wires provide the critical current density sufficient to increase the nominal operation field in accelerator magnets up to 15-16 T. Magnets with this level of nominal field are considered for the use in the LHC Energy Doubler and a future Very High Energy pp Collider. Analysis shows that due to larger coil volume the persistent current effect becomes even larger and, therefore, more important in 15-16 T Nb₃Sn dipoles. This paper presents the results of analysis of the coil magnetization effect in the 15 T Nb₃Sn dipole demonstrator being developed at Fermilab and describes different possibilities of its correction including coil geometry, iron shims and passive superconducting wires.

THA1C005 **Thermal Modeling and Cryogenic Design of a Helical Superconducting Undulator Cryostat**10:00 ¹⁵ **Y. Shiroyanagi, J.D. Fuerst, Q.B. Hasse, Y. Ivanyushenkov** (*ANL*)

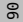
A conceptual design for a helical superconducting undulator (HSCU) for the Advanced Photon Source (APS) at Argonne National Laboratory (ANL) has been completed. The device differs sufficiently from the existing APS planar superconducting undulator (SCU) design to warrant development of a new cryostat based on value engineering and lessons learned from the existing planar SCU. Changes include optimization of the existing cryocooler-based refrigeration system and thermal shield as well as cost reduction through the use of standard vacuum hardware. The end result is a design that provides significantly larger 4.2 K refrigeration margin in a smaller package for greater installation flexibility in the APS storage ring. This paper presents ANSYS-based thermal analysis of the cryostat, including estimated static and dynamic (beam-induced) heating, and compares the new design with the existing planar SCU cryostat.

THA1C006 **Status of Development of Superconducting Undulators for Storage Rings and Free Electron Lasers at the Advanced Photon Source***10:15 ¹⁵ **Y. Ivanyushenkov, C.L. Doose, J.F. Fuerst, E. Gluskin, K.C. Harkay, Q.B. Hasse, M. Kasa, Y. Shiroyanagi, D. Skiadopoulos, E. Trakhtenberg** (*ANL*) **P. Emma** (*SLAC*)

Development of superconducting undulator (SCU) technology continues at the Advanced Photon Source (APS). Experience of building and successful operation of the first short-length, 16-mm period length superconducting undulator SCU0 paved a way for the second 1-m long, 18-mm period device, SCU1, which is in operation since May 2015. The APS SCU team has also built and tested a 1.5-m long, 21-mm period undulator as a part of LCLS SCU R&D program aiming at demonstration of SCU technology availability for free electron lasers. This undulator successfully achieved all the requirements including a phase error of 5 degree rms. Our team is currently completing one more 1-m, 18-mm period undulator that will replace the SCU0. We are also working on a helical SCU for the APS. The status of these projects will be presented.

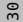
- THB1TU01

08:30



Risk Management of Complex Systems
J. Thomas (*MIT*)
Based on the US PAS class "Risk Management of Complex Systems" by John Thomas
- THB1I002

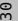
10:00



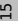
Lightweight Superconducting Magnet Technology for Medical Applications
S. Caspi (*LBNL*)
Lawrence Berkeley National Laboratory, the Paul Scherrer Institute, and Varian Particle Therapy, Inc. will develop light-weight superconducting magnet technology that will reduce the size and cost of particle beam delivery systems by nearly a factor of 10. Leveraging technologies and techniques developed for the magnets of the Large Hadron Collider, a prototype gantry bending magnet will be built and tested.

THA2 — Oral Presentations (MC7)**Chair:** A.V. Zlobin (Fermilab)**THA2I001 High Field SC Magnet Program in the US and Worldwide: Goals, Challenges, Plans**11:00  **S.A. Gourlay** (LBNL)


This talk will give an overview of the high field SC magnet program in the US and Worldwide. In particular, the goals, challenges and plans for SC magnet R&D for VHEPP, HE-LHC, SPPC, FCC-PP will be presented.

THA2I002 High Gradient Permanent Magnet Technology for Ultra-High Brightness Rings11:30  **G. Le Bec** (ESRF)


Permanent magnets have since long been major components in accelerator based light sources, particularly as part of insertion devices. However, their use as main lattice magnets (dipoles, quadrupoles) has been so far somewhat limited. The present trend towards small magnet apertures, exemplified by various multiband achromat designs currently under commissioning or design/construction opens up once more the discussion on the large scale use of permanent magnets as a means to achieve extremely high gradients in future diffraction limited storage rings. This talk will review the current R&D programs on the use of permanent magnets in the lattice of high brightness storage rings.

THA2C003 S-Band 1.4 Cell Photoinjector Design for High Brightness Beam Generation12:00  **E. Pirez**, **P. Musumeci** (UCLA) **D. Alesini** (INFN/LNF) **J.M. Maxson** (Cornell University)

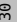
In this paper, we study in detail the design of a novel S-band radiofrequency photogun structure to maximize the accelerating field at the time of injection. This is a critical quantity for electron sources as it directly sets a limit of the maximum brightness achievable. The proposed design is based on a modification of the latest generation of S-band RF photoinjectors including novel fabrication approaches. The gun is designed to operate at a 120MV/m gradient and at an optimal injection phase of 70 degrees providing the beam quality required to enable novel electron beam applications such as single shot time-resolved transmission electron microscopy and ultrafast electron nanodiffraction.

THA2C004 Bench Measurement of a Multifrequency Cavity of the Ultra-fast RF Kicker for ERL Circular Cooler Ring of JLEIC12:15  **Y.L. Huang** (IMP/CAS) **R.A. Rimmer**, **H. Wang**, **S. Wang** (JLab)

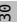
An ultra-fast kicker system is being developed for the ERL based electron Circular Cooler Ring (CCR) in the proposed Jefferson Lab Electron Ion Collider (JLEIC, previously named MEIC). In the CCR, the injected electron bunches can be recirculating and performing cooling for 10^{-30} turns before the extraction, thus reducing the ERL beam current to 1/10 - 1/30 (150mA - 50mA) of the cooling beam current (up to 1.5A). Assuming a bunch repetition rate of 476.3MHz and a recirculating factor of 10 in the CCR, the kicker is required to operate at a pulse repetition rate of 47.63MHz with pulse width of around 2ns, so that only every 10th bunch in the CCR will experience the transverse kick while the rest of the bunches won't be disturbed. Such a kicker pulse can be synthesized by 10 harmonic modes of the 47.63MHz kicker pulse repetition frequency, using four quarter wavelength resonator based deflecting cavities. A prototype cavity which could excite 5 odd modes simultaneously was fabricated with copper, and a 3-D bead pull system was built. Bench measurement for the kick scheme, electric center, stub tuner and multipole field was done on the prototype cavity.

THB2 — Oral Presentations (MC8)**Chair:** P.N. Ratoff (Lancaster University)**THB2I001 Applications of High-Power Accelerators to Cargo Inspection****11:00**  **S.E. Korbly** (*Passport Systems Inc*)

High-power accelerators and new radiation detection technologies are being brought together to advance the state of the art in cargo inspection at the nation's ports. This presentation will discuss recent developments in the use of high-power accelerators, both normal-conducting and superconducting, to build effective, non-intrusive, cargo inspection facilities.

THB2I002 Production of Medical Isotopes With Electron Linacs**11:30**  **D.A. Rotsch** (*ANL*)

Radioisotopes play important roles in numerous areas ranging from medical treatments to national security and basic research. Radionuclide production technology for medical applications has been pursued since the early 1900s both commercially and in nuclear science centers. Many medical isotopes are now in routine production and are used in day-to-day medical procedures. Despite these advancements, research is accelerating around the world to improve the existing production methodologies as well as to develop novel radionuclides for new medical applications. Electron linear accelerators (linacs) are unique sources of radioisotopes. Even though the basic technology has been around for decades, only recently have electron linacs capable of producing photons with sufficient energy and flux for radioisotope production become available. Housed in Argonne National Laboratory's building 211 is a newly upgraded 50 MeV/30-kW electron linear accelerator, capable of producing a wide range of radioisotopes. This talk will focus on the work being performed for the production of the medical isotopes ⁹⁹Mo (⁹⁹Mo/^{99m}Tc generator), ⁶⁷Cu, and ⁴⁷Sc.

THB2I003 Fulfilling the Mission of Brookhaven ATF as a DOE's Flagship User Facility in Accelerator Stewardship**12:00**  **I. Pogorelsky, I. Ben-Zvi, M.A. Palmer** (*BNL*)

25 years ago, Brookhaven Accelerator Test Facility (ATF), sponsored by the U.S. Department of Energy's (DOE's) Office of High-Energy Physics (HEP), pioneered a concept of a proposal-driven user facility for advanced accelerator research using lasers and electron beams. Since then, the ATF became an internationally recognized destination for researchers to benefit from free access to unique equipment not affordable otherwise to individual institutions and businesses. We will show by examples how collaborative user research achieves high productivity when supported by the ATF's capabilities. Researchers from academia, industry and national laboratories coming to ATF successfully investigate wide range of topics. Recently endorsed as an Office of Science National User Facility and a flagship in Accelerator Stewardship, ATF continues broadening its user community. DOE is now planning a considerable expansion of the ATF's capabilities via simultaneously upgrading the parameters of the e-beam and laser.

THPOA02 Nonlinear Stability in the Transport of Intense Bunched Beams**R. Pakter**, F.B. Rizzato, T.M.C. da Silva (IF-UFRGS)

In this work, we investigate the envelope dynamics for an intense bunched beam. While the linear stability analysis shows the absence of effective coupling between longitudinal and transverse evolutions, when we consider finite mismatches the system may become unstable. In such cases, we see a large energy exchange between these degrees-of-freedom. We construct stability maps showing the parameter regions where the system is unstable and investigate the dynamical features that lead to the instability. The theoretical results are compared to self-consistent simulations.

THPOA04 Maximum Brightness of Linac-Driven Electron Beams in the Presence of Collective Effects**S. Di Mitri** (Elettra-Sincrotrone Trieste S.C.p.A.)

Linear accelerators capable of delivering high brightness electron beams are essential components of a number of research tools, such as free electron lasers (FELs) and elementary particle colliders. In these facilities the charge density is high enough to drive undesirable collective effects (wakefields) that may increase the beam emittance relative to the injection level, eventually degrading the nominal brightness. We formulate a limit on the final electron beam brightness, imposed by the interplay of geometric transverse wakefield in accelerating structures and coherent synchrotron radiation in energy dispersive regions*. Numerous experimental data of VUV and X-ray FEL drivers validate our model. This is then used to show that a normalized brightness of 10^{16} A/m², promised so far by ultra-low charge beams (1-10 pC), can in fact be reached with a 100 pC charge beam in the Italian FERMI FEL linac, with the existing machine configuration.**

THPOA05 Intra-Beam Scattering in High Brightness Electron Linacs**S. Di Mitri** (Elettra-Sincrotrone Trieste S.C.p.A.)

The role played by Intra-Beam Scattering (IBS) in high brightness electron linacs, like those driving free electron lasers, is studied analytically and with particle tracking. We found that IBS typically plays no significant role in the microbunching instability that develops in such accelerators*. A partial damping of the instability through IBS is envisaged, however, with dedicated magnetic insertions. The feasibility of linear and circular lattice designs to cumulate relevant IBS-induced energy spread, and the interplay with microbunching instability, are discussed theoretically, and with the help of tracking codes.

THPOA06 CSR-Immune Arc Compressors for Recirculating Accelerators Driving High Brightness Electron Beams**S. Di Mitri**, M. Cornacchia (Elettra-Sincrotrone Trieste S.C.p.A.)

The advent of short electron bunches in high brightness linear accelerators has raised the awareness of the accelerator community to the degradation of the beam transverse emittance by coherent synchrotron radiation (CSR) emitted in magnetic bunch length compressors, transfer lines and turnaround arcs. We reformulate the concept of CSR-driven beam optics balance, and apply it to the general case of varying bunch length in an achromatic cell*. The dependence of the CSR-perturbed emittance to beam optics, mean energy, and bunch charge is shown. The analytical findings are compared with particle tracking results**. Practical considerations on CSR-induced energy loss and nonlinear particle dynamics are included. As a result, we identify the range of parameters that allows feasibility of an arc compressor in a recirculating accelerator driving, for example, a free electron laser or a linear collider.

THPOA07 Probabilistic Estimation of Low Energy Electron Trapping in Quadrupoles.**K.G. Sonnad** (KEK), J.A. Crittenden (Cornell University (CLASSE), Cornell Laboratory for Accelerator-Based Sciences and Education)

Electron cloud formation in quadrupoles is important for storage rings because they have the potential of being trapped for a time period that exceeds the revolution period of the beam. This can result in a turn by turn build up of cloud, that could potentially interfere with beam motion. The mechanism of electron trapping can be understood based on dynamics associated with the motion of an isolated charged particle in a magnetic field. In such a system, energy is conserved and so is the magnetic moment of the gyrating electron which is an adiabatic invariant. This leads to determination of a so called loss cone in velocity space. Using these principles we describe a method to estimate the probability distribution of trapping across the cross-section of a quadrupole for a given field gradient and electron energy. Such an estimate can serve as a precursor to more detailed numerical studies of electron cloud build and trapping in quadrupoles.

THPOA08 Transformer Ratio Enhancement Experiment Based on Emittance Exchanger in Argonne Wakefield Accelerator**Q. Gao**, H.B. Chen, J. Shi (TUB) S.P. Antipov, W. Gai, C.-J. Jing, J.G. Power (ANL) S.P. Antipov, C.-J. Jing (Euclid Beamlabs LLC) C.-J. Jing (Euclid TechLabs, LLC)

The transformer ratio is an important property in colinear wakefield acceleration, it indicates the efficiency of energy transferring from drive bunch to witness bunch. For the gaussian bunch, this ratio has its limit as 2. To obtain higher transformer ratio, we need bunch with specific longitudinal shape. One of that technique is emittance exchange, which has been demonstrated in Argonne Wakefield Accelerator. Now we optimize the beamline and mask in order to generate a triangular beam with quadratic head, which has theoretically transformer ratio as 9.4. An experiment to prove this high transformer ratio has been designed in Argonne Wakefield Accelerator laboratory.

THPOA10 Quantum Mechanics of Beam Optics**S.A. Khan** (CAAS)

Charged-particle optics, or the theory of transport of charged-particle beams through electromagnetic systems, is traditionally dealt with using classical mechanics. Though the classical treatment has been very successful, in designing and working of numerous charged-particle optical devices, it is natural to look for a prescription based on the quantum theory, since any system is quantum mechanical at the fundamental level. With this motivation the quantum theory of charged-particle beam optics, is being developed by Jagannathan et al. The quantum theory gives rise to interesting additional contributions to the classical paraxial and aberrating behaviour. In the classical limit the quantum formalism reproduces the well-known Lie algebraic formalism. This formalism is further applied to the study of the spin-dynamics of a Dirac particle with anomalous magnetic moment being transported through magnetic optical element. This naturally leads to a unified treatment of both the orbital (the Lorentz and Stern-Gerlach forces) and the spin (Thomas-Bargmann-Michel-Telegdi equation) motions.

- THPOA11 Quantum Methods in Light Beam Optics**
S.A. Khan (CAAS)
 A unified treatment of light beam optics and polarization, using the standard mathematical machinery of quantum mechanics is presented. Dirac-like form of the Maxwell equations is well known in literature. Starting with the Dirac-like form of the Maxwell's equations a unified treatment of light beam optics and polarization has been obtained. The traditional results (including aberrations) of the scalar optics are modified by the wavelength-dependent contributions. Some of the well-known results in polarization studies are realized as the leading-order limit of a more general framework of our formalism.
- THPOA12 Need to Create International Synchrotron Radiation Facilities**
S.A. Khan (CAAS)
 We address the theme of international collaborations based on accelerator sciences, citing examples of the European institutions and their large-scale science projects. The proposal for International Synchrotron Radiation Facilities (ISRF) is presented, in some detail along with the technological feasibility and importantly the financial viability. Such facilities when created shall meet the synchrotron radiation requirements of the participating countries.
- THPOA13 Modeling of Dipole and Quadrupole Fringe-Field Effects for the Advanced Photon Source Upgrade Lattice**
M. Borland (ANL)
 The proposed upgrade of the Advanced Photon Source (APS) to a multibend-achromat lattice requires shorter and much stronger quadrupole magnets than are present in the existing ring. This results in longitudinal gradient profiles that differ significantly from a hard-edge model. Additionally, the lattice assumes the use of five-segment longitudinal gradient dipoles. Under these circumstances, the effects of fringe fields and detailed field distributions are of interest. We evaluated the effect of soft-edge fringe fields on the linear optics and chromaticity, finding that compensation for these effects is readily accomplished. In addition, we evaluated the reliability of standard methods of simulating hard-edge nonlinear fringe effects in quadrupoles.
- THPOA14 Ion Effects in the APS Particle Accumulator Ring**
J.R. Calvey, J.A. Carter, K.C. Harkay, C. Yao (ANL)
 Trapped ions in the APS Particle Accumulator Ring (PAR) lead to a positive coherent tune shift in both planes, which increases along the PAR cycle as more ions accumulate. This effect has been studied using an ion simulation code developed at SLAC. After modifying the code to include a realistic vacuum profile, multiple ionization, and the effect of shaking the beam to measure the tune, the simulation agrees well with our measurements. This code has also been used to evaluate the possibility of ion instabilities at the high bunch charge needed for the APS-Upgrade.
- THPOA15 Adaptive Space Charge Calculations in MADX-SC**
Y.I. Alexahin, V.V. Kapin (Fermilab) **F. Schmidt, R. Wasef** (CERN)
 Since a few years MAD-X allows to simulate beam dynamics with frozen space charge à la Bassetti-Erskine. The limitation of simulation with a fixed distribution is somewhat overcome by an adaptive approach that consists of updating the emittances once per turn and by recalculating the Twiss parameters after certain intervals, typically every 1,000 turns to avoid an excessive slowdown of the simulations. The technique has been benchmarked for the PS machines over 800,000 turns. MADX-SC code developments are being discussed that include the re-introduction of acceleration into MAD-X and more advanced beam sigma calculations that will avoid code interruptions for the Twiss parameters calculation.
- THPOA16 Gaseous H₂-Filled Helical FOFO Snake for Initial 6D Ionization Cooling of Muons**
Y.I. Alexahin (Fermilab)
 H₂ gas-filled channel for 6D ionization cooling of muons is described which consists of periodically inclined solenoids of alternating polarity with 325MHz RF cavities inside them. To provide sufficient longitudinal cooling LiH wedge absorbers are placed at the minima of transverse beta-function between the solenoids. An important feature of such channel (called Helical FOFO snake) is that it can cool simultaneously muons of both signs. Theoretical considerations as well as results of simulations with G4beamline are presented.
- THPOA17 Computing Eigen-Emittances from Tracking Data**
Y.I. Alexahin (Fermilab)
 In a strongly nonlinear system the particle distribution in the phase space may develop long tails which contribution to the covariance (sigma) matrix should be suppressed for a correct estimate of the beam emittance. A method is offered based on Gaussian approximation of the original particle distribution in the phase space (Klimontovich distribution) which leads to an equation for the sigma matrix which provides efficient suppression of the tails and cannot be obtained by introducing weights. This equation is easily solved by iterations in the multi-dimensional case. It is also shown how the eigen-emittances and coupled optics functions can be retrieved from the sigma matrix in a strongly coupled system.
- THPOA18 Simulating Batch-on-Batch Slip-Stacking in the Fermilab Recycler Using a New Multiple Interacting Bunch Capability in Synergia**
E.G. Stern, J.F. Amundson, Q. Lu (Fermilab)
 The Recycler is an 8 GeV/c proton storage ring at Fermilab. To achieve the 700 MW beam power goals for the NOvA neutrino oscillation experiment, the Recycler accumulates 12 batches of 80-bunch trains from the Booster using slip-stacking. One set of bunch trains are injected into the ring and decelerated, then a second set is injected at the nominal momentum. The trains slip past each other longitudinally due to their momenta difference. We have recently extended the multi-bunch portion of the Synergia beam simulation program to allow co-propagation of bunch trains at different momenta. In doing so, we have expanded the applicability of the massively parallel multi-bunch physics portion of Synergia to include new categories of bunch-bunch interactions. We present results from our first application of these capabilities to batch-on-batch slip stacking in the Recycler.
- THPOA19 Lattice Optimization for Proposed Fermilab Integrable RCS**
J.S. Eldred, A. Valishev (Fermilab)
 Integrable optics is an innovation in particle accelerator design that provides strong nonlinear focusing while avoiding parametric resonances. One promising application of integrable optics is to overcome the traditional limits on accelerator intensity imposed by betatron tune-spread and collective instabilities. The efficacy of high-intensity integrable accelerators will be undergo comprehensive testing over the next several years at the Fermilab Integrable Optics Test Accelerator (IOTA) and the University of Maryland Electron Ring (UMER). We propose an integrable RCS (iRCS) as a replacement for the Fermilab Booster to achieve multi-MW beam power for the Fermilab high-energy neutrino program. We provide an overview of the machine parameters and discuss an approach

to lattice optimization. Integrable optics requires arcs with integer- π phase advance followed by drifts with matched beta functions. We provide an example integrable lattice with features of a modern RCS - long dispersion-free drifts, low momentum compaction, superperiodicity, chromaticity correction with harmonic sextupoles, separate-function magnets, and bounded beta functions.

THPOA20 Simulation of Multipacting with Space Charge Effect in PIP-II 650 MHz Cavities

G.V. Romanov (Fermilab)

The central element of the Proton Improvement Plan -II at Fermilab is a new 800 MeV superconducting linac, injecting into the existing Booster. Multipacting affects superconducting RF cavities in the entire range from high energy elliptical cavities to coaxial resonators for low-beta part of the linac. The extensive simulations of multipacting in the cavities with updated material properties and comparison of the results with experimental data are routinely performed during electromagnetic design at Fermilab. This work is focused on multipacting study in the low-beta and high-beta 650 MHz elliptical cavities. The new advanced computing capabilities made it possible to take the space charge effect into account in this study. The results of the simulations and new features of multipacting due to the space charge effect are discussed.

THPOA21 Multipacting in HOM Coupler of LCLS-2 1.3 GHz SC Cavity

G.V. Romanov, T.N. Khabiboulline, A. Lunin (Fermilab)

During high power tests of the 1.3 GHz LCLS-2 cavity on the test stand at Fermilab an anomalous rise of temperature of the pickup antenna in the higher order mode (HOM) couplers was detected in accelerating gradient range of 5-10 MV/m. It was suggested that the multipacting in the HOM coupler may be a cause of this temperature rise. In this work the suggestion was studied, and the conditions and the location, where multipacting can develop, were found.

THPOA22 Linear Lattice and Trajectory Reconstruction and Correction at FAST Linear Accelerator

A.L. Romanov, D.R. Edstrom (Fermilab) **A. Halavanau** (Northern Illinois University)

Low energy part of FAST linear accelerator based on 1.3 GHz superconducting RF cavities was successfully commissioned. During commissioning, beam based model dependent methods were used to correct linear lattice and trajectory. Lattice correction algorithm is based on analysis of beam shape from profile monitors and trajectory responses to dipole correctors. Trajectory responses to field gradient variations in quadrupoles and phase variations in superconducting RF cavities were used to correct bunch offsets in quadrupoles and accelerating cavities relative to its magnetic axes. Details of used methods and experimental results are presented.

THPOA23 Adaptive Matching of the IOTA Ring Linear Optics for Space Charge Compensation

A.L. Romanov, A. Valishev (Fermilab) **D.L. Bruhwiler, N.M. Cook, C.C. Hall** (RadiaSoft LLC)

Many present and future accelerators must operate with high intensity beams when distortions induced by space charge forces are among major limiting factors. Betatron tune depression of above approximately 0.1 per cell leads to significant distortions of linear optics. Many aspects of machine operation depend on proper relations between lattice functions and phase advances, and can be improved with proper treatment of space charge effects. We implement an adaptive algorithm for linear lattice re-matching with full account of space charge in the linear approximation for the case of Fermilab's IOTA ring. The method is based on a search for initial second moments that give closed solution and, at the same time, satisfy predefined set of goals for emittances, beta functions, dispersions and phase advances at and between points of interest. Iterative singular value decomposition based technique is used to search for optimum by varying wide array of model parameters.

THPOA24 Testing of Advanced Technique for Linear Lattice and Closed Orbit Correction by Modeling Its Application for IOTA Ring at Fermilab

A.L. Romanov (Fermilab)

Many modern and most future accelerators rely on precise configuration of lattice and trajectory. Integrable Optics Test Accelerator (IOTA) at Fermilab that is coming to final stages of construction will be used to test advanced approaches of control over particles dynamics. Various experiments planned at IOTA require high flexibility of lattice configuration as well as high precision of lattice and closed orbit control. Dense element placement does not allow to have ideal configuration of diagnostics and correctors for all planned experiments. To overcome this limitations advanced method of lattice analysis is proposed that can also be beneficial for other machines. Developed algorithm is based on LOCO approach, extended with various sets of other experimental data, such as dispersion, BPM-to-BPM phase advances, beam shape information from synchrotron light monitors, responses of closed orbit bumps to variations of focusing elements and other. Extensive modeling of corrections for a big number of random seed errors is used to illustrate benefits from developed approach.

THPOA25 Effect of Higher Order Terms in Particle Transport Through Combined Function Sector Magnets

E.G. Stern, J.F. Amundson, K.E. Badgley, T. Zolkin (Fermilab)

The simulation of particle transport through combined function sector magnets in widely used programs such as MAD-X/PTC follows calculations described in Brown* and Iselin**. These papers integrate the equations of motion through the magnetic elements using a magnetic potential that satisfies Laplace equations only to second order. We evaluate the effect of the approximation using symplectic integration and exact field solutions in the Synergia accelerator simulation program. The magnetic field in the vicinity of the particle trajectory may be expanded in polynomials of powers of x/R and y/R where R is the bend radius of the element. The effect of truncating the magnetic field series would be expected to be enhanced for small radius rings such as the CERN PS Booster. Lattice properties that depend only on first order derivatives such as particle tunes are insensitive to this approximation but second order quantities such as chromaticity show differences exceeding 5% between the approximate and exact field solutions calculations in the PS Booster.

THPOA27 Triggers and Mitigation Strategies of Systematic Errors for the Muon g-2 Experiment at Fermilab

D. Stratakis, M.E. Convery, J.P. Morgan, M.J. Syphers, J.C.T. Thangaraj (Fermilab) **J.D. Crnkovic, W. Morse** (BNL) **M.J. Syphers** (Northern Illinois University)

The Muon g-2 experiment at Fermilab aims to measure the anomalous magnetic moment of the muon to a precision of 140 ppb $|-|$ a fourfold improvement over the 540 ppb precision obtained in BNL experiment E821. Obtaining this precision requires controlling total systematic errors at the 100 ppb level. One form of systematic error on the measurement of the anomalous magnetic moment occurs when the muon beam injected and stored in the ring has a correlation between the muon's spin direction and its momentum. In this paper, we first analyze the creation and transport of muon polarization from the production target to the Muon g-2 storage ring. Then, we detail the spin-momentum and spin-orbit correlations and estimate their impact on the final measurement. Finally, we outline mitigation strategies that could potentially circumvent this problem.

- THPOA28 Limitations of Space Charge Algorithms for Bunched Beams**
A. Valishev, E. Prebys (Fermilab) D.L. Bruhwiler, N.M. Cook, C.C. Hall, R.A. Kishek, S.D. Webb (RadiaSoft LLC) C.E. Mitchell, G. Penn (BNL)
 Particle tracking simulations accounting for space-charge effects have become an important tool in studying the beam dynamics in high intensity accelerators. Owing to the complexity of algorithms and software systems it is important to understand their limitations in order to produce reliable predictions. We undertook a campaign of careful evaluation of several space-charge codes including Synergia, Warp, ImpactZ, and MADX for the case of bunched beam dynamics in the IOTA ring and present our findings.
- THPOA29 PIP-II Transfer Lines Design**
A. Vivoli (Fermilab)
 The U.S. Particle Physics Project Prioritization Panel (P5) report encouraged the realization of Fermilab's Proton Improvement Plan II (PIP-II) to support future neutrino programs in the United States. PIP-II aims at enhancing the capabilities of the Fermilab existing accelerator complex while simultaneously providing a flexible platform for its future upgrades. The central part of PIP-II project is the construction of a new 800 MeV H^- Superconducting (SC) Linac together with upgrades of the Booster and Main Injector synchrotrons. New transfer lines will also be needed to deliver beam to the downstream accelerators and facilities. In this paper we present the recent development of the design of the transfer lines discussing the principles that guided their design, the constraints and requirements imposed by the existing accelerator complex and the following modifications implemented to comply with a better understanding of the limitations and further requirements that emerged during the development of the project.
- THPOA30 SCHARGEV 1.0 - Strong Space Charge Vlasov Solver**
T. Zolkin, A.V. Burov (Fermilab)
 The space charge (SC) is known to be one of the major limitations for the collective transverse beam stability. When SC is strong (i.e. space charge tune shift \gg synchrotron tune) the problem allows an exact analytical solution. For that practically important case we present a fast and effective Vlasov solver SCHARGEV which calculates a complete eigensystem (spatial shapes of modes and bunch spectra) and therefore provides the growth rates and the thresholds of instabilities. SCHARGEV allows an inclusion of driving and detuning wake forces, coupled bunch motion, any feedback system and Landau damping. In this presentation we will consider a Gaussian bunch under the action of resistive wall wakes and damper. A numerical example for FermiLab Recycler Ring is given.
- THPOA31 Sector Magnets or Transverse Electromagnetic Fields in Cylindrical Coordinates**
T. Zolkin (Fermilab)
 Laplace's equation is considered for scalar and vector potentials describing electric or magnetic fields in cylindrical coordinates, with invariance along the azimuthal coordinate. A series of special functions are found which, when expanded to lowest order in power series in radial and vertical coordinates, replicate harmonic polynomials in two variables. These functions are based on radial harmonics found by Edwin~M.~McMillan forty years ago. In addition to McMillan's harmonics, a second family of radial harmonics is introduced to provide a symmetric description between electric and magnetic fields and to describe fields and potentials in terms of the same functions. Formulas are provided which relate any transverse fields specified by the coefficients in the power series expansion in radial or vertical planes in cylindrical coordinates with the set of new functions. This result is important for potential theory and for theoretical study, design and proper modeling of sector dipoles, combined function dipoles and any general sector element for accelerator physics. All results are presented in connection with these problems. A numerical example for CERN PS Ring is given.
- THPOA32 Sensitivity of the Microbunching Instability to Irregularities in Cathode Current in the LCLS-II Beam Delivery System**
C.E. Mitchell, J. Qiang, M. Venturini (BNL) P. Emma (SLAC)
 LCLS-II is a high-repetition rate (1 MHz) Free Electron Laser (FEL) X-ray light source now under construction at SLAC National Accelerator Laboratory. During transport to the FEL undulators, the electron beam is subject to a space charge-driven microbunching instability that can degrade the electron beam quality and lower the FEL performance if left uncontrolled. The present LCLS-II design is well-optimized to control the growth of this instability out of the electron beam shot noise. However, the instability may also be seeded by irregularities in the beam current profile at the cathode (due to non-uniformities in the temporal profile of the photogun drive laser pulse). In this paper, we describe the sensitivity of the microbunching instability to small-amplitude temporal modulations on the emitted beam current profile at the cathode, using high-resolution simulations of the LCLS-II beam delivery system.
- THPOA33 A Preliminary Beam Impedance Model of the Advanced Light Source Upgrade**
S. Persichelli, J.M. Byrd, S. De Santis, D. Li, T.H. Luo, M. Venturini, Y. Yang (BNL)
 The proposed upgrade of the Advanced Light Source (ALS-U) consists of a multibend achromat ultralow emittance lattice for the production of diffraction-limited soft x-rays. Vacuum chamber apertures of few millimeters are a key feature of low-emittance machines, especially for the insertion device straight sections, and can result in a significant increase in the beam impedance. The impedance may limit the peak current of individual bunches and can limit the total beam current. Although the vacuum chamber design is in an early stage, this paper presents a preliminary beam impedance budget using a combination of electromagnetic simulations, analytical calculations, and scaling of components from other light source projects. We include the impedance of cavities, kickers and vacuum instrumentation. We also estimated the resistive wall and space charge impedance in a multi-layered beam chamber, considering the effect of the NEG coating.
- THPOA34 Beam Coupling Impedance Studies for FCC-ee**
S. Persichelli (BNL) R. Kersevan, M. Migliorati (CERN) M. Migliorati (University of Rome "La Sapienza") M. Zobov (INFN/LNF)
 The goal of the Future Circular Collider Study (FCC) at CERN is to push the energy and intensity limits of particle accelerators, reaching collision energies of 100 TeV, in the search for new physics. The FCC-ee project, as part of the Future Circular Collider design project, is a high-luminosity, high-precision e^+e^- circular collider envisioned in a new 80-100 km tunnel in the Geneva area. It represents the first step towards the long-term goal of a 100 TeV proton-proton collider. This new accelerator complex represents a great challenge for R&D on beam dynamics. One very critical point in this context is represented by beam instabilities induced by the beam coupling impedance, limiting the maximum foreseen beam current and machine performances. It is therefore very important to be able to predict these effects and to study in details potential solutions to prevent them. In this paper the resistive wall and some other critical geometrical sources of beam coupling impedance for the FCC-ee accelerator are identified

and evaluated, and their impact on the beam dynamics is discussed. We are also presenting a preliminary impedance model of the machine.

THPOA35 Analysis of Microbunching Structures in Transverse and Longitudinal Phase Spaces

C.-Y. Tsai (Virginia Polytechnic Institute and State University) **R. Li** (JLab)

Microbunching instability (MBI) has been a challenging issue in high-brightness electron beam transport for modern accelerators. The existing Vlasov analysis of MBI is based on single-pass configuration*. For multi-pass recirculation or a long beamline, the intuitive argument of quantifying MBI, by successive multiplication of MBI gains, was found to underestimate the effect**. More thorough analyses based on concatenation of gain matrices aimed to combine both density and energy modulations for a general beamline**. Yet, quantification still focuses on characterizing longitudinal phase space; microbunching residing in (x,z) or (x',z) was observed in particle tracking simulation. Inclusion of such cross-plane microbunching structures in Vlasov analysis shall be a crucial step to systematically characterize MBI for a beamline complex in terms of concatenating individual beamline segments. We derived a semi-analytical formulation to include the microbunching structures in longitudinal and transverse phase spaces. Having numerically implemented the generalized formulae, an example lattice*** is studied and reasonable agreement achieved when compared with particle tracking simulation.

THPOA36 Efficient Multiphysics Accelerator Modeling on Advanced Hardware

J.R. Cary, **G.R. Werner** (CIPS) **B.M. Cowan**, **S.W. Sides** (Tech-X)

Computational Accelerator Physics (and computational science, more generally) has been facing the daunting task of supporting an increasing array of devices (multicore, many-core, GPU). Extracting performance now requires that code be adaptable to vector instructions (AVX and GPU), threading, and distributed memory parallelism. Each of these types of parallelism brings new requirements in many ways, including data layout, avoidance of race conditions, and computation ordering. Moreover, accessing parallelism on different devices is done differently, with possibly OpenMP or thread launches for off-cpu devices. Finally, in a multiphysics computation, like beam propagation with secondary electron emission, and collisional interactions, different parts of the calculation can make use of different types of parallelism. The present work describes developments that reduce the total code that one needs to write to support the variety of platforms and coding methodologies. The use of strip mining, separation of iteration from computation, and flexible data ordering are shown to assist in reducing the code that one must write and maintain.

THPOA37 Study of 2D CSR Effects in a Compression Chicane

C.C. Hall (RadiaSoft LLC) **S. Biedron**, **S.V. Milton** (CSU)

The study of coherent synchrotron radiation (CSR) has been an area of great interest because of its negative impact on FEL performance. The modeling of CSR is frequently performed using a 1D approximation*, as 2D and 3D models can become extremely computational intensive. While experimental evidence is lacking in this area most studies show reasonable agreement between 1D and 2D CSR models for beam parameters in existing accelerators. In this work we focus on 2D modeling of CSR in a four-dipole chicane lattice based on the Jefferson Lab FEL. Comparison is shown between several models and measurement for energy loss due to CSR in the chicane. While good agreement is generally observed we also present investigation of several key differences observed in simulation. In particular, showing how the 1D and 2D CSR models deviate in regards to CSR and beam interaction within the drift spaces of the chicane and the downstream drift at the chicane end.

THPOA38 Efficient Simulations of Energy Recovery Linacs With Multiple High-Order Modes

S.D. Webb, **D.T. Abell**, **N.M. Cook**, **C.C. Hall** (RadiaSoft LLC)

The full, self-consistent numerical simulation of beam energy recovery in linacs is presently a supercomputing problem. We present an efficient computational approach, based on a variational principle, to solving the self-consistent problem. The algorithm naturally includes an arbitrary number of high-order RF cavity modes, thus making possible the studies of many-mode dynamics. Its computational efficiency opens the perspective of running simulations on a single desktop computer.

THPOA39 Analytic Treatment of Collective Effects in Nonlinear Integrable Optics

S.D. Webb, **D.L. Bruhwiler**, **N.M. Cook**, **C.C. Hall** (RadiaSoft LLC)

Collective effects, such as transverse wake fields and space charge, can be detrimental to the nonlinear integrable optics. We present the effects of quadrupole wakes and space charge on the dynamics using a perturbative transfer map formalism. From this, we draw a number of design considerations for nonlinear optics rings.

THPOA40 Multi-Scale Modeling for Beam-Beam Depolarization

D.T. Abell, **I.V. Pogorelov** (Tech-X) **F. Méot**, **V.H. Ranjbar** (BNL)

Highly polarized beams are essential for efficient experiments designed to study the origin of nuclear spin. The beam-beam collision has the potential—through both direct and indirect effects—to cause significant depolarization. The two types of effects occur on very different scales. We present a new simulation capability that captures both these scales by linking a pair of complementary codes: gpuSpinTrack, which performs fast spin-orbit tracking in storage rings, and Vorpai, for self-consistent 3D simulations of the beam-beam interaction. We have recently extended Vorpai so that it can also track the spin degree of freedom. By coupling the inputs and outputs of these two codes, we now have a tool that enables scientists to study in detail the effect of multi-pass beam-beam collisions on the polarization of both beams in various designs for future electron-ion colliders. This presentation will describe the codes, their coupling, and some initial results.

THPOA41 Simulations of Hole Injection in Diamond Detectors

G.I. Bell, **D.A. Dimitrov**, **C.D. Zhou** (Tech-X) **I. Ben-Zvi**, **M. Gaowei**, **T. Rao**, **J. Smedley** (BNL) **E.M. Muller** (SBU)

We present simulations of a semiconductor beam detector using the code VSIM. The 3D simulations involve the movement and scattering of electrons and holes in the semiconductor, voltages which may be applied to external contacts, and self-consistent electrostatic fields inside the device. Electrons may experience a Schottky barrier when attempting to move from the semiconductor into a metal contact. The strong field near the contact, due to trapped electrons, can result in hole injection into the semiconductor due to transmission of electrons from the valence band of the semiconductor into the metal contact. Injected holes are transported in the applied field leading to current through the detector. We compare our simulation results with experimental results from a prototype diamond X-ray detector.

THPOA42 3D Modeling and Simulations of Electron Emission From Photocathodes With Controlled Rough Surfaces

D.A. Dimitrov, **G.I. Bell**, **D.N. Smithe**, **C.D. Zhou** (Tech-X) **I. Ben-Zvi**, **J. Smedley** (BNL) **S.S. Karkare**, **H.A. Padmore** (LBNL)

Developments in materials design and synthesis have resulted in photocathodes that can have a high quantum efficiency (QE),

operate at visible wavelengths, and are robust enough to operate in high electric field gradient photoguns, for application to free electron lasers and in dynamic electron microscopy and diffraction. However, synthesis often results in roughness, ranging from the nano to the microscale. The effect of this roughness in a high gradient accelerator is to produce a small transverse accelerating gradient, which therefore results in emittance growth. Although analytical formulations of the effects of roughness have been developed, a full theoretical model and experimental verification are lacking, and our work aims to bridge this gap. We report results on electron emission modeling and 3D simulations from photocathodes with controlled surface roughness similar to grating surfaces that have been fabricated by nanolithography. The simulations include both charge carrier dynamics in the photocathode material and a general electron emission modeling that includes field enhancement effects at rough surfaces. The models are being implemented in the VSim code.

THPOA43 **Algorithm for Mitigating Particle Integration Error in Highly-Relativistic Laser Plasma Simulations**

A.V. Higuera, D.T. Abell, J.R. Cary, B.M. Cowan (Tech-X) K.J. Weichman (The University of Texas at Austin)

In particle-in-cell simulations of laser wakefield accelerators driven by laser pulses with normalized vector potentials greater than unity, errors in particle trajectories produce incorrect beam charges and energies. In order to avoid these errors, the simulation time step must resolve a time scale smaller than the laser period by a factor of the normalized vector potential*. If the Yee algorithm is used to advance the fields with this time step, the laser wavelength must be over-resolved by a factor of the normalized vector potential. Here is presented a new electromagnetic integration algorithm that corrects the dispersion errors in the Yee algorithm for time steps obeying the Courant-Friedrichs-Lewy condition but otherwise arbitrary, reducing the computational requirements of simulations by a factor of the normalized vector potential.

THPOA44 **Single-Pass Cooling Simulations for the CeC Proof-of-Principle Experiment**

I.V. Pogorelov, G.I. Bell (Tech-X) V. Litvinenko, G. Wang (BNL) V. Litvinenko (Stony Brook University)

Efficient cooling of ion beams is a key challenge in achieving high luminosity required by the next generation of electron-ion and hadron-hadron colliders. Coherent electron cooling (CeC) is a novel technique that promises to significantly boost the efficiency of cooling high-intensity proton beams at 100 GeV and above. We present and discuss the results of single-pass simulations for the parameters of the CeC Proof-of-Principle Experiment at RHIC. Modeling the three-stage CeC cooler requires careful coupling of the 6D phase space distribution from the Vorpil simulations of the modulator into the GENESIS simulations of the FEL amplifier, with the e-beam distribution out of the amplifier fed into the Vorpil EM PIC simulations of the kicker section to determine the net energy kick on the ion. In particular, we discuss the advantages of the novel "perturbative trajectory" approach compared to the delta-f PIC Vorpil simulation previously used for modeling the CeC modulator.

THPOA45 **Update of the SEY Measurement at Fermilab Main Injector**

Y. Ji (IIT)

The studies of in-situ Secondary electron yield (SEY) measurement at Main Injector started at 2013. These studies aimed at understand how the conditioning of different materials evolve at Main Injector. The engineering run was finished at 2014. From 2014 to 2016 the Fermilab accelerator intensity has increased from $24 \cdot 10^{12}$ Protons to $42 \cdot 10^{12}$ Protons. The conditioning effect of SS116L and TiN coated SS116L have been observed during such period. A on going process of improving the data acquisition procedure and hardware has been performed. A deconditioning process was observed during the accelerator annual shut down at 2016.

THPOA46 **Benchmark of RF Photoinjector and Beamline in OPAL-T and GPT**

N.R. Neveu (IIT) G. Ha (POSTECH) G. Ha, J.G. Power (ANL)

Accurate simulations of RF photoinjector beamlines is critical to many modern accelerator applications, including SASE FEL light sources and advanced accelerator concepts such as two beam acceleration. These beamlines typically start with an RF photocathode gun and are followed by accelerating structures, bunch compressors, and a variety of magnets. Accurate beam dynamics simulations must include single particle effects (e.g. time step) as well as collective effects such as space charge, wakefields, and coherent synchrotron radiation (CSR). Using portions of the Argonne Wakefield Accelerator as the benchmark model, we simulated beam dynamics using OPAL-T, and GPT for several charge values between 0.1nC and 100nC. In this paper, we present the results, and discuss the similarities or differences between the codes in each case.

THPOA47 **Impedance Measurement of the Vacuum Chamber Components for the Advance Photon Source (APS) Upgrade**

M.P. Sangroula, C.U. Segre (IIT) R.R. Lindberg (ANL)

The Advanced Photon Source (APS) at Argonne National Lab has proposed an upgrade to a multi-bend achromat (MBA) that would improve the x-ray brightness by two to three orders of magnitude. One of the main design challenges of the upgrade is to minimize rf heating and collective instabilities associated with the impedance of the small-aperture vacuum components. As part of this effort, my research focuses on impedance measurement and simulation of various MBA vacuum components. Here, we present our planned measurement technique with some preliminary simulation and measurement results.

THPOA48 **Model of Electron Cloud Instability in Fermilab Recycler**

S. A. Antipov (University of Chicago) A.V. Burov, S. Nagaitsev (Fermilab)

An electron cloud instability might limit the intensity in the Fermilab Recycler after the PIP-II upgrade. A multibunch instability typically develops in the horizontal plane within a hundred turns and, in certain conditions, leads to beam loss. Recent studies have indicated that the instability is caused by an electron cloud, trapped in the Recycler index dipole magnets. We developed an analytical model of an electron cloud driven instability with the electrons trapped in combined function dipoles. The resulting instability growth rate of about 30 revolutions is consistent with experimental observations and qualitatively agrees with the simulation in the PEI code. The model allows an estimation of the instability rate for the future in-tensity upgrades.

THPOA49 **Electron Cloud Trapping in Recycler Combined Function Dipole Magnets**


S. A. Antipov (University of Chicago) S. Nagaitsev (Fermilab)

Electron cloud can lead to a fast instability in intense proton and positron beams in circular accelerators. In the Fermilab Recycler the electron cloud is confined within its combined function magnets. We show that combined function magnets trap the electron cloud with their magnetic field, present the results of analytical estimates of trapping, and compare them to numerical simulations of electron cloud formation. The electron cloud in a combined function magnet is located at the beam center and up to 1% of the particles can be trapped by its magnetic field. Since the process of electron cloud build-up is exponential, once trapped this amount of electrons significantly increases the density of the cloud on the next revolution. In a Recycler combined function dipole this multi-turn accumulations allows the electron cloud reaching final intensities orders of magnitude greater than in a pure dipole. The multi-turn build-up can be stopped by injection of a single clearing bunch of $1 \cdot 10^{10}$ p at any position in the ring.

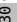
- THPOA50 Development of an Optical Cavity for LCS Sources at the Compact ERL**
T. Akagi, S. Araki, Y. Honda, A. Kosuge, N. Terunuma, J. Urakawa (KEK) R. Hajima, M. Mori, R. Nagai, T. Shizuma (QST)
 High-energy photons from the laser Compton scattering (LCS) sources are expected to be applied in various fields in a wide range photon energies from keV to GeV. High-flux and narrow-bandwidth LCS photon beam is realized in an energy recovery linac (ERL). An electron beam of high-average current and small-emittance collides with accumulating laser pulses in an enhancement cavity for generating high-flux LCS photon beam. We have developed the high-finesse bow-tie ring cavity for the LCS experiment at the Compact ERL (cERL) in KEK. In this presentation, we will report the detail of the optical cavity.
- THPOA51 Improvement of X-Ray Generation by Using Laser Compton Scattering in Laser Undulator Compact X-Ray Source(LUCX)**
M.K. Fukuda, S. Araki, Y. Honda, N. Terunuma, J. Urakawa (KEK) K. Sakaue (Waseda University, Waseda Institute for Advanced Study) M. Washio (RISE)
 We have been developing a compact X-ray source via laser Compton scattering(LCS) at Laser Undulator Compact X-ray source(LUCX) accelerator in KEK. We have started to take X-ray images such as refraction contrast images and phase contrast imaging with Talbot interferometer. In this accelerator, 6-10keV X-rays are generated by colliding a multi-bunch electron beam whose energy is 18-24MeV with a laser pulse stored with the wavelength of 1064nm. An electron beam is produced by a 3.6cell rf-gun and accelerated to 18-24MeV by a 12cell booster. A laser pulse is stored in a 4-mirror planar optical cavity to enhance the power. Presently, to increase the flux and the energy of LCS X-rays, optimization of the beam-loading compensation, improvement of the intensity and the focal size at the collision point and increase of stored RF power in accelerating cavity by rf-aging have been continued. We will report the result of the X-ray generation in this accelerator.
- THPOA52 A Simulation for Bright THz Light Source from Wiggler Radiation at KEK LUCX**
Y. Sumitomo, S. Araki, A. Aryshev, M.K. Fukuda, M. Shevelev, N. Terunuma, J. Urakawa (KEK) A. Deshpande (SAMEER) N. Terunuma (Sokendai)
 We study a bright THz light source generated by a wiggler radiation at KEK LUCX THz experiment, where an injected 4 pre-micro-bunched electron beam with few hundreds femto-seconds separation plays a crucial role. The energy of pre-bunched beam reaches 10 MeV at an S-band 3.6 cell RF Gun, and hence the space-charge effect is not negligible. We simulate the beam optics by ASTRA code, a charged beam optics simulator with space-charge effect, and then the resultant particle distribution is passed to GENESIS, a FEL simulator to deal with the wiggler radiation. The simulation results including a suitable 4 micro-bunch structure are compared with measured profile at KEK LUCX THz experiment, where the wiggler is installed around 8.5m position from the cathode. The major advantage of this system is a compactness of total setup that is expected to generate a 10 MW peak power THz beam by the coherent radiation.
- THPOA53 Luminosity Increase in Laser-Compton Scattering by Crab Crossing Method**
Y. Koshihara, D. Igarashi, S. Ohta, T. Takahashi, M. Washio (RISE) K. Sakaue (Waseda University, Waseda Institute for Advanced Study) J. Urakawa (KEK)
 In collider experiments such as KEKB, crab crossing method is a promising way to increase the luminosity and KEK (High Energy Accelerator Research Organization) has achieved the luminosity record in 2009. We are planning to apply crab crossing to laser-Compton scattering, which is a collision of electron beam and laser, to gain a higher luminosity leading to a higher brightness X-ray source. It is well known that the collision angle between electron beam and laser affects the luminosity. It is the best when the collision angle is zero, head-on collision, to get a higher luminosity but difficult to construct such system especially when using an optical cavity for laser. Concerning this difficulty, we are planning crab crossing by tilting the electron beam using an rf-deflector. Although crab crossing in laser-Compton scattering has been already proposed*, nowhere has demonstrated yet. We are going to demonstrate and conduct experimental study at our compact accelerator system in Waseda University. In this conference, we will report about our compact accelerator system, laser system for laser-Compton scattering, and expected results of crab crossing laser-Compton scattering.
- THPOA54 HOM Power and HOM spectrum of the RW HOM Damping Scheme***
Y. Gao (PKU) I. Ben-Zvi, H. Hahn, K.S. Smith, W. Xu (BNL)
 A HOM damping scheme, with combination of six ridge waveguides and beampipe absorber, is proposed to damp the high power, broadband HOMs for eRHIC 647 MHz SRF cavity. A time domain calculation is conducted to quantify the HOM power distribution in the waveguide dampers and beam pipe absorbers. HOM power density in each waveguide mode is looked into, so that the coupling between cavity and waveguide is well-understood. This paper will describe the HOM damping scheme for eRHIC cavity and HOM power distribution estimation on each load. The coupling of the cavity to waveguide will be discussed as well.
- THPOA55 Experimental Characterization of Coherent Synchrotron Radiation in a Magnetic Chicane**
Z. Zhang, Y.-C. Du, W.-H. Huang, X.L. Su, C.-X. Tang, Q.L. Tian, D. Wang, L.X. Yan, Z. Zhou (TUB) W. Gai (ANL)
 Coherent synchrotron radiation (CSR) in a magnetic chicane is observed and studied experimentally. The primary goal of this work is to characterize the CSR effect on the electron beam by the method that has been widely applied in the wakefield studies. We first let two or more electron bunches pass through a chicane and use the head one as the witness bunch. Varying the distance from the witness bunch to the drive bunch, the CSR effects can be characterized by measuring the corresponding beam energy loss. We will present some scaling laws between CSR effects and some experimental parameters. Simulations are performed as a comparison with the experimental measurements.
- THPOA56 Primary Study of the Photocathode Electron Gun With a Cone Cathode and Radial Polarization Laser**
R. Huang, Q.K. Jia (USTC/NSRL)
 The linearly polarized laser with oblique incidence can achieve a higher quantum efficiency (QE) of metal cathodes than that with the normal incidence, which however requires the wavefront shaping for better performance. To simplify the system and maintain the high QE, we propose a cone cathode electron gun with a radial polarization laser at normal incidence. The primary analytical estimation and numerical simulations are explored for its effect on the emittance of the electron beam.
- THPOA57 EEHG-Based Soft X-Ray Generation Scheme at HLSII Storage Ring**
W.W. Gao (Fujian University of Technology) H.T. Li, W. Li, L. Wang (USTC/NSRL)
 In this paper we study the feasibility of HLSII light source to radiate soft x-ray by storage ring based echo-enabled harmonic generation (EEHG) free electron laser (FEL). We hold the significant features of HLSII, short circumferences, that the whole ring is used as the first dispersion section. Hence, one modulator is saved compared to the conventional EEHG-FEL scheme.

- THPOA58 Multiple Bunch Length Operation Mode Design at HLSII Storage Ring**
W.W. Gao (*Fujian University of Technology*), **W. Li, L. Wang** (*USTC/NSRL*)
 In this paper we design a multiple bunch length operation mode by installing two harmonic cavities in a low momentum compaction factor lattice. The short bunch designed in this work can satisfy the coherent THz radiation experiment, and the long bunch can efficiently increase the total beam current. So that the multiple bunch length operation mode allowed that the current synchrotron users and THz user may carry out there experiment simultaneously.
- THPOA59 Development of 6 MeV Medical Linac for Cancer Therapy**
Y. Kim, P. Buaphad, S.S. Cha (*KAERI*)
 At KAERI, we have been developing a 6 MeV S-band medical linear accelerator for the cancer therapy. In this paper, we describe details of design, fabrication, and commissioning of the 6 MeV medical linear accelerator.
- THPOA60 Status of PLSII Operation**
T.-Y. Lee (*PAL*)
 As an upgrade of PLS, PLSII is a 3 GeV light source in 12 super-periods (281.8 m circumference) with 5.8 nm design emittance and can store electron beam up to 400 mA with 3 superconducting RF cavities. Its most unique characteristic is that it has a short straight section and a long straight section for each cell (24 straight sections) and up to 20 insertion devices can be installed. But, as the installed insertion devices, particularly in-vacuum insertion devices, are sources of high impedance, these are quite challenging for high current operation. Current status of PLSII operation and future plans are described in this paper.
- THPOA61 A Possible Emittance Reduction Scheme for PLSII**
T.-Y. Lee (*PAL*)
 As the upgrade of PLS, PLSII is a 3 GeV light source in 12 super-periods (281.8 m circumference) with 5.8 nm design emittance and can store electron beam up to 400 mA with 3 superconducting RF cavities. PLSII lattice is a double bend achromatic (DBA) lattice with 2 straight sections for each cell (24 straight sections). After completion of PLSII, multi-bend achromatic lattice has widely been adopted to accomplish low emittance. This paper discusses how a minimal change can modify the PLSII's DBA to a quadrupole bend achromatic (QBA) lattice and reduce the emittance to about a half value.
- THPOA62 Clearing Magnet Design for APS-U**
M. Abliz, J.H. Grimmer, Y. Jaski, M. Ramanathan, F. Westferro (*ANL*)
 Abstract Advanced Photon Source is in the process of developing an upgrade of the storage ring. The Upgrade will be converting the current double bend lattice to a multi-bend lattice (MBA). In addition, the storage ring will be operated at 6 GeV and 200 mA with regular swap-out injection to keep the stored beam current constant. The swap-out injection will take place with beamline shutters open. For radiation safety to ensure that no electrons can exit the storage ring, a passive method of protecting the beamline and containing the electrons inside the storage ring tunnel is proposed. A clearing magnet will be located in all beamline front ends inside the storage ring tunnel. This article will discuss the principle, design and mechanical design of the clearing magnet scheme for the APS-Upgrade.
- THPOA63 Septum Magnet Design for APS-U**
M. Abliz, M. Borland, H. Cease, G. Decker, M.S. Jaski, J.S. Kerby, U. Wienands, A. Xiao (*ANL*)
 The Advanced Photon Source is in the process of developing an upgrade (APS-U) of the storage ring from a double-bend to a multi-bend lattice. A swap-out injection is planned for the APS-U lattice to keep a constant beam current and accommodate small, dynamic aperture. A septum magnet that has a minimum thickness of 2 mm with an injection field of 1.06 T has been designed. The stored beam chamber has an 8 mm x 6 mm super-ellipsoidal aperture. The required total deflecting angle is 89 mrad with a ring energy of 6 GeV. The magnet is straight, but is tilted in yaw, roll, and pitch from the stored beam chamber in order to meet the swap out injection requirements for the APS-U lattice. In order to minimize the leakage field inside the stored beam chamber, four different techniques were utilized in the design. As a result, the horizontal deflecting angle of the stored beam was held to only 5 μ rad, and the integrated skew quadrupole inside the stored beam chamber was held to 0.09 T. The detailed techniques that were applied to the design, the field multipoles, and the resulting trajectories of the injected and stored beams are reported.
- THPOA64 MAX IV Storage Ring Magnets Installation Procedure**
K. Åhnberg, M.A.G. Johansson, P.F. Tavares, L. Th'nell (*MAX IV Laboratory, Lund University*)
 The MAX IV facility consists of a 3 GeV storage ring, a 1.5 GeV storage ring and a full energy injector linac. The storage ring magnets are based on an integrated "magnet block" concept. Each magnet block holds several consecutive magnet elements. The 3 GeV ring consists of 140 magnet blocks and 1.5 GeV ring has 12 magnet blocks. During the installation issues with deflection of the magnet blocks occurred and were solved. This article discusses the installation procedure from a mechanical point of view and presents measurement data of block straightness and ring performance.
- THPOA65 Double Triple Bend Achromat for Next Generation 3 GeV Light Sources**
A. Alekou, R. Bartolini (*Oxford University, Physics Department*) **A. Alekou, R. Bartolini** (*JAI*) **A. Alekou, R. Bartolini, T. Pulampong, R.P. Walker** (*DLS*) **N. Carmignani, S.M. Liuzzo, P. Raimondi** (*ESRF*)
 The Double Triple Bend Achromat (DTBA) is a newly designed cell for a next generation 3 GeV synchrotron light sources. DTBA comes from a modification of the ESRF HMBA 6 GeV cell and is inspired by the Double-Double Bend Achromat (DDBA) cell designed for Diamond, combining in this way the best characteristics of each lattice. The cell achieves a natural emittance as low as 115 pm, together with a large Dynamic Aperture (DA) and lifetime. Two cells are designed with different end-drift lengths providing two different Long Straight Sections for insertion devices, 5 and 7.5 m long, in addition to the middle-straight section of 3 m. The characteristics of the lattice together with the results on emittance, DA and Touschek lifetime are presented after extensive linear and non-linear optimisations, with and without the presence of errors and corrections.
- THPOA66 Longitudinal Electron Beam Measurements at the MAX IV 3 GeV Linac**
F. Curbis, M. Kotur, F. Lindau, E. Mansten, S. Thorin (*MAX IV Laboratory, Lund University*)
 The MAX IV 3 GeV linac (Lund, Sweden) is equipped with a thermionic and a photocathode gun and it used as the injector for the two storage rings as well as to drive the short pulse facility (SPF). When using the photo-cathode beam for the SPF, the compression is made by two double-achromats structures that are separated by the so-called 'main linac'. We can circumvent the lack of a transverse deflecting cavity via a relative measurement of the bunch length, done by running part of the main linac at zero-crossing phase and using a dispersive dipole as spectrometer. In this way, we will be able to characterize the performance of the first bunch compressor retrieving the longitudinal bunch profile. We can also compare the bunch length with an indirect measurement of the photon pulse done at the SPF via cross-correlation in a crystal.


- THPOA67 **A Concept of Tabletop Laser Wakefield Accelerator of Carbon Beams for Radiation Therapy**
C. Rangacharyulu, R.T. Tannous, M.Z. Zhu Song (University of Saskatchewan) C.V. Chau Van, Q.B. Nguyễn Điền (HCMUS)
 In recent years, laser wake field accelerators have achieved high field gradients to generate a few GeV electron beams in a few centimeters *. We are then led to consider if this technology maybe exploited to generate 200-300 MeV/nucleon ion beams to be useful for radiation therapy as compact accelerators. Such accelerators will minimize the need for expensive real estate and associated maintenance costs. If successful, such facilities may become affordable to be deployed in several countries. While this technology may not yield highly mono energetic beams without discarding the low and high energy tails of the spectrum, it may not be a serious issue since medical applications prefer finite energy spreads of ion beams. This is due to the fact that Spread Out Bragg Peak (SOBP) is desirable for tumor therapies. The challenge is to ensure that a non-relativistic ion will see an accelerating field in the electron bubble and achieve desired energies. We started a simulation program to identify optimal wake field plasma densities and laser parameters etc. In this presentation, we report our preliminary results along with our plans for future works.
- THPOA68 **The First Particle-Based Proof of Principle Numerical Simulation of Electron Cooling**
S. Abeyratne, B. Erdelyi (Northern Illinois University) B. Erdelyi (ANL)
 Envisioned particle accelerators such as JLEIC demand unprecedented luminosities of 10^{34} cm⁻² s⁻¹ and small emittances are key to achieve them. Electron cooling, where a 'cold' electron beam and the 'hot' proton or ion beam co-propagate in the cooling section of the accelerator, can be used to reduce the emittance growth. It is required to precisely calculate the cooling force among particles to estimate accurately the cooling time. There are different methods to simulate electron cooling. We have developed a novel code, Particles' High-order Adaptive Dynamics (PHAD), for electron cooling. This code differs from other established methods since it is the first particle-based simulation method employing full particle nonlinear dynamics. In this paper we present the first results obtained that establish electron cooling of heavy ions.
- THPOA69 **Evolution of the Design of the Magnet Structure for the APS Superconducting Undulators**
E. Trakhtenberg, Y. Ivanyushenkov, M. Kasa (ANL)
 Abstract A number of superconducting planar undulators (SCU) with different pole gaps and periods were designed, manufactured, and successfully operated at the Advanced Photon Source (APS) storage ring. A key component of the project is the precision machining of the magnet structure and the precision of the coil winding. The design of the magnet core had a number of modifications during the evolution of the design in order to achieve the best magnetic performance. The current design of the magnet structure is based on the assembled jaws with individual poles, while previous designs utilized solid cores with machined coil grooves. The winding procedure also changed from the first test cores to the current final design. Details of the magnet structure's design, manufacturing, winding and jaw assembly, and changes made from the first prototype system to the production unit, are presented.

THA3 — Oral Presentations (MC4)**Chair:** K.W. Jones (ORNL)**THA3I001 FNAL Accelerator Complex Upgrade Possibilities**14:00 **I. Kourbanis**, S.D. Holmes, V.A. Lebedev (*Fermilab*)


Proton Improvement Plan-II (PIP-II) is the centerpiece of Fermilab's plan for upgrading the accelerator complex to establish the leading facility in the world for particle physics research based on intense proton beams. PIP-II has been developed to provide 1.2 MW of proton beam power at the start of operations of the Long Baseline Neutrino Experiment (LBNE), while simultaneously providing a platform for eventual extension of LBNE beam power to >2 MW and enabling future initiatives in rare processes research based on high duty factor/higher beam power operations. PIP-II is based on the construction of a new 800 MeV superconducting linac, augmented by improvements to the existing Booster, Recycler, and Main Injector complex. PIP-II is currently in the development stage with an R&D program underway targeting the front end and superconducting RF acceleration technologies. This paper will describe the status of the PIP-II conceptual development, the associated technology R&D programs, and the strategy for project implementation.

THA3I002 The ESS Accelerator14:30 **J.G. Weisend** (*ESS*)

The ESS accelerator construction has started and the tunnel and RF gallery will be handed over to the accelerator division in 2016 with the installation of the cryoplant starting later in the year. Beam should be delivered in June 2019 at 570 MeV and 1.5 MW with full 5 MW capability being available in 2023. The project is a highly contributed project with more than 50% of the total budget being contributed by more than 25 IK partners. The talk will review the project status reflecting the IK nature of the project with the many partners contributions and with some focus on the cryogenics systems.

THA3C003 Beam Commissioning Activities and Issues at Demo Facility of C-ADS Injector II15:00 **Z.J. Wang**, Y. He (*IMP/CAS*)

To develop the next generation of safe and cleaner nuclear energy, the ADS (Accelerator Driven Sub-critical System) emerges as one of the most attractive technologies. The prototype of the Chinese ADS (C-ADS) proton accelerator comprises two injectors and a 1.5 GeV, 10 mA Continuous Wave (CW) superconducting main linac. The Injector Scheme II at the C-ADS demo facility inside Institute of Modern Physics is a 10 MeV CW superconducting linac with designed beam current of 10 mA. The commissioning activities have been carried out since June 2014. Through around two years hard work, Injector II has been operated with tens high beam power successfully. In this paper, the beam commissioning activities and issues at the demo facility of C-ADS Injector II are reported.


THA3C004 Space Charge Compensation Using Electron Columns and Electron Lenses at IOTA15:15 **C.S. Park**, D. Milana, V.D. Shiltsev, G. Stancari, J.C.T. Thangaraj (*Fermilab*) D. Milana (*Politecnico/Milano*)

The ability to transport a high current proton beam in a ring is ultimately limited by space charge effects. A cost effective way to overcome this limit in a proton ring is by taking advantage of residual gas ionization induced neutralization to create an electron column (e-column). Theory predicts that an appropriately confined e-column can completely compensate the space charge through neutralization, both transversely and longitudinally. The primary advantage of this scheme lies in using the proton beam itself to generate electrons and match the proton beam profile. With the WARP beam dynamics code, we modeled a 2.5 MeV proton beam passing through a meter long e-column with solenoid magnetic field and bias voltage on the electrodes. In this work, we report how the IOTA e-column compensates space charge with the WARP simulations. The dynamics of proton beams inside of the e-column column is understood by changing the magnetic field of a solenoid and the voltage on the electrodes, and by looking for electron accumulation, as well as by considering various beam dynamics in the IOTA ring. These simulations will guide the planned experiments at IOTA.

THB3 — Oral Presentations (MC8)

Chair: M. Tigner (Cornell University (CLASSE), Cornell Laboratory for Accelerator-Based Sciences and Education)

THB3I001 Development of a High Brightness Source for Fast Neutron Imaging*

14:00  **B. Rusnak**, S.G. Anderson, D.L. Bleuel, M.L. Crank, P. Fitsos, D.J. Gibson, M. Hall, M. S. Johnson, R.A. Marsh, J.D. Sain, R. Souza, W. Wiedrick (LLNL)

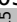
Lawrence Livermore National Lab is developing an intense, high-brightness fast neutron source to create high resolution neutron radiographs and images. An intense source (10^{11} n/s/sr at 0 degrees) of fast neutrons (10 MeV) allows: penetrating very thick, dense objects; maintaining high scintillator response efficiency; and remaining below the air activation threshold for (n,p) reactions. Fast neutrons will be produced using a pulsed 7 MeV, 300 microamp average-current commercial ion accelerator that will deliver deuterons to a 3 atmosphere deuterium gas cell. To achieve high resolution, a small (1.5 mm diameter) beam spot size will be used, and to reduce scattering from lower energy neutrons, a transmission gas cell will be used to produce a quasi-monoenergetic neutron beam. Because of the high power density of such a tightly focused, modest-energy ion beam, the gas target is a major engineering challenge that combines a 'windowless' rotating aperture, a rotary valve to meter cross-flowing high pressure gases, a novel gas beam stop, and recirculating gas compressor systems. A summary of the progress of the system design and building effort shall be presented.

THB3I002 Review of Potential Accelerator Systems for Energy and Environmental Applications

14:30  **S. Henderson** (ANL)


Review potential accelerator concepts for Energy and Environmental applications. The talk should cover several potential applications and address the technological requirements and the issues that must be addressed to reach successful market insertion.

THB3C003 Thermoacoustic Range Verification for Ion Therapy

15:00  **S.K. Patch**, Y.M. Qadadha (UWM) R. Albright, P. Bloemhard, K. Campbell, A.P. Donoghue, T.L. Gimpel, A. Jackson, M.B. Johnson, M. Kireeff Covo, B. Ninemire, L. Phair, C.R. Siero, S.M. Small (LBNL)

The potential of particle therapy due to focused dose deposition in the Bragg peak has not yet been fully realized due to inaccuracies in range verification. We report correlation of the Bragg peak location with target structure, by overlaying thermoacoustic localization of the Bragg peak onto a standard ultrasound image. Pulsed delivery of 50 MeV protons was accomplished by a fast chopper installed between the ion source and the inflector of the 88" cyclotron at Lawrence Berkeley National Lab. 2 Gy were delivered in 2 μ s by a beam with peak current of 2 μ A. Thermoacoustic emissions were detected by a clinical ultrasound array, which also generated a grayscale ultrasound image. Data was collected in a room temperature water bath and gelatin phantom with a cavity designed to mimic the intestine, where gas pockets can displace the Bragg peak. Experiments were performed with the cavity both empty and filled with olive oil. In the waterbath overlays of the Bragg peak agreed with Monte Carlo simulations to within 800 ± 170 μ m. Agreement within 1.3 ± 0.2 mm was achieved in the gelatin phantom, for which stopping power was estimated to first order from CT scans.

THB3C004 The Design and Monte Carlo Simulation of the Energy Loss Used in Proton Radiography


15:15  **N. Zheng**, Q.G. Jia, H.B. Xu (Institute of Applied Physics and Computational Mathematics)

High-energy proton radiography provides a new and quantitative technique to determine the geometric configuration and physical characteristic for hydrotest experiment. In the traditional high-energy proton radiography, a point-to-point magnetic quadrupole imaging system named Zumbro lens is used to control the proton beam. In the proton radiography, the information of the flux attenuation and the angular scattering of the protons is used to diagnose the properties of the object, and the energy loss of the incident proton is the main reason to debase the image quality because of the chromatic blur. As we know, the energy loss of the incident proton is also relate to the sample. In this paper, a new type of imaging beamline which can modulate the energy rang of the imaging protons is proposed with a specially designed imaging lens, a new method which will use the energy loss in the density reconstruction is proposed, a program which can simulate the energy loss in the proton radiography has been developed in the frame of the Geant4, and the preliminary design of this proton energy-loss radiography concept has been verified by the Monte Carlo simulation.

THPL — Louis Costrell Honorary Awards Session

Chair: M. White (ANL)

THPLI001 What Life Is Like as a Scientist in Congress

16:00 

G.W. Foster (*Fermilab*)

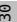
Bill Foster has given several excellent talks pointing out that scientists and engineers are greatly underrepresented in politics, and that the people making decisions about science funding do not have adequate background to make informed decisions themselves. He has excellent suggestions in the talk as to how we can contribute.

FRA1 — Oral Presentations (MC6)


Chair: S. Biedron (CSU)

FRA1I001 Single Particle Detection With a Schottky Resonator08:30  **M. Steck** (GSI)

Presentation would address underlying physics, experimental method / instrumentation and experimental outcomes.

FRA1I002 State of the Art X-Ray Photon BPMs for Next Generation Storage Ring Light Sources09:00  **B.X. Yang** (ANL) *R. Ischebeck* (PSI)


From <http://journals.aps.org/prab/pdf/10.1103/PhysRevSTAB.18.082802>: "A transverse profile imager for ultrabright electron beams is presented, which overcomes resolution issues in present designs by observing the Scheimpflug imaging condition as well as the Snell- Descartes law of refraction in the scintillating crystal. Coherent optical transition radiation emitted by highly compressed electron bunches on the surface of the crystal is directed away from the camera, allowing to use the monitor for profile measurements of electron bunches suitable for X-ray free electron lasers. . ." The detector design and it's integration for routine use with a transverse mode deflecting cavity will be reviewed with experimental data from the SwissFEL Injector Test Facility.

FRA1C003 An Ultra-High Resolution Pulsed-Wire Magnet Measurement System09:30  **A. D'Audney**, *S. Biedron, S.V. Milton* (CSU) *G. Fiorito, R. Geometrante* (KYMA)


The performance of a Free-Electron Laser (FEL) depends in part on the quality of the magnetic field in the undulator. Imperfections in the magnetic field of an undulator lead to an imperfect electron trajectory, both offset and angle, as well as a relative phase error between the oscillation phase of the electrons and the generated electromagnetic field. The result of such errors is a reduction of laser gain impacting overall FEL performance. A pulsed-wire method can be used to determine the profile of the magnetic field. This is achieved by sending a square-current pulse through a wire placed along the length of the axis that will induce a Lorentz-force interaction with the magnetic field. Measurement of the resulting displacement in the wire over time using a motion detector yields the first or second integrals of the magnetic field and so provides a measure of the local magnetic field strength. Dispersion in the wire can be corrected using algorithms, with a resulting increase in overall accuracy of the measurement. We have designed, constructed and tested a pulsed-wire magnetic measurement system and used this system to characterize the CSU FEL undulator.

FRA1C004 6D Phase Space Measurement of Low Energy, High Intensity Hadron Beam09:45  **B.L. Cathey** (ORNL RAD)


The goal of this project is to demonstrate a method for measuring the full 6D phase space of an low energy, high intensity hadron beam. This is done by combining 4D emittance measurement techniques along with dispersion measurement and a beam shape monitor to provide the energy and phase space components. The measurement will be performed on new Beam Testing Facility (BTF) at the Spallation Neutron Source (SNS), a 2.5 MeV functional duplicate of the SNS accelerator front end.

FRA1C005 Progress of Gas-Filled Multi-RF-Cavity Beam Profile Monitor for Intense Neutrino Beam10:00  **K. Yonehara**, *M. Backfish, A. Moretti, A.V. Tollestrup, A.C. Watts, R.M. Zwaska* (Fermilab) *M.A.C. Cummings, A. Dudas, R.P. Johnson, G.M. Kazakevich, M.L. Neubauer* (Muons, Inc) *B.T. Freemire* (IIT) *Q. Liu* (Case Western Reserve University)

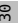
A novel pressurized gas-filled multi-RF-cavity beam profile monitor has been studied that is simple and robust in high-radiation environments. Charged particles passing through each RF-cavity in the monitor produce intensity-dependent ionized plasma, which changes the gas permittivity. The sensitivity to beam intensity is adjustable using gas pressure and RF gradient. The performance of the gas-filled beam profile monitor has been numerically simulated to evaluate the sensitivity of permittivity measurements. The result indicates that the RF resonator will be useful to measure the beam profile with a charged beam intensity range from 10^6 to 10^{13} protons/bunch. The range covers the expected beam intensities in NuMI and LBNF. The demonstration of the monitor with intense proton beams are taken place at Fermilab to validate the simulation result. The result will be given in this presentation.

FRA1C006 Measurement of Coherent Transition Radiation Using Interferometer and Photoconductive Antenna10:15  **K. Kan**, *M. Gohdo, T. Kondoh, I. Nozawa, J. Yang, Y. Yoshida* (ISIR)


Ultrashort electron beams are essential for light sources and time-resolved measurements. Electron beams can emit terahertz (THz) pulses using coherent transition radiation (CTR). Michelson interferometer* is one of candidates for analyzing the pulse width of an electron beam based on frequency-domain analysis. Recently, electron beam measurement using a photoconductive antenna (PCA)** based on time-domain analysis has been investigated. In this presentation, measurement of femtosecond electron beam with 35 MeV energy and < 1 nC from a photocathode based linac will be reported. Frequency- and time- domain analysis of THz pulse of CTR by combining the interferometer and PCA will be carried out.

FRB1 — Tutorial (MC7) / Oral Presentation (MC8)**Chair:** W. Leemans (LBNL)**FRB1TU01 RF Superconductivity**08:30 **J.R. Delayen** (ODU)


Tutorial, based on the "RF Superconductivity" course taught by J. Delayen at the US PAS

FRB1I002 ADAM: LIGHT a Linear Accelerator for Proton Therapy10:00 **D. Ungaro, P. Stabile** (ADAM)


ADAM, Application of Detectors and Accelerators to Medicine is a Swiss Company based in Geneva Switzerland established on 20th December 2007. ADAM was founded to promote scientific know-how and innovations in medical technology for cancer treatment. In 2007 a first partnership agreement was signed with CERN and in 2011 ADAM has been officially recognized as CERN spin-off. After the first research results other partnership agreements were signed between ADAM and CERN with the main goal of establishing a framework within which the two parties can collaborate to develop novel technologies for detectors and accelerators. Currently ADAM research activity is mainly focused on the construction and testing of its first linear accelerator for medical application: LIGHT (Linac for Image-Guided Hadron Therapy). LIGHT is an innovative linear accelerator designed to revolutionise hadron therapy facilities by simplifying the infrastructure and make them profitable from an industrial point of view while providing a better quality beam. The current design allow LIGHT to accelerate proton beam up to 230MeV with several advantages comparing to the current solutions present in the market.

FRA2 — Oral Presentations (MC6)**Chair:** B.E. Carlsten (LANL)**FRA2I001 Development and Application of on-Line Accelerator Optimization Algorithms**11:00  **X. Huang** (SLAC)


Automated tuning is an online optimization process. It is more efficient than manual tuning and can lead to better performance. It may also substitute or improve upon model based methods. Noise tolerance is a fundamental challenge to online optimization algorithms. We will discuss our experience in developing high efficiency, noise-tolerant optimization algorithms and the successful application of the algorithms to various real-life accelerator problems.

FRA2I002 High Precision RF Control for the LCLS-II11:30  **G. Huang, L.R. Doolittle** (LBNL)


The LCLS-II is CW superconducting linac driving an FEL. The energy and timing stability requirements of the FEL drive the need for very high precision RF control. This talk will summarize the design and early demonstration of the performance on a test cryomodule.

FRA2C003 Study of the Electrical Center of a Resonant Cavity Beam Position Monitor (RF-BPM) and Its Integration With the a Main Beam Quadrupole for Alignment Purposes12:00  **S. Zorzetti, M. Wendt** (CERN) **L. Fanucci** (Università di Pisa)


To achieve the luminosity goals in a next generation linear collider, acceleration and preservation of ultra-low emittance particle beams is mission critical and requires a precise alignment between the main accelerator components. PACMAN is an innovative doctoral training program, hosted by CERN, with the goal of developing high accuracy metrology and alignment methods and tools to integrate those components in a standalone, automatic test bench. The method will be validated on CLIC components, a proposed Compact Linear Collider currently studied at CERN. The alignment between the electrical center of the Beam Position Monitor (BPM) and the magnetic center of the associated Main Beam Quadrupole (MBQ) is of particular importance to minimize the emittance blow-up, and therefore in the focus of the PACMAN project. The two components have been independently characterized on separated test benches by stretched and vibrating wire techniques. Preliminary conclusions are presented in this paper, with emphasis on the characterization of the electrical center of the BPM.

FRA2C004 Status of the SRF Cavities Resonance Control F&D Work at FNAL12:15  **Y.M. Pischnalnikov, J.P. Holzbauer, W. Schappert** (Fermilab)

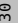
There are several new machines under construction or development at this moment. Some machines, (LCLS II and PIP II) will operate with the relatively low beam currents and high cavity quality factors. SRF cavities for these projects will be operated with small RF bandwidths, meaning that they will be highly sensitive to microphonics and Lorentz force detuning. Other future projects such as ESS will be operate with SRF cavities tuned for larger RF bandwidth but will still have significant Lorentz Force Detuning. Work is ongoing at FNAL to develop active resonance stabilization techniques using fast piezoelectric tuners in support of PIP-II and LCLS II. These techniques as well as testing and development results using a prototype, dressed low-beta single-spoke cavity and 9-cell elliptical cavities will be presented along with an outlook for future efforts.

FRB2 — Oral Presentations (MC8)**Chair:** V.V. Parkhomchuk (BINP SB RAS)**FRB2I001 Application of Superconducting Technology for Proton Therapy**11:00 **V.P. Derenchuk** (*ProNova Solutions*)

ProNova is developing SC cyclotrons and gantries for application in cancer therapy with proton beams. Superconducting magnets have multiple benefits; not only are they dramatically smaller in size, weight and power consumption, they also have a magnetic field 2x higher than those used in today's cyclotrons and gantries, in addition to a 0.5x bend radius. Taking advantage of this technology, the SC360 system maintains 360° rotation similar to radiation therapy, while the dramatically smaller size and weight allows for ample room for full ring imaging at isocenter and simplified shipping and installation, reducing cost and time to market.

FRB2I002 4 K Superconducting Linacs for Commercial Applications11:30 **C.H. Boulware** (*Niowave, Inc.*)

Developments in low-frequency superconducting RF accelerating structures have created a commercial niche for 4 K superconducting electron accelerator systems at high powers. This presentation will discuss niobium accelerating structures, the liquid helium refrigerator, high power microwave source, radiation shielding and licensing for high-average-power commercial electron accelerators. Applications to be briefly reviewed include radioisotope production, high-power x-ray generation (for cargo scanning, industrial sterilization, etc.), high-flux neutron sources, high intensity positron sources, and high-power free-electron lasers.

FRB2I003 GEM*STAR Accelerator-Driven Subcritical System for Improved Safety, Waste Management, and Plutonium Disposition12:00 **M.A.C. Cummings, R.J. Abrams, R.P. Johnson, T.J. Roberts** (*Muons, Inc*)

Operation of high-power SRF particle accelerators at two US national laboratories allows us to consider a less-expensive nuclear reactor that operates without the need for a critical core, fuel enrichment, or reprocessing. A multipurpose reactor design that takes advantage of this new accelerator capability includes an internal spallation neutron target and high-temperature molten-salt fuel with continuous purging of volatile radioactive fission products. The reactor contains less than a critical mass and almost a million times fewer volatile radioactive fission products than conventional reactors like those at Fukushima. We describe GEMSTAR, a reactor that without redesign will burn spent nuclear fuel, natural uranium, thorium, or surplus weapons material. A first application is to burn 34 tonnes of excess weapons grade plutonium as an important step in nuclear disarmament under the 2000 Plutonium Management and Disposition Agreement **. The process heat generated by this W-Pu can be used for the Fischer-Tropsch conversion of natural gas and renewable carbon into 42 billion gallons of low-CO₂-footprint, drop-in, synthetic diesel fuel for the DOD.

FRPL — Closing Session**Chair:** S.R. Koscielniak (TRIUMF, Canada's National Laboratory for Particle and Nuclear Physics)**FRPLI001 The Need for Compact Coherent Light Sources - an Example - X-Ray Phase Contrast Tomography Reveals the Secrets of Herculaneum Papyri**

14:00

45

V. Mocella (IMM)

We present the first experimental demonstration of a non-destructive technique that reveal the text of a carbonized and thus extremely fragile Herculaneum papyrus. Buried by the famous eruption of Vesuvius in 79 AD, the Herculaneum papyri represent a unique treasure for humanity. Overcoming the difficulties of the other techniques we prove that x-ray phase contrast tomography technique can detect the text within scrolls, thanks to the coherence and high energy properties of a synchrotron source. This new imaging technique represents a turning point for the study of literature and ancient philosophy, disclosing texts that were believed to be completely lost. These and related applications require the development and implementation of compact, portable, bright, and coherent light sources. This talk describes a prime example for the need of such a source.

— A —

Abell, D.T.	THP0A38, THP0A40 , THP0A43
Abeyratne, S.	THP0A68
Abliz, M.	THP0A62 , THP0A63
Abrams, R.J.	TUP0A56, WEP0B34 , FRB2I003
Acosta, J.G.	MOB3C004, TUP0B44
Adamson, P.	WEP0A14, WEP0A16
Adli, E.	TUA4C003
Afanasev, A.	TUP0B32 , TUP0B35, WEP0A54
Agustsson, R.B.	MOP0B72, TUP0A68, TUB3C004, TUP0B39, TUP0B42, WEP0B46, WEP0B47, WEP0B48
Åhnberg, K.	THP0A64
Ainsworth, R.	WEP0A14 , WEP0A16
Akagi, T.	THP0A50
Al Marzouk, A.A.	SUP001 , TUP0B14
Albert, M.	MOB3I002
Albright, R.	THB3C003
Alekou, A.	THP0A65
Aleman-Fernandez, R.	MOB3I002
Alesini, D.	SUP033, THA2C003
Alessi, J.G.	MOB3C003, MOA4I001
Alexahin, Y.I.	MOB4C003 , WEP0A17 , THP0A15 , THP0A16 , THP0A17
Allaria, E.	TUB2I002
Altinbas, Z.	MOA3I001, WEP0B54, WEP0B60
Alverson, S.C.	SUP022, WEP0B49
Ambrosio, G.	WEB3I002
Ammigan, K.	MOP0B13 , MOP0B14 , MOP0B35
Amundson, J.F.	WEA4C003, THP0A18, THP0A25
An, W.	WEP0A48
Anastasio, M.A.	TUP0A27
Anderson, G.G.	SUP018, TUP0A61, WEP0B35, WEP0B38
Anderson, K.	MOP0B35
Anderson, S.G.	THB3I001
Andersson, Å.	WEA3C004
Andonian, G.	TUP0A72
Andorf, M.B.	TUP0A47, WEP0A38
Andrews, R.	WEP0A15
Anerella, M.	MOP0B74
Angelo, J.J.	MOP0B25
Antipov, S.A.	SUP006 , THP0A48 , THP0A49
Antipov, S.P.	WEP0B19, WEP0B20, THP0A08
Antonsen, T.M.	TUA4C004
Apollinari, G.	MOP0B41
Araki, S.	MOP0B03, THP0A50, THP0A51, THP0A52
Arodzero, A.	TUP0A68
Aryshev, A.	THP0A52
Asner, D.	MOP0B13
Assadi, S.	MOB2C003, TUA1C004
Atherton, A.R.	MOP0B14
Attenkofer, K.	WEP0B52
Auchmann, B.	MOP0B41
Avagyan, V.S.	MOP0B01
Avrakhov, P.V.	TUP0B02, TUP0B03
Awida, M.H.	MOP0B15 , MOP0B16 , WEP0B27

— B —

Babzien, M.	WEP0A24, WEP0A58, WEP0B46
Bacha, B.	TUP0B50, WEA1C005
Backfish, M.	SUP024, MOP0B52, TUP0A44, FRA1C005
Badgley, K.E.	TUA1C004, WEA2I002, THP0A25
Baffes, C.M.	MOP0B25, TUP0A19, WEP0A15

Banerjee, N.	MOP0B60
Bao, Y.	TUP0B35, TUP0B38 , WEPOA53 , WEPOA54
Baptiste, K.M.	MOP0B47
Barber, B.R.	SUP002 , WEB3C004
Barnard, J.J.	WEPOA29
Barnes, C.W.	TUB4I001
Baros, D.	MOA3C003
Bartnik, A.C.	SUP003, TUP0A58
Bartnik, L.Y.	TUP0B22
Bartolini, R.	THP0A65
Barty, C.P.J.	SUP018, TUP0A61, WEP0B35, WEP0B38
Barzi, E.Z.	MOP0B41
Bassi, G.	TUP0B45 , TUP0B46 , TUP0B48, TUP0B49, TUP0B50, TUP0B51, TUP0B56, WEA1C005
Batygin, Y.K.	SUP012 , TUP0A64, TUP0B26
Baumgartner, H.	SUP055 , TUP0A45, TUP0B11
Bazarov, I.V.	SUP003, TUP0A58, WEP0A61
Beaudoin, B.	SUP036, SUP055, TUP0A45 , TUP0B11, TUP0B12, WEP0A08
Beavis, D.R.	WEP0B54
Beck, K.	TUP0A68
Beebe, E.N.	MOB3C003, MOA4I001
Beebe-Wang, J.	TUP0B56
Bell, G.I.	THP0A41 , THP0A42, THP0A44
Bellavia, S.	WEP0B54
Ben-Zvi, I.	MOP0B76, THB2I003, THP0A41, THP0A42, THP0A54
Benesch, J. F.	WEB4C003
Bengtsson, J.	TUP0B52
Bennett, L.C.	TUP0A54
Benson, S.V.	TUP0A53, TUP0B36
Berg, J.S.	MOP0B74, MOP0B75, TUP0B56, WEP0A61
Berg, W.	WEP0B48
Bergan, W.F.	SUP003 , TUP0A57 , TUP0A58
Bernal, S.	TUP0A45
Berry, R.D.B.	TUP0A68
Betz, M.	MOP0B47
Bevilacqua, R.	WEPOA07
Bhandari, H.	WEP0B52
Biedron, S.	SUP010, SUP042, SUP043, MOP0B17, MOP0B56, MOP0B57, TUP0A51, TUP0A52, TUP0A53, WEP0A42, WEP0A43, THP0A37, FRA1C003, TUP0A43
Billing, M.G.	TUP0B22
Bischofberger, K.	WEP0B39
Blaclard, G.	WEPOA30
Blaskiewicz, M.	MOB3C003, TUP0B56, TUP0B58, WEP0A61, WEA3I001 , WEA4C005, WEP0B62
Blednykh, A.	TUP0B45, TUP0B46, TUP0B48 , TUP0B49 , TUP0B50 , TUP0B51 , WEA1C005 , WEP0B08
Bleuel, D.L.	THB3I001
Bloemhard, P.	THB3C003
Bogacz, S.A.	TUP0B34
Bohler, D.K.	SUP022, WEP0B49
Bonnema, E.C.	TUP0A67
Borissov, E.	MOP0B32, MOP0B33
Borland, M.	TUB2I001 , WEP0B01 , WEP0B02 , WEP0B08, WEP0B09, WEP0B14, WEP0B15, WEP0B22, THP0A13 , THP0A63, TUP0B61
Boruchowski, M.	TUP0A09
Boucher, S.	TUP0A68, WEP0B48, MOP0B72
Boulware, C.H.	MOP0B67 , WEP0A47, WEP0B37, FRB2I002
Bowden, G.B.	WEP0B42
Bowring, D.L.	SUP010, MOP0B17, MOP0B52, TUP0A51
Bradley III, J.T.	TUP0A63
Brajuskovic, B.	MOP0B11
Brameld, M.	TUP0A04
Bravin, E.	MOB3I002
Breitschopf, J.	MOB2C003, MOP0B54
Brennan, J.M.	MOB3C003

Briegel, C.I.	TUP0A19
Broemmelsiek, D.R.	TUP0A19, TUP0A73, TUP0B18
Bromberek, D.J.	WEP0B70
Brooks, S.J.	TUP0B60, WEP0A61
Brown, B.C.	WEP0A16
Brown, K.A.	MOB3C003
Bruhaug, G.M.	TUP0A74
Bruhwieler, D.L.	TUP0B10 , TUP0B13, WEA2I002 , WEP0A31, WEA4C002, WEP0B17, THP0A23, THP0A28, THP0A39
Bruno, D.	MOB3C003, WEP0B54
Brutus, J.C.B.	WEP0B60
Buaphad, P.	THP0A59
Bultman, N.K.	MOP0B55
Burke, D.C.	MOP0B59
Burkhardt, E.E.	MOP0B55
Burov, A.V.	WEP0A14, WEP0A17, WEA3C003 , WEA4C003, THP0A30, THP0A48
Butcher, M.E.J.	MOP0B14
Butler, J.J.	MOB3C003
Butler, N.	MOP0B44, MOP0B45, TUP0B09
Byer, R.L.	WEP0A32
Byrd, J.M.	SUP009, SUP052, MOP0B47, TUP0A08, TUP0A39 , TUP0A41, THP0A33

— C —

Cahill, A.D.	SUP004 , WEP0B41 , WEP0B42
Cai, Y.	TUP0B29, TUP0B31
Calaga, R.	MOB2C004
Caldwell, A.	TUA2I001
Calvey, J.R.	WEA1C003 , THP0A14
Calviani, M.	MOP0B14
Campbell, K.	THB3C003
Campese, T.J.	WEP0B46, WEP0B48
Cao, W.	MOP0B68
Capista, D.	WEP0A16
Capobianco-Hogan, K.G.	SUP005 , TUP0B43
Cappadoro, P.L.	WEP0B57
Caretta, O.	MOP0B14
Carlson, C.	MOA3I001
Carlson, K.	TUP0A19
Carlsten, B.E.	TUP0A62
Carmignani, N.	THP0A65
Carneiro, J.-P.	TUP0B64 , TUP0B66
Carpenter, A.	WEB4C003
Carter, J.A.	SUP048, MOP0B07 , MOP0B10, MOP0B11, WEP0B18, THP0A14
Carver, R.L.	SUP027, TUP0A38
Carwardine, J.	WEP0B24
Cary, J.R.	THP0A36 , THP0A43
Casella, A.M.	MOP0B13
Caspi, S.	THB1I002
Castellano, L.J.	TUP0A63
Cathey, B.L.	SUP007 , FRA1C004
Cease, H.	MOP0B11, WEP0B03, THP0A63
Cerutti, F.	WEP0A07
Cha, S.S.	THP0A59
Champion, M.S.	MOP0B71
Chandrashekar, C.	WEP0A48, WEP0A58
Chang, P.S.	TUP0B42
Chase, B.E.	SUP010, MOA3I002 , MOP0B17, TUP0A18, TUP0A19, TUP0A51, TUP0A52
Chasman, C.	MOA3I001
Chau Van, C.V.	THP0A67
Chaurize, S.	WEP0A18
Chavez, D.	MOB2C003, MOP0B54
Cheatam, J.R.	TUA3C003

Checchin, M.	SUP008, MOP0B19, MOP0B20, MOP0B34
Chen, A.Z.	WEPOA15
Chen, H.B.	THPOA08
Chen, Q.	SUP009, TUPOA08
Chen, Y.C.	TUPOA68, WEPOB47, WEPOB48
Chen, Y.J.	TUPOB24, TUPOB25
Chen-Wiegart, Y.	WEA1C005
Cheng, G.	WEPOB44
Cheng, W.X.	MOA2I002, TUPOA71 , WEA1C005
Cheng, Y.-S.	TUPOA12
Chiu, P.C.	TUPOA12
Chlachidze, G.	MOP0B41
Choi, C.U.	TUPOA10
Choi, H.S.	MOP0B78
Chouhan, V.	MOP0B61
Chow, K.	TUB1C003
Chubar, O.V.	WEA1C005, WEPOB57
Chung, M.	TUPOA10
Collins, J.T.	WEPOB03
Colocho, W.S.	WEPOB43
Conde, M.E.	SUP049, TUA2I002 , TUPOA13, WEPOB19, WEPOB20
Connolly, R.	MOB3C003
Convery, M.E.	MOA4I002 , THPOA27
Conway, Z.A.	MOB4C004, WEPOA11
Cook, N.M.	WEA2I002, WEPOA31 , WEA4C002, THPOA23, THPOA28, THPOA38, THPOA39
Cornacchia, M.	TUB1C002, THPOA06
Costanzo, M.R.	MOA3I001, MOA4I001, WEPOA57, WEPOB54
Cours, A.R.	WEPOB24
Cowan, B.M.	WEPOA32 , THPOA36, THPOA43
Crank, M.L.	THB3I001
Crawford, A.C.	MOP0B34
Crawford, D.J.	TUPOA15 , TUPOA19, TUPOB18
Cremaldi, L.M.	MOB3C004, TUPOB44
Crittenden, J.A.	MOP0B59, TUPOB23 , WEA2C003, WEPOA61, THPOA07
Crnkovic, J.D.	THPOA27
Crockford, G.E.	MOB3I002
Crowley, C.F.	MOP0B35
Cullerton, E.	TUPOA18, TUPOA19
Cullinan, F.J.	WEA3C004
Cummings, M.A.C.	SUP024, TUPOA44, TUPOA56, TUPOB06, WEPOB34, FRA1C005, FRB2I003
Curbis, F.	THPOA66
Curcio, A.J.	WEPOB60

— D —

D'Audney, A.	FRA1C003
D'Ottavio, T.	MOB3C003
da Silva, T.M.C.	THPOA02
Dalichaouch, T.N.	WEPOA49
Danielyan, V.	MOP0B01
Davenne, T.R.	MOP0B14
Davidson, A.W.	WEPOA49
De Maria, R.	TUPOB17
De Monte, V.	WEPOB58
De Santis, S.	MOP0B47, THPOA33
De Silva, S.U.	WEB2I002
Decker, E.-J.	WEPOB43
Decker, G.	WEPOB03, THPOA63
Degen, C.	MOA3I001
Deitrick, K.E.	WEPOB45
Dejus, R.J.	WEPOB03 , WEPOB09
Dekhtiarov, S.G.	MOP0B01

Delayen, J.R.	WEPOB45, FRB1TU01
Den Hartog, P.K.	MOP0B10, WEPOB17
Densham, C.J.	MOP0B14, MOP0B35
Derbenev, A.A.	WEA1C005
Derbenev, Y.S.	TUP0B05, TUP0B29, TUP0B30, TUP0B31, TUP0B32, TUP0B35, TUP0B36, WEA2C004, WEPOA54
Derenchuk, V.P.	FRB2I001
Derwent, P.	WEPOA15
DeSanto, L.	MOA4I001, WEPOB58
Deshpande, A.	MOPLI004
Deshpande, A.	THPOA52
Dey, J.E.	MOP0B28
Di Lieto, A.	WEPOB60
Di Mitri, S.	TUB1C002, THPOA04, THPOA05, THPOA06
Diamond, J.S.	TUPOA16 , TUPOA19, TUPOA29
DiMarco, J.	MOP0B41
Dimitrov, D.A.	THPOA41, THPOA42
Ding, Y.	WEPOB30
Ding, Z.	WEPOB52
Dishman, R.	TUPOA60
Dobbins, J.	MOP0B60, WEPOA61
Dolgashev, V.A.	SUP004, WEPOB41, WEPOB42
Domenge, J.	MOP0B46
Donnelly, A.T.	WEPOB03, WEPOB09
Donoghue, A.P.	THB3C003
Dooling, J.C.	MOA3C004, MOP0B08 , WEPOB05, WEPOB48
Doolittle, L.R.	SUP009, SUP052, TUPOA08, TUPOA14, TUPOA39, TUPOA40, TUPOA41, FRA2I002
Doose, C.L.	TUB4C004, WEPOB03, WEPOB09, THA1C006
Doran, D.S.	SUP049, TUPOA13, WEPOB19, WEPOB20
Dorda, U.	TUA4I002
Douglas, D.	WEA2C004, WEPOA61
Downer, M.	TUPOA28, WEPOA58
Downey, J.S.	WEPOB09
Draganic, I.N.D.	MOA3C003
Drees, K.A.	MOA3I001, M0B3C003
Drury, M.A.	THA1I002
Du, Q.	SUP052, TUPOA39, TUPOA41
Du, Y.-C.	THPOA55
Dudas, A.	MOP0B58, FRA1C005
Dudnikov, A.V.	WEPOA44
Dudnikov, V.G.	WEPOA44, WEPOA45
Dudnikova, G.	WEPOA45
Duel, K.L.	MOP0B28
Duffy, L.D.	WEPOB39
Dunham, B.M.	TUPOA59, WEPOA61
Dunne, A.M.	MOPLI003
Duris, J.P.	SUP045, WEPOB40

— E —

Eddy, N.	TUPOA17 , TUPOA19, TUPOA24, TUPOA29
Edelen, A.L.	SUP010, MOP0B17, TUPOA51 , TUA3C003, TUPOA43
Edelen, J.P.	SUP010, MOP0B17, TUPOA18 , TUPOA51, WEPOB25, WEPOB26
Edstrom, D.R.	TUPOA19 , TUPOA25, TUPOA26, TUPOA73, THPOA22
Eichhorn, R.G.	MOP0B60, WEPOA61
Einstein, J.	TUPOA52 , TUPOA18
Eldred, J.S.	THPOA19
Elementi, L.	MOP0B22, TUPOA20
Ellison, J.S.	WEPOA34
Ellsworth, L.	TUP0B24, TUP0B25
Elsayed-Ali, H.	MOP0B68
Emery, L.	WEPOB04
Emma, C.	SUP011, TUB3C003

Emma, P.	WEPOB30, THA1C006, THPOA32
England, R.J.	WEPOA32
Ent, R.	MOPLI004
Erdelyi, B.	SUP001, SUP013, TUP0B14, TUP0B15, THPOA68, TUP0B04
Eremeev, G.V.	SUP034, WEB1C002
Erickson, J.L.	TUB4I001
Erwin, L.	WEPOB48
Esposito, L.S.	WEPOA07
Evans, N.J.	MOA2I001

— F —

Fagerberg, G.	WEPOA40
Faillace, L.	MOA4C004
Fanucci, L.	SUP054, FRA2C003
Fedotov, A.V.	TUP0B56, TUP0B58, WEA4C005 , WEPOB54, WEPOB56, WEPOB61, WEPOB62, WEPOB68
Fedurin, M.G.	TUP0A72 , WEPOA24, WEPOA58, WEPOB46
Feinberg, E.	WEPOA29
Fellenz, B.J.	TUP0A19, TUP0A29
Feng, G.	TUB2C004
Fernandes, H.C.	WEPOB57
Ferracin, P.	WEB1TU01
Ferrari, E.	TUB2I002
Feschenko, A.	MOA3C003
Figora, M.	WEPOA40
Filatov, Y.	TUP0B30
Filippetto, D.	TUP0A39
Fiorito, G.	FRA1C003
Fischer, J.F.	WEPOB44
Fischer, W.	MOA3I001, MOB3C003, TUP0B56, WEA4C005
Fitsos, P.	THB3I001
Fitterer, M.	WEA1C004
Fitton, M.D.	MOP0B14
Fitzgerald, J.	TUP0A29
Folz, C.	WEPOB60
Fonseca, R.A.	WEPOA49
Forest, T.A.	WEPOA47
Forster, M.J.	TUP0A57, TUP0B22
Fortgang, C.M.	MOA3C003
Foster, G.W.	THPLI001
Franck, D.	MOP0B25
Freemire, B.T.	SUP024, MOP0B52 , TUP0A44, FRA1C005
Friedman, A.	WEPOA29
Frisch, H.J.	WEPOB52
Froemming, N.S.	WEPOA46
Fronk, T.T.	SUP012, TUP0B26, TUP0B27
Fry, A.R.	SUP022, WEPOB49
Fu, W.	WEPOB59, WEPOB60
Fuchsberger, K.	MOB3I002
Fuerst, J.D.	TUB4C004, THA1C005
Fuerst, J.F.	THA1C006
Fukasawa, A.	WEPOB42
Fukuda, M.K.	MOP0B03, THPOA51 , THPOA52
Fulkerson, M.	WEPOA24
Funakoshi, Y.	MOB3I001
Furuta, F.	MOP0B60 , MOP0B61 , MOP0B62, MOP0B66
Fuwa, Y.	MOP0B04 , WEPOA04
Fystro, G.I.	WEPOB04

— G —

Gai, W.	SUP049, TUA2I002, TUP0A13, WEPOB19, WEPOB20, THPOA08, THPOA55
Gaidash, V.	MOA3C003

Gao, Q.	THPOA08
Gao, W.W.	TUP0B01, THPOA57 , THPOA58
Gao, Y.	THPOA54
Gaowei, M.	WEPOB52 , THPOA41
Garcia, F.G.	MOA4I002
Gardner, C.J.	MOB3C003
Garnett, R.W.	MOA3C003
Garson, A.B.	TUP0A27
Gassner, D.M.	MOA3I001, MOB3C003, WEPOB54, WEPOB60, WEPOB61
Gaudreau, M.P.J.	MOP0B44, MOP0B45 , MOP0B46, TUP0B09
Gavryushkin, D.I.	MOP0B72
Ge, G.M.	MOP0B60, MOP0B61, MOP0B62 , MOP0B64
Gee, A.J.	SUP013 , TUP0B15
Geelhoed, M.G.	TUP0A21
Geometrante, R.	TUP0A03 , FRA1C003
Gerity, J.	MOB2C003, MOP0B54, TUA1C004, TUA3C003, TUP0B13
Ghosh, A.K.	MOP0B49
Giachino, R.	MOB3I002
Gianfelice-Wendt, E.	WEPOA17
Gibson, D.J.	SUP018, TUP0A61 , WEPOB35, WEPOB38, THB3I001
Gilevich, S.	SUP022, WEPOB43, WEPOB49
Gilson, E.P.	WEPOA29
Gimpel, T.L.	THB3C003
Giovannozzi, M.	MOB3I002
Gluskin, E.	TUB4C004, WEPOB23, THA1C006
Godfrey, B.B.	WEPOA30
Goel, A.	MOA4C004
Gohdo, M.	FRA1C006
Gonin, I.V.	TUP0A22 , WEB3C003, WEPOB27
Gonnella, D.	MOP0B60, MOP0B65
Gorelov, D.	WEPOA47, WEPOB37
Gorev, V.V.	TUP0A11
Gourlay, S.A.	MOP0B49, THA2I001
Grange, J.M.	WEPOA26
Grassellino, A.	SUP008, MOP0B19, MOP0B20, MOP0B34, THA1I001
Grebe, A.V.	TUP0A32
Green, A.T.	TUP0A46 , TUP0B18, WEPOA39, WEPOA40
Grimm, C.J.	WEB3C003
Grimm, T.L.	MOP0B67, WEPOA47, WEPOB37
Grimmer, J.H.	THPOA62
Grote, D.P.	WEPOA29
Gruber, T.	MOP0B61, MOP0B62
Gschwendtner, E.	SUP047, WEPOA09
Gu, X.	MOA3I001, MOB3C003
Guertg, M.W.	SUP011, TUB3C003
Guinchard, M.	MOP0B14
Gulliford, C.M.	TUP0B58
Gupta, L.	SUP014 , WEPOB32
Gupta, R.C.	MOP0B49

— H —

Ha, G.	SUP031, THPOA46, WEPOB20
Ha, K.	MOA2I002
Ha, T.	MOP0B78
Haber, I.	SUP036, SUP055, TUP0A45, TUP0B11, TUP0B12
Hahn, H.	THPOA54
Hajima, R.	THPOA50
Halavanau, A.	SUP015 , TUP0A19, TUP0A48, TUP0B16 , THPOA22
Halinski, J.	WEPOB54
Hall, C.C.	TUP0B10, TUP0B13, WEA2I002, WEPOA31, WEA4C002 , THPOA23, THPOA28, THPOA37 , THPOA38, THPOA39
Hall, D.L.	MOP0B63 , MOP0B66

Hall, M.	THB3I001
Hall, P.	SUP016, TUP0A23
Hamdi, K.	MOA3I001, WEP0B54, WEP0B58
Han, B.	WEP0A45
Hanna, B.M.	TUP0B64, WEP0A15
Hanuka, A.	WEP0A32
Hao, H.	SUP021, SUP053, TUP0B01, TUP0B19, WEP0B33
Hao, Y.	SUP040, MOB3C003, MOP0B76, TUP0B56, TUP0B59, TUP0B62, WEP0B59, WEP0B60, WEP0B67
Harder, D.A.	WEP0B57
Harkay, K.C.	MOA3C004, MOP0B07, WEA1C003, WEP0B05 , THA1C006, THP0A14
Harms, E.R.	SUP044, MOP0B50, TUP0A19
Harris, J.R.	WEP0B25, WEP0B26
Hart, T.L.	MOB3C004, TUP0B44
Hartsell, B.D.	MOP0B14, MOP0B35, WEP0A15
Hartzell, J.J.	MOP0B72, TUP0A68, TUB3C004, WEP0B48
Harvey, M.	MOB3C003, WEP0B59, WEP0B60
Hasse, Q.B.	THA1C005, THA1C006
Hayano, H.	MOP0B61
Hayes, T.	MOB3C003, WEP0B59, WEP0B60
Hazelwood, K.J.	WEP0A16
He, H.	SUP003, TUP0A58
He, T.	SUP053, WEP0B33
He, Y.	THA3C003
Hearth, S.N.	WEA2C003
Hemelseoet, G.H.	MOB3I002
Henderson, C.	MOP0B62
Henderson, S.	THB3I002
Hernalsteens, C.	WEP0A08
Hershcovitch, A.	TUP0B56
Hettel, R.O.	TUB2I001
Hetzel, C.	TUP0B50
Hidaka, Y.	MOA2C003 , TUP0B48, TUP0B49, TUP0B52
Hidas, D.A.	WEP0B53 , WEP0B57
Higuera, A.V.	THP0A43
Hirshfield, J.L.	WEP0A21
Hock, J.	MOA3I001
Höfle, W.	MOB3I002
Hoffstaetter, G.H.	MOP0B60, WEP0A61, WEP0A62
Hogan, M.J.	TUA3I002
Hogstrom, H.R.	SUP027, TUP0A38
Holland, K.	MOP0B55
Hollister, J.L.	WEP0A47
Holmes, S.D.	THA3I001
Holtzapple, R.	TUP0B22
Holzbauer, J.P.	MOP0B32, MOP0B33, FRA2C004
Honda, Y.	MOP0B03, THP0A50, THP0A51
Hoyt, J.E.	MOP0B11
Hoyt, K.J.	MOP0B72
Hsu, K.T.	TUP0A12
Hu, K.H.	TUP0A12
Huang, G.	SUP009, SUP052, TUP0A08, TUP0A39, TUP0A40 , TUP0A41, TUP0A42, FRA2I002
Huang, H.	MOB3C003
Huang, R.	THP0A56
Huang, W.-H.	THP0A55
Huang, X.	FRA2I001
Huang, X.	TUP0A06
Huang, Y.L.	SUP017, THA2C004
Huang, Z.	SUP022, WEP0B30, WEP0B43, WEP0B49
Hulsart, R.L.	MOB3C003, TUP0B55, WEP0B60
Humphry, F.	THA1I002
Hurh, P.	MOP0B13, MOP0B14, MOP0B23 , MOP0B35
Hussain, A.	MOP0B55

Hwang, K.	WEPOA28 , WEPOB29
Hwang, Y.	SUP018 , WEPOB35 , WEPOB38
Hylen, J.	MOP0B35, WEPOA43
Hyun, J.	TUP0A19, TUP0A73

— I —

Ibrahim, A.	TUP0A16
Ida, Y.I.	MOP0B61
Igarashi, D.	THP0A53
Ikeda, S.	MOA4I001
Ikeda, S.	WEPOA56 , WEPOA57
Ikegami, M.	TUA1I001
Ingrassia, P.F.	MOB3C003
Insepov, Z.	TUP0A49
Ischebeck, R.	FRA1I002
Ivanyushenkov, Y.	TUB4C004, THA1C005, THA1C006 , THP0A69
Iwashita, Y.	MOP0B04, WEPOA04
Izquierdo Bermudez, S.	MOP0B41

— J —

Jackson, A.	THB3C003
Jacobson, B.T.	TUP0A68, WEPOB48
Jacquet, D.	MOB3I002
Jain, A.K.	MOP0B49, TUP0B60, WEPOB03, WEPOB09, WEPOB64
Jain, V.	WEB3C003
Jamilkowski, J.P.	MOB3C003, MOA4I001, WEPOB54, WEPOB59, WEPOB60
Jansma, W.G.	WEPOB03, WEPOB70
Jaski, M.S.	WEPOB03, WEPOB09, THP0A63
Jaski, Y.	THP0A62
Jeon, D.	MOP0B78
Ji, Q.	WEPOA29
Ji, Y.	SUP019 , TUP0B63 , THP0A45
Jia, Q.G.	THB3C004
Jia, Q.K.	THP0A56
Jimbo, K.	WEPOA03
Jing, C.-J.	TUA2I002, WEPOB19, WEPOB20, THP0A08
Jing, Y.C.	WEPOA58, WEPOB59, WEPOB60, WEPOB67
Johansson, M.A.G.	MOP0B06 , MOP0B80 , TUP0A09, THA1C003 , THP0A64
Johnson, M. S.	THB3I001
Johnson, M.B.	THB3C003
Johnson, R.P.	SUP024, MOP0B52, MOP0B58, TUA2C003, TUP0A44, TUP0A56 , TUP0B32, TUP0B35, WEPOA45, WEPOA54, WEPOB34, FRA1C005, FRB2I003
Johnstone, C.	TUP0A36
Johnstone, J.A.	TUP0A36, WEPOA41
Jones, K.W.	TUA1I003
Joo, J.	MOP0B62
Joshi, C.	WEPOA50

— K —

Kaganovich, I.	WEPOA29
Kahn, S.A.	MOP0B58 , WEPOB34
Kan, K.	FRA1C006
Kanareykin, A.	TUP0B02, TUP0B03
Kanesue, T.	MOA4I001, WEPOA56, WEPOA57
Kang, Y.W.	MOP0B71, WEPOA52
Kankiya, P. K.	WEPOB59, WEPOB60
Kapin, V.V.	WEPOA18 , WEPOA19 , WEPOA20 , THP0A15
Karaś, K.	MOP0B06, MOP0B80, TUP0A09, THA1C003
Karkare, S.S.	THP0A42
Karppinen, M.	MOP0B41
Kasa, M.	TUB4C004 , THA1C006, THP0A69

Kashikhin, V.V.	MOP0B42, THA1C004
Kasper, P.H.	MOP0B35
Kato, S.	MOP0B61
Kaufman, J.J.	MOP0B61, MOP0B63, MOP0B64, MOP0B66
Kautz, N.A.	MOP0B77
Kayran, D.	TUP0B58, WEA4C005, WEPOB54 , WEP0B56, WEP0B59, WEP0B60, WEP0B61, WEP0B62, WEP0B67
Kazakevich, G.M.	SUP024, TUA2C003 , TUP0A44, WEP0B34, FRA1C005
Kazakov, S.	MOP0B24 , WEP0A21, WEP0B27
Kedzie, M.	WEP0A11
Kellams, J.N.	MOB2C003, MOP0B54
Kellermann, R.	WEP0B59, WEP0B60
Kellett, R.J.	MOP0B25
Kelley, M.J.	SUP034, WEB1C002
Kelly, M.P.	WEB2I001 , WEP0A11
Kempkes, M.K.	MOP0B44, MOP0B45, MOP0B46, TUP0B09
Kendziora, K.R.	MOP0B25
Kephart, R.D.	TUP0A22
Kerby, J.S.	THP0A63
Kersevan, R.	THP0A34
Kewisch, J.	TUP0B58, WEA4C005, WEP0B54, WEPOB55 , WEPOB56 , WEP0B62, WEP0B68
Khabiboulline, T.N.	MOP0B15, MOP0B16, MOP0B33, TUP0A22, TUP0B03, WEB3C003, WEPOB27 , THP0A21
Khan, S.A.	THP0A10 , THP0A11 , THP0A12
Khare, P.	MOP0B36
Khorshidi, A.	TUP0A02
Kim, J.-W.	MOP0B62, WEP0A05
Kim, J.H.	MOP0B78
Kim, K.-J.	SUP014, WEP0B32
Kim, S.-C.	WEP0A26, WEPOA46
Kim, S.H.	WEPOB06
Kim, S.H.	MOP0B09 , WEP0A11
Kim, W.K.	MOP0B62
Kim, Y.	THP0A59
Kim, Y.K.	MOPLI002 , WEP0A62
King, L.K.	THA1I002
Kinross-Wright, J.	MOP0B45, TUP0B09
Kirchen, M.	WEP0A30
Kireeff Covo, M.	THB3C003
Kiselev, Yu.V.	MOA3C003
Kishek, R.A.	WEA2I002, WEP0A31, WEA4C002, THP0A28, SUP041, MOP0B53, TUP0A45
Kitegi, C.A.	WEPOB57
Knapp, D.J.	TUP0A63
Kobak, P.	TUP0A19
Kochemirovskiy, A.V.	MOP0B26 , MOP0B52
Koeth, T.W.	SUP036, SUP055, TUP0A45, TUP0B11, TUP0B12, WEP0A08
Kolski, J.S.	TUP0B27
Kondoh, T.	FRA1C006
Kondrashev, S.A.	WEPOA05
Kondratenko, A.M.	TUP0B30
Kondratenko, M.A.	TUP0B30
Kononenko, O.	MOB2C004
Korbly, S.E.	THB2I001
Korenev, S.	TUP0A60
Korysko, P.	SUP020 , TUP0B53
Koshiba, Y.	THP0A53
Kostin, R.A.	TUP0B02 , TUP0B03
Kosuge, A.	THP0A50
Kotelnikov, S.	MOP0B27
Kotur, M.	THP0A66
Koufalis, P.N.	MOP0B64
Kourbanis, I.	WEP0A14, WEP0A16, THA3I001
Krafczyk, G.E.	MOP0B35
Krafft, G.A.	WEP0B45

Krasnov, A.A.	WEB4C004
Król, P.	TUP0A09
Kucera, M.J.	TUP0A19
Kuharik, J.	MOP0B28
Kuksenko, V.I.	MOP0B14
Kunz, J.D.	WEPOA37
Kuroda, R.	TUP0A04
Kusche, K.	TUP0A72, WEPOA24, WEPOA58
Kustom, R.	WEPOB07
Kutsaev, S.V.	MOA4C004, TUP0A68 , TUB3C004 , TUP0B40
Kwiatkowski, S.	MOP0B47
Kwon, S.	TUP0A63
Kwon, Y.K.	WEPOA05

— L —

Lajoie, A.	TUA3C003
Lambiase, R.F.	MOA4I001, WEPOA57
Lamont, M.	MOB3I002
Lancelot, J.L.	MOP0B46
Lari, L.	WEPOA07
Laster, J.S.	MOB3C003
Laurich, A.	TUP0A68
Lawler, G.	TUA3C003
Le Bec, G.	THA2I002
Lebedev, V.A.	TUA2C003, WEPOA17, WEPOA19, WEPOA20, WEPOA38, WEA4C004, THA3I001
Lee, A.	MOP0B35
Lee, D.	TUP0A12
Lee, H.-S.	TUP0A10
Lee, J.	TUP0A10
Lee, J.	MOP0B62
Lee, P.	WEPOA30
Lee, S.W.	MOP0B71 , WEPOA52
Lee, T.-Y.	TUP0A10 , THPOA60 , THPOA61
Leemann, S.C.	TUB2I001, TUB3I001
Lehé, R.	WEPOA30
Lehn, D.	MOA4I001
Leibfritz, J.R.	TUP0A19
Lenkszus, F.	WEPOB24
Lerch, J.E.	MOP0B10
Leveling, A.F.	TUP0A32
Lewandowski, J.R.	WEPOB43
Lewellen, J.W.	WEPOB25, WEPOB26, WEPOB39
Li, B.	SUP021 , TUP0B19
Li, D.	MOP0B48, THPOA33
Li, F.	WEPOA49, WEPOA50
Li, G.	MOP0B05
Li, H.	WEPOA58
Li, H.T.	THPOA57
Li, J.J.	WEPOA24
Li, J.Y.	SUP021, TUP0B19
Li, R.	SUP046, TUB1TU01 , TUP0B28 , WEA2C004, THPOA35
Li, S.	SUP022 , WEPOB49
Li, W.	TUP0B01 , THPOA57, THPOA58
Li, Y.	WEPOA61
Li, Y.	TUP0B54 , WEPOB65
Li, Y.S.	SUP023 , TUP0B37
Li, Z.	MOB2C004
Liao, C.Y.	TUP0A12
Liaw, C.J.	MOA4I001, WEPOA57, WEPOB54, WEPOB58
Licciardi, W.	WEPOB57
Liepe, M.	MOP0B60, MOP0B61, MOP0B62, MOP0B63, MOP0B64, MOP0B65, MOP0B66

Lill, R.M.	MOP0B11
Limberg, T.	TUB2C004
Lin, F.	MOA4C003, TUP0B29 , TUP0B30, TUP0B31
Lindau, F.	THP0A66
Lindberg, R.R.	SUP014, SUP038, MOP0B11, TUB2C003 , TUP0B51, WEA1C003, WEP0B08 , WEP0B14, WEP0B32, WEP0B48, THP0A47
Lishilin, O.	TUA3C003
Litvinenko, V.	SUP026, SUP029, MOB3C003, WEP0A55, WEP0A58 , WEP0A59 , WEP0B50, WEP0B59, WEP0B60, WEP0B67, THP0A44
Liu, A.	MOA2C004 , WEP0A22
Liu, C.	MOB3C003, TUP0B55 , WEP0B68 , WEP0B69
Liu, J.	WEP0B03, WEP0B09
Liu, N.	TUP0A16, TUP0A24
Liu, Q.	SUP024 , TUP0A44 , FRA1C005
Liu, W.	SUP049, TUP0A13, WEP0B20
Liuzzo, S.M.	THP0A65
Lobet, M.	WEP0A30
Losito, R.	MOP0B14
Lotov, K.V.	SUP047, WEP0A09
Lou, W.	WEP0A61
Loveridge, P.	MOP0B14
Lu, Q.	THP0A18
Lu, T.	TUP0A32
Lu, W.	WEP0A49, WEP0A50, WEP0A58
Lu, X.Y.	SUP025 , WEP0A33
Ludewigt, B.A.	WEP0A29
Lumpkin, A.H.	MOP0B08, TUP0A19, TUP0A25 , TUP0A26 , TUP0A27 , TUP0A28 , TUP0B18
Lund, S.M.	SUP050, WEA4I001
Lundberg, B.G.	MOP0B35
Lunin, A.	WEP0B27, THP0A21
Luo, T.H.	MOP0B47 , MOP0B48 , THP0A33
Luo, Y.	MOA3I001, MOB3C003, TUP0B56
Lutman, A.A.	SUP011, TUB3C003, WEP0B43
Lyles, J.T.M.	TUP0A63

— M —

Ma, H.	TUP0A14
Ma, J.	SUP026 , WEP0A55
Macha, K.	MOP0B68, WEP0B44
Macridin, A.	WEA4C003
Madrak, R.L.	MOP0B28 , MOP0B29
Maggi, P.E.	SUP027 , TUP0A38
Mahler, G.J.	TUP0B60, WEP0A61, WEP0B54, WEP0B59, WEP0B60, WEP0B61
Makasyuk, I.V.	WEP0A32
Makulski, A.	MOP0B27
Malone, R.	WEP0A24
Maloy, S.A.	WEP0A47
Malyzhenkov, A.	TUP0A62 , TUB4C003
Mamtimin, M.	WEP0A47
Maniscalco, J.T.	MOP0B65
Mansten, E.	THP0A66
Mapes, M.	MOB3C003, WEP0B58, WEP0B59, WEP0B60
Marchionni, A.	MOP0B35
Marinelli, A.	SUP011, TUB3C003
Marr, G.J.	MOB3C003
Marsh, R.A.	SUP018, TUP0A61, WEP0B35, WEP0B38 , THB3I001
Marshall, M. S. J.	WEP0B52
Marti, F.	MOP0B55
Martin Yebra, A.	TUP0A60
Martinello, M.	SUP008, SUP028 , MOP0B19, MOP0B20, MOP0B34, WEB1C003
Marusic, A.	MOA3I001, MOB3C003

Matthew, D.B.	SUP055, TUP0B11
Matthews II, K.L.	SUP027, TUP0A38
Maxson, J.M.	SUP033, THA2C003
Maxwell, T.J.	SUP011, TUB3C003, WEA1I001
Mayes, C.E.	MOP0B59, WEPOA61
McCafferty, D.R.	MOA4I001
McCarter, J.L.	WEPOA47, WEPOB37
McCaughan, M.D.	THA1I002
McCrary, R.C.	MOA3C003, TUP0A64, TUP0B27
McIntyre, G.T.	MOB3C003
McIntyre, P.M.	MOB2C003, MOP0B54, TUA1C004, TUP0B13
McNevin, J.D.	TUP0B39, TUP0B42
Mead, J.	MOA2I002
Melnychuk, O.S.	MOP0B34
Meng, W.	WEPOB61
Méot, F.	SUP020, TUP0B53, TUP0B60, WEPOA61, THPOA40
Mereghetti, A.	WEPOA07
Merio, M.	WEB2C004
Mernick, K.	MOB3C003, TUP0B55, WEPOB59, WEPOB60
Meshcheryakov, N.D.	TUP0A60
Miahnahri, A.	SUP022, WEPOB49
Miao, C.M.	TUA4C004
Michnoff, R.J.	MOB3C003, TUP0B55, WEPOA61, WEPOB60
Migliorati, M.	THPOA34
Mihalcea, D.	TUP0A19, TUP0A73
Mihara, K.	WEPOB59, WEPOB60, SUP029, WEPOB50
Mikhailov, S.F.	SUP053, WEPOB33
Milana, D.	THA3C004
Miller, K.E.	MOP0B79
Miller, M.	WEPOA08
Miller, T.A.	MOA3I001, WEPOB54, WEPOB59, WEPOB60, WEPOB62
Milner, R.	MOPLI004
Milton, S.V.	SUP010, SUP042, SUP043, MOP0B17, MOP0B56, MOP0B57, TUP0A51, TUP0A52, TUP0A53, WEPOA42, WEPOA43, THPOA37, FRA1C003, TUP0A43
Minty, M.G.	MOA3I001, MOB3C003, TUP0B55, TUP0B58, WEPOA61, WEPOB68
Mishra, C.S.	WEB3C003
Mitchell, C.E.	THPOA28, THPOA32
Mitchell, D.V.	WEB3C003
Miyamoto, R.	WEPOA07
Mocella, V.	FRPLI001
Moens, V.	TUP0B13
Mohayai, T.A.	SUP030, WEPOA35, WEPOA36
Mokhov, N.V.	MOP0B35, TUP0A32, TUP0A33, WEPOA16, WEPOA18, WEPOA20
Montag, C.	MOB3C003, TUP0B56
Moon, K.	TUA3C003
Moore, C.D.	MOP0B35
Moretti, A.	SUP024, MOP0B52, TUP0A44, FRA1C005
Morgan, J.P.	THPOA27
Mori, M.	THPOA50
Mori, W.B.	WEPOA48, WEPOA49, WEPOA50, WEPOA58
Morozov, V.S.	MOB2I002, MOA4C003, TUP0B05, TUP0B29, TUP0B30, TUP0B31, TUP0B32, TUP0B35, WEPOA54
Morris, D.K.	WEPOA16
Morris, J.	MOB3C003, MOA4I001
Morrison, L.H.	WEPOB24
Morse, W.	THPOA27
Motta, C.C.	MOP0B02
Muggli, P.	TUA2I001, WEPOA01, WEPOA02, TUA4C003
Muller, E.M.	WEPOB52, THPOA41
Munderville, M.G.	MOP0B44, MOP0B45, MOP0B46, TUP0B09
Munroe, B.J.	SUP051, WEPOB31
Murokh, A.Y.	MOP0B72, TUP0A68, TUP0A69, WEPOB46, WEPOB48, TUB3C004
Murrey, S.	WEPOA45

Musardo, M.	WEP0B57
Musson, J.	MOP0B68
Mustapha, B.	MOA4C004, MOB4C004, TUP0B04 , TUP0B05
Musumeci, P.	SUP033, SUP045, WEP0B40, THA2C003

— N —

Nagai, R.	THP0A50
Nagaitsev, S.	SUP006, TUA3I001 , WEA1C006, WEA2I002, THP0A48, THP0A49
Nagaoka, R.	WEA3C004
Narayan, G.	WEP0B59, WEP0B60
Nassiri, A.	MOA4C004, TUP0A14, TUB3C004, WEP0B07
Naulleau, P.	TUP0A69
Nayak, S.K.	WEP0B54
Naylor, C.	MOB3C003
Nemesure, S.	MOB3C003
Neubauer, M.L.	MOP0B58, TUA2C003, TUP0A56, FRA1C005
Neuffer, D.V.	SUP030, TUP0B06 , TUP0B44, WEP0A23, WEP0A35 , WEP0A36, WEP0A53
Neveu, N.R.	SUP031 , THP0A46
Nguyễn Điền, Q.B.	THP0A67
Nichols, K.E.	TUP0A62
Nicklaus, D.J.	TUP0A19
Nicol, T.H.	MOP0B36, WEB3C003
Niell, F.M.	MOP0B45
Nietubyc, R.	MOP0B06, MOP0B80, THA1C003
Nietubyc, R.	TUP0A09
Nii, K.N.	MOP0B61
Ninemire, B.	THB3C003
Nisbet, D.	MOB3I002
Nishida, M.	TUP0A04
Nissen, E.W.	TUP0B33 , TUP0B34
Nobrega, A.	MOP0B41
Nogiec, J.M.	MOP0B27
Noonan, J. R.	MOP0B11
Norem, J.	TUP0A49
Normann, L.	MOB3I002
Nosochkov, Y.	MOA4C003, TUP0B29, TUP0B31
Novitski, I.	MOP0B30, MOP0B41, MOP0B42, TUP0A33
Nozawa, I.	FRA1C006

— O —

O'Connell, T.I.	MOP0B60, MOP0B62
O'Dell, J.	MOP0B14
O'Hara, J.F.	MOA3C003
O'Shea, F.H.	TUP0B39, TUP0B42 , WEP0B47 , WEP0B48
Ohnishi, Y.	MOB3I001
Ohta, S.	THP0A53
Oide, K.	MOB4I001
Okamura, M.	MOA4I001 , WEP0A56, WEP0A57
Olivas, E.R.	WEP0A47
Oliveros, S.J.	MOB3C004 , TUP0B44
Olsen, R.H.	MOA4I001
Olsen, V.K.B.	TUA4C003
Orfin, P.	WEP0B60
Orlov, Y.O.	MOP0B36
Ostroumov, P.N.	MOA4C004 , MOB4C004, TUP0B04, TUP0B05, WEP0A11
Ovodenko, A.G.	WEP0B46
Öz, E.	WEP0A01

— P —

Padmore, H.A.	WEP0B52, THP0A42
Pakter, R.	THP0A02

Palastro, J.	TUA4C004
Palczewski, A.D.	MOP0B70
Palmer, M.A.	TUP0B06, WEPOA24 , THB2I003, WEPOA23
Palmer, R.B.	TUP0B56
Palmowski, A. J.	WEPOB47
Paniccia, M.C.	WEPOB59
Papadimitriou, V.	SUP024, MOP0B35, TUP0A44
Papaphilippou, Y.	TUP0B17
Papotti, G.	MOB3I002
Parise, M.	MOP0B31
Park, C.S.	TUP0B13, THA3C004
Park, Y.H.	WEPOA05
Parker, B.	TUP0B56
Parkhomchuk, V.V.	WEPOA06
Pasky, S.J.	WEPOB48
Patapenka, A.S.	TUP0B17
Patch, S.K.	THB3C003
Patel, N.	TUP0A29
Patrick, R.J.	WEB4C004
Patterson, J.R.	WEPOA61, WEPOA62
Pavlovic, Z.	WEPOA26
Pavlovsky, I.	TUP0A60
Peggs, S.	TUP0B56, WEPOA61
Pekrul, W.E.	WEPOB59
Pellegrini, C.	SUP011, TUB3C003
Pellemoine, F.	WEB2C003
Pellico, W.	MOA4I002, MOP0B28, MOP0B29, WEPOA18
Penn, G.	THP0A28
Pennisi, T.R.	WEPOA45
Peralta, E.A.	WEPOA32
Perrin, J.D.	WEA2C003
Persaud, A.	WEPOA29
Persichelli, S.	MOP0B47, MOP0B48, THP0A33 , THP0A34
Petersen, T.B.	TUP0A30 , TUP0A31
Peterson, D.W.	MOP0B52
Petit, E.	TUA1I002
Petrenko, A.V.	SUP047, WEPOA09
Petrushina, I.	SUP032 , TUP0A70 , WEPOB59, WEPOB60
Pfeffer, H.	MOP0B39
Phair, L.	THB3C003
Pham, A.N.	TUA1C005
Phillips, D.	WEPOB60
Phillips, H.L.	MOP0B68, MOP0B70
Pierre, C.	WEPOA07
Pikin, A.I.	MOA3I001, MOA4I001
Pilat, F.C.	MOA4C003, TUP0B29, TUP0B31
Piller, C.	WEPOA45
Pinayev, I.	SUP029, MOB3C003, WEPOB50, WEPOB59 , WEPOB60 , WEPOB67
Piot, P.	SUP015, TUP0A47 , TUP0A48 , TUP0B16, WEPOA38, TUP0A19, TUP0A73
Pirez, E.	SUP033 , THA2C003
Pischalnikov, Y.M.	MOP0B32 , MOP0B33 , WEB3C003, FRA2C004
Plastun, A.S.	MOA4C004, MOB4C004
Plum, M.A.	TUA1I003
Podobedov, B.	MOA2I002, MOA2C003, TUP0B52
Pogorelov, I.V.	THP0A40, THP0A44
Pogorelsky, I.	WEPOA58, WEPOB46, THB2I003
Pogue, N.	MOB2C003, TUA1C004
Pojer, M.	MOB3I002
Polikhov, S.A.	WEB4C004
Polyanskiy, M.N.	WEPOA58, WEPOB46
Ponce, L.	MOB3I002
Ponter, T.S.	WEPOA08

Popov, V.	SUP053, WEP0B33
Popović, S.	MOP0B70
Poprocki, S.	TUP0B23, WEA2C003
Porter, R.D.	MOP0B63, MOP0B66
Portmann, G.J.	MOA2I002
Posen, S.	SUP008, MOP0B20, MOP0B34, WEB2C004
Power, J.G.	SUP031, SUP049, TUA2I002, TUP0A13, WEP0B19, WEP0B20, THP0A08, THP0A46
Pozdeyev, G.	TUA1I001
Prager, J.	MOP0B79
Prebys, E.	TUP0A19, WEA2I002, THP0A28
Prestemon, S.	WEB1TU01
Prieto, P.S.	TUP0A19
Prokop, M.S.	TUP0A63
Pronitchev, O.V.	MOP0B24
Pronskikh, V.S.	TUP0A32, TUP0A33, TUP0A34
Prost, L.R.	TUP0B64, TUP0B66, WEP0A15
Ptitsyn, V.	MOB4I002, MOP0B76, TUP0B56, TUP0B60, WEP0A61
Pudasaini, U.	SUP034, WEB1C002
Pulampong, T.	THP0A65
Pushka, D.	MOP0B35

— Q —

Qadadha, Y.M.	THB3C003
Qiang, J.	TUP0B62, WEP0A28, WEA3I002, WEP0B29, WEP0B30, THP0A32
Qiang, Q.	TUP0A42
Qin, Q.	MOB4I001
Qiu, J.Q.	SUP049, TUP0A13
Quigley, P.	MOP0B60

— R —

Raab, F.H.	MOP0B51
Raimondi, P.	THP0A65
Rakhno, I.L.	MOP0B35
Ramanathan, M.	THP0A62
Rangacharyulu, C.	THP0A67
Ranjbar, V.H.	MOB3C003, TUP0B56, TUP0B57, WEA2I001, THP0A40
Rank, J.	WEP0B57
Rao, T.	WEP0B54, WEP0B58, WEP0B59, WEP0B60, WEP0B67, THP0A41
Raparia, D.	MOB3C003
Ratner, D.F.	SUP022, WEP0B30, WEP0B49
Ratti, A.	TUP0A14
Raubenheimer, T.O.	WEP0B30
Ravaioli, E.	WEB4I002
Ravikumar, D.	SUP035, MOP0B73
Ready, R.	TUA1C005
Redaelli, S.	MOB3I002
Reece, C.E.	SUP034, WEB1C002
Rees, D.	TUP0A63
Reid, J.	MOP0B28, TUP0A19
Reid, T.	WEP0A11
Reitzner, S.D.	MOP0B35
Rhein, C.	WEP0B57
Rider, N.T.	TUP0A57, TUP0B22
Riemer, K.H.	MOP0B40
Rimmer, R.A.	SUP017, THA2C004
Rizzato, F.B.	THP0A02
Robert-Demolaize, G.	SUP020, MOB3C003, TUP0B53
Roberts, S.G.	MOP0B14
Roberts, T.J.	TUP0A56, TUP0B21, TUP0B38, FRB2I003
Robin, D.	TUB1C003, TUB2I001
Robinson, J.	SUP022, WEP0B49

Roblin, Y.	TUP0B36
Rogacki, A.	MOP0B67
Roger, V.	MOP0B36
Rogers, C.T.	SUP030, WEP0A36
Romanenko, A.	SUP008, MOP0B19, MOP0B20, MOP0B34, MOP0B37, MOP0B38 , MOP0B77, WEB2C004
Romanov, A.L.	WEA2I002, WEP0A31, WEA4C002, THPOA22, THPOA23, THPOA24
Romanov, G.V.	MOP0B28, MOP0B29, THPOA20, THPOA21
Rose, J.	WEP0B65
Rosenzweig, J.B.	SUP004, WEP0B41, WEP0B42, WEP0B46
Roser, T.	MOB3C003, WEP0A61
Rossi, L.	MOP0B41
Roth, I.	MOP0B44, MOP0B46
Rotsch, D.A.	THB2I002
Rowe, A.M.	TUP0B03, WEB3C003
Roy, P.K.	TUP0A64 , TUP0B27
Ruan, J.	TUP0A19, TUP0A25, TUP0A26, WEP0A38
Rubin, D. L.	WEP0A46, SUP003, TUP0A57, TUP0A58, WEA2C003, WEP0B36
Ruelas, M.	TUP0A69, WEP0B48
Ruisard, K.J.	SUP036 , SUP055, TUP0A45, TUP0B11, TUP0B12 , WEP0A08
Rule, D.W.	TUP0A28
Rush, W.D.	TUP0A19, TUP0A73
Rusnak, B.	THB3I001
Russell, S.J.	WEP0B39
Russo, T.	MOP0B55
Rybarczyk, L.	MOA3C003
Ryne, R.D.	TUP0B62

— S —

Sabbi, G.L.	MOP0B49
Sabol, D.M.	MOP0B60
Saeki, T.	MOP0B61
Saewert, G.W.	MOP0B39
Sahai, A. A.	TUA3C003, WEP0A10
Sain, J.D.	THB3I001
Saini, A.	WEP0A60
Saito, Y.	SUP037, TUP0A05
Sajaev, V.	MOA3C004, WEP0B01, WEP0B05, WEP0B10 , WEP0B14
Sakai, Y.	WEP0B46
Sakaue, K.	MOP0B03 , TUP0A04, THPOA51, THPOA53
Salvachua, B.	MOB3I002
Sampson, P.	MOB3C003
Samulyak, V.	SUP026, WEP0A55
San Soucie, J.E.	TUP0B23
Sandberg, J.	MOB3C003
Sangroula, M.P.	SUP038 , MOP0B11, THPOA47
Sannibale, F.	TUB3I002
Santana, M.	WEP0A45
Santucci, J.K.	TUP0A19, TUP0A26
Sattarov, A.	MOB2C003, MOP0B54, TUA1C004
Savard, N.	WEP0A01
Savary, F.	MOP0B41
Savin, E.A.	TUB3C004, TUP0B40, MOA4C004, TUP0A68
Scarpine, V.E.	TUP0A29, WEP0A15
Schappert, W.	TUA2C003, FRA2C004
Schaub, S.C.	TUA2C004
Scheinker, A.	TUP0A63
Schenkel, T.	WEP0A29
Schmalzle, J.	MOP0B74
Schmidt, F.	THPOA15
Schmookler, B.A.	TUP0A57
Schnepp, A.B.	WEP0B37

Schoefer, V.	MOB3C003
Schoepfer, R.	MOA4I001
Schubert, S.G.	WEP0B52
Sears, J.	MOP0B60, MOP0B61, MOP0B62
Segre, C.U.	SUP038, THP0A47
Seidl, P.A.	WEP0A29
Seletskiy, S.	TUP0B56, TUP0B58 , WEA4C005, WEP0B54, WEP0B56, WEP0B61 , WEP0B62
Semenov, A.	TUP0A16
Sen, T.	SUP023, TUP0A19, TUP0A73, TUP0B37
Senor, D.J.	MOP0B13
Sereno, N.	WEP0B48
Sergatskov, D.A.	MOP0B34
Seryi, A.	TUA3C003
Sethna, J.P.	SUP003, TUP0A58
Severino, F.	MOB3C003, WEP0B59, WEP0B60
Shaftan, T.V.	TUP0B50, TUP0B56, WEP0A24, WEP0B46, WEP0B64, WEP0B65
Shang, H.	MOA3C004, WEP0B04
Shanks, J.P.	TUP0B22, WEP0B36
Shapiro, M.A.	SUP025, SUP051, TUA2C004, WEP0A33, WEP0B31
Sharkov, G.B.	WEB4C004
Sharma, M.K.	SUP039 , TUP0A01
Sharma, N.K.	WEB3C003
Shchegolkov, D.Y.	WEP0B39
Sheehy, B.	TUP0B58, WEP0B54, WEP0B59, WEP0B60
Sheffield, R.L.	TUB4I001
Shemyakin, A.V.	TUP0B64, TUP0B66, WEP0A15
Sheppard, J.C.	WEP0B43
Shevelev, M.	THP0A52
Shi, J.	THP0A08
Shih, K.	SUP040 , TUP0B59 , TUA3C003
Shiltsev, V.D.	TUP0A19, TUP0B07 , WEP0A25 , THA3C004
Shin, I.	MOP0B62
Shin, S.	WEP0A12, TUP0A10
Shin, Y.-M.	TUP0A46, TUP0B18 , WEP0A39 , WEP0A40
Shiroyanagi, Y.	THA1C005 , THA1C006
Shizuma, T.	THP0A50
Shrey, T.C.	MOB3C003
Sibener, S.J.	MOP0B77
Siddiqi, M.	SUP041 , MOP0B53
Sides, S.W.	THP0A36
Sidorov, V.I.	MOP0B35, WEP0A16
Siero, C.R.	THB3C003
Silverman, M.S.	WEP0A29
Simakov, E.I.	WEP0A51
Simonyan, A.S.	MOP0B01
Simpson, R.E.	MOP0B44, MOP0B45, MOP0B46, TUP0B09
Sinsheimer, J.	WEP0B52
Sipahi, N.	SUP042 , WEP0A42
Sipahi, T.	SUP043 , MOP0B56 , MOP0B57 , WEP0A43
Sirorattanakul, K.	SUP044 , MOP0B50
Skaritka, J.	WEP0B59, WEP0B60
Skiadopoulos, D.	THA1C006
Skripka, G.	WEA3C004
Slabaugh, M.	MOP0B28, WEP0A18
Slominski, C.J.	WEB4C003
Small, S.M.	THB3C003
Smaluk, V.V.	TUP0B45, TUP0B46, TUP0B48, TUP0B49, TUP0B50, TUP0B51, TUP0B56, WEA1C005, WEP0B65
Smart, L.	WEP0B60
Smedley, J.	WEP0B52, WEP0B63 , THP0A41, THP0A42
Smekens, D.	MOP0B41
Smirnov, A.V.	TUP0B41 , WEP0B48 , MOP0B72 , TUB3C004, TUP0B40
Smirnov, A.Yu.	TUP0A68

Smirnov, I.B.	TUP0A60
Smith, E.N.	MOP0B60
Smith, K.S.	MOB3C003, MOP0B76, WEP0B59, WEP0B60, THP0A54
Smith, M.L.	WEP0B04
Smith, T.L.	TUP0A14, WEP0B11 , WEP0B70
Smithe, D.N.	THP0A42
Smolenski, K.W.	MOP0B59, TUP0A59 , WEP0A61, WEP0B58
Snopok, P.	SUP030, WEP0A34, WEP0A36, WEP0A37, WEP0A35
Snydstrup, L.	WEP0A24
Solfaroli Camillocci, M.	MOB3I002
Solopova, A.D.	THA1I002
Solyak, N.	TUP0A22, TUP0B02, TUP0B03
Son, H.J.	WEP0A05
Son, H.J.	MOP0B78
Sonnad, K.G.	THP0A07
Soong, K.	WEP0A32
Soria, V.	WEP0B60
Sorrell, Z.	WEP0B60
Sosedkin, A.	SUP047, WEP0A09
Souda, H.	WEP0A03
Souza, R.	THB3I001
Spentzouris, L.K.	TUP0B63
Spentzouris, P.	WEA4C003
Spranza, E.	WEP0B47, WEP0B48
Sprau, G.S.	MOP0B12
Stabile, P.	FRB1I002
Stancari, G.	TUP0A19, TUP0B13, WEA1C004, WEA2I002, THA3C004
Stanley, S.	MOP0B62
Starovoitova, V.N.	WEP0A47, WEP0B37
Steck, M.	FRA1I001
Stefanik, A.M.	MOP0B35
Steier, C.	TUB1C003
Steimel, J.	SUP010, MOP0B17, TUP0A51, TUP0B66, WEP0A15
Steinke, S.	TUA4I001
Stepanov, A.D.	WEP0A29
Stern, E.G.	WEP0A16, WEA4C003, THP0A18 , THP0A25
Steszyn, A.N.	MOA4I001, WEP0B58
Stillwell, B.K.	MOP0B07, MOP0B11 , WEP0B17
Stinson, C.	WEP0A45
Stockli, M.P.	WEP0A45
Stoynev, S.	MOP0B40 , MOP0B41
Stratakis, D.	TUP0B06, WEP0A26 , WEP0A46, THP0A27
Strauss, T.	MOP0B41
Strelnikov, N.O.	WEP0B23
Striganov, S.I.	WEP0A20
Stupakov, G.	TUP0A69, TUP0B48
Su, X.L.	THP0A55
Sudar, N.S.	SUP045 , WEP0B40
Sullivan, M.K.	TUP0B29, TUP0B31
Sullivan, T.	WEP0A18
Sulyman, A.A.	WEP0A29
Sumitomo, Y.	THP0A52
Summers, D.J.	MOB3C004, TUP0B06, TUP0B44, WEP0A35
Sun, D.	MOP0B28
Sun, X.	WEP0B16 , WEP0B24
Sun, Y.-E.	TUP0A14, TUB3C004, WEP0A12 , WEP0B25, WEP0B26, WEP0B48
Sun, Y.P.	WEP0B01, WEP0B10, WEP0B12 , WEP0B13 , WEP0B14 , WEP0B15
Suthar, K.J.	SUP048, MOP0B11, WEP0B07, WEP0B17 , WEP0B18
Sutter, D.F.	TUP0A45
Suykerbuyk, R.	MOB3I002
Swinson, C.	TUP0A72, WEP0A24, WEP0A58, WEP0B46
Sy, A.V.	TUP0B32, TUP0B35 , WEP0A54

Syphers, M.J.

MOB2I001, WEP0A41, THPOA27, TUA1C005

— T —

Taebi, B.	TUP0A34
Taira, Y.	TUP0A04
Tajima, T.	SUP018, WEP0B35
Takahashi, T.	THPOA53
Tan, C.-Y.	MOP0B28, MOP0B29
Tanabe, T.	WEP0B57
Tang, C.-X.	THPOA55
Tannous, R.T.	THPOA67
Tantawi, S.G.	SUP004, WEB4I001 , WEP0B41, WEP0B42
Tarazona, D.	TUP0B20
Tariq, S.	MOP0B35
Tavares, P.F.	TUB3I001 , WEA3C004, THPOA64
Tchelidze, L.	WEP0A07
Temkin, R.J.	SUP025, SUP051, TUA2C004, WEP0A33, WEP0B31
Tennant, C.	TUB1TU01, WEA2C004
Teperman, M.R.	SUP055, TUP0B11
Tepikian, S.	MOB3C003, TUP0B56
Terechkine, I.	MOP0B28, MOP0B29
Terunuma, N.	MOP0B03, THPOA50, THPOA51, THPOA52
Teryaev, V.E.	WEP0A21
Tesarek, R.	TUP0A35 , WEP0A18
Than, R.	SUP035, MOB3C003, MOP0B73, WEP0B60
Thangaraj, J.C.T.	TUP0A19, THPOA27, THA3C004
Thieberger, P.	MOA3I001 , MOB3C003, WEP0A61, WEP0B62
Thomas, J.	THB1TU01
Thorin, S.	THPOA66
Thurman-Keup, R.M.	TUP0A19, TUP0A26, TUP0B18
Th'nell, L.	TUP0A09, THPOA64
Tian, Q.L.	THPOA55
To, H.L.	TUP0A69
Tokarek, R.	TUP0A16
Tollestrup, A.V.	SUP024, MOP0B52, TUP0A44, FRA1C005
Torrez, P.A.	TUP0A63
Torun, Y.	SUP024, TUP0A44, MOP0B52
Trakhtenberg, E.	THA1C006, THPOA69
Trbojevic, D.	TUP0B60, WEP0A61
Trenikhina, Y.	MOP0B34, WEB2C004
Triplett, A.K.	WEP0A18
Trombly-Freytag, K.	MOP0B27
Tropin, I.S.	WEP0A16, WEP0A20
Tsai, C.-Y.	SUP046 , TUP0B28, WEA2C004 , THPOA35
Tsoupas, N.	TUP0B60 , WEP0A61
Tuggle, J.	SUP034, WEB1C002
Tuozzolo, J.E.	MOB3C003, WEA4C005, WEP0B54, WEP0B58, WEP0B59, WEP0B60
Tuozzolo, J.L.	WEP0A61
Turner, J.L.	WEP0B43
Turner, M.	SUP047 , TUA3C003 , WEP0A09 , WEP0A10
Turrioni, D.	MOP0B41
Tyutyunnikov, S.I.	TUP0A33

— U —

Ungaro, D.	FRB1I002
Upadhyay, J.	MOP0B70 , WEP0A51
Urakawa, J.	MOP0B03, THPOA50, THPOA51, THPOA52, THPOA53

— V —

Vafaei, N.	WEP0A58
Valente-Feliciano, A-M.	MOP0B70

Valicenti, T.T.	SUP048, WEP0B18
Valishev, A.	TUP0A19, TUP0B17, WEA1C004, WEA2I002, WEP0A17, WEP0A31, WEA4C002, WEA4C004 , THP0A19, THP0A23, THP0A28
Varghese, P.	TUP0A18
Vasserman, I.	WEP0B23
Vassiliev, O. N.	TUP0A54
Vay, J.-L.	WEP0A30
Vaziri, K.	MOP0B35
Veit, R.D.	MOP0B77
Velev, G.	MOP0B41
Venturini, M.	TUB1C003, THP0A32, THP0A33
Verma, A.	TUP0A68, TUB3C004
Veshcherevich, V.	MOP0B60, MOP0B62
Vetter, K.	MOA2I002
Vetter, S.	WEP0B43
Vieira, J.	TUA4C003, WEP0A49, WEP0A01
Villabona, T.J.	MOP0B72
Vincenti, H.	WEP0A30
Vivoli, A.	THP0A29
Vušković, L.	MOP0B70

— W —

Wacker, V.	TUP0A72
Walbridge, D.G.C.	MOP0B27
Waldron, W.L.	WEP0A29
Waldschmidt, G.J.	TUB3C004, WEP0B07, WEP0B11, WEP0B70
Walker, R.P.	THP0A65
Walsh, J.	WEP0B52, WEP0B58
Wanderer, P.	MOP0B49
Wang, C.H.	TUP0A07
Wang, D.	THP0A55
Wang, E.	WEP0B59, WEP0B60, WEP0B67
Wang, G.	SUP026, MOP3C003, WEP0A55, WEP0B59, WEP0B60, WEP0B67, THP0A44
Wang, G.M.	WEP0B64, WEP0B65, WEP0B66
Wang, H.	SUP017, MOP0B58, MOP0B69 , WEP0B44, THA2C004
Wang, J.	MOP0B12 , WEP0B05, WEP0B24
Wang, L.	THP0A57, THP0A58
Wang, S.	SUP017, THA2C004
Wang, S.	WEA2C003, WEP0B36
Wang, X.	MOP0B49
Wang, Y.R.	SUP049, TUP0A13
Wang, Z.J.	THA3C003
Warner, A.	TUP0A19
Wasef, R.	THP0A15
Washio, M.	THP0A51, THP0A53, MOP0B03, TUP0A04
Watts, A.C.	TUP0A36 , FRA1C005
Webb, S.D.	TUA3C004 , TUP0B10, WEA2I002, WEP0A31, WEA4C002, THP0A28, THP0A38, THP0A39
Wei, G.H.	MOA4C003 , TUP0B29, TUP0B31
Wei, J.	TUA1I001
Weichman, K.J.	THP0A43
Weisend, J.G.	THA3I002
Welch, J.R.	WEP0A58
Welton, R.F.	WEP0A45
Wendt, M.	SUP054, FRA2C003
Wenninger, J.	MOP3I002
Werner, G.R.	THP0A36
Wesseln, S.J.	TUP0A19
Westferro, F.	WEP0B24, THP0A62
White, M.	MOPLI001
White, S.M.	MOA3I001
Whiteford, C.	SUP049, TUP0A13, WEP0B19, WEP0B20

Wichmann, R.	TUB4I002
Wiechecki, J.J.	TUP0A09
Wiedrick, W.	THB3I001
Wiemerslage, G.E.	MOP0B10, MOP0B11
Wienands, U.	THP0A63
Wilcox, R.B.	SUP052, M0A2I001 , TUP0A39, TUP0A41, TUP0A42
Willeke, F.J.	TUP0B56, WEP0A24, WEP0B64
Williams, J.E.	TUP0A53
Williams, K.E.	MOP0B35
Wisniewski, E.E.	SUP049, TUP0A13, WEP0B19 , WEP0B20
Witte, H.	MOP0B74 , MOP0B75 , TUP0B56, WEP0A61
Wojtsekhowski, B.	TUP0A57
Woloshun, K.A.	WEP0A47
Wong, C.Y.	SUP050 , TUA3C003, WEA4I001
Wootton, K.P.	WEP0A32
Wu, C.Y.	TUP0A12
Wu, J.	SUP011, TUB3C003
Wu, Q.	M0B3C003, TUP0B56
Wu, Wu, Y.H.	TUP0B24 , TUP0B25
Wu, Y.K.	SUP021, SUP053, TUP0B01, TUP0B19, WEP0B33
Wu, Z.	WEP0A32

— X —

Xiao, A.	WEP0B10, WEP0B21 , WEP0B22 , THP0A63
Xiao, B. P.	WEP0B60
Xiao, M.	TUP0B08
Xie, J.	WEP0B52
Xu, C.	SUP035, MOP0B73, MOP0B76
Xu, H.	SUP051 , WEP0B31
Xu, H.B.	THB3C004
Xu, J.Z.	WEP0B23
Xu, T.	WEB3I001
Xu, T.	WEB3I001
Xu, W.	MOP0B76, WEP0B59, WEP0B60, THP0A54
Xu, X.L.	WEP0A49, WEP0A50
Xu, Y.L.	SUP052 , TUP0A40, TUP0A41 , TUP0A42

— Y —

Yakimenko, V.	TUA3I002
Yakovlev, V.P.	TUA2C003, TUP0A22, TUP0B02, TUP0B03, WEB3C003, WEP0B27
Yamaguchi, T.Y.	MOP0B61
Yamazaki, Y.	MOP0B55
Yampolsky, N.A.	TUB4C003
Yan, J.	SUP053 , WEP0B33
Yan, L.X.	THP0A55
Yancey, J.A.	MOP0B67
Yang, B.X.	WEP0B21, FRA1I002
Yang, J.	FRA1C006
Yang, J.	TUP0A40
Yang, M.-J.	WEP0A16
Yang, W.J.	MOP0B55
Yang, Y.	SUP052, MOP0B48, TUP0A41, TUP0A42 , THP0A33
Yao, C.	WEA1C003, WEP0B16, WEP0B24 , THP0A14
Yao, Q.G.	MOP0B55
Yonehara, K.	SUP024, MOP0B52, TUP0A44, FRA1C005
Yoshida, Y.	FRA1C006
Yu, L.	TUP0B54
Yu, P.	WEP0A49
Yun, J.C.	MOP0B32, MOP0B33

Zagorodnov, I.	TUB2C004, WEA1I002
Zaltsman, A.	M0B3C003, M0P0B76, WEP0B59, WEP0B60
Zanoni, C.	M0B2C004
Zasadzinski, J.	SUP008, M0P0B19, M0P0B20
Zennamo, J.A.	WEP0A26
Zeno, K.	M0B3C003
Zerbe, B.	TUA3C003
Zgad Zaj, R.	WEP0A58
Zhang, C.J.	WEP0A49, WEP0A58
Zhang, H.	TUP0B36
Zhang, S.	TUP0A53
Zhang, S.Y.	M0B3C003
Zhang, W.	M0B3C003
Zhang, Y.	M0A4C003, TUP0B05, TUP0B29, TUP0B30, TUP0B31, TUP0B36
Zhang, Z.	THP0A55
Zhang, Z.M.	SUP049, TUP0A13
Zhao, Q.	M0P0B55
Zhao, Z.	TUP0B58, WEP0B59, WEP0B60
Zheng, N.	THB3C004
Zholents, A.	TUB3C004, WEP0A12, WEP0B48
Zhou, C.D.	THP0A41, THP0A42
Zhou, F.	SUP022, WEP0B49
Zhou, N.	WEP0A13
Zhou, Z.	THP0A55
Zhu Song, M.Z.	THP0A67
Ziemba, T.M.	M0P0B79
Zientek, J.	M0P0B11
Zimmer, M.	WEP0A29
Zlobin, A.V.	M0P0B30, M0P0B40, M0P0B41, M0P0B42, THA1C004
Zobov, M.	THP0A34
Zolkin, T.	WEA1C006, THP0A25, THP0A30, THP0A31
Zorzetti, S.	SUP054, FRA2C003
Zwaska, R.M.	SUP024, M0A4I002, M0P0B13, M0P0B14, M0P0B35, M0P0B43, TUP0A37, TUP0A44, TUP0B63, WEP0A27, WEP0A43, FRA1C005

Participants

Abeyratne, Sumana (Northern Illinois University)	Caldwell, Allen (MPI-P)
Abliz, Melike (ANL)	Calvey, Joseph (ANL)
Abrams, Robert (Muons, Inc)	Capobianco-Hogan, Kyle (SBU)
Ahl, Anton (Scanditronix Magnet AB)	Carlsten, Bruce (LANL)
Ainsworth, Robert (Fermilab)	Carneiro, Jean-Paul (Fermilab)
Akagi, Tomoya (KEK)	Carpenter, Adam (JLab)
Al Marzouk, Afnan (Northern Illinois University)	Carter, Jason (ANL)
Alekou, Androula (DLS)	Caspi, Shlomo (LBNL)
Alexahin, Yuri (Fermilab)	Cathey, Brandon (ORNL RAD)
Alvarez, Matthew (Fermilab)	Champion, Mark (ORNL)
Ambrosio, Giorgio (Fermilab)	Chase, Brian (Fermilab)
Ammigan, Kevin (Fermilab)	Checchin, Mattia (Fermilab)
Amundson, James (Fermilab)	Chen, Qi (IMP/CAS)
An, Sun (PLAI)	Cheng, Weixing (BNL)
An, Weiming (UCLA)	Conde, Manoel (ANL)
Andorf, Matthew (Northern Illinois University)	Convery, Mary (Fermilab)
Andrist, John (ANL)	Conway, Zachary (ANL)
Antipov, Sergey (Fermilab)	Cook, Nathan (RadiaSoft LLC)
Awida, Mohamed (Fermilab)	Crawford, Darren (Fermilab)
Baffes, Curtis (Fermilab)	Crittenden, James (Cornell University (CLASSE))
Baker, Samuel (ANL)	Crofford, Mark (ORNL)
Bao, Yu (UCR)	Cullinan, Francis (SOLEIL)
Baumgartner, Heidi (UMD)	Cummings, Thomas (Fermilab)
Beaudoin, Brian (UMD)	Cummings, Mary Anne Clare (Muons, Inc)
Bell, George (Tech-X)	Dalichaouch, Thamine (UCLA)
Belomestnykh, Sergey (Fermilab)	Danielyan, Vahe (CANDLE SRI)
Bennett, Laura (M.D.A.C.C.)	dashtestani, Sepideh (Rejected)
Ben-Zvi, Ilan (BNL)	D'Audney, Alex (CSU)
Bergan, William (Cornell University (CLASSE))	De Silva, Subashini (ODU)
Bergoz, Julien (GMW Associates)	Degiovanni, Alberto (ADAM)
Billing, Michael (Cornell University (CLASSE))	Dejus, Roger (ANL)
Blaskiewicz, Michael (BNL)	Delayen, Jean (ODU)
Blednykh, Alexei (BNL)	Den Hartog, Patric (ANL)
Borland, Michael (ANL)	Denisov, Dmitri (Fermilab)
Boulware, Charles (Niowave, Inc.)	Derenchuk, Vladimir (ProNova Solutions)
Bourseau, Isabelle (SOLCERA)	Di Mitri, Simone (Elettra-Sincrotrone Trieste S.C.p.A.)
Bowring, Daniel (Fermilab)	Diamond, John (Fermilab)
Brodbar, Debbie (APS)	Dimitrov, Dimitre (Tech-X)
Bromberek, David (ANL)	Dooling, Jeffrey (ANL)
Bruhaug, Gerrit (Fermilab)	Doose, Charles (ANL)
Bruhwiller, David (RadiaSoft LLC)	Dorda, Ulrich (DESY)
Burov, Alexey (Fermilab)	Draganic, Ilija (LANL)
Byrd, John (LBNL)	Drury, Michael (JLab)
Byrne, Warren (LBNL)	Dudnikov, Vadim (Muons, Inc)
Cahill, Alexander (UCLA)	

Duffy, Leanne (LANL)
 Dunne, Mike (LLNL)
 Eddy, Nathan (Fermilab)
 Edelen, Auralee (CSU)
 Edelen, Jonathan (CSU)
 Edstrom, Dean (Fermilab)
 El Fikky, Niazi (Saudi Electricity Company)
 Eldred, Jeffery (Fermilab)
 Ellison, James (IIT)
 Emery, Louis (ANL)
 Emma, Claudio (UCLA)
 Ent, Rolf (JLab)
 Erdmann, Mark (ANL)
 Fedotov, Alexei (BNL)
 Fedurin, Mikhail (BNL)
 Ferrari, Eugenio (EPFL)
 Fitterer, Miriam (CERN)
 Fronk, Tyler (LANL)
 Fukuda, Masafumi (KEK)
 Fuwa, Yasuhiro (Kyoto ICR)
 Ge, Mingqi (Cornell University (CLASSE))
 Gee, Anthony (Northern Illinois University)
 Gerity, James (Texas A&M University)
 Gianfelice-Wendt, Eliana (DESY)
 Gibson, David (LLNL)
 Gourlay, Stephen (LBNL)
 Grassellino, Anna (Fermilab)
 Green, Andrew (Northern Illinois University)
 Grimm, Terry (Niowave, Inc.)
 Gu, Xiaofeng (BNL)
 Gupta, Lipi (Cornell University (CLASSE))
 Ha, Taekyun (PAL)
 Halavanau, Aliaksei (Northern Illinois University)
 Hall, Christopher (CSU)
 Hall, Patricia (Fermilab)
 Harding, David (Fermilab)
 Harkay, Katherine (ANL)
 He, Ping (BNL)
 Henderson, Stuart (ANL)
 Hidaka, Yoshiteru (BNL)
 Hidas, Dean (BNL)
 Higuera, Adam (Tech-X)
 Huang, Dazhang (SINAP)
 Huang, Gang (LBNL)
 Huang, Xiaobiao (SLAC)
 Huang, Yulu (IMP/CAS)
 Hurh, Patrick (Fermilab)
 Hwang, Kilean (LBNL)

Hwang, Yoonwoo (Cornell University (CLASSE))
 Ikeda, Shunsuke (BNL)
 Ivanyushenkov, Yury (ANL)
 Iwawaki, Tomoyuki (Mitsubishi Electric Corporation)
 Izzo, Scott (ANL)
 Jain, Vikas (Fermilab)
 Jaski, Mark (ANL)
 Jensen Jr., Don (ANL)
 Ji, Yichen (IIT)
 Jimbo, Kouichi (Kyoto University)
 Johansson, Martin (MAX IV Laboratory)
 Johnson, Rolland (Muons, Inc)
 Jones, Kevin (ORNL)
 Kahn, Stephen (Muons, Inc)
 Kan, Koichi (ISIR)
 Kapin, Valery (Fermilab)
 Kasa, Matthew (ANL)
 Kayran, Dmitry (BNL)
 Kazakevich, Grigory (Euclid TechLabs, LLC)
 Kendziora, Kyle (Fermilab)
 Kewisch, Jorg (BNL)
 Khabiboulline, Timergali (Fermilab)
 Khorshidi, Abdollah (Gerash Research Institute)
 Kim, Sang-Hoon (ANL)
 Kim, SeungCheon (Cornell University (CLASSE))
 Kim, Suk Hong (ANL)
 Kim, Young-Kee (University of Chicago)
 Kitegi, Charles (BNL)
 Kleinschmidt, Ron (Lambda)
 Kondrashev, Sergey (IBS)
 Kononenko, Oleksiy (SLAC)
 Koscielniak, Shane (TRIUMF)
 Koshiba, Yuya (RISE)
 Kostin, Roman (Euclid Beamlabs LLC)
 Kotelnikov, Sergey (Fermilab)
 Kourbanis, Ioanis (Fermilab)
 Kustom, Robert (ANL)
 Kutsaev, Sergey (RadiaBeam Systems)
 Lari, Luisella (CERN)
 Le Bec, Gaël (ESRF)
 Lebedev, Valeri (Fermilab)
 Lee, Sung-Woo (ORNL)
 Lee, Tae-Yeon (PAL)
 Leemans, Wim (LBNL)
 Leibfritz, Jerry (Fermilab)
 Len, Lek (US DOE)
 Leopoldes, David (Sigmaphi Electronics)

Lerch, Jason (ANL)
 Levin, Mark (LANL)
 Li, Bing (FEL/Duke University)
 Li, Ge (ASIPP)
 Li, Rui (JLab)
 Li, Siqi (SLAC)
 Li, Yongjun (BNL)
 Li, Yuan Shen (Carleton College)
 Liaw, Chong-Jer (BNL)
 Lidia, Steven (FRIB)
 Lindberg, Ryan (ANL)
 Litvinenko, Vladimir (BNL)
 Liu, Ao (Fermilab)
 Liu, Chuyu (BNL)
 Liu, Jie (ANL)
 Liu, Ning (Fermilab)
 Liu, Qiaoyi (Case Western Reserve University)
 Lott, John (Sandia National Laboratories)
 Lumpkin, Alex (Fermilab)
 Ma, Hengjie (ANL)
 Ma, Jun (SBU)
 Macridin, Alexandru (Fermilab)
 Madrak, Robyn (Fermilab)
 Maggi, Paul (LSU)
 Martinello, Martina (Fermilab)
 Maxwell, Timothy (Fermilab)
 Mayes, Christopher (Cornell University (CLASSE))
 McCarter, James (Niowave, Inc.)
 McVea, James (Thales Components Corporation)
 Meot, Francois (BNL)
 Miao, Chenlong (UMD)
 Mitchell, Chad (LBNL)
 Mohayai, Tanaz (IIT)
 Moog, Elizabeth (ANL)
 Moretti, Alfred (Fermilab)
 Morozov, Vasilii (JLab)
 Motta, Claudio (USP)
 Murokh, Alex (RadiaBeam Systems)
 Musson, John (JLab)
 Nagaitsev, Sergei (Fermilab)
 Neubauer, Michael (Muons, Inc)
 Neuffer, David (Fermilab)
 Neveu, Nicole (ANL)
 Nguyen, Dinh (LANL)
 Nishida, Mariko (Waseda University)
 Nissen, Edward (JLab)
 Norem, Jim (Nano Synergy, Inc.)
 Oganessian, Koryun (ANSL)

Ohnishi, Yuki Yoshi (KEK)
 Okamura, Masahiro (BNL)
 Oliveros, Sandra (UMiss)
 Olsen, Veronica (University of Oslo)
 O'Neill, Maria (ANL)
 Oprondek, Samuel (ANL)
 Osen, Lauren (UCLA Anderson School of Management)
 O'Shea, Finn (RadiaBeam)
 Ostroumov, Peter (ANL)
 Pakter, Renato (IF-UFRGS)
 Palmer, Mark (BNL)
 Papotti, Giulia (CERN)
 Park, Chong Shik (Fermilab)
 Parkhomchuk, Vasily (BINP SB RAS)
 Patch, Sarah (UWM)
 Patel, Niral (Fermilab)
 Patrick, James (Fermilab)
 Patterson, J. Ritchie (Cornell University (CLASSE))
 Petersen, Troy (Fermilab)
 Petit, Eric (GANIL)
 Pham, Alfonse (NSCL)
 Phelps, Tyler (Roark Custom Metal Fabrication)
 Pilat, Fulvia (JLab)
 Pile, Geoffery (ANL)
 Pinayev, Igor (BNL)
 Pirez, Eylene (UCLA)
 Pischalnikov, Yuriy (Fermilab)
 Plastun, Alexander (ANL)
 Pogorelsky, Igor (BNL)
 Poprocki, Stephen (Cornell University (CLASSE))
 Posen, Sam (Fermilab)
 Power, Maria (ANL)
 Pozdeyev, Eduard (FRIB)
 Prager, James (EHT)
 Pronitchchev, Oleg (Fermilab)
 Pronskikh, Vitaly (Fermilab)
 Ptitsyn, Vadim (BNL)
 Pudasaini, Uttar (The College of William and Mary)
 Pushka, David (Fermilab)
 Qiang, Ji (LBNL)
 Qin, Qing (IHEP)
 Raab, Frederick (Green Mountain Radio Research)
 Rangacharyulu, Chary (University of Saskatchewan)
 Ranjbar, Vahid (BNL)

Ratoff, Peter (Lancaster University)
 Raubenheimer, Tor (SLAC)
 Ravaioli, Emmanuele (LBNL)
 Richter, Brian (GMW Associates)
 Roark, Ted (Roark Custom Metal Fabrication)
 Roberts, Thomas (Muons, Inc)
 Roger, Vincent (Fermilab)
 Romanenko, Alexander (Fermilab)
 Romanov, Alexander (Fermilab)
 Romanov, Gennady (Fermilab)
 Rotsch, David (ANL)
 Roy, Prabir (LANL)
 Rubin, David (Cornell University (CLASSE))
 Ruisard, Kiersten (UMD)
 Rusthoven, Brian (ANL)
 Saewert, Gregory (Fermilab)
 Saini, Arun (Fermilab)
 Saito, Yutaro (Waseda University)
 Sajaev, Vadim (ANL)
 Sakaue, Kazuyuki (RISE)
 Sangroula, Medani (IIT)
 Sannibale, Fernando (LBNL)
 Santucci, James (Fermilab)
 Sayler, Jeffrey (The University of Chicago)
 Scherma, George (Lambda)
 Schriber, Stan (Private Address)
 Seidl, Peter (LBNL)
 Seletskiy, Sergei (BNL)
 Sen, Tanaji (Fermilab)
 Seryi, Andrei (JAI)
 Shapiro, Michael (MIT/PSFC)
 Shiltsev, Vladimir (Fermilab)
 Shin, Seunghwan (ANL)
 Shin, Young-Min (Fermilab)
 Shiroyanagi, Yuko (ANL)
 Siddiqi, Moiz (UMD)
 Sipahi, Nihan (CSU)
 Sipahi, Taylan (CSU)
 Skiadopoulos, Denise (ANL)
 Smirnov, Alexei (RadiaBeam)
 Smith, Terry (ANL)
 Snopok, Pavel (Fermilab)
 Son, Hyungjoo (IBS)
 Spentzouris, Linda (Illinois Institute of Technology)
 Stancari, Giulio (Fermilab)
 Steck, Markus (GSI)
 Steier, Christoph (LBNL)

Steinke, Sven (LBNL)
 Stillwell, Benjamin (ANL)
 Streiffer, Stephen (ANL)
 Stupakov, Gennady (SLAC)
 Sudar, Nicholas (UCLA)
 Sumitomo, Yoske (KEK)
 Sun, Xiang (ANL)
 Sun, Yin-E (ANL)
 Sun, Yipeng (ANL)
 Suthar, Kamlesh (ANL)
 Sutter, David (UMD)
 Sy, Amy (JLab)
 Syphers, Michael (MSU)
 Tantawi, Sami (SLAC)
 Tariq, Salman (Fermilab)
 Tavares, Pedro (MAX IV Laboratory)
 Taylor, Charles (LANL)
 Thieberger, Peter (BNL)
 Tigner, Maury (Cornell University (CLASSE))
 Trakhtenberg, Emil (ANL)
 Trbojevic, Dejan (BNL)
 Tropin, Igor (Fermilab)
 Tsai, Cheng-Ying (JLab)
 Tsoupas, Nicholas (BNL)
 Turner, Marlene (CERN)
 Upadhyay, Janardan (LANL)
 Valicenti, Timothy (ANL)
 Valishev, Alexander (Fermilab)
 Vay, Jean-Luc (LBNL)
 Veit, Richard (The University of Chicago)
 Verboncoeur, John (Michigan State University)
 Vetter, Kurt (ORNL)
 Vieweg, Mikael (Scanditronix Magnet AB)
 Vivoli, Alessandro (Fermilab)
 Walbridge, Dana (Fermilab)
 Waldschmidt, Geoff (ANL)
 Wang, ChunHong (IHEP)
 Wang, Erdong (BNL)
 Wang, Guimei (BNL)
 Wang, Haipeng (JLab)
 Wang, Ju (ANL)
 Wang, Yanru (AAI/ANL)
 Wang, Zhijun (IMP/CAS)
 Watts, Adam (Fermilab)
 Webb, Stephen (RadiaSoft LLC)
 Wei, Guohui (JLab)
 Weisend, John (ESS)
 White, Marion (ANL)

Wichmann, Riko (DESY)
Wiemerslage, Greg (ANL)
Wilcox, Russell (LBNL)
Willeke, Ferdinand (BNL)
Wisniewski, Eric (ANL)
Wong, Chun Yan Jonathan (NSCL)
Wu, Chunyi (NSRRC)
Wu, Yuan Hui (LLNL)
Xiao, Meiqin (Fermilab)
Xu, Haoran (MIT/PSFC)
Xu, Joseph (ANL)
Xu, Ting (FRIB)
Xu, Xinlu (UCLA)
Xu, Yilun (TUB)
Yan, Jun (FEL/Duke University)
Yang, Bingxin (ANL)
Yang, Yawei (ANL)
Yao, Chihyuan (ANL)
Yonehara, Katsuya (Fermilab)
Yuan, Alex (Fermilab)
Zagorodnov, Igor (DESY)
Zhang, Qi (TUB)
Zheng, Na (Institute of Applied Physics and
Computational Mathematics)
Zholents, Alexander (ANL)
Zhou, Ning (ANL)
Ziemba, Timothy (EHT)
Zientek, John (ANL)
Zlobin, Alexander (Fermilab)
Zolkin, Timofey (Fermilab)
Zorzetti, Silvia (CERN)
Zwaska, Robert (Fermilab)

NAPAC16 Schedule																																				
Time	Sunday, October 9, 2016	Monday, October 10, 2016			Tuesday, October 11, 2016			Wednesday, October 12, 2016			Thursday, October 13, 2016			Friday, October 14, 2016		Saturday, October 15, 2016																				
		Chicago VI	Chicago VII	Riverwalk	Chicago VI	Chicago VII	Riverwalk	Chicago VI	Chicago VII	Riverwalk	Chicago VI	Chicago VII	Riverwalk	Chicago VI	Chicago VII																					
		MOPL			TUA1	TUB1	Morning Poster Session	WEA1	WEB1	Morning Poster Session	THA1	THB1	Morning Poster Session	FRA1	FRB1	Tours of Argonne National Laboratory and Fermi National Accelerator Laboratory																				
830	IEEE Short Courses (Millennium Park, Jackson Park, Grant Park)	Welcome			Status of FRIB <i>Eduard Pozdeyev (FRIB)</i>	Tutorial A Discussion on Phase Space and Beam Emittance <i>Rui Li (JLab)</i>	TUPOA MC6 & MC8	Demonstration of Energy-Chirp Control in Relativistic Electron Bunches at LCLS Using a Corrugated Structure <i>Timothy Maxwell (SLAC)</i>	Tutorial Superconducting Accelerators Magnets Soren Prestemon (LBNL)	WEPOA MC3 & MC4	Progress in High Q SRF Cavities Development: From Single Cell to Cryomodule <i>Anna Grassellino (Fermilab)</i>	Tutorial Risk Management of Complex Systems <i>John Thomas (MIT)</i>	THPOA MC2 & MC5	Single Particle Detection With a Schottky Resonator <i>Markus Steck (GSJ)</i>	Tutorial RF Superconductivity <i>Jean Delayen (ODU)</i>																					
845		(0845-0920) High Energy Physics as a Global Enterprise: Report from ICHEP XXVIII (Chicago, Aug. 2016) <i>Young-Kee Kim (University of Chicago)</i>			Status Report on the SPIRAL2 Facility at GANIL <i>Eric Petit (GANIL)</i>			Computation of Electromagnetic Fields Generated by Relativistic Beams in Complicated Structures <i>Igor Zagorodnov (DESY)</i>			Results of the 2015 Helium Processing of CEBAF Cryomodules <i>Michael Drury (JLab)</i>			State of the Art X-Ray Photon BPMs for Next Generation Storage Ring Light Sources <i>Bingxin Yang (ANL)</i>																						
900		(0920-0955) A Billion Times Brighter: An Overview of the Scientific Impact and Future Opportunities of X-Ray Free Electron Lasers <i>Michael Dunne (SLAC)</i>			Technological Challenges in the Path to 3.0 MW at the SNS Accelerator <i>Kevin Jones (ORNL)</i>			Simulations of Booster Injection Efficiency for the APS-Upgrade <i>Joseph Calvey (ANL)</i>			MAX IV & Solaris 1.5 GeV Storage Rings Magnet Block Production Series Measurement Results <i>Martin Johansson (MAX IV Laboratory)</i>			An Ultra-High Resolution Pulsed-Wire Magnet Measurement System <i>Stephen Milton (CSU)</i>																						
915		(0955-1030) Nuclear Physics at the Electron Ion Collider Plenary <i>Rolf Ent (JLab)</i>			Simulation of Beam Dynamics in a Strong-focusing Cyclotron <i>Karie Badgley (Fermilab)</i>			Hollow Electron Beam Collimation for HL-LHC - Effect on the Beam Core <i>Miriam Fitterer (Fermilab)</i>			Persistent Current Effect in 15-16 T Nb3Sn Accelerator Dipoles & Its Correction <i>Alexander Zlobin (Fermilab)</i>			6D Phase Space Measurement of Low Energy, High Intensity Hadron Beam <i>Brandon Cathey (ORNL RAD)</i>																						
930					Design of a Compact Ring for Pulse Structure Manipulation of Heavy Ion Beams at the NSCL <i>Alfonse Pham (NSCL)</i>			Microwave Instability Studies in NSLS-II <i>Alexei Blednykh (BNL)</i>			Thermal Modeling & Cryogenic Design of a Helical Superconducting Undulator Cryostat <i>Yuko Shiroyanagi (ANL)</i>			Progress of Gas-Filled Multi-RF-cavity Beam Profile Monitor for Intense Neutrino Beam <i>Katsuya Yonehara (Fermilab)</i>																						
945					ALS-U: A Soft X-Ray Diffraction Limited Light Source <i>Christoph Steier (LBNL)</i>			Analytical Theory for McMillan Map <i>Timofey Zolkin (Fermilab)</i>			Status of Development of Superconducting Undulators for Storage Rings & Free Electron Lasers at the APS <i>Yury Ivanushchenkov (ANL)</i>			Measurement of Coherent Transition Radiation Using Interferometer and Photoconductive Antenna <i>Koichi Kan (ISIR)</i>																						
1000					Morning Coffee			Morning Coffee			Morning Coffee			Morning Coffee																						
1015																																				
1030 - 1100																																				
1100																																				
1115																																				
1130																																				
1145																																				
1200	Student Poster Session (Riverwalk A & B)	Measurement of Tune Shift with Amplitude from BPM Data with a Single Kicker Pulse <i>Yoshiteru Hidaka (BNL)</i>			Collider in the Sea: A New Vision for a 700 TeV World Laboratory <i>Peter M. McIntyre (Texas A&M Univ.)</i>			A Novel Technique of Power Control in Magnetrans <i>Grigory Kazakevich (Muons, Inc)</i>			S-Band 1.4 Cell Photoinjector Design for High Brightness Beam Generation <i>Eylene Pirez (UCLA)</i>			Study of the Electrical Center of a Resonant Cavity Beam Position Monitor (RF-BPM) & Its Integration with the Main Beam Quadrupole for Alignment Purposes - <i>Silvia Zorzetti (CERN)</i>																						
1215		MICE Operation and Demonstration of Muon Ionization Cooling <i>Ao Liu (Fermilab)</i>			Multiphysics Analysis of Crab Cavities for High Luminosity LHC Upgrade <i>Oleksiy Kononenko (SLAC)</i>			Vacuum Breakdown Research at 110 GHz <i>Samuel Schaub (MIT)</i>			High Power Production Target for FRIB <i>Frederique Pellemoine (FRIB)</i>			Fulfilling the Mission of Brookhaven ATF as a DOE'S Flagship User Facility in Accelerator Stewardship <i>Igor Pogorelsky (BNL)</i>																						
1230 - 1400		Lunch			Lunch			Lunch			Lunch			Lunch																						
1400		MOA3			TUA3			WEA3			THA3			FRPL																						
1415		MOB3			TUB3			WEB3			THB3																									
1430		High energy Coulomb Scattered Electrons Detected in Air used as the Main Beam Overlap Diagnostics for Tuning the RHIC Electron Lenses <i>Peter Thieberger (BNL)</i>			Commissioning of the Phase-I SuperKEKB B-Factory and Update on the Overall Status <i>Yukiyoishi Ohnishi (KEK)</i>			Possible Road Maps for High-Energy Collider Based on Advanced Acceleration Techniques <i>Sergei Nagaitsev (Fermilab)</i>			Commissioning of Max-IV, the First Light Source Using a Multi Bend Achromat <i>Pedro Tavares (MAX IV Laboratory)</i>			Emittance Growth from Modulated Focusing in Bunched Beam Cooling <i>Michael Blaskiewicz (BNL)</i>																						
1445		Precision Vector Control of a Superconducting RF Cavity driven by an Injection Locked Magnetron <i>Brian Chase (Fermilab)</i>			LHC Operation at 6.5 TeV : Status and Beam Physics Issues <i>Giulia Papotti (CERN)</i>			FACET Results and FACET II Perspective <i>Vitaly Yakimenko (SLAC)</i>			Overview of Electron Source Development for High Repetition Rate FEL Facilities <i>Fernando Sannibale (LBNL)</i>			Start-to-End Beam Dynamics Optimization of X-Ray FEL Light Source Accelerators <i>Ji Qiang (LBNL)</i>																						
1500		The Bunch Shape Monitor Measurements at the LANSCE Linac <i>Ilija N. Draganic (LANL)</i>			RHIC Au-Au Operation at 100 GeV in Run16 <i>Xiaofeng Gu (BNL)</i>			Compact Ring-based X-ray Source with On-orbit and On-energy Laser-plasma Injection <i>Marlene Turner (CERN)</i>			Demonstration of Fresh Slice Self Seeding in a Hard X-ray Free Electron Laser <i>Claudio Emma (UCLA)</i>			Efficiency of Feedbacks for Suppression of Transverse Instabilities of Bunched Beams <i>Alexey Burov (Fermilab)</i>																						
1515		Operational Experience with Fast Fiber-Optic Beam Loss Monitors for the APS Storage Ring SCUs <i>Jeffrey Dooling (ANL)</i>			High Luminosity 100 TeV Proton-Antiproton Collider <i>Sandra Oliveros (UMiss)</i>			Kinetic Limits to Average Power in Plasma Wakefield Accelerators <i>Stephen Webb (RadiaSoft LLC)</i>			A New Thermionic RF Electron Gun for Synchrotron Light Sources <i>Sergey V Kutsaev (RadiaBeam Systems)</i>			Impedance Characterization and Collective Effects in the MAX IV 3 GeV Ring <i>Francis Cullinan (SOLEIL)</i>																						
1530 - 1600		Afternoon Coffee			Afternoon Coffee			Afternoon Coffee			Afternoon Coffee			Afternoon Coffee																						
1600	Welcome Reception (Riverwalk A & B - 1800-2100)	MOA4			TUA4			WEA4			THPL - Award Session																									
1615		MOB4			TUB4			WEB4																												
1630		Performance of the Low Charge State Laser Ion Source in BNL <i>Masahiro Okamura (BNL)</i>			Specifics of Electron Dynamics in High Energy Circular e+e- Colliders <i>Qing Qin (IHEP)</i>			Staging Results at BELLA and Plans for BELLA (k-BELLA) <i>Sven Steinke (LBNL)</i>			Status of the MaRIEProject <i>John Erickson (LANL)</i>			Dynamics of Beams With Canonical Angular Momentum in Non-Axisymmetric Optical Elements <i>Chun Yan Jonathan Wong (NSCL)</i>																						
1645		Recent Progress in High Intensity Operation of the Fermilab Accelerator Complex <i>Mary Convery (Fermilab)</i>			Linac-ring and Ring-ring designs for the eRHIC Electron-Ion Collider <i>Vadim Pitsyn (BNL)</i>			Eupraxia: A Compact European Plasma Accelerator With Superior Beam Quality <i>Ulrich Dorda (DESY)</i>			Accelerator Physics Challenges, Technical Progress and Commissioning Results from the European XFEL <i>Riko Wichmann (DESY)</i>			Impact of Space Charge on Beam Dynamics and Integrability in the IOTA Ring <i>Christopher Hall (RadiaSoft LLC)</i>																						
1700		Complete Beam Dynamics of the JLEIC Ion Collider Ring Including Imperfections, Corrections, and Detector Solenoid Effects <i>Guohui Wei (JLab)</i>			Design of Muon Collider Lattices <i>Yuri Alexahin (Fermilab)</i>			Loading of Wakefields in a Plasma Accelerator Section Driven by a Self-Modulated Proton Beam <i>Veronica Olsen (University of Oslo)</i>			Optimization of Compton source Performance through Electron Beam Shaping <i>Alexander Malyzhenkov (LANL)</i>			Intrinsic Landau Damping for Bunched Beams in the Proximity of Transverse Coupling Resonance <i>Alexandru Macridin (Fermilab)</i>																						
1715		Compact Carbon Ion Linac <i>Peter Ostroumov (ANL)</i>			Design of the Room-temperature Front-end for a Multi-ion Linac Injector <i>Alexander Plastun (ANL)</i>			High-Power Tunable THz Generation in Corrugated Plasma Waveguides <i>Chenlong Miao (UMD)</i>			Progress on the Magnetic Performance of Planar Superconducting Undulators <i>Matthew Kasa (ANL)</i>			Suppression of Half-Integer Resonance in FNAL Booster and Space Charge Losses at Injection <i>Alexander Valishev (Fermilab)</i>																						
1730														Accelerator Physics Design and Challenges of RF Based Electron Cooler LEReC <i>Alexei Fedotov (BNL)</i>																						
					Women in Science and Engineering (WISE) Event (starting at 1900 - location TBA)			Teachers' Day (0815-1700)			Conference Banquet																									
																Legend																				
														1: Circular and Linear Colliders																						
														7: Accelerator Technology Main Systems																						
														2: Photon Sources and Electron Accelerators																						
														8: Applications of Accelerators, Tech Transfer, and Industrial Relations																						
														3: Advanced Acceleration Techniques and Alternative Particle Sources																						
														9: Opening, Closing, and Special Presentations																						
														4: Hadron Accelerators																						
														Posters																						
														5: Beam Dynamics and EM Fields																						
														Posters Staffed																						
														6: Accelerator Systems: Beam Instrumentation, Controls, Feedback, and Operational Aspects																						

